PB-251 581

RADIONUCLIDE PRODUCTION, TRANSPORT, AND RELEASE FROM NORMAL OPERATION OF LIQUID-METAL-COOLED FAST BREEDER REACTORS

Virginia University

Prepared for:

Office of Radiation Programs

November 1975

DISTRIBUTED BY:

NTIS
National Technical Information Service
U. S. DEPARTMENT OF COMMERCE

PB 251 581

REPRODUCED BY
NATIONAL TECHNICAL
INFORMATION SERVICE
U. S. DEPARTMENT OF COMMERCE
SPRINGFIELD, VA. 22161

BIBLIOGRAPHIC DATA SHEET	1. Report No. EPA-520/3-75-019	2.	3. Recipient's Accession No.

4. Title and Subtitle
Radionuclide Production, Transport, and Release from Normal Operation of Liquid-Metal-Cooled Fast Breeder Reactors

5. Report Date November 1975 (date published)

6.

7. Author(s) C. A. Erdman, J. L. Kelly, M. Kirbiyik, A. B. Reynolds
(All affiliated with University of Virginia, Charlottesville)

8. Performing Organization Rept. No. NE-4146-102-73

9. Performing Organization Name and Address
University of Virginia
Office of Sponsored Programs
P. O. Box 3901
Charlottesville, Virginia 22903

10. Project/Task/Work Unit No.

11. Contract/Grant No.
68-01-0547

12. Sponsoring Organization Name and Address
Environmental Protection Agency
Office of Radiation Programs
Washington, D. C. 20460

13. Type of Report & Period Covered
Final

14.

15. Supplementary Notes
Extracted portions of this report were published in NUCLEAR SAFETY, Vol. 16-1 (Jan/Feb 1975) and Vol 16-3 (May/June 1975)

16. Abstracts Sources of radioactivity from the normal operation of an LMFBR and the transport of this radioactivity, were studied. Reliance was placed predominantly on published results although some new calculations were made where needed. Results were normalized to a 1000 MWe LMFBR and compared to values for a 1000 MWe LWR. The radioactivity sources studied included plutonium and other transuranium elements, fission products, tritium, corrosion products, and tramp fuel. Radionuclide transport studies included fission products and fuel from failed fuel, behavior of radioactivity in sodium and cold traps, and operation of gaseous radwaste systems. Operating experience was reviewed, including data from the fast reactors EBR-II, Fermi, SEFOR, Dounreay, Rapsodie, and BR-5, and limited data from the thermal reactors SRE, S8ER, and Hallam. The authors completed this study in September 1973. Since that time, a number of technical papers, reports, and studies have been published which might serve to extend or refine some of the conclusions of the present study (and in some cases may even refute results in the study). Therefore, the users of this report are cautioned to keep in mind the September, 1973 "cutoff" date for the references cited and used in preparing this study.

17. Key Words and Document Analysis. 17a. Descriptors

Radioactive Wastes (1807)
  Fission Products
  Radioactive Isotopes
  Radioactive Waste Processing

Radioactivity (1808)
  Fission Products
  Radioactive Materials
  Induced Radioactivity

Nuclear Reactors (1809)
  Breeder Reactors
  Fast Reactors (nuclear)
  Liquid Metal Cooled Reactors

17b. Identifiers/Open-Ended Terms

17c. COSATI Field/Group

PRICES SUBJECT TO CHANGE

18. Availability Statement Release unlimited - Limited number of copies available free from: U. S. EPA, Technology Assessment Division (AW-459), 401 "M" Street, SW, Washington, D.C. 20460

19. Security Class (This Report) UNCLASSIFIED

20. Security Class (This Page) UNCLASSIFIED

21. No. of Pages 244

22. Price $8.00-2.25

FORM NTIS-35 (REV. 10-73) ENDORSED BY ANSI AND UNESCO. THIS FORM MAY BE REPRODUCED USCOMM-DC 8265-P74

This report was prepared as an account of work sponsored by the Environmental Protection Agency (EPA) of the United States Government under Contract No. 68-01-0547. The report has been reviewed and edited by the EPA and approved for publication. However, approval does not signify that the contents of the report necessarily reflect the views and policies of the EPA. Neither the United States nor the EPA makes any warranty, express or implied, or assumes any legal liability or responsibility for the accuracy, completeness or usefulness of any information, apparatus, product or process disclosed, or represents that its use would not infringe privately owned rights.

FOREWORD

This report was prepared for the Environmental Protection Agency by the University of Virginia, Department of Nuclear Engineering, for the purpose of summarizing the available information on radioactivity discharges from liquid metal fast breeder reactors (LMFBR's). The Energy Research and Development Administration has underway an extensive effort to perfect this reactor type for commercial operation to produce electricity. While producing electricity, the LMFBR will at the same time breed more fissile material than is consumed by the reactor. This is accomplished by using excess neutrons from the fission process to convert the abundant isotope of uranium (^{238}U) to the fissile plutonium isotope ^{239}Pu. (Smaller quantities of other plutonium isotopes, some fissile and some non-fissile, are also produced in the process, by successive neutron absorptions and beta decays.) The plutonium so produced can then be extracted and used to refuel the LMFBR, or to provide fuel for other LMFBR's or other reactor types. Present-day light-water reactors operate by fissioning ^{235}U, which comprises only 0.7% of natural uranium, the balance being essentially all ^{238}U. By converting this 138-times more abundant ^{238}U isotope to fissile material the LMFBR will effect a many-fold increase in the amount of electrical energy which in principle can be produced from the available uranium deposits.

This report is being published so that it will be available as a resource to the scientific community and the general public. The results of the report will assist EPA in assessing the environmenal impacts of the LMFBR program as a whole as well as those of related individual facilities as they are developed. The information also will be used to assist EPA in developing generally applicable environmental radiation standards for LMFBR-related facilities, and may be of assistance in our evaluations of LMFBR accidents.

We solicit, and will appreciate receiving, any corrections or critical comments on the information and conclusions contained in this report. Please send any such comments to the Environmental Protection Agency, Office of Radiation Programs (AW-459), Washington, D.C. 20460.

W. D. Rowe, Ph.D.
Deputy Assistant Administrator
for Radiation Programs (AW-458)

ABSTRACT

Sources of radioactivity from the normal operation of an LMFBR, and the transport of this radioactivity, were studied. Reliance was placed predominantly on published results although some new calculations were made where needed. Results were normalized to a 1000 MWe LMFBR and compared to values for a 1000 MWe LWR.

Sources of radioactivity which were studied included plutonium and other transuranium elements, fission products, tritium, corrosion products, activation products, and tramp fuel.

The study of the transport of radionuclides included reviews of transport of fission products and fuel from failed fuel, behavior of radioactivity in sodium and cold traps, and operation of gaseous radwaste systems.

Operating experience for liquid metal cooled reactors relating to radioactivity was reviewed. Included were data from the fast reactors EBR-II, Fermi, SEFOR, Dounreay, Rapsodie, and BR-5, and limited data from the thermal reactors SRE, S8ER, and Hallam.

The authors conpleted this study in September, 1973. Since that date a number of technical papers, reports, and studies have been published which might serve to extend or refine some of the conclusions of the present study (and in some cases may even refute results in this study). Therefore, the users of this report are cautioned to keep in mind the September, 1973 "cutoff date" for the references cited and used in preparing this study.

TABLE OF CONTENTS

Page
1. INTRODUCTION 1
   - 1.1 Objectives of the Present Study 1
   - 1.2 Some General Results of the Study 2
2. SUMMARY 3
   - 2.1 Objectives and Methods 3
   - 2.2 Sources 4
     - 2.2.1 Plutonium and Other Transuranium Elements 4
     - 2.2.2 Fission Products 5
     - 2.2.3 Tritium 6
     - 2.2.4 Activated Corrosion Products 6
     - 2.2.5 Cladding Activation 7
     - 2.2.6 Sodium Activation 7
     - 2.2.7 Miscellaneous Activation Products 8
     - 2.2.8 Tramp Fuel 8
   - 2.3 Transport of Fission Products and Fuel from Failed Pins 8
   - 2.4 Radioactivity in the Sodium System 10
   - 2.5 Gaseous Radwaste Management 11
   - 2.6 Liquid and Solid Radwaste Management at EBR-II 11
3. PLUTONIUM AND OTHER TRANSURANIUM ELEMENTS 14
   - 3.1 Plutonium Inventories 15
   - 3.2 Isotopic Composition of Plutonium 17
   - 3.3 The Higher Actinides 17
4. FISSION PRODUCT GENERATION 25
   - 4.1 LMFBR Fission Product Generation 25
   - 4.2 Comparison with LWR Fission Product Generation 38
5. OTHER SOURCES 45
   - 5.1 Tritium and Its Transport 45
     - 5.1.1 Summary 45
     - 5.1.2 Sources 46
       - 5.1.2.1 Ternary Fission 46
       - 5.1.2.2 Boron Carbide Control Rods 48
       - 5.1.2.3 Lithium Contamination 53
     - 5.1.3 Transport of Tritium in an LMFBR System 54
       - 5.1.3.1 Escape into Sodium System 54
       - 5.1.3.2 Transport in the Sodium and Steam Systems (including EBR-II Experience) 55
   - 5.2 Activated Corrosion Products 61
     - 5.2.1 Estimated Corrosion Product Activity in 1000 MWe LMFBR 63
     - 5.2.2 Distribution of Corrosion Products in the Primary System 69
     - 5.2.3 Calculational Method 70
     - 5.2.4 Corrosion of ^{182}Ta from Tantalum Control Rods 72
     - 5.2.5 Activated Corrosion Product Experience at Operating Sodium-Cooled Reactors 73

TABLE OF CONTENTS

(Continued - Page 2)

Page

5.2.5.1 Summary.......................... 73
5.2.5.2 EBR-II........................... 75
5.2.5.3 Rapsodie......................... 75
5.2.5.4 SRE.............................. 75
5.2.5.5 SEFOR............................ 76
5.3 Activation Products.................................. 78
5.3.1 Sodium Activation............................ 78
5.3.1.1 Sodium-24........................ 78
5.3.1.2 Sodium-22........................ 79
5.3.2 Cladding Activation.......................... 85
5.3.3 Activation Products ^{39}Ar, ^{41}Ar and ^{23}Ne.... 87
5.3.4 Miscellaneous Activation..................... 89
5.3.4.1 From Fission Products............ 89
5.3.4.2 From Impurities in Sodium Systems. 89
5.4 Tramp Fuel... 90
5.4.1 SEFOR.. 90
5.4.2 EBR-II....................................... 90
5.4.3 Rapsodie..................................... 90
5.4.4 Extrapolation to 1000 MWe LMFBR.............. 91
6. TRANSPORT OF FISSION PRODUCTS FROM FAILED FUEL......... 92
6.1 Introduction... 92
6.2 Brief Background Description of Irradation Experience Relating to Fission Product Release.... 93
6.3 Tritium Release from Fuel Pins (see also Section 5.1)...................................... 95
6.4 Release Fractions for Noble Gases from Oxide Fuels.. 95
6.5 Fuel Failure Rates................................... 101
6.6 Leakage of Fission Products from Failed Fuel--Gaseous and Solid................................ 102
6.6.1 Escape Rates from Plenum to Sodium.......... 102
6.6.2 Transit Time from Failure to Cover Gas...... 103
6.6.3 Time for Diffusion out of the Fuel.......... 104
6.6.4 Diffusion Direction.......................... 104
6.6.5 Experimental Data on Transport of Specific Fission Products to the Sodium or NaK Coolant.............................. 105
6.6.6 Theoretical Models for Fission Product Transport.................................... 107
6.7 Vented Fuel.. 107
6.8 Example Calculations of Releases of a Few Selected Radionuclides to the Primary Coolant and the Cover Gas System..................................... 110
7. FISSION PRODUCTS IN SODIUM SYSTEMS..................... 123
7.1 Fission Product Behavior in Sodium................... 123
7.1.1 Behavior of Each Fission-Product Type...... 124
7.1.1.1 Noble Gases...................... 124
7.1.1.2 Iodine........................... 125
7.1.1.3 Alkali Metals (e.g. Cesium)...... 125

TABLE OF CONTENTS
(Continued - Page 3)

Page

7.1.1.4 Alkaline-Earth Metals (e.g. Strontium)........................ 126
7.1.1.5 Rare Earths........................ 126
7.1.1.6 Transition Metals................. 127
7.1.1.7 Noble Metals....................... 127
7.1.1.8 Tritium (see Section 5.1.3)....... 127
7.1.2 Operating Experience with Fission Products in Sodium (or NaK) Cooled Reactors (Excluding Experience with Cold Traps)...... 127
7.1.2.1 Summary............................ 127
7.1.2.2 EBR-II............................. 127
7.1.2.3 BR-5............................... 130
7.1.2.4 Dounreay........................... 130
7.1.2.5 Rapsodie........................... 132
7.1.2.6 SRE................................ 132
7.1.2.7 SEFOR.............................. 136
7.2 Cold Traps.. 136
7.2.1 Brief Description of Cold Trap Technology.. 136
7.2.2 Cold Trap Decontamination Terminology...... 139
7.2.3 Experiments on Cold Trapping of Particular Radionuclides.............................. 142
7.2.3.1 Cesium............................. 142
7.2.3.2 Iodine............................. 144
7.2.3.3 Strontium, Barium and Zirconium... 145
7.2.3.4 Tritium (see Section 5.1.3.2)..... 145
7.2.4 Operating Experience on Cold Trapping of Fission Products at Sodium-Cooled Reactors. 145
7.2.4.1 Summary............................ 145
7.2.4.2 EBR-II............................. 146
7.2.4.3 BR-5............................... 146
7.2.4.4 SRE................................ 146
7.2.4.5 SEFOR and Fermi (see also Section 7.2.1).................... 148
8. GASEOUS RADWASTE MANAGEMENT.............................. 151
8.1 FFTF Gaseous Radwaste Systems...................... 151
8.1.1 Primary Sodium System Seals................ 152
8.1.2 Radioactive Argon Processing System (RAPS). 153
8.1.3 Cell Atmosphere Processing System (CAPS)... 156
8.2 EBR-II Gaseous Radwaste Systems.................. 156
8.2.1 Present Operation.......................... 156
8.2.1.1 Normal Operation.................. 158
8.2.1.2 Fast Gas Purge System............. 158
8.2.2 Proposed Gas Radwaste System................ 158
8.2.2.1 Criteria........................... 159
8.2.2.2 Cover Gas Cleanup System.......... 160
8.2.2.3 Seven-Day-Delay System............ 160
8.2.2.4 24-Hour-Delay System.............. 162

TABLE OF CONTENTS

(Continued - Page 4)

Page

8.3 Gaseous Radwaste Experience in Other Operating Fast Reactors.......... 162
  8.3.1 Fermi.......... 162
  8.3.2 SEFOR.......... 165
  8.3.3 Rapsodie.......... 165
  8.3.4 Dounreay.......... 165
8.4 Comparison of LWR and LMFBR Radgas Effluents.......... 165
  8.4.1 LWR Gaseous Releases.......... 166
    8.4.1.1 ORNL Study.......... 166
    8.4.1.2 USAEC Regulatory Study.......... 168
  8.4.2 Comparison of LWR and LMFBR Radioactive Gas Releases.......... 168
9. LIQUID AND SOLID RADWASTE MANAGEMENT AT EBR-II.......... 172
  9.1 Liquid Radwaste System.......... 172
  9.2 Solid Radwaste Management.......... 173

APPENDICES

A. Environmental Operating Data for Fermi, SEFOR, and EBR-II.......... 177
B. Fission Product Data.......... 224

TABLES

Table		Page
2.1	Radionuclides Observed in the Primary Coolant System of Sodium-Cooled Reactors	12
3.1	1000 MWe Reactor Charges, Discharges, and Inventories of Plutonium	16
3.2	Isotopic Composition of Plutonium in Discharged Fuels (wt %)	18
3.3	Average Annual Amounts and Activities of Selected Actinides Discharged from Reactors	19
3.4	Neutron and Alpha Particle Yields from Selected Actinides and Their Compounds	22
4.1	Fuel Mass and Fission Product Activity Discharged Annually from an LMFBR and Fission Product Power of Discharged Fuel	26
4.2	Operating Conditions for Two 1000 MWe Designs	27
4.3	Fission Product Activity of Core Discharge Fuel from AI 1000 MWe Reference Oxide Design (80,000 MWd/MT Exposure) as a Funciton of Cooling Time	28
4.4	Fission Product Activity of Axial Blanket Discharge from AI 1000 MWe Reference Oxide Design, as a Function of Cooling Time	31
4.5	Fission Product Activity of Radial Blanket Discharge from AI 1000 MWe Reference Oxide Design, as a Function of Cooling Time	33
4.6	Fission Product Activity of Core Discharge Fuel from GE 1000 MWe Follow-on Design (100,000 MWd/MT Exposure), as a Function of Cooling Time	35
4.7	Energy Generation Rate from Fission Product Decay for the AI 1000 MWe Reference Oxide Design as a Function of Cooling Time	36
4.8	Total Activity of Noble Gas and Iodine Nuclides During Operation of a 1000 MWe LMFBR	37
4.9	LWR Fission Product Activities as a Function of Cooling Time	39

TABLES (Cont'd)

Table Page

4.10 Fission Product Activity Transported Annually From a 1000 MWe LMFBR 42

4.11 Yields of Selected Fission Products from Thermal and Fast Fission 43

5.1 Estimated Tritium Production Rates in a 1000 MWe LMFBR 46

5.2 Summary of EBR-II Tritium Data 57

5.3 Tritium Concentrations in EBR-II 58

5.4 Activation Reactions in Stainless Steel 62

5.5 Data for Corrosion Product Calculation 63

5.6 Estimates of Activated Corrosion Products in the Primary System of the 1000 MWe LMFBR After 30 Years Operation 64

5.7 Corrosion Product Neutron Cross Sections 67

5.8 Comparison of HEDL, AI, and ORNL Cross Sections Averaged Over an LMFBR Core Energy Spectrum 68

5.9 316 Stainless Steel Composition and Isotopic Abundance 69

5.10 Fraction of Nuclides Deposited in Primary System Components - HEDL and GE Results 70

5.11 Corrosion Products in Sodium-Cooled Reactors 74

5.12 Weight Percent of Impurities in SEFOR Cold Traps 76

5.13 Cladding Activity of Spent LMFBR Core Fuel as a Function of Cooling Time 86

5.14 Cladding Activity Discharged Annually From 1000 MWe LMFBR 86

6.1 Oxide Fuel Pins Irradiated in LMFBR's 96

6.2 General Electric F2 Series of Fuel Pin Irradiations 98

6.3 ANL Irradiations in EBR-II 99

TABLES (Cont'd)

Table		Page
6.4	Percent of Fission Gas Released vs Fuel Burnup	100
6.5	Leaching Results from Grossly Defected Oxide Pin in NaK	106
6.6	Loss of Fission Products from Grossly Defected Oxide Fuel in Flowing Sodium	108
6.7	Isotopic Release Fractions from GE Vented Fuel Test	111
6.8	Example Equilibrium Cover-Gas Activity from Failed Fuel for Various Delay Times after Birth for Gaseous Radionuclides	114
6.9	Calculated Annual Activities of Long-Lived Radionuclides Entering Primary Sodium from Failed Fuel	115
7.1	Fission Products Observed in the Primary System of Sodium and NaK Cooled Reactors (other than Tritium)	128
7.2	Fission Product Activity in BR-5 During First Stage of Operation (1962-64)	131
7.3	Gamma Activity of Fission Products in DFR Coolant, 6 Days After Sampling	131
7.4	Typical Radioactivity Levels of SRE Primary Sodium Prior to Run 14	133
7.5	Initial Fission Product Analysis of SRE Primary Sodium After Run 14	134
7.6	Fission Product Analysis of SRE Primary Sodium as a Function of Time After Run 14	135
7.7	Example of SRE Primary Pipe Wall Fission-Product Contamination from HCl Etch at Pipe Surface	137
7.8	Fission Products Observed in Primary Cold Traps of Sodium or NaK Cooled Reactors	145
7.9	Comparison of Impurity Levels in SRE Cold Trap to those in Sodium Coolant	147
8.1	Radioactive Argon Processing System Delay Times	155

TABLES (Cont'd)

Table		Page
8.2	Xenon and Krypton Conditions in Delay Beds	163
8.3	Typical Annual Gaseous Releases from a 1000 MWe PWR Operating with 0.25% Defective Fuel	167
8.4	Summary of Variables for PWR Gaseous Radwaste Treatment Systems	169
8.5	Estimated Annual Releases of Radioactive Gaseous Effluents from 1000 MWe PWR with 0.25% Defective Fuel	170
9.1	EBR-II Solid Waste Management	175
A.1 through A.31	Environmental Operating Data for Fermi, SEFOR, and EBR-II	177
B.1	Half Lives and Fission Yields of Fission Products Listed in Section 4	225

FIGURES

Figure Page

3.1 Formation Scheme for Important Actinides 20

5.1 Tritium in Primary Sodium (EBR-II) 56

8.1 Radioactive Argon Processing System 154

8.2 Cell Atmosphere Processing System 157

8.3 Seven-Day-Delay Cover Gas Cleanup System for EBR-II 161

8.4 24-Hour-Delay Cover Gas Cleanup System for EBR-II 164

9.1 EBR-II Liquid Radwaste System 174

B.1 Fission Product Decay Schemes Used for Calculations in Section 4 228

1. INTRODUCTION

1.1 Objectives of the Present Study

Radioactivity produced in a Liquid Metal Fast Breeder Reactor (LMFBR) must either decay or ultimately leave the reactor site (or remain at the site after decommissioning the plant.) The purpose of this study is to examine all sources of radioactivity in an LMFBR power reactor and to determine the ultimate fate of this activity during the normal operation of the plant. This investigation is concerned with the quantity and form of the radioactivity that leaves the site. The "environment" is defined as anything beyond the site boundary, so all radioactivity leaving the site enters the "environment". Nearly all of the radioactivity leaving will be contained; but then this radioactivity becomes the source at the next stage in an environmental study. An attempt is made to identify the small amounts of radioactivity that leave the site uncontained and enter the atmosphere and water directly.

It should be emphasized that the study is limited to normal operation and therefore does not include accident situations. Normal operation does assume operation with some failed fuel, however.

The study also includes numerous comparisons between the operation of an LMFBR and a light water reactor (LWR).

Numerical results are based on a 1000 MWe plant. For the LMFBR, and efficiency of 40% was assumed, so that the thermal power was 2500 MW(th). For the LWR an efficiency of 34% was assumed, which gives a thermal power of 2940 MW(th).

Environmental statements for the LMFBR Demonstration Plant (WASH-1509) and for the FFTF (WASH-1510) were published in April, 1972 and May, 1972. The statement for the Demonstration Plant contains a general description of the LMFBR program, including history, the projected U. S. program, and European, USSR, and Japanese programs. Therefore, this type of discussion is not presented in the present report.

A study related to parts of the present one, and which also included a review of accidents, was reported in March, 1969 by ORNL (G. W. Keilholtz and G. C. Battle, Jr., "Fission Product Release and Transport in Liquid Metal Fast Breeder Reactors," ORNL-NSIC-37, March, 1969). Since that time much has been reported and further experience with several fast reactors has been obtained; this new material in addition to the old is included in the present report.

The present study includes a review of operating experience with liquid metal cooled fast reactors and also some data from sodium cooled thermal reactors. The reactors reviewed include:

U.S. Fast Reactors:
    Experimental Breeder Reactor-II (EBR-II)
    Enrico Fermi Fast Reactor (Fermi)
    Southwest Experimental Fast Oxide Reactor (SEFOR)
U. S. Thermal Reactors:
    Sodium Reactor Experiment (SRE)
    Hallam Nuclear Power Facility (HNPF)
    Snap-8 Experimental Facility (S8ER)
UK Fast Reactor:
    Dounreay Fast Reactor (DFR)
French Fast Reactor:
    Rapsodie
USSR Fast Reactor:
    BR-5

All of these reactors were sodium cooled except Dounreay and S8ER, which were cooled by NaK. It was more useful to treat various results from the operation of these reactors throughout the report under the different functional sections rather than to devote a separate overall section to operating reactor experience.

1.2 Some General Results of the Study

Despite the vast amount of material reviewed and discussed in the present report it is clear that there is still much to learn concerning transport of the radionuclides produced in an LMFBR. The quantities of the radionuclides produced in an LMFBR, which include the isotopes of plutonium and other transuranium elements (Section 3) and the contained fission products (Section 4) are fairly accurate and well defined. Their disposition and safeguarding are of concern with respect to the reprocessing and fuel fabrication plants, transportation, and the waste disposal systems. The areas which are still poorly defined concern fuel failure during normal operation (Section 6), the transport of fission products from failed fuel (Section 6), and the fate of the non-noble gas fission products in the sodium (Section 7). The status of knowledge on tritium and corrosion products (Section 5) is better than that of the above problems, but still is not adequate. Only long-term operation of power LMFBR's (for example, the Clinch River Breeder Reactor Plant, the Fast Flux Test Facility, and the currently operating demonstration plants in the U. K., France and the USSR) will provide experience in these problem areas to replace the early estimates reported here.

If an efficient gaseous radwaste system is used on all fast power reactors, as proposed for the FFTF, it is expected that during normal operation the gaseous effluent released to the environment (i.e. to the atmosphere at the reactor site) can be made as low as required. In a sodium reactor leakage of coolant to the environment cannot be permitted during normal operation. The only liquid waste (other than tritiated water) will come from experimental and cleanup facilities, which can be made to contain little waste if necessary as in the case of EBR-II (Section 9). The only major source of radioactivity released to the atmosphere and water at the plant site which is difficult to eliminate is tritium, but even here the cold traps in an LMFBR appear to provide a reduction below effluent levels typical for light water reactors. Based on EBR-II experience (which is a very limited basis for extrapolation to a large power reactor) and the estimated tritium sources in a large plant, the annual tritium release rate to the surrounding atmosphere from 1000 MWe LMFBR is of the order of 100 Ci/yr and is less than 10 Ci/yr to the condenser water (Section 5.1). This liquid effluent rate compares to predicted tritium releases of 100 Ci/yr and 600 Ci/yr in the liquid effluent of a 1000 MWe BWR and PWR respectively (Section 5.1)

For these reasons, it appears that the principal environmental problems for normal operation of an LMFBR will involve offsite handling of the larger amounts of plutonium and transuranium elements and fission products shipped away from the site in the irradiated fuel, storage of the ^{85}Kr, storage of the cold traps shipped away from the plant, and storage of sodium and primary system equipment after decommissioning of the power plant. The problems concerning sodium and sodium cold trap disposal do not exist, of course, for water reactors. The quantities of plutonium and the decreased ^{240}Pu in radial blanket material lead to a worsening of the plutonium problem for the LMFBR over the "Pu Recycle LWR", but not greatly so (Section 3). The other environmental problems from normal operation of the LMFBR (e.g. fuel reprocessing, transportation, long-term storage of fission products) are similar to those of a light water reactor.

2. SUMMARY

2.1 Objectives and Methods

The purpose of this investigation was to examine all sources of radioactivity in an LMFBR power reactor and to determine the ultimate fate of this radioactivity. Only normal operation was considered. There was particular concern with the form and quantity of radioactivity which leaves the reactor site; this radioactivity was considered to enter the "environment", meaning that this activity must be dealt with at a reprocessing plant, a storage facility, or elsewhere.

The method of the study was predominantly to obtain numbers from published values in the literature. These were augmented by some original estimates where needed. Operating experience of liquid metal cooled reactors was reviewed, including EBR-II, Fermi, SEFOR, Dounreay, Rapsodie, BR-5, SRE, SBER, and Hallam. Numerical results are presented on the basis* of the normal operation of a 1000 MWe LMFBR.

2.2 Sources

Radionuclides which are transported to the environment from normal operation of an LMFBR include:

- plutonium and other transuranium elements
- fission products
- tritium
- corrosion products
- activation products (^{24}Na, ^{22}Na, ^{39}A, ^{41}A, ^{23}Ne, cladding)
- tramp fuel

Transport to the environment refers to any transport from the reactor site. Planned transport paths include shipments from the plant of irradiated fuel, cold traps or other used primary equipment, bottled gas from the gaseous radwaste system, wastes in water solutions, solid wastes, and sodium and primary equipment after decommissioning of the plant. Unplanned leakage to the environment includes gas leakage through the building ventilation system and tritium leakage through the secondary sodium system to the steam systems and thence to the condenser water.

2.2.1 Plutonium and Other Transuranium Elements

Depending on the specific design, a 1000 MWe LMFBR will have from 1100 to 1850 kg of plutonium loaded into it annually, and from 1540 to 2000 kg of plutonium will be unloaded annually. The maximum plutonium inventory will be on the order of 3000 to 3300 kg. The typical isotopic content of the discharged plutonium for the mixed blankets and core is shown below.

Isotope	Wt. % of Total Pu
^{238}Pu	1
^{239}Pu	69
^{240}Pu	22
^{241}Pu	5
^{242}Pu	3

---

* In general, extrapolation of data to correspond to the 1000 MWe size LMFBR has been done by assuming proportionality to reactor thermal power. Most parameters do change linearly in such a scale-up, and the assumption of linearity is generally a good approximation. However, there are some important parameters which do not change linearly, and caution should be exercised in making any such extrapolations.

For comparison, a 1000 MWe LWR will charge 0 to 730 kg of plutonium annually, will discharge 250 to 400 kg annually, and will have maximum plutonium inventories on the order of 500 to 2000 kg, depending on whether they are based on ^{235}U fuel or plutonium recycle.

The amounts and activities of uranium and the various transuranium elements discharged annually from core and blankets of a 1000 MWe LMFBR are shown below for a plutonium discharge of 2000 kg.

	At Discharge		Ci after
Element	kg	Ci	90 d
U	2×10^4	7	7
Np	8	1.2×10^9	1.2×10^3
Pu	2000	1.5×10^7	1.5×10^7
Am	17	3.4×10^6	4.6×10^4
Cm	1	1.8×10^6	1.2×10^6

2.2.2 Fission Products

The important fission products still in the fuel one year after the fuel is removed from an LMFBR (i.e. those of activities still greater than 10^4 Ci/year in the fuel discharged from a 1000 MWe plant) are

^{85}Kr
^{89}Sr
^{90}Sr-Y
^{91}Y
^{95}Zr-Nb
^{103}Ru-Rh
^{106}Ru-Rh
^{125}Sb
^{125m}Te
^{127}Te-Te
^{134}Cs
^{137}Cs-Ba
^{141}Ce
^{144}Ce-Pr
^{147}Pm
^{151}Sm
^{155}Eu
^{162}Gd-Tb

The total fission product activity in the fuel discharged annually from a typical 1000 MWe LMFBR, together with the associated fission product power, are shown below as a function of cooling time after discharge.

	Cooling Time				
	30d	90d	150d	300d	30yr
Activity (Ci/yr)	4.3×10^8	2.4×10^8	1.6×10^8	8.6×10^7	3.4×10^6
Power (MW)	1.9	1.0	0.7	0.4	0.01

2.2.3 Tritium

Tritium is produced in ternary fission, but in an LMFBR nearly all of this tritium escapes from the fuel. Tritium is also produced in boron carbide control rods, but it is unclear how much of this escapes to the sodium. The annual estimated tritium production rates are summarized as follows:

Source	Annual Production Rate (Ci/yr)
Ternary fission	20,000
Control rods: $^{10}B(n,t)\,2\alpha$	7,000
$^{7}Li(n,nt)\alpha$	2,500
Lithium contamination: $^{6}Li(n,t)\alpha$	
In fuel (maximum)	4,000
In sodium	100
TOTAL	∿ 30,000

Tritium leaks to the environment, both as a gas to the atmosphere and as a liquid in the condenser water. Based on direct extrapolation from EBR-II (60 MWth) to a 1000 MWe LMFBR, the annual leakage rates would be ∿ 60 Ci/yr of tritium to the atmosphere and ∿ 3 Ci/yr to the condenser water. This value compares to BWR and PWR liquid effluent rates of ∿ 100 Ci/yr and ∿ 600 Ci/yr, respectively. Most of the tritium in an LMFBR is held up in cold traps, and is eventually shipped from the site with the cold traps.

2.2.4 Activated Corrosion Products

Activated steel cladding and steel structures in and near the core are slowly corroded by sodium. The principal activated corrosion products are ^{60}Co, ^{58}Co and ^{54}Mn. Most of the corrosion products plate out on the walls of the primary system, while some are held up in the cold traps and some remain in solution in the sodium. Estimates of the corrosion products which will enter the sodium and still be present in the primary sodium system after 30 years of operation in the 1000 MWe LMFBR, together with the principal reactions and the half lives, are summarized below.

Nuclide	Formation Reaction	Half Life	Primary-System Corrosion Product Activity After 30 Years (Ci)
$^{60}\mathrm{Co}$	$^{59}\mathrm{Co}(n,\gamma)$	5.24 yr	19,000
	$^{60}\mathrm{Fe}(n,p)$		1,000
$^{58}\mathrm{Co}$	$^{58}\mathrm{Ni}(n,p)$	71 d	23,000
$^{54}\mathrm{Mn}$	$^{54}\mathrm{Fe}(n,p)$	313 d	19,000
$^{59}\mathrm{Fe}$	$^{58}\mathrm{Fe}(n,\gamma)$	45 d	1,000
$^{51}\mathrm{Cr}$	$^{50}\mathrm{Cr}(n,\gamma)$	28 d	7,000
$^{182}\mathrm{Ta}$	$^{181}\mathrm{Ta}(n,\gamma)$	115 d	$<6{,}000$

2.2.5 Cladding Activation

The cladding and channel walls are activated and the activity is shipped to the reprocessing plant with the fuel. Estimates of the cladding activity shipped from a 1000 MWe LMFBR annually with the discharged fuel are given below as a function of cooling time:

	Cooling Time				
	30 d	90 d	150 d	300 d	30 y
Activity (Ci/yr)	5×10^{6}	3×10^{6}	2×10^{6}	1×10^{6}	1×10^{3}

Two activation products not considered among the activated corrosion products are $^{59}\mathrm{Ni}$ and $^{63}\mathrm{Ni}$ (half lives of 8×10^{4} yr and 92 yr respectively) which contribute 20 Ci and 500 Ci respectively to the 1000 Ci total at 30 years.

2.2.6 Sodium Activation

Sodium activates to $^{24}\mathrm{Na}$ (by an n,γ reaction) and $^{22}\mathrm{Na}$ (by $n,2n$). Sodium-24 has a relatively short half life (15 hr) but $^{22}\mathrm{Na}$ has a 2.6 year half life. At $\sim$ 8 days after shutdown the $^{22}\mathrm{Na}$ becomes dominant activity. The equilibrium activities of the primary system of a 1000 MWe LMFBR are estimated at 2×10^{7} Ci for $^{24}\mathrm{Na}$ and 3000 Ci for $^{22}\mathrm{Na}$.

2.2.7 Miscellaneous Activation Products

Argon-39 is produced by activation of ^{39}K in sodium and is significant because of its long half-life (269 yr). Although no reported observations of ^{39}A were found for operating fast reactors, the calculated ^{39}A production rate for a 1000 MWe LMFBR (assuming 300 ppm potassium in the coolant) is ~30 Ci/yr.

Small amounts of the following activation products are found in operating fast reactors:

^{41}A, ^{23}Ne -- Gaseous activation products always present in LMFBR's.

^{65}Zn, ^{110}Ag, ^{125}Sb, ^{210}Po -- Activation products observed in some fast reactors.

Also, ^{134}Cs, ^{154} Eu, and several other isotopes listed in this report under fission products are actually activation products produced from activation of fission products.

2.2.8 Tramp Fuel

Tramp fuel will probably not be a concern in large LMFBR's. Total tramp fuel inventories of the order of half a gram of heavy metal atoms can be predicted based on other reactor experience. This results in an equilibrium fission product inventory in the primary circuit of about 300 Ci of fission products and 20 to 30 Ci of actinide activities. The long-lived isotopic buildup would be to a few tens of curies of fission products and a few curies of long-lived actinides over the plant life.

2.3 Transport of Fission Products and Fuel from Failed Pins

Estimation of the transport of activity from failed fuel pins to the primary circuit is an extremely difficult problem. On the basis of limited experimental results and operating experience, the following conservative assumptions were used to calculate releases.

1% failed pins
90% of failed pins are leakers
10% of failed pins have gross cladding failures
75% of the noble fission gases are released from the fuel proper, i.e., pellets, of failed pins

For gross failures, the escape fractions assumed are

Fuel	1%
Br, I, Cs	15%
Te, Ru, Tc, Mo	5%
All Others	1%

The plutonium fraction in the escaped fuel is assumed to be only one-tenth of the original Pu fraction because of the observed preferential leaching of the U and the inward migration of Pu. The releases calculated from the above assumptions can easily be adjusted to other failure or release fractions if experience or judgement dictates.

Annual releases of a few selected fission products and plutonium, to the primary sodium or cover gas, together with the total released activity still present one year after a 30 year operating period, are given below.

Radionuclide	Annual Release (Ci)	Activity Present One Year After a 30 Year Operating Period (Ci)
^{85}Kr	1900	25,000
^{90}Sr-Y	30	600
^{106}Ru-Rh	4600	6,000
^{125}Sb	---	40
^{125m}Te	---	10
^{134}Cs	---	350
^{137}Cs-Ba	1100	30,000
^{144}Ce-Pr	900	800
^{147}Pm	100	500
^{151}Sm	---	50
^{154}Eu	---	4
^{155}Eu	---	60
^{241}Pu(β)	20	400
Pu(α)	0.6	20
Pu	2.5 grams	75 grams

A reduction in failed pins from 1% to 0.1% and a corresponding reduction in gross cladding failures from 0.1% to 0.01% would reduce all of the above releases, including the ^{85}Kr release, by a factor of ten. If the assumption concerning relatively higher leaching of uranium than plutonium is correct, this reduction in failure rates would reduce the annual plutonium release to the same order of magnitude as the plutonium in tramp fuel (~0.1 gm.). Also, the fraction of fuel leached from gross cladding failures may be significantly less than 1% in most cases, further lowering the Pu release.

2.4 Radioactivity in the Sodium System

The primary sodium system of an LMFBR becomes highly radioactive. Fission products and small quantities of fuel enter the sodium from failed fuel pins, tritium and activated corrosion products enter the sodium, sodium becomes activated to ^{24}Na and ^{22}Na, and small amounts of other activation products and tramp fuel are present. Sodium leakage from the primary system (other than very small leakage to the secondary sodium) cannot be tolerated. Hence, coolant leakage is not a source of fission products in the environment as is the case with LWR's. Activated sodium causes maintenance problems, but only to plant personnel. An important environmental concern is the periodic removal from the site of cold traps which contain radioactive material. Also, after decommissioning of the reactor, the radioactive sodium and contaminated primary system components must be removed from the site and stored somewhere in the environment.

Many experimental studies on fission product behavior in sodium have been reported, some of which are reviewed in this report. One of the principal purposes for those studies is to determine the activity in the sodium in the case of an accidental sodium fire or sodium release, and these considerations are beyond the scope of this report.

Cold traps are used in LMFBR's to purify the sodium. Although the primary function of the cold trap is to maintain a low oxygen concentration, cold traps also remove much of the radioactivity from sodium during normal operation. These cold traps must be removed periodically, shipped from the site, and stored somewhere in the environment. Iodine and tritium are effectively removed from sodium by cold traps. Much of the cesium is removed, but according to EBR-II experience cold traps are not adequate for cesium removal. At low temperatures, much of the cesium will plate out on the walls of the primary system. Also, most activated corrosion products plate out on the primary system. Nobel gases are volatile in liquid sodium, except for small amounts that remain in solution, and quickly escape to the cover gas.

A summary table of experience with the sodium (or NaK) system of operating sodium (or NaK) cooled reactors is given on the next two pages. The table only lists radioactive isotopes that have been observed. Further details on levels of activity are given in Section 7 of this report.

2.5 Gaseous Radwaste Management

Information on the gaseous radwaste systems of FFTF, EBR-II, Fermi, SEFOR, Rapsodie, and Dounreay was reviewed.

The amount of gaseous activity released from FFTF is expected to be trivial as a result of two factors: (a) a sophisticated gaseous radwaste system is used, which includes charcoal delay beds and a cryogenic distillation column, and (b) virtually no coolant leakage is permitted from a liquid metal cooled reactor. In this system, ^{85}Kr will be bottled and shipped offsite for storage.

Assuming the same type of gaseous radwaste system on an LMFBR power plant, the ^{85}Kr release to the atmosphere from a 1000 MWe LMFBR would be 3 Ci/year, based on scaleup of the FFTF projected values and assuming operation with 1% failed fuel. In addition the 30 Ci/yr of ^{39}A (produced from 300 ppm potassium in the coolant) would all be released to the environment.

EBR-II has a gaseous waste system that does not presently allow operation with failed fuel. A proposed system using charcoal delay beds and ^{85}Kr storage, will allow operation with up to twelve failed test oxide fuel pins.

For comparison, short-lived noble gas and ^{85}Kr leakage to the atmosphere is much higher for typical LWR's than for an LMFBR with an FFTF-type gaseous radwaste system. For a typical LWR with 0.25% defective fuel the ^{85}Kr release rate is 800 Ci/year. Unlike the LMFBR, an important source of fission product gas leakage to the environment from an LWR is primary coolant leakage. Gaseous radwaste systems can be added to an LWR to reduce the ^{85}Kr leakage to values nearly as low as for the LMFBR, however, if required. The ^{39}A source is not present in a LWR.

2.6 Liquid and Solid Radwaste Management at EBR-II

The only fast reactor operating experience with liquid and solid radwaste which was reviewed was for EBR-II. At present the EBR-II liquid radwaste system has a decontamination factor of 10^2 to 10^3. A modified system composed of a settling tank, evaporators, condensers, filters, mist separator, centrifuge, and ion exchange bed is being installed to increase the decontamination factor to 10^4.

Low, intermediate, and high level solid wastes are processed at EBR-II. About 13,000 cu ft/year are processed, most of which is low level. In 1971, 1.5 x 10^6 Ci of high level waste were processed, with a volume of only 150 cu ft. Small amounts of plutonium contamination were shipped from the site.

Table 2.1
Radionuclides Observed in the Primary Coolant System of Sodium (and NaK) Cooled Reactors (other than ^{24}Na and ^{22}Na)

		Fermi	BR-5	EBR-II	Dounreay	Rapsodie
Observed in Primary Coolant	Fission Products	^{140}Ba-La, ^{137}Cs ^{89}Sr, ^{131}I	^{144}Ce, ^{141}Ce, ^{144}Pr, ^{140}Ba-La, ^{137}Cs, ^{136}Cs, ^{106}Ru, ^{90}Sr, ^{95}Zr-Nb, ^{131}I	^{134}Cs, ^{3}H	^{141}Ce, ^{144}Ce, ^{132}Te ^{131}I, ^{103}Ru, ^{106}Ru ^{132}I, ^{137}Cs, ^{95}Zr-Nb ^{140}Ba-La, ^{138}Cs	^{137}Cs
	Activated Corrosion Products			^{54}Mn		
	Other Activation Products		^{65}Zn	^{65}Zn, ^{124}Sb, ^{125}Sb, ^{110m}Ag, ^{113}Sn, ^{113m}In, ^{117m}Sn, ^{210}Po,		^{210}Po
Observed on Primary System Surfaces	Fission Products	^{141}Ce, ^{144}Ce, ^{133}I, ^{103}Ru, ^{95}Zr-Nb	^{144}Ce, ^{141}Ce, ^{144}Pr, ^{140}Ba-La, ^{137}Cs, ^{136}Cs, ^{106}Ru, ^{90}Sr, ^{95}Zr-Nb, ^{131}I	^{137}Cs	^{140}Ba-La	^{141}Ce, ^{137}Cs, ^{131}I, ^{132}I, ^{140}Ba-La, ^{95}Zr-Nb, ^{91}Y, ^{90}Sr-Y
	Activated Corrosion Products			^{54}Mn, ^{60}Co		^{54}Mn, ^{58}Co, ^{60}Co
	Other Activation Products			^{65}Zn, ^{182}Ta		^{65}Zn
Observed in Cold Traps	Fission Products		^{137}Cs, ^{136}Cs, ^{131}I ^{133}I, ^{95}Zr-Nb, ^{135}I, ^{140}Ba-La	^{137}Cs, ^{134}Cs ^{3}H, I	^{137}Cs	
	Activated Corrosion Products			^{54}Mn, ^{60}Co		^{54}Mn, ^{58}Co, ^{60}Co
	Other Activation Products			^{65}Zn, ^{124}Sb		^{65}Zn

Table 2.1. (continued - page 2)
Radionuclides Observed in the Primary Coolant System of Sodium (and NaK) Cooled Reactors

		SEFOR	SRE	S8ER	Hallam
Observed in Primary Coolant	Fission Products	^{86}Rb	^{134}Cs, ^{137}Cs, ^{89}Sr, ^{90}Sr, ^{131}I, ^{141}Ce, ^{144}Ce, ^{103}Ru, ^{106}Ru, ^{95}Zr-Nb ^{140}Ba-La		
	Activated Corrosion Products	^{60}Co	^{51}Cr, ^{54}Mn, ^{59}Fe, ^{60}Co	^{56}Mn, ^{60}Co	
	Other Activation Products	^{65}Zn, ^{124}Sb ^{110}Ag	^{125}Sb		
Observed on Primary System Surfaces	Fission Products		^{89}Sr, ^{90}Sr, ^{144}Ce, ^{95}Zr-Nb, ^{106}Ru ^{137}Cs	^{89}Sr, ^{90}Sr, ^{103}Ru, ^{106}Ru-Rh, ^{141}Ce, ^{144}Ce, ^{95}Zr-Nb ^{140}Ba-La	
	Activated Corrosion Products		^{51}Ci, ^{54}Mn, ^{59}Fe, ^{60}Co	^{54}Mn, ^{59}Fe, ^{58}Co, ^{60}Co	^{54}Mn, ^{60}Co
	Other Activation Products				
Observed in Cold Traps	Fission Products		^{137}Cs, ^{106}Ru, ^{144}Ce-Pr, ^{110}Ag		
	Activated Corrosion Products	(Cu, Fe, Cr, Ni, Mn)	^{54}Mn, ^{59}Fe, ^{60}Co,	^{54}Mn, ^{59}Fe	^{54}Mn, ^{60}Co
	Other Activation Products		^{125}Sb		

Both solid and liquid waste quantities from EBR-II are larger than would be expected from an LMFBR power reactor due to the extensive use of hot cells for experiments there.

3. PLUTONIUM AND OTHER TRANSURANIUM ELEMENTS

The LMFBR will have larger inventories of plutonium and other higher actinides than are found in enriched-uranium-fueled light water reactors (LWR's). In comparing LMFBR's and LWR's, it is also interesting to consider LWR's fueled with recycled plutonium, because plutonium recycle has already become a reality with the Big Rock Reactor. All three types of fuel-reactor combinations are considered in this section in the predictions of transuranium element production.

There are important environmental concerns raised by the increased plutonium inventories forecast for planned LMFBR's. These concerns are related to the extremely toxic nature of plutonium[1], the possible diversion of plutonium for clandestine weapons production[2], and the increased production in high-plutonium-content fuels of other transuranium elements in the form of extremely high specific activity nuclides.

The general conclusions of this section, which address most of the concerns raised above are as follows:

(1) The average plutonium inventory in an LMFBR, while significantly greater than that in a uranium-fueled LWR of the same size, will be less than an order of magnitude greater than in the LWR.

(2) The average plutonium inventory in an LWR fueled with recycled plutonium will be about half the inventory in an LMFBR, thus posing similar toxicity control problems.

(3) Plutonium derived from reprocessed fuel either from uranium-fueled LWR's or from LMFBR's can be used to construct an explosive nuclear weapon. The major differences are that the LMFBR has "blankets" of ^{238}U to increase plutonium production, the plutonium from the radial blanket of an LMFBR would be exceptionally good for weapons, and the separate diversion of the radial blankets is possible because of the normal physical segregation of radial blanket and core.

(4) The overall implication of conclusions (1), (2), and (3) above is that the plutonium problem, whether with respect to toxicity control or fissile material safeguards, is not created by the LMFBR but rather is aggravated by it.

(5) Of the transplutonium isotopes, only ^{241}Am and ^{243}Am will be produced in kilogram quantities each year in a large LMFBR.

However, the much smaller quantities of ^{242}Cm and ^{244}Cm produced will yield higher alpha and neutron activities than both the americium isotopes and the vastly more abundant plutonium isotopes combined. (The plutonium will have a higher overall activity because of the beta decay of ^{241}Pu). Indeed the spontaneous fission activity from the curium isotopes will be much greater than that of the plutonium isotopes in discharged LMFBR fuel despite the huge difference in inventories. Thus the curium isotopes deserve special attention in LMFBR fuels and pose even more of a concern in plutonium recycle fuel from LWR's.

3.1 Plutonium Inventories

Calculated plutonium charges, inventories, and discharges for four reactors are shown in Table 3.1. Results for a pressurized water reactor (PWR) fueled with uranium and for a PWR fueled with plutonium are both presented[3].

Similar results are presented for two LMFBR conceptual designs: the 1000 MWe AI Reference Oxide LMFBR[4] and the GE 1000 MWe LMFBR[5].

The AI LMFBR is considered here because it has been used as the basis for many literature characterizations of the LMFBR. A design such as the GE LMFBR is probably closer to that which will be seen in the first generation of large LMFBR's.

The plutonium which is used in the fuel for the LMFBR's and for the plutonium-fueled PWR shown in Table 3.1 is plutonium obtained from uranium-fueled light water reactors. [3,4,5] This would be the situation for the first several years of a plutonium-fueled reactor industry because of the available plutonium stocks. By 1985 there may be as much as $1.7 billion worth of plutonium available from reprocessing of uranium fuels.[6]

The fuel reloading schemes for the various reactors in Table 3.1 differ significantly as can be seen from the table. Therefore, the most important factors for comparison are the maximum plutonium inventories and the average amounts of plutonium charged and discharged per year. The larger amounts associated with the LMFBR, as opposed to the uranium-fueled PWR, are clearly shown. However, just as there should be serious concern over the 3000 kg of plutonium present in an LMFBR and the 1500 kg shipped to and from the plant each year, there must also be appropriate concern over the 500 kg of plutonium present in a uranium-fueled LWR and the 250 kg shipped from the LWR plant each year. As stated previously, the plutonium problem already exists with LWR's and is simply aggravated by the LMFBR.

Note also that the reduction in the amount of plutonium involved in a plutonium-fueled LWR relative to an LMFBR is not nearly as dramatic as for the comparison of a uranium-fueled LWR and an LMFBR.

Table 3.1

1000 MWe Reactor Charges, Discharges, and Inventories of Plutonium

Reactor		Fuel fraction replaced per charge	Ave. Residence time (days)	Pu discharged* (Kg)	Pu Charged* (Kg)	Maximum Pu Inventory (Kg)	Ave. Amount of Pu (Kg)		Ave. Burnup of Core Fuel (MWd/MT)
							Discharged per year	Charged per year	
PWR[3] (U-Fueled)		1/3	1100	256	—	512	256	—	33,000
PWR[3] (Fueled with Pu from U-Fueled PWR)		1/3	1200	442	800	2042	403	730	33,000
AI Ref. Oxide LMFBR[4] (Fueled with Pu from U-Fueled PWR)	Core and Axial Blanket	1/2	540	1270	1380	2740	1716	1865	80,000
	Radial Blanket	.28	970	223	—	560	302	—	
	Total			1493	1380	3300	2018	1865	
GE LMFBR[5] (Fueled with Pu from U-Fueled BWR)	Core and Axial Blanket	.46	796	1304	1094	2713	1304	1094	100,000
	Radial Blanket	.29	1260	157	—	356	157	—	
	Total			1461	1094	3069	1461	1094	

* Refers to Pu charged or discharged at an actual refueling. Refueling recurred annually for the PWR (U-fueled) and GE LMFBR reactors so that these numbers agree with the average annual amounts for these reactors. Refueling was not annual for the PWR (Pu-fueled) and AI LMFBR reactors.

3.2 Isotopic Composition of Plutonium

Table 3.2 gives information on the isotopic composition of plutonium in fuels discharged from specific reactor types [3,4,5,7,8,9] and also shows the estimated average composition of plutonium available for recycle.

The table shows that discharged fuel with the lowest percentage of fissile plutonium (^{239}Pu and ^{241}Pu) is that from plutonium-fueled LWR's. This plutonium is much lower in fissile content than that from either uranium-fueled LWR's or LMFBR's. Next lowest in fissile content is plutonium from uranium-fueled LWR's. The plutonium with the highest fissile content (and thus most easily used in constructing a nuclear explosive) comes from the LMFBR and in particular from the radial blanket.

It is important to remember, however, that (aside from possible diversion) high fissile isotopic content is extremely desirable for reactor fuels. Higher fissile content means better utilization, or more complete "burning" of the plutonium and it also means an overall smaller plutonium inventory for reactors designed to use high fissile plutonium.

Isotopic composition also has a strong effect on the quantity and character of the radiation from plutonium. A good description of the contributions made by the various plutonium isotopes to the activity of interest in fuel manufacturing is provided in Reference 7. He discusses the neutron doses from spontaneous fission and from (α,n) reactions with light nuclei. Also the importance of the gamma activity from the ^{236}Pu chain is noted. However, for environmental considerations, the alpha and beta activity of the various plutonium isotopes is probably the overriding concern. (All of the plutonium isotopes of interest are alpha emitters except ^{241}Pu, a beta emitter.) Moreover, the potential for biological damage from reactor fuels is related not only to the plutonium content but also, to some extent, to the presence of other higher actinides.

3.3 The Higher Actinides

Although it is theoretically possible to produce elements all the way up through the highest in the actinide series by successive neutron absorptions in a reactor, only a few of the higher actinides are produced in sufficient quantities to be of interest as potential sources of danger to the environment. Figure 3.1 shows the isotopes of interest and the principal means of producing them in reactors. This figure is an elaboration of a figure from Reference 10. Most of these isotopes will be produced in significant quantities in both LWR's and LMFBR's. Calculations and some measurements on the quantities and activities of the various actinide nuclides present in reactor fuel during and after exposure have been made.[3,4,10] Table 3.3 shows average amounts and activities of several nuclides of interest that would be discharged each year from various reactor

Table 3.2

Isotopic Composition of Plutonium in Discharged Fuels (wt %)

I. Uranium-Fueled Reactors

Reactor	PWR[3]	Yankee Rowe[7]			BWR[5]	BWR[8]	Dresden-I[7]	
Burnup (MWd/MT)	33,000	23,900	33,000	38,900	20,000	27,500	23,000	38,400
^{238}Pu	1.8	1.00	1.92	2.15	---	1.0 *	.80	1.71
^{239}Pu	58.7	67.7	63.3	56.4	58.9	57.2	63.4	53.3
^{240}Pu	24.2	18.8	19.2	21.9	25.7	25.7	24.8	28.8
^{241}Pu	11.4	10.0	11.7	13.8	12.2	11.6	8.32	10.3
^{242}Pu	3.9	2.51	3.88	5.77	3.2	4.5	2.73	5.85

*Estimated

II. Estimated Average Composition of Pu Available for Recycle[9]

Year	1975	1980	1985
^{238}Pu	1.0	1.5	1.7
^{239}Pu	64	58	54
^{240}Pu	22	24	25
^{241}Pu	10	11	12
^{242}Pu	3	5	7

III. Plutonium-Fueled Reactors

Reactor	PWR[3]	AI Ref. Oxide LMFBR[4]			GE LMFBR[5]		
		core & axial blanket	radial blanket	core & blankets averaged	core & axial blanket	radial blanket	core & blankets averaged
Burnup (MWd/MT) Pu Source	33,000 U-Fueled PWR		-Core: 80,000- U-Fueled PWR			-Core: 100,000- U-Fueled PWR	
^{238}Pu	2.7	.9	.02	.8	—	—	—
^{239}Pu	39.3	61.5	97.6	66.8	67.5	94.9	70.5
^{240}Pu	25.6	26.0	2.33	22.5	24.5	4.9	22.4
^{241}Pu	17.3	7.2	.04	6.2	5.2	.2	4.6
^{242}Pu	15.1	4.5	—	3.8	2.8	—	2.5

Table 3.3

Average Annual Amounts and Activities of Selected Actinides Discharged from Reactors

	U-Fueled PWR[3]			Pu-Fueled PWR[3]			LMFBR[4]		
Isotope	Kg	Curies	Curies after 90d	Kg	Curies	Curies after 90d	Kg	Curies	Curies after 90d
^{235}U	231	.50	.50	53	.11	.11	33.4	.07	.07
^{236}U	129	8.20	8.20	25.7	1.63	1.63	.88	.06	.06
^{238}U	$2.69x10^{4}$	8.97	8.97	$2.67x10^{4}$	8.88	8.88	$2.07x10^{4}$	6.87	6.87
^{237}Np	13.5	9.51	9.74	3.55	2.50	2.55	2.92	2.06	2.10
^{239}Np	2.22	$5.17x10^{8}$	489	2.09	$4.88x10^{8}$	$5.78x10^{3}$	5.02	$1.17x10^{9}$	$1.16x10^{3}$
^{236}Pu	$1.85x10^{-5}$	9.86	9.31	$2.24x10^{-5}$	11.9	11.2	$1.84x10^{-5}$	9.81	9.27
^{238}Pu	4.63	$7.83x10^{4}$	$8.06x10^{4}$	10.7	$1.80x10^{5}$	$1.92x10^{5}$	15.6	$2.64x10^{5}$	$2.66x10^{5}$
^{239}Pu	149	$9.14x10^{3}$	$9.28x10^{3}$	158	$9.70x10^{3}$	$9.84x10^{3}$	$1.35x10^{3}$	$8.28x10^{4}$	$8.31x10^{4}$
^{240}Pu	61.4	$1.35x10^{4}$	$1.35x10^{4}$	103	$2.28x10^{4}$	$2.29x10^{4}$	454	$1.00x10^{5}$	$1.00x10^{5}$
^{241}Pu	29.1	$3.31x10^{6}$	$3.29x10^{6}$	69.9	$7.98x10^{6}$	$7.87x10^{6}$	124	$1.42x10^{7}$	$1.40x10^{7}$
^{242}Pu	9.86	38.6	38.6	60.9	238	238	77	299	299
Pu	—	—	$3.39x10^{6}$	—	—	$8.09x10^{6}$	—	—	$1.44x10^{7}$
^{241}Am	.79	$2.58x10^{3}$	$3.80x10^{3}$	3.47	$1.13x10^{4}$	$1.42x10^{4}$	10.8	$3.51x10^{4}$	$4.05x10^{4}$
^{242m}Am	$1.3x10^{-3}$	130	130	.069	668	665	.21	$2.04x10^{3}$	$2.04x10^{3}$
^{242}Am	$2.7x10^{-3}$	$2.17x10^{6}$	130	.011	$9.02x10^{6}$	665	$4.1x10^{-3}$	$3.34x10^{6}$	$2.04x10^{3}$
^{243}Am	2.54	489	489	30.2	$5.78x10^{3}$	$5.78x10^{3}$	6.05	$1.16x10^{3}$	$1.16x10^{3}$
Am	—	—	$4.55x10^{3}$	—	—	$2.13x10^{4}$	—	—	$4.57x10^{4}$
^{242}Cm	.35	$1.16x10^{6}$	$7.94x10^{5}$	2.29	$7.58x10^{6}$	$5.27x10^{6}$	.52	$1.74x10^{6}$	$1.20x10^{6}$
^{243}Cm	$4.0x10^{-3}$	175	174	$4.4x10^{-2}$	$2.05x10^{3}$	$2.04x10^{3}$	.02	911	906
^{244}Cm	.87	$7.06x10^{4}$	$7.00x10^{4}$	19.7	$1.60x10^{6}$	$1.58x10^{6}$	.36	$2.92x10^{4}$	$2.89x10^{4}$
Cm	—	—	$8.64x10^{5}$	—	—	$6.85x10^{6}$	—	—	$1.23x10^{6}$
Subtotal	—	$5.60x10^{8}$	$4.26x10^{6}$	—	$5.19x10^{8}$	$1.50x10^{7}$	—	$1.19x10^{9}$	$1.57x10^{7}$
Total	—	$1.09x10^{9}$	$4.26x10^{6}$	—	$1.11x10^{9}$	$1.50x10^{7}$	—	$2.38x10^{9}$	$1.57x10^{7}$

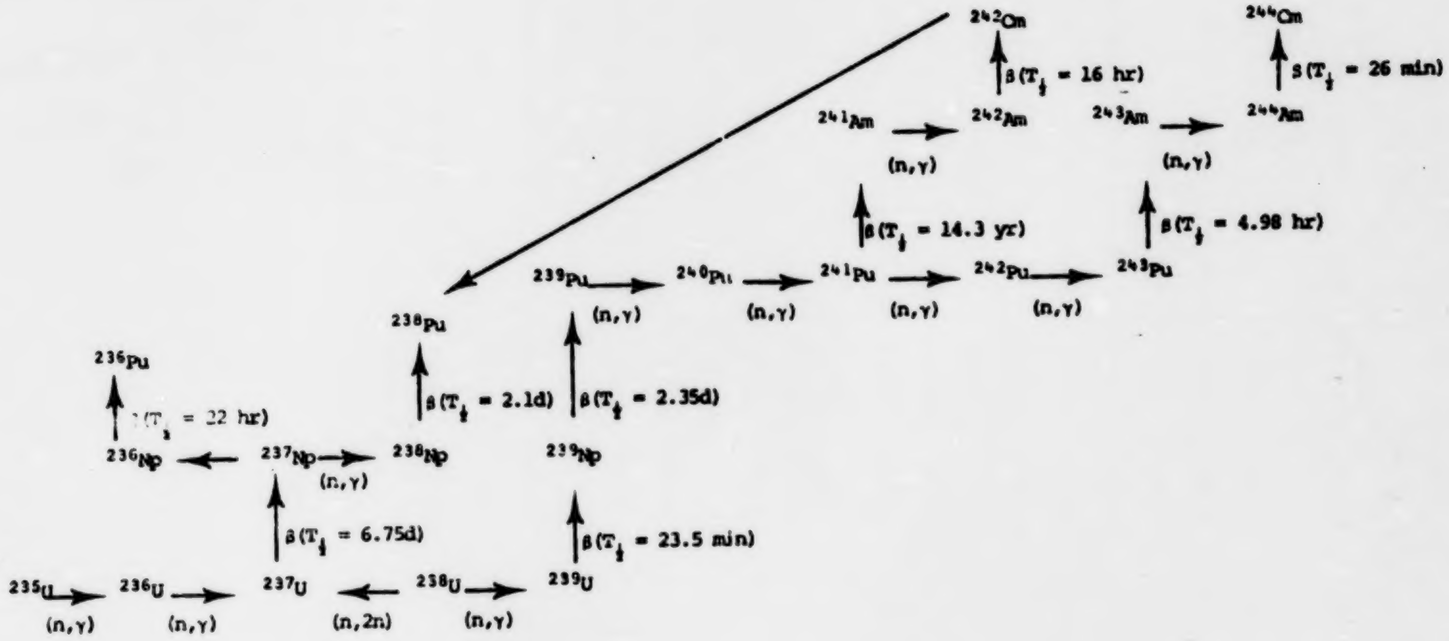
242Cm
244Cm
β(T½ = 16 hr)
S(T½ = 26 min)
241Am
242Am
243Am
244Am
(n,γ)
(n,γ)
β(T½ = 14.3 yr)
β(T½ = 4.98 hr)
239Pu
240Pu
241Pu
242Pu
243Pu
238Pu
(n,γ)
(n,γ)
(n,γ)
(n,γ)
236Pu
β(T½ = 2.1d)
β(T½ = 2.35d)
(T½ = 22 hr)
236Np
237Np
238Np
239Np
(n,γ)
β(T½ = 6.75d)
β(T½ = 23.5 min)
235U
236U
237U
238U
239U
(n,γ)
(n,γ)
(n,2n)
(n,γ)

Figure 3.1 Formation Scheme for Important Actinides

types. Also the activities are shown after a 90 day cooling period.

Note that the LMFBR will indeed have the most heavy metal activity at discharge by about a factor of two over either the uranium-fueled or plutonium-fueled PWR's, with the major activity being that of the beta decay of ^{239}Np to ^{239}Pu in all fuels considered. The situation changes significantly after 90 days of cooling.

The relative amounts of total actinide activities after 90 days of cooling for the LMFBR, plutonium-fueled PWR, and uranium-fueled PWR respectively are : 1, 0.96, and 0.27. The similar ratios for total plutonium activities are 1, 0.56, and 0.24. The percentages of total actinide activity which are due to plutonium alone are respectively 92%, 54%, and 80% for the three types of discharged fuels.

The last comparison above is significant. It means that a reclamation of the plutonium from the uranium-fueled PWR or from LMFBR discharges would result in separation of most of the actinide activity. This is not true with the plutonium-fueled PWR discharges. About seven megacuries of americium and curium isotopes would have to be handled for the plutonium-fueled PWR discharged fuel after 90 days, while the uranium-fueled PWR and the LMFBR would each have about one megacurie of americium and curium isotopes to handle.

The beta emitters among the higher actinides (indicated in Figure 3.1) all have half-lives of the order of days or less except ^{241}Pu. Therefore, the activities shown at 90 days in Table 3.3 are mostly alpha activities. The total plutonium activity in 90 day cooled LMFBR fuel is 1.44×10^7 curies, but 1.40×10^7 curies of this is the beta activity from ^{241}Pu. Thus about 4.5×10^5 curies of plutonium alpha activity are present compared to 1.23×10^6 curies of curium alpha activity.

The alpha activity of ^{241}Am will continue to build as the ^{241}Pu decays. At three years after discharge, there will be about 8.8×10^4 curies of ^{241}Am alpha activity. At 30 years after discharge this activity would be about 3.5×10^5 curies.

The gamma radiation from the various isotopes and their daughters is mostly low energy, with less than 1% of the photons exceeding 400 KeV[7]. There are a few exceptions such as the 2.6 MeV gamma ray from ^{208}Tl, a daughter of ^{236}Pu. This particular exception would probably only be important in uranium-fueled reactors.

The neutron production from spent reactor fuels can be significant as mentioned previously,[7,10] both from spontaneous fission and from (α,n) reactions in light elements. Table 3.4 summarizes neutron production estimates for several nuclides and compounds. The plutonium and americium results are from Reference 7 except where indicated. The curium results are from Reference 10.

Tables 3.3 and 3.4 together show that the neutron production from curium isotopes in discharged fuel will be greater than the neutron

Table 3.4

Neutron and Alpha Particle Yields From Selected Actinides and Their Compounds

n/(g-sec) of Heavy Isotope

Chemical Form	Isotope	Spontaneous Fission	(α,n)	Total	α/(g-sec) of Heavy Isotope
Pu	^{236}Pu	$3.7x10^4$	---	$3.7x10^4$	$1.97x10^{13}$
PuO_2	^{238}Pu	$2.62x10^3$	$1.4x10^4$	$1.66x10^4$	$6.47x10^{11}$
*PuO_2	^{238}Pu	$2.4\ x10^3$	$2x10^4$	$2.2x10^4$	$6.47x10^{11}$
PuO_2	^{239}Pu	.03	45	45	$2.27x10^9$
PuO_2	^{240}Pu	$1.02x10^3$	$1.6x10^4$	$1.7x10^4$	$8.38x10^9$
PuO_2	^{242}Pu	$1.7x10^3$	2.7	$1.7x10^3$	$1.44x10^8$
Pu	^{244}Pu	$5.1x10^3$	---	$5.1x10^3$	$6.54x10^5$
AmO_2	^{241}Am	---	$2.6x10^3$	$2.6x10^3$	$1.20x10^{11}$
*AmO_2	^{241}Am	---	$4x10^3$	$4x10^3$	$1.20x10^{11}$
Cm_2O_3	^{242}Cm	$2.30x10^7$	$2.00x10^7$	$4.3x10^7$	$1.23x10^{14}$
CmO_2	^{242}Cm	$2.30x10^7$	$2.67x10^7$	$4.97x10^7$	$1.23x10^{14}$
Cm_2O_3	^{244}Cm	$1.19x10^7$	$4.29x10^5$	$1.23x10^7$	$3.08x10^{12}$
CmO_2	^{244}Cm	$1.19x10^7$	$5.72x10^5$	$1.25x10^7$	$3.08x10^{12}$

*All neutron yields for plutonium and americium are from Reference 7 except these two, which, along with the curium neutron yields, are from Reference 10.

production from the plutonium despite the two to three orders of mangitude difference in masses of the two elements which are present in the fuel.

Moreover, the alpha activity of the curium isotopes will be greater than that of the plutonium, although the total plutonium activity is higher due to beta decay of ^{241}Pu.

It should be mentioned here that, because of the high toxicity and very long half-lives of the transuranics, and the unique waste disposal problems created by their presence, work is proceeding to develop the capability of recycling the actinides along with the plutonium. This would eliminate the need for handling the transuranics as waste, but would increase the concentration of these undesirable nuclides in the recycled reactor fuel material.

REFERENCES (Section 3)

1. Plutonium Handbook, A Guide to the Technology, ed. by O. J. Wick, Vol. II, Gordon and Breach, New York, 1967.

2. R. Romethsch, "Implementation of International Safeguards - Background and Future," Trans. Am. Nucl. Soc., 15, 989 (1972).

3. M. J. Bell, "Heavy Element Composition of Spent Power Reactor Fuels," ORNL-TM-2897, May 1970.

4. "Aqueous Processing of LMFBR Fuels: Technical Assessment and Experimental Program Definition," ORNL-4436, June 1970.

5. "Conceptual Plant Design, System Descriptions, and Costs for a 1000 MWe Sodium Cooled Fast Reactor," GEAP-5678, Dec. 1968.

6. L. C. Schmid, "A Review of Plutonium Utilization in Thermal Reactors," Nucl. Tech., 18, 78 (May 1973).

7. R. C. Smith, L. G. Gaust, L. W. Brackenbush, "Plutonium Fuel Technology Part II: Radiation Exposure from Plutonium in LWR Fuel Manufacture," Nucl. Tech., 18, 97 (May 1973).

8. "Current Status and Future Technical and Economic Potential of Light Water Reactors," WASH-1082, January 1968, p. 5-9.

9. D. E. Deonigi, "The Value of Plutonium Recycle in Thermal Reactors," Nucl. Tech., 18, 80 (May 1973).

10. H. S. Bailey, R. N. Evatt, G. L. Gyorey, and C. P. Ruiz, "Neutron Shielding Problems in the Shipping of High Burnup Thermal Reactor Fuels," Nucl. Tech., 17, 217 (March 1973).

4. FISSION PRODUCT GENERATION

4.1 LMFBR Fission Product Generation

Fission product production rates were calculated for two representative 1000 MWe LMFBR's. Extensive data was available for the AI Reference Oxide Design,[1] but the target burnup for this design was only 80,000 MWd/MT. Since frequently LMFBR comparisons have been made for a target burnup of 100,000 MWd/MT, similar results are reported for a GE 1000 MWe design[2] that assumes this burnup. Total fission product generation should be about equal for the two designs, except for minor differences such as assumed load factors, different fractions of power and Pu/U fission ratios in the various core and blanket regions, and different residence times for the fuel.

A summary of results is presented in Table 4.1. (Although tritium is a fission product, it is discussed separately in Section 5.1, and is not included in Section 4). Table 4.1 provides total fuel discharged annually from each reactor (in metric tons, MT), total fission product activity discharged with the fuel per year and fission product power in the discharged fuel, for various cooling times after reactor shutdown.

The conditions (exposure, specific power, power distribution, length of time in the core, etc.) for both the AI and the GE designs are given in Table 4.2.

In Reference 1, values are reported for fission product activities for the AI design for all fission products which were not negligible 30 days after reactor shutdown. The Reference 1 calculations for the core were repeated for the most important of these nuclides (i.e. those which still contributed significantly at 150 days after shutdown) using fission yields from Reference 3. An energy yield of 215 MeV/fission* was used, which leads to 2.90×10^{16} fissions/sec MW, instead of the 203 MeV/fission (3.07×10^{16} fission/sec MW) used in Reference 1. For the less important nuclides activity values from Reference 1 for the core were used; also Reference 1 values were used for all activities in the axial and radial blankets. (Those nuclide activities which were calculated are marked with an asterisk in Table 4.3). It was assumed that 87% of the fissions in the core occurred in ^{239}Pu and 13% occurred in ^{238}U. (Activities of several nuclides were checked using the same input as Reference 1 to assure agreement with the methods of Reference 1).

*This value is higher than for LWR's primarily because of a higher value for the kinetic energy of fission products from plutonium fission than from uranium fission and high gamma energies from neutron absorption by steel in LMFBR's.

Table 4.1

Fuel Mass and Fission Product Activity Discharged Annually From an LMFBR and Fission Product Power of Discharged Fuel

I. FUEL MASS DISCHARGED

	AI Design	GE Design
Discharge from Core (MT/yr)	8.517	6.169
Discharge from Axial Blanket (MT/yr)	4.948	6.912
Discharge from Radial Blanket (MT/yr)	10.07	4.869

II. FISSION PRODUCT ACTIVITY DISCHARGED

	Activity Discharged/Yr (Ci/yr)				
	Cooling Time				
AI Design	30d	90d	150d	300d	30y
Core	3.77×10^{8}	2.08×10^{8}	1.40×10^{8}	7.81×10^{7}	2.96×10^{6}
Axial Blanket	0.10×10^{8}	0.05×10^{8}	0.03×10^{8}	0.18×10^{7}	0.06×10^{6}
Radial Blanket	0.44×10^{8}	0.23×10^{8}	0.16×10^{8}	0.60×10^{7}	0.37×10^{6}
Total	4.30×10^{8}	2.36×10^{8}	1.59×10^{8}	8.59×10^{7}	3.38×10^{6}
GE Design					
Core Only	3.08×10^{8}	1.67×10^{8}	1.14×10^{8}	6.10×10^{7}	2.70×10^{6}

III. FISSION PRODUCT POWER

	Fission Product Power of Fuel Discharged/Year (Megawatts)*				
	Cooling Time				
AI Design	30d	90d	150d	300d	30y
Core plus Blankets	1.89	1.02	0.71	0.38	0.010

*Equal to the product of MW/MT and MT discharged/year.

Table 4.2

Operating Conditions for Two 1000 MWe Designs

	AI Reference Oxide Design [7]	GE Follow-on Design [5]
Average core exposure (MWd/MT	80,000	100,000
Core specific power (MW/MT(U+Pu))	175	157
Average irradiation time (equivalent full power days)	458	638
Average chronological (residence) time in core (days)	540	796
Load factor	0.85	0.80
Fraction of power at mid-burnup, equilibrium fuel cycle (%)		
Core	87.8	87.6
Axial Blanket	1.6	7.6
Radial Blanket	10.6	4.8

Table 4.3

Fission Product Activity of Core Discharge Fuel from AI 1000 MWe Reference Oxide Design (80,000 MWd/MT Exposure), as a Function of Cooling Time

	Activity (Ci/MT(U+Pu))					
	Cooling Time					
Fission Product	0	30d	90d	150d	300d	30 yr
*^{85}Kr	1.542×10^{4}	1.535×10^{4}	1.519×10^{4}	1.503×10^{4}	1.464×10^{4}	2.240×10^{3}
^{86}Rb^{a}	7.699×10^{3}	2.522×10^{3}	2.720×10^{2}	29.28		
*^{89}Sr	2.190×10^{6}	1.455×10^{6}	6.420×10^{5}	2.835×10^{5}	3.700×10^{4}	
*^{90}Sr+^{90}Y	1.810×10^{5}	1.813×10^{5}	1.806×10^{5}	1.799×10^{5}	1.781×10^{5}	8.820×10^{4}
*^{91}Y	3.164×10^{6}	2.238×10^{6}	1.103×10^{6}	0.544×10^{6}	0.092×10^{6}	
*^{95}Zr	5.457×10^{6}	3.973×10^{6}	2.106×10^{6}	1.116×10^{6}	0.228×10^{6}	
*^{95m}Nb	7.093×10^{4}	5.466×10^{4}	2.898×10^{4}	1.536×10^{4}	3.142×10^{3}	
*^{95}Nb	5.436×10^{6}	5.065×10^{6}	3.470×10^{6}	2.079×10^{6}	0.475×10^{6}	
^{99}Mo+^{99m}Tc	13.18×10^{6}	8.039×10^{3}	0.00273			
*^{103}Ru+^{103m}Rh	15.05×10^{6}	8.93×10^{6}	3.142×10^{6}	1.105×10^{6}	0.081×10^{6}	
*^{106}Ru+^{106}Rh	6.372×10^{6}	6.022×10^{6}	5.378×10^{6}	4.804×10^{6}	3.622×10^{6}	0.004
^{110m}Ag^{a}	4.303×10^{3}	4.043×10^{3}	3.439×10^{3}	2.909×10^{3}	1.950×10^{3}	
^{110}Ag^{a}	3.051×10^{5}	5.262×10^{2}	4.459×10^{2}	3.788×10^{2}	2.960×10^{2}	
^{111}Ag	4.770×10^{5}	2.985×10^{4}	1.162×10^{2}	0.455		
^{113m}Cd^{a}	3.221×10^{2}	3.212×10^{2}	3.183×10^{2}	3.155×10^{2}	3.095×10^{2}	73.02
^{115m}Cd	9.011×10^{2}	5.271×10^{2}	2.116×10^{2}	80.29	11.12	
^{119m}Sn	47.13	43.45	36.74	31.078	19.90	
^{121m}Sn	1.341×10^{2}	1.341×10^{2}	1.341×10^{2}	1.341×10^{2}	1.340×10^{2}	1.020×10^{2}
^{123m}Sn	1.955×10^{3}	1.653×10^{3}	1.181×10^{3}	8.502×10^{2}	3.600×10^{2}	
^{125}Sn	1.145×10^{5}	1.578×10^{4}	1.889×10^{2}	2.267		
*^{125}Sb	6.525×10^{4}	6.453×10^{4}	6.198×10^{4}	5.945×10^{4}	5.356×10^{4}	32.52
^{125m}Te	1.615×10^{4}	1.691×10^{4}	1.766×10^{4}	1.757×10^{4}	1.590×10^{4}	9.163
^{126}Sb	9.635×10^{4}	1.833×10^{3}	69.71	6.471	5.000	4.119
^{127}Sb	5.199×10^{5}	2.209×10^{3}	0.039			
^{127m}Te+^{127}Te	9.664×10^{5}	2.976×10^{5}	2.012×10^{5}	1.375×10^{5}	5.125×10^{4}	
^{129m}Te	7.727×10^{5}	4.213×10^{5}	1.237×10^{5}	3.646×10^{4}	1.650×10^{3}	
^{129}Te	1.851×10^{6}	2.702×10^{5}	7.944×10^{4}	2.343×10^{4}	1.095×10^{3}	
^{129}I	0.122	0.124	0.125	0.126	0.126	0.126
*^{131}I	4.791×10^{6}	0.374×10^{6}	2155.810	12.43		
^{131m}Xe	4.260×10^{4}	1.426×10^{4}	5.488×10^{2}	16.90		
^{132}Te+^{132}I	11.468×10^{6}	1.936×10^{4}	0.055			

Table 4.3

(continued-page 2)

Fission Product Activity of Core Discharge Fuel from AI 1000 MWe Reference Oxide Design (80,000 MWd/MT Exposure), as a Function of Cooling Time
Activity (Ci/MT(U+Pu))

	Cooling Time					
Fission Product	0	30d	90d	150d	300d	30 yr
*^{133}Xe	7.867×10^{6}	0.186×10^{6}	69.68	0.026		
^{134}Cs^{a}	7.425×10^{4}	7.226×10^{4}	6.839×10^{4}	6.461×10^{4}	5.400×10^{4}	2.985
^{136}Cs	3.448×10^{5}	6.971×10^{4}	2.843×10^{3}	1.162×10^{2}	0.045	
*^{137}Cs+^{137m}Ba	4.903×10^{5}	4.894×10^{5}	4.875×10^{5}	4.857×10^{5}	4.811×10^{5}	2.463×10^{5}
^{140}Ba+^{140}La	12.242×10^{6}	2.541×10^{6}	9.871×10^{4}	3.835×10^{3}	1.050	
*^{141}Ce	6.978×10^{6}	3.701×10^{6}	1.031×10^{6}	0.287×10^{6}	0.012×10^{6}	
^{143}Pr	6.027×10^{6}	1.748×10^{6}	8.407×10^{4}	4.034×10^{3}	5.100	
*^{144}Ce+^{144}Pr	6.337×10^{6}	5.886×10^{6}	5.186×10^{6}	4.394×10^{6}	3.048×10^{6}	
^{147}Nd	2.673×10^{6}	4.100×10^{5}	9.730×10^{3}	2.286×10^{2}	0.015	
*^{147}Pm	7.673×10^{5}	7.743×10^{5}	7.454×10^{5}	7.138×10^{5}	6.404×10^{5}	2.874×10^{2}
^{148m}Pm^{a}	1.672×10^{5}	1.020×10^{5}	3.779×10^{4}	1.407×10^{4}	2.000×10^{3}	
*^{151}Sm	1.058×10^{4}	1.061×10^{4}	1.059×10^{4}	1.058×10^{4}	1.055×10^{4}	0.849×10^{4}
^{154}Eu^{a}	2.390×10^{3}	2.380×10^{3}	2.362×10^{3}	2.352×10^{3}	2.300×10^{3}	6.518×10^{2}
*^{155}Eu	5.221×10^{4}	5.162×10^{4}	5.046×10^{4}	4.932×10^{4}	4.659×10^{4}	8.165×10^{2}
^{156}Eu	2.872×10^{5}	7.330×10^{4}	4.581×10^{3}	2.862×10^{2}	0.350	
^{160}Tb^{a}	3.221×10^{4}	2.418×10^{4}	1.360×10^{4}	7.623×10^{3}	2.000×10^{3}	
^{161}Tb	4.478×10^{4}	2.201×10^{3}	5.299	0.013		
^{162}Gd+^{162m}Tb	2.286×10^{4}	2.154×10^{4}	1.927×10^{4}	1.714×10^{4}	1.200×10^{4}	
Total Activity	(11.70×10^{7})	4.421×10^{7}	2.441×10^{7}	1.647×10^{7}	9.169×10^{6}	3.472×10^{5}

* These nuclide activities were calculated during the present investigation. Others were obtained from Reference 1.

a. Activation products, produced by neutron activation of a fission product.

The yields and half lives of the fission products (from Reference 3) are given in Appendix B. Also the decay schemes of the nuclides whose activities were calculated are illustrated in Appendix B.

Results for the activities of the important radionuclides are listed in Tables 4.3, 4.4, and 4.5 for the core, axial blanket, and radial blanket of the AI 1000 MWe Reference Oxide Design. Results are listed as curies per metric ton of metal (U + Pu). Also listed and noted in the tables are a number of activation products which result from neutron activation of fission products. Core activities for the GE 1000 MWe Follow-On Design are listed in Table 4.6. Totals in Table 4.6 for those nuclides not specifically calculated are based on results from Reference 1. In Tables 4.3 - 4.6 the totals at zero cooling time are only the totals for those nuclides shown (hence, they are shown in parentheses). By 30 days these are the only nuclides which are not negligible so that the totals from 30 days on are correct.

In Table 4.7 are listed the gamma and beta energy production rates as a function of cooling time, also listed per MT of metal (U + Pu).

Noble gases and iodine have special significance since they can be released to the cover gas. These fission product sources are listed separately in Table 4.8. Saturated activities in a 1000 MWe reactor are listed, except for ^{85}Kr and ^{129}I. The ^{85}Kr and ^{129}I are the amounts at shutdown for the GE 1000 MWe design, with average core discharge exposure of 100,000 MWd/MT. The longest half-lives of the noble gases or iodine other than ^{85}Kr and ^{129}I are the 11.96 day ^{131m}Xe and 9.065 day ^{131}I. As can be seen from Table 4.3, the only nuclide in Table 4.8 still important after one year is ^{85}Kr; hence, all but ^{85}Kr are short-term hazards only.

Table 4.4

Fission Product Activity of Axial Blanket Discharge from AI 1000 MWe
Reference Oxide Design, as a Function of Cooling Time

	Activity [Ci/MT(U+Pu)]					
	Cooling Time					
Fission Product	0	30d	90d	150d	300d	30 yr
^{85}Kr	$7.878x10^2$	$7.840x10^2$	$7.755x10^2$	$7.670x10^2$	$7.260x10^2$	$1.143x10^2$
^{86}Rb^a	72.64	23.80	2.569	0.277		
^{89}Sr	$1.294x10^5$	$8.70x10^4$	$3.911x10^4$	$1.757x10^4$	$2.500x10^3$	
^{90}Sr+^{90}Y	$7.944x10^3$	$7.897x10^3$	$7.859x10^3$	$7.840x10^3$	$7.600x10^3$	$3.779x10^3$
^{91}Y	$1.766x10^5$	$1.247x10^5$	$6.140x10^4$	$3.023x10^4$	$5.325x10^3$	
^{95}Zr	$2.834x10^5$	$2.059x10^5$	$1.086x10^5$	$5.724x10^4$	$1.175x10^4$	
^{95m}Nb	$5.668x10^3$	$4.364x10^3$	$2.305x10^3$	$1.219x10^3$	$2.800x10^2$	
^{95}Nb	$2.626x10^5$	$2.522x10^5$	$1.757x10^5$	$1.058x10^5$	$2.600x10^4$	
^{99}Mo+^{99m}Tc	$6.480x10^5$	$3.949x10^2$	$1.338x10^{-4}$			
^{103}Ru+^{103m}Rh	$6.612x10^5$	$3.911x10^5$	$1.371x10^5$	$4.799x10^4$	$4.500x10^2$	
^{106}Ru+^{106}Rh	$1.608x10^5$	$1.519x10^5$	$1.356x10^5$	$1.211x10^5$	$8.780x10^4$	
^{110m}Ag^a	8.162	7.519	6.376	5.413	3.500	
^{110}Ag^a	$7.378x10^2$	0.973	0.829	0.704	0.450	
^{111}Ag	$1.162x10^4$	$7.283x10^2$	2.843	0.011		
^{113m}Cd^a	0.580	0.578	0.573	0.568	0.550	0.131
^{115m}Cd	95.40	58.66	22.29	8.473	0.815	
^{119m}Sn	3.306	3.042	2.569	2.182	1.475	
^{121m}Sn	1.001	1.001	1.001	1.001	1.000	0.763
^{123m}Sn	38.730	32.779	23.521	16.814	7.900	
^{125}Sn	$4.090x10^3$	$4.478x10^2$	5.365	0.064		
^{125}Sb	$9.730x10^2$	$9.824x10^2$	$9.446x10^2$	$9.097x10^2$	$7.85x10^2$	0.456
^{125m}Te	$2.947x10^2$	$3.221x10^2$	$3.495x10^2$	$3.561x10^2$	$3.500x10^2$	0.189
^{126}Sb	$1.455x10^3$	$2.758x10^2$	9.919	0.398	0.042	0.042
^{127}Sb	$1.918x10^4$	91.82	0.002			
^{127m}Te+^{127}Te	$2.097x10^4$	$4.865x10^3$	$3.533x10^3$	$2.409x10^3$	$8.900x10^2$	
^{129m}Te	$2.872x10^4$	$1.568x10^4$	$4.610x10^3$	$1.360x10^3$	66.00	
^{129}Te	$7.236x10^4$	$1.001x10^4$	$2.957x10^3$	$8.691x10^2$	40.00	
^{129}I	0.003	0.003	0.003	0.003	0.003	0.003
^{131}I	$1.861x10^5$	$1.445x10^4$	82.466	0.470		
^{131m}Xe	$1.644x10^3$	$5.970x10^2$	23.521	0.721		

Table 4.4

(continued–page 2)

Fission Product Activity of Axial Blanket Discharge from AI 1000 MWe Reference Oxide Design, ad a Function of Cooling Time

Activity [Ci/MT(U+Pu)]

	Cooling Time					
Fission Product	0	30d	90d	150d	300d	30 yr
^{132}Te+^{132}I	5.318×10^{4}	8.908×10^{2}	0.003			
^{133}Xe	3.278×10^{5}	7.651×10^{2}	2.862	0.001		
^{134}Cs^{a}	3.750×10^{2}	3.646×10^{2}	3.457×10^{2}	3.268×10^{2}	2.800×10^{2}	0.015
^{136}Cs	6.981×10^{3}	1.407×10^{3}	57.528	2.343		
^{137}Cs+^{137m}Ba	1.495×10^{4}	1.492×10^{4}	1.486×10^{4}	1.481×10^{4}	1.425×10^{4}	7.472×10^{3}
^{140}Ba+^{140}La	6.083×10^{5}	1.282×10^{5}	4.978×10^{3}	1.927×10^{2}	0.070	
^{141}Ce	3.070×10^{5}	1.625×10^{5}	4.496×10^{4}	1.247×10^{4}	4.500×10^{2}	
^{143}Pr	2.806×10^{5}	6.949×10^{4}	3.287×10^{3}	1.578×10^{2}	0.110	
^{144}Ce+^{144}Pr	2.598×10^{5}	2.399×10^{5}	2.059×10^{5}	1.785×10^{5}	1.780×10^{5}	
^{147}Nd	1.672×10^{5}	2.569×10^{4}	6.064×10^{2}	14.264		
^{147}Pm	3.731×10^{4}	3.807×10^{4}	3.675×10^{4}	3.523×10^{4}	3.100×10^{4}	13.98
^{148m}Pm^{a}	1.861×10^{3}	1.134×10^{3}	4.204×10^{2}	1.559×10^{2}	12.55	
^{151}Sm	4.704×10^{2}	4.723×10^{2}	4.723×10^{2}	4.714×10^{2}	4.680×10^{2}	3.722×10^{2}
^{154}Eu^{a}	19.27	19.17	19.08	18.89	18.50	5.252
^{155}Eu	3.324×10^{3}	3.221×10^{3}	3.023×10^{3}	2.834×10^{3}	2.350×10^{3}	0.034
^{156}Eu	6.660×10^{3}	1.710×10^{3}	1.067×10^{2}	6.679	0.004	
^{160}Tb^{a}	56.58	42.41	23.80	13.41	0.280	
^{161}Tb	7.916×10^{2}	38.919	0.094	2.258×10^{-4}		
^{162}Gd+^{162m}Tb	2.418×10^{2}	2.286×10^{2}	2.040×10^{2}	1.816×10^{2}	1.330×10^{2}	
Total Activity	(4.714×10^{6})	1.963×10^{6}	9.973×10^{5}	6.411×10^{5}	3.715×10^{5}	1.176×10^{4}

Fission Product Activity of Radial Blanket Discharge from AI 1000 MWe Reference
Oxide Design, as a Function of Cooling Time

Activity (Ci/MT(U+Pu)

	Cooling Time					
Fission Product	0	30d	90d	150d	300d	30yr
^{85}Kr	2.428×10^{3}	2.409×10^{3}	2.390×10^{3}	2.362×10^{3}	2.300×10^{3}	3.505×10^{2}
^{86}Rb[a]	3.363×10^{2}	1.105×10^{2}	11.90	1.285		
^{89}Sr	2.465×10^{5}	1.653×10^{5}	7.415×10^{4}	3.335×10^{4}	4.285×10^{3}	
^{90}Sr+^{90}Y	2.371×10^{4}	2.362×10^{4}	2.343×10^{4}	2.343×10^{4}	2.290×10^{4}	1.126×10^{4}
^{91}Y	3.372×10^{5}	2.371×10^{5}	1.171×10^{5}	5.772×10^{4}	9.150×10^{3}	
^{95}Zr	6.102×10^{5}	4.430×10^{5}	2.333×10^{5}	1.237×10^{5}	2.500×10^{4}	
^{95m}Nb	1.219×10^{4}	9.403×10^{3}	4.959×10^{3}	2.617×10^{3}	5.100×10^{2}	
^{95}Nb	5.819×10^{5}	5.526×10^{5}	3.826×10^{5}	2.295×10^{5}	5.500×10^{4}	
^{99}Mo+^{99m}Tc	1.330×10^{6}	8.105×10^{2}	2.749×10^{-4}			
^{103}Ru+^{103}Rh	1.351×10^{6}	8.001×10^{5}	2.796×10^{5}	5.063×10^{4}	9.500×10^{2}	
^{106}Ru+^{106}Rh	4.742×10^{5}	4.411×10^{5}	4.005×10^{5}	3.571×10^{5}	2.675×10^{4}	
^{110m}Ag[a]	77.36	71.22	60.45	51.29	34.00	
^{110}Ag	5.120×10^{3}	9.257	7.859	6.669	4.300	
^{111}Ag	3.316×10^{4}	2.078×10^{3}	8.105	0.032		
^{113m}Cd[a]	6.017	5.989	5.942	5.894	5.795	1.360
^{115m}Cd	1.568×10^{2}	96.35	36.74	13.98	1.150	
^{119m}Sn	8.643	7.954	6.735	5.6[illegible]6	3.750	
^{121m}Sn	5.885	5.876	5.866	5.857	5.800	4.478
^{123m}Sn	1.190×10^{2}	1.001×10^{2}	71.98	51.14	21.90	
^{125}Sn	1.077×10^{4}	1.171×10^{3}	14.07	0.169		
^{125}Sb	3.344×10^{3}	3.363×10^{3}	3.231×10^{3}	3.098×10^{3}	2.800×10^{3}	1.549
^{125m}Te	1.115×10^{3}	1.171×10^{3}	1.228×10^{3}	1.237×10^{3}	1.200×10^{3}	0.643
^{126}Sb	2.125×10^{3}	4.034×10^{2}	14.73	0.727	0.300	0.208
^{127}Sb	5.507×10^{4}	2.626×10^{2}	0.006			
^{127m}Te+^{127}Te	6.253×10^{4}	1.719×10^{4}	1.159×10^{4}	7.907×10^{3}	2.500×10^{3}	
^{129m}Te	6.546×10^{4}	3.571×10^{4}	1.049×10^{4}	3.089×10^{3}	1.45×10^{2}	
^{129}Te	1.625×10^{5}	2.286×10^{4}	6.735×10^{3}	1.984×10^{3}	1.300×10^{2}	
^{129}I	0.010	0.011	0.011	0.011	0.011	0.011
^{131}I	3.939×10^{5}	3.061×10^{4}	1.748×10^{2}	0.992		

Table 4.5
(continued-page 2)

Fission Product Activity of Radial Blanket Discharge from AI 1000 MWe Reference Oxide Design as a Function of Cooling Time

Activity (Ci/MT(U+Pu))

	Cooling Time					
Fission Product	0	30d	90d	150d	300d	30yr
^{131m}Xe	3.760×10^3	1.313×10^3	51.20	1.578		
^{132}Te+^{132}I	1.118×10^6	1.880×10^3	0.005			
^{133}Xe	7.047×10^5	1.625×10^4	6.083	0.002		
^{134}Cs^a	2.645×10^3	2.579×10^3	2.437×10^3	2.305×10^3	2.000×10^3	0.107
^{136}Cs	1.880×10^4	3.797×10^3	1.549×10^2	6.320		
^{137}Cs+^{137m}Ba	4.770×10^4	4.770×10^4	4.751×10^4	4.734×10^4	4.700×10^4	2.370×10^4
^{140}Ba+^{140}La	1.254×10^6	2.626×10^5	1.020×10^4	3.958×10^2	0.180	
^{141}Ce	6.310×10^5	3.335×10^5	9.248×10^4	2.560×10^4	1.000×10^3	
^{143}Pr	5.913×10^5	1.445×10^5	6.924×10^3	3.325×10^2	0.140	
^{144}Ce+^{144}Pr	6.320×10^5	5.800×10^5	5.007×10^5	4.326×10^5	3.975×10^5	
^{147}Nd	3.164×10^5	4.865×10^4	1.152×10^2	27.11	0.900	
^{147}Pm	1.020×10^5	1.030×10^5	9.919×10^4	9.541×10^4	8.200×10^4	37.88
^{148m}Pm^a	7.784×10^3	4.742×10^3	1.757×10^3	6.546×10^2	49.00	
^{151}Sm	1.370×10^3	1.379×10^3	1.370×10^3	1.370×10^3	1.360×10^3	1.086×10^3
^{154}Eu^a	1.275×10^2	1.275×10^2	1.266×10^2	1.256×10^2	1.220×10^2	34.85
^{155}Eu	1.219×10^4	1.181×10^4	1.115×10^4	1.049×10^4	8.900×10^3	0.125
^{156}Eu	1.833×10^4	4.695×10^3	2.938×10^2	18.326	0.022	
^{160}Tb^a	5.129×10^2	3.845×10^2	2.163×10^2	1.209×10^2	27.50	
^{161}Tb	2.513×10^2	1.237×10^2	0.299	0.001		
^{162}Gd+^{162m}Tb	1.096×10^3	1.035×10^3	9.238×10^2	8.237×10^2	6.100×10^2	
Total Activity	(11.23×10^7)	4.361×10^6	2.327×10^6	1.515×10^5	5.943×10^5	3.648×10^4

Table 4.6

Fission Product Activity of Core Discharge Fuel from GE 1000 MWe Follow-on Design (100,000 MWd/MT Exposure), as a Function of Cooling Time

Activity(Ci/MT(U+Pu))

	Cooling Time					
Fission Product	0	30d	90d	150d	300d	30yr
^{85}Kr	1.915×10^4	1.906×10^4	1.886×10^4	1.866×10^4	1.817×10^4	0.277×10^4
^{89}Sr	2.322×10^6	1.542×10^6	0.680×10^6	0.300×10^6	0.039×10^6	
^{90}Sr+^{90}Y	2.260×10^5	2.263×10^5	2.254×10^5	2.245×10^5	2.223×10^5	1.104×10^5
^{91}Y	3.357×10^6	2.374×10^6	1.171×10^6	0.577×10^6	0.099×10^6	
^{95}Zr	5.795×10^6	4.219×10^6	2.236×10^6	1.185×10^6	0.242×10^6	
^{95m}Nb	7.533×10^4	5.805×10^4	3.078×10^4	1.631×10^4	0.334×10^4	
^{95}Nb	5.787×10^6	5.387×10	3.687×10^6	2.209×10^6	0.505×10^6	
^{103}Ru+^{103m}Rh	15.95×10^6	9.199×10^6	3.330×10^6	1.072×10^6	0.086×10^6	0.008
^{106}Ru+^{106}Rh	7.396×10^6	6.990×10^6	6.244×10^6	5.576×10^6	4.204×10^6	39.44
^{125}Sb	7.925×10^4	7.829×10^4	7.517×10^4	7.210×10^4	6.496×10^4	
^{127}Sb	5.510×10^5	2.341×10^3	0.041			
^{131}I	5.077×10	0.396×10^6	2284.590	13.17		
^{133}Xe	8.336×10^6	0.197×10^6	73.84	0.028		
^{137}Cs+^{137m}Ba	6.120×10^5	6.109×10^5	6.086×10^5	6.063×10^5	6.006×10^5	3.075×10^5
^{141}Cr	7.395×10^6	3.922×10^6	1.093×10^6	0.304×10^6	1.246×10^4	
^{144}Ce+^{144}Pr	7.238×10^6	6.723×10^6	5.809×10^6	5.019×10^6	3.482×10^6	3.482×10^2
^{147}Pm	9.339×10^5	9.387×10^5	9.031×10^5	8.648×10^5	7.758×10^5	1.062×10^4
^{151}Sm	1.324×10^4	1.327×10^4	1.325×10^4	1.323×10^4	1.319×10^4	0.100×10^4
^{155}Eu	6.421×10^4	6.348×10^4	6.205×10^4	6.066×10^4	5.730×10^4	
Total for calculated nuclides		4.296×10^7	2.619×10^7	1.812×10^7	0.973×10^7	4.37×10^5
Total for uncalculated nuclides		0.697×10^7	$.085\times10^7$	0.037×10^7	0.016×10^7	.01
Total		4.99×10^7	2.70×10^7	1.85×10^7	0.99×10^7	4.4×10^5

Table 4.7

Energy Generation Rate from Fission Product Decay for the AI 1000 MWe Reference Oxide Design as a Function of Cooling Time

Specific Power[Watts/MT (U+Pu)]

	Cooling Time				
	30d	90d	150d	300d	30yr
Core					
Gamma Decay	9.56×10^4	4.39×10^4	2.57×10^4	1.12×10^4	$.49\times10^3$
Beta Decay	10.00×10^4	6.21×10^4	4.87×10^4	2.81×10^4	$.59\times10^3$
Axial Blanket					
Gamma Decay	4.07×10^3	1.77×10^3	1.00×10^3	$.43\times10^3$	15.
Beta Decay	4.07×10^3	2.29×10^3	1.69×10^3	$.91\times10^3$	21.
Radial Blanket					
Gamma Decay	8.83×10^3	3.94×10^3	2.27×10^3	0.98×10^3	48.
Beta Decay	9.37×10^3	5.60×10^3	4.29×10^3	2.45×10^3	66.

Table 4.8

Total Activity of Noble Gas and Iodine Nuclides During Operation of a 1000 MWe LMFBR

Radio-nuclide	Saturated Activity, Ci	Half-life	Accumulated Yields (Fast Fission) ^{239}Pu	^{238}U
			(%)	(%)
^{83m}Kr	7.016x10^{6}	1.86h	0.350	0.412
^{85m}Kr	1.301x10^{7}	4.4h	0.642	0.811
^{85}Kr	2.4x10^{5}*	10.76y	0.142	0.173
^{87}Kr	2.250x10^{7}	76m	1.108	1.416
^{88}Kr	2.759x10^{7}	2.79h	1.368	1.677
^{89}Kr	3.585x10^{7}	3.18m	1.653	3.010
^{131m}Xe	4.822x10^{5}	11.96d	0.025	0.022
^{133m}Xe	3.785x10^{6}	2.26d	0.195	0.181
^{133}Xe	1.328x10^{8}	5.27d	6.824	6.471
^{135m}Xe	3.459x10^{7}	15.7m	1.902	0.852
^{135}Xe	1.416x10^{8}	9.16h	7.447	5.748
^{137}Xe	1.138x10^{8}	3.82m	5.785	5.951
^{138}Xe	7.828x10^{7}	14.2m	3.709	5.908
^{129}I	1.7*	1.6x10^{7}y	0.922	0.653
^{131}I	8.086x10^{7}	8.065d	4.196	3.662
^{132}I	1.050x10^{8}	2.284h	5.366	5.300
^{133}I	1.327x10^{8}	20.8h	6.817	6.471
^{134}I	1.392x10^{8}	52.3m	7.186	6.553
^{135}I	1.217x10^{8}	6.7h	6.290	5.673

*Approximate values in the reactor (1000 MWe GE design) at shutdown for refueling.

4.2 Comparison with LWR Fission Product Generation

The fission products generated by a reference LWR have been estimated by ORNL staff in their study of siting for fuel reprocessing plants and waste management facilities.[4] The reference LWR is a pressurized water type fueled with Zircaloy-clad UO_2 (3.3% ^{235}U), operating at an average power level of 30 MW/MTU and achieving a fuel exposure of 33,000 MWd/MTU. The Diablo Canyon Nuclear Power Plant Reactor served as a prototype for the reference design.

Values for LWR fission product inventories after cooling times of 90 and 150 days, as taken from Table 3.9 of the ORNL study,[4] are presented in Table 4.9. Comparison of these values with the corresponding values for an LMFBR core discharge (see Tables 4.3 and 4.6) reveals that the fission product inventories per metric ton (U + Pu) are much lower for the LWR than for the LMFBR, as expected from the large difference in MWd exposure per MT.

The total fuel charge in the PWR is 88.6 MTU, of which one third (or 29.5 MTU) is discharged each year. The total fission product activity associated with the fuel shipped annually is given in Table 4.10 as a function of cooling time. On comparing these values with the corresponding AI LMFBR values of Table 4.1 (i.e. 2.36×10^8 Ci/yr shipped after a 90-day cooling period and 1.59×10^8 Ci/yr after a 150-day cooling period), it is evident that the 1000 MWe LMFBR will ship annually a greater quantity of activity from the plant site than will the 1000 MWe PWR, assuming equal cooling times. This result does not change by including also the actinide activity (see Table 3.3) and the cladding activity (Table 5.13). (A comparison between the GE design and the PWR cannot be made without a calculation of the blanket discharge activities.)

The higher overall fission product activity in the discharged LMFBR fuel results primarily from the shorter residence time of LMFBR fuel in the reactor, i.e., 540 days for the AI LMFBR design vs. 3 years for the PWR. Considering freshly discharged LWR and LMFBR fuels, the average time elapsed since a particular fuel atom fissioned is roughly 550 days for the LWR compared to only 270 days for the LMFBR. The longer average decay time prior to reactor shut-down for the PWR far outweighs the effects of differences between the two reactor types in fuel exposure, thermal efficiency, energy release per fission, and isotopic fission product yields. It is of interest, however, to compare the isotopic yields of several important fission products. Table 4.11 gives yields of specific nuclides from thermal fission of ^{235}U and ^{239}Pu and from fast fission of ^{238}U and ^{239}Pu. These are cumulative yields. The table indicates significantly lower production rates for ^{90}Sr and ^{85}Kr and a higher production rate for ^{131}I in the LMFBR.

Table 4.9

LWR Fission Product Activities as a Function of Cooling Time

Nuclide	Curies/Metric Ton Discharged Fuel 90 days	 150 days
^{3}H	6.98E 02	6.92E 02
^{85}Kr	1.13E 04	1.12E 04
^{86}Rb	1.72E 01	1.85E 00
^{89}Sr	2.16E 05	9.60E 04
^{90}Sr	7.69E 04	7.66E 04
^{90}Y	7.69E 04	7.66E 04
^{91}Y	3.22E 05	1.59E 05
^{93}Zr	1.88E 00	1.88E 00
^{95}Zr	5.24E 05	2.76E 05
^{95m}Nb	1.11E 04	5.86E 03
^{95}Nb	8.69E 05	5.18E 05
^{99}Tc	1.42E 01	1.42E 01
^{103}Ru	2.55E 05	8.91E 04
^{103m}Rh	2.55E 05	8.91E 04
^{106}Ru	4.59E 05	4.10E 05
^{110m}Ag	3.08E 02	2.61E 02
^{110}Ag	4.01E 01	3.40E 01
^{115}Cd	1.17E 02	4.43E 01
^{119}Sn	1.29E 01	1.09E 01
^{123m}Sn	5.11E 02	3.66E 02
^{124}Sb	1.73E 02	8.63E 01
^{125}Sn	1.67E 01	2.00E 01

Table 4.9
(Continued - 2)

LWR Fission Product Activities as a Function of Cooling Time

	Curies/Metric Ton Discharged Fuel	
Nuclide	90 days	150 days
^{125}Sb	8.48E 03	8.13E 03
^{125m}Te	3.32E 03	3.28E 03
^{127m}Te	9.04E 03	6.18E 03
^{127}Te	8.94E 03	6.11E 03
^{129m}Te	2.27E 04	6.69E 03
^{129}Te	1.46E 04	4.29E 03
^{131}I	3.81E 02	2.17E 00
^{131m}Xe	1.06E 02	3.27E 00
^{134}Cs	2.25E 05	2.13E 05
^{136}Cs	5.10E 02	2.08E 01
^{137}Cs	1.07E 05	1.06E 05
^{137m}Ba	9.99E 04	9.96E 04
^{140}Ba	1.11E 04	4.30E 02
^{140}La	1.28E 04	4.95E 02
^{141}Ce	2.05E 05	5.67E 04
^{143}Pr	1.44E 04	6.94E 02
^{144}Ce	8.92E 05	7.70E 05
^{144}Pr	8.92E 05	7.70E 05
^{147}Nd	2.16E 03	5.10E 01
^{147}Pm	1.04E 05	9.94E 04
^{148m}Pm	1.06E 03	3.92E 02
^{148}Pm	8.82E 01	3.15E 01

Table 4.9

(Continued - 3)

LWR Fission Product Activities as a Function of Cooling Time

	Curies/Metric Ton Discharged Fuel	
Nuclide	90 days	150 days
^{151}Sm	1.15E 03	1.15E 03
^{152}Eu	1.16E 01	1.15E 01
^{153}Gd	2.66E 01	2.24E 01
^{154}Eu	6.87E 03	6.82E 03
^{155}Eu	6.79E 03	6.37E 03
^{156}Eu	3.51E 03	2.19E 02
^{160}Tb	5.34E 02	3.00E 02
^{62}Gd	1.86E 02	1.66E 02
^{62}Tb	1.86E 02	1.66E 02
Total	6.19E 06	4.39E 06

Table 4.10

Fission Product Activity Transported Annually From a 1000 MWe PWR

Cooling Time, days	Activity Transported, Ci/yr
90	1.83×10^8
150	1.30×10^8

Table 4.11

Yields of Selected Fission Products from Thermal and Fast Fission

Nuclide	Thermal Fission Yields (%) from		Fast Fission Yields (%) from	
	^{235}U	^{239}Pu	^{239}Pu	^{238}U
^{85m}Kr	1.332	.598	.642	.811
^{85}Kr	.285	.144	.142	.173
^{131}I	2.774	3.889	4.196	3.662
^{90}Sr	5.935	2.121	2.089	3.282
^{137}Cs	6.228	6.534	6.625	5.952
^{133}Xe	6.766	6.838	6.824	6.471

REFERENCES (Section 4)

1. Staff, Chemical Technology Division, ORNL, "Aqueous Processing of LMFBR Fuels: Technical Assessment and Experimental Program Definition," ORNL-4436 (June 1970).

2. "Task II Report, Conceptual Plant Design, System Descriptions, and Costs for a 1000 MWe Sodium-Cooled Fast Reactor, GEAP-5678 (December 1968).

3. M. E. Meek and B. F. Rider, "Compilation of Fission Product Yields, Vallecitos Nuclear Center - 1972, "NEDO-12154 (January 1972).

4. ORNL-4451 "Siting of Fuel Reprocessing Plants and Waste Management Facilities," July 1971, Staff of ORNL.

5. OTHER SOURCES*

5.1 Tritium and Its Transport

Tritium produced in an LMFBR comes from two principal sources - ternary fissions in the fuel and n,t reactions in boron control rods. Lithium contamination in the fuel might lead to another important source, and Lithium contamination in the sodium is a minor source.

An estimate of tritium production rates in thermal reactors was given by Peterson, Martin, Weaver, and Harward, [1,2] who also presented results for tritium production rates from fast fission in a Pu-fueled fast reactor. More recently Sehgal and Rempert reported calculated tritium production rates for EBR-II and FFTF.[3] Kabele reported tritium calculations for FFTF,[4] but the references other than the ANS summary were preliminary and not available to the public at the time of this investigation.[5] Limited information on the details of Reference 4 were obtained from Westinghouse personnel.[6] Data on tritium production and transport throughout the EBR-II reactor system have been reported.[7,8] Data on tritium transport through fuel cladding in fast reactors have been reported;[8,9] data on tritium transport through control rod cladding have been obtained[10] but have not been publicly reported.

5.1.1 Summary

A summary of estimated annual tritium production rates in a 1000 MWe LMFBR is given in Table 5.1. Results could easily be off by a factor of two.

Most of the tritium may enter the primary system. It is known that nearly all of the tritium produced in ternary fission enters the primary sodium. Some unpublished experimental results indicate that only a fraction (i.e. ~ 30%) of the tritium in the control rods enters the sodium. Until firm data is presented to show this, however, it should be assumed that all the tritium enters the sodium.

EBR-II experience indicates that ~ 0.2% of the tritium that enters the sodium escapes to the atmospher and ~ 0.01% escapes to the condenser water (EBR-II has a complete steam cycle). It is unclear to what extent these percentages will apply to an LMFBR power reactor, but they represent the best indication currently available.

---

*References are indicated at the end of each subsection of Section 5, unlike the procedure used in other sections.

Table 5.1

Estimated Tritium Production Rates in a 1000 MWe LMFBR

Source	Annual Activity Production Rate
Ternary Fission	20,000 Ci/yr
B_4C control rods (shim and safety), $^{10}B(n,t)2\alpha$	7,000
Lithium produced in control rods $^{7}Li(n,nt)\alpha$	2,500
Lithium contamination in fuel (20 ppm Li in fuel) $^{6}Li(n,t)\alpha$	4,000
Lithium contamination in sodium (5ppm Li in Na) $^{6}Li(n,t)\alpha$	100
TOTAL	∿ 30,000 Ci/yr

Extrapolation of the above EBR-II leak rates to the LMFBR would indicate leakage rates for a 1000 MWe LMFBR of the order of 60 Ci/yr to the atmosphere and 3 Ci/yr to the condenser water. This value for leakage to the condenser water compares to liquid effluent tritium rates of 100 Ci/yr for a BWR and 600 Ci/yr for a PWR reported in the AEC draft statement on the proposed Appendix I to 10 CFR 50.[24]

5.1.2 Sources

5.1.2.1 Ternary Fission

Tritium production rate from ternary fission in a 1000 MWe LMFBR (2500 MWt) is estimated to be 20,000 curies/year. This value could be as much as a factor of two lower than the true value, however, since the tritium production rate from fast fission of ^{239}Pu is so poorly known. AEC funding to establish this value more precisely has been terminated.

The production rate of 20,000 Ci/yr is based on the following parameters: Tritium yield from ^{239}Pu fast fission ∿ 2 x 10^{-4} t/f (Reference 11). Tritium yield from ^{238}U fission is assumed to be the same as from ^{239}Pu fast fission. N = number of tritons produced/year, and is roughly equal to:

$$\left(2 \times 10^{-4} \frac{\text{tritons}}{\text{fission}}\right) \left(2.9 \times 10^{16} \frac{\text{fissions}}{\text{MW-sec}}\right) (2500 \text{ MW}) \left(.864\text{x}10^{5} \frac{\text{sec}}{\text{day}}\right)$$

$$\left(.8 \times 365 \frac{\text{operating days}}{\text{year}}\right)$$

$$= 3.7 \times 10^{23}$$

$T_{1/2}$ (tritium) = 12.4 yr.

$\lambda = 1.77 \times 10^{-9} \text{ sec}^{-1}$

Neglecting decay during the year, the annual activity production rate from ternary fission is:

$$\text{Activity} = \frac{N\lambda}{3.7 \times 10^{10} \text{ dis/sec/Ci}} \approx 20{,}000 \text{ Ci/yr}$$

The tritium yield data in Reference 11 consist of three points, as follows:

Neutron Energy	Tritium yield/fission
425 ± 45 keV	$(1.9 \pm 0.9) \times 10^{-4}$
483 ± 52 keV	$(2.3 \pm 1.0) \times 10^{-4}$
540 ± 55 keV	$(1.1 \pm 0.4) \times 10^{-4}$

These values are preliminary and so are not reported in a public document. The tritium yields for thermal fission of ^{239}Pu are not well known. Hence it is difficult to compare behavior of tritium yields of ^{239}Pu with tritium yields from ^{235}U as a function of fission energy. Such a comparison would be useful since both the thermal and fast fission yields for tritium from ^{235}U are fairly well established.

Four measurements of the thermal fission yield for ^{235}U reported since 1960 all lie between 0.8×10^{-4} and 1×10^{-4} tritons/fission, with the latest value of Dudey, Fluss, and Malewicki[12] being $0.85 \pm 0.09 \times 10^{-4}$. Dudey, et al. report values for fast fission (i.e. between 200 and 800 keV) between 1.5 and 3.0×10^{-4}, with an average near 2.0×10^{-4} which is nearly constant over the 200 to 800 keV energy range.[12] Hence the tritium yield from fast fission of ^{235}U is about 2.5 times the yield from thermal fission.

Unfortunately there are no reliable thermal fission tritium yields for ^{239}Pu. Horrocks and White[13] report preliminary values ranging from 1.8 to 5.0×10^{-4} tritons/fission. An independent estimate of tritons/fission can be inferred from two intermediate results which have been reported--alphas/fission and alphas/triton from fission. The number of alphas/fission for thermal fissions of ^{239}Pu is $\sim$2 x 10^{-3}.[12] The number of alphas/triton is $\sim$6.[14,15] This gives a value of 3 x 10^{-4} tritons/fission. Dudey reports a theoretical prediction of 2.3 x 10^{-4} tritons/fission, even though he says the theory is inadequate.[16]

On comparing the preliminary values for tritium yield in fast fission of ^{239}Pu from Reference 11 with the above range of thermal fission yields, it is noted that the increase in yield with energy observed for ^{235}U fission may not apply for ^{239}Pu fission.

The tritium yield for ^{239}Pu assumed by Sehgal and Rempert[3] to calculate tritium production in FFTF was 1.8 x 10^{-4}, a value which they estimated as the thermal fission yield for ^{239}Pu. They report an annual tritium production rate of 1670 Ci/yr for ternary fission, assuming 300 MW(th) operation at a load factor of 0.7.

For comparison the annual tritium production rate from ternary fission in a 1000 MWe light water reactor (for 34% thermal efficiency and 0.8 load factor) can be calculated to be $\sim$15,000 Ci/yr. This value is based on the following assumptions: 55% of the fissions occur in ^{235}U, 41% in ^{239}Pu, and 4% in ^{238}U; the tritons/fission in ^{238}U are the same as ^{239}Pu; thermal fission yields are used; and the number of tritons per thermal fission in ^{235}U and ^{239}Pu fission are 0.85 x 10^{-4} and 2 x 10^{-4}, respectively. This compares to value of 18,700 Ci/yr for a 1000 MWe light water reactor reported in Reference 1, in which a higher thermal fission yield for ^{235}U (1.3 x 10^{-4}) was used.

5.1.2.2 Boron Carbide Control Rods

It is likely that B_4C will be used for shim control in the LMFBR. Boron carbide is being used for the early demonstration plants (e.g. PFR, Phenix, FFTF, U. S. Demonstration Plant). Tantalum was selected as the shim control material for all five 1000 MWe follow-on conceptual designs[17] (i.e. GE, W, CE, AI, and B & W), while B_4C, was chosen for safety rods for some of them. Since operating and planned reactors use B_4C, however, it is prudent at this time to assume that B_4C will continue to be used for our present purpose of predicting tritium production.

The principal reaction accounting for tritium production in boron carbide control rods of an LMFBR is the $^{10}B(n,t)2\alpha$ reaction. This reaction has a threshold at about 1 MeV and has a cross section averaged over the fission spectrum of $\sim$30 millibarns. A second reaction, $^{7}Li(n,nt)\alpha$, contributes some tritium; ^{7}Li is produced from the $^{10}B(n,\alpha)^{7}Li$ reaction which is the neutron absorption reaction that leads to the use of B_4C as neutron control material. The threshold for the $^{7}Li(n,nt)\alpha$ reaction is 2.8 MeV. A third reaction that produces tritium is $^{11}B(n,t)^{9}Be$, but this reaction has such a high threshold (9.6 MeV) that it contributes little to the total tritium production rate.

No reported tritium production rates from control rods were found for a large power LMFBR that uses B_4C shim control. Sehgal and Rempert have reported calculated tritium production rates from B_4C control rods in EBR II and FFTF.[3] Kabele reports total predicted tritium production rates for FFTF.[4] These calculations cannot be used directly for a large power reactor, however, because the tritium production rate depends upon the fuel cycle adopted and the amount of B_4C needed in the core for shim control for the particular reactor design.

For this reason, an example calculation of tritium production in a 1000 MWe LMFBR has been made based on control requirements and results reported for the GE 1000 MWe follow-on design.[18] The basis for this design is:

- 12 month refueling interval. The required shim reactivity was 4.76$ (1.80% δk/k).
- 16$ worth of safety control (including the backup control system which is located in the axial blanket during operation).

The GE design assumed tantalum rods for shim control and B_4C rods for safety control. Reference 18 provides a neutron balance at mid-cycle for an equilibrium fuel cycle, which provides tantalum absorption rates in the core and axial blanket and boron absorption rates in the axial blanket. The fraction of neutrons absorbed by tantalum in the core is 0.00875, which is one half of the shim control requirement of 0.0180. Hence, the nertron balance is reported for the true mid-cycle case, i.e. with half of the shim control rods withdrawn from the core. Half the shim rods represents the average amount of control in the core during the entire equilibrium fuel cycle.

For the example calculation, the tantalum absorptions were replaced with the required number of boron absorptions to provide the same shim control in order to simulate boron-carbide shim control rods. Reference 18 gives (a) the total neutron flux, (b) the core average flux spectrum, (c) the core adjoint flux, ϕ_i^*, (d) the fraction of fissions in the core, and (e) the Ta capture-to-fission ratio in the core at mid-burnup. The core fission rate can be calculated to give a total reactor power of 2500 MW(th). A sixteen group cross section set is also available from General Electric which contains natural boron and tantalum capture cross sections, both self-shielded for a control pin array equivalent to a 2-inch rod diameter. These data permit calculation of the number of ^{10}B atoms in the core required for shim control by forcing

$$N(^{10}B)\sum_i \sigma_{c_i}(^{10}B)\phi_i\phi_i^* = N(Ta)\sum_i \sigma_{c_i}(Ta)\phi_i\phi_i^*.$$

The neutron spectrum changes caused by replacing the tantalum with boron were ignored.

For reference, the intermediate results are:

A capture in boron and a capture in Ta have almost equivalent effects on reactivity. Only 1% more absorptions were required in B than Ta to provide equal reactivity control.

Core average fission rate = 1.7×10^{13} fissions/cm^3 sec

From the neutron balance, $\dfrac{\text{core control-rod captures (mid-cycle)}}{\text{core fission}} = \dfrac{0.00875}{0.299}$

Tantalum absorption rate in core = 4.9×10^{11} absorptions/cm^3 sec

Boron absorptions in core for same Δk = 4.9×10^{11} absorptions/cm^3 sec

$$\sum_{i=1}^{16} \sigma_{c_i}(^{10}B)\phi_i = 1.57 \times 10^{-8}\ \text{sec}^{-1}$$

^{10}B concentration: $N(^{10}B) = 3.1 \times 10^{19}\ \dfrac{\text{atoms}}{\text{cm}^3}$

Volume of core: $V = 3.66 \times 10^6\ \text{cm}^3$

With these values it was possible to calculate the reaction rate for tritium production in the core from the reaction $^{10}B(n,t)\,2\alpha$. This reaction rate is:

$$N(^{10}B)V\int_{E_{th}}^{\infty} \sigma(E)\ \phi(E)dE \text{ (reactions in core/sec)}$$

where E_{th} is the threshold energy for the reaction ($\sim$ 1.3 MeV).

The curve for $\sigma(E)$ was that recommended by Irving[19] for the ENDF-B evaluation. The flux was assumed to follow the fission spectrum in the first energy group, i.e. above 2.2 MeV. A plot of the flux spectrum from Reference 18 was used to obtain the spectrum below 2.2 MeV. The spectra were normalized to the group 1 and group 2 fluxes, the two groups in which the $^{10}B(n,t)2\alpha$ reaction occurs. The group 1 flux (for which the lower energy limit was 2.2 MeV) was:

$\phi^1 = 2.8 \times 10^{14}$ n/cm^2 sec. The group 2 flux (lower limit of 0.825 MeV) was:

$\phi^2 = 7.0 \times 10^{14}$ n/cm^2 sec. The integral for the $^{10}B(n,t)2\alpha$ reaction was:

$$\int_{E_{th}}^{\infty} \sigma(E)\ \phi(E)dE = 2.9 \times 10^{-11}\ \text{sec}^{-1}$$

Hence, the triton production rate from ^{10}B in the core was:

$$N(^{10}B)V = \int_{E_{th}}^{\infty} \sigma(E) \; \phi(E)dE - 3.3 \times 10^{15} \text{ tritons/sec}$$

This results in an annual tritium activity production rate from ^{10}B in the core, A(shim, core), of:

$$A(\text{shim,core}) = 4000 \text{ Ci/yr}$$

There are two more contributions to the tritium activity from ^{10}B--(1) reactions in the part of the shim rods in the axial blanket and (2) reactions in the safety and shutdown rods which are present in the axial blanket. The tritium production from these two sources can be estimated by using again the neutron balance data from the GE design and by assuming that the ratio of $^{10}B(n,\alpha)^7Li$ reactions and the $^{10}B(n,t)2\alpha$ reactions is the same in the axial blanket and the core. This assumption is not exact because the spectrum is softer in the axial blanket so that the assumption leads to a small overestimate of the tritium production.

From the GE neutron balance, the ratio of tantalum capture in the shim rods in the axial blanket to that in the core is 0.00300/0.00875. The ratio of boron captures in the safety rods in the axial blanket to the tantalum absorptions in the core is 0.00364/0.00875 and this ratio would be the same (within 1%) if B_4C had been used for shim control. Hence the tritium production rate, if the shim rods were B_4C, would be

$$A(\text{shim, ax. blanket}) = A(\text{shim,core}) \; \frac{0.00300}{0.00875} = 1400 \text{ Ci/yr}$$

$$A(\text{Safety-shutdown, ax. blanket}) = A(\text{shim,core}) \; \frac{0.00364}{0.00875} = 1700 \text{ Ci/yr}$$

Hence the total tritium production rate in the control rods is:

$$A \gtrsim 7000 \text{ Ci/yr}$$

This tritium production rate from ^{10}B capture is significantly lower than the values which would be extrapolated directly from References 3 and 4. Both Sehgal-Rempert and Kabele calculate higher tritium production rates in FFTF from ^{10}B capture than from ternary fission, a result opposite from that shown here for a power reactor operating with a typical fuel cycle. Sehgal and Rempert report an annual tritium production rate for FFTF of 3980 Ci/yr from ^{10}B, based on 300 MW(th) operation at 0.7 load factor.[3] Direct extrapolation to a 2500 MW(th) LMFBR at 0.8 load factor gives a value of 38,000 Ci/yr.

Kabele reports a total of 40 Ci/day generation for tritium production rate in FFTF.[4] It is known from conversations with Westinghouse personnel that ∿ 80% of this is from boron capture in the B_4C control rods. Assuming Kabele used 400 MW(th) (the rated power level for FFTF) and 0.7 load factor, a direct extrapolation to a 1000 MWe LMFBR would give 64,000 Ci/yr. Hence, Kabele's number is significantly higher than Sehgal and Rempert's, and the tritium production rate from ^{10}B in a power reactor is grossly overestimated by extrapolating either calculation to a power reactor. This overestimate is probably due to the relatively large amounts of boron needed for control purposes in a test reactor.

Tritium can also be produced by the $^{7}Li(n,t)\alpha$ reaction in a boron carbide control rod. Lithium-7 builds up in a control rod since it is the product of the $^{10}B(n,\alpha)^{7}Li$ reaction that provides the control.

Again, the GE neutron balance[18] provides a means of estimating the tritium production from this source. During one year of operation, the number of fissions that occur in the core is:

$$\left(1.7 \times 10^{13}\ \frac{\text{fissions}}{\text{cm}^3\text{-sec}}\right) \left(3.66 \times 10^{6}\ \text{cm}^3\right) \left(.864 \times 10^{5}\ \frac{\text{sec}}{\text{day}}\right) \left(0.8 \times 365\ \frac{\text{day}}{\text{yr}}\right)$$

$$= 1.6 \times 10^{27}$$

From the neutron balance, the number of $^{10}B(n,\alpha)^{7}Li$ reactions in the core is:

$$\left(\frac{.00875}{.299}\right) \left(1.6 \times 10^{27}\right) = 5 \times 10^{25}$$

The ratio of the integrals $\int \sigma(E)\,\phi(E)dE$ for the $^{7}Li(n,t)\alpha$ reaction and the $^{10}B(n,t)2\alpha$ reaction is:

$$\frac{^{7}Li}{^{10}B} = \frac{\int_{2.8}^{\infty} \sigma_{Li}(E)\ \phi(E)dE}{\int_{1.3}^{\infty} \sigma_B(E)\ \phi(E)\,dE} = \frac{2.4 \times 10^{-11}}{3.0 \times 10^{-11}} = .8$$

where the $^{7}Li(n,t)\alpha$ cross section was obtained from BNL-325[20].

Since the number of ^{10}B atoms in the core at mid-cycle is 1.1×10^{26}, at which time the tritium production rate from $^{10}B(n,t)2\alpha$ in the core is 4000 Ci/yr, the tritium production rate from $^{7}Li(n,nt)\alpha$ in the core after one year, after refueling, is

$$4000\ \frac{\text{Ci}}{\text{Yr}} \times \frac{5 \times 10^{25}}{1.1 \times 10^{26}} \times .8 = 1500\ \text{Ci/yr}$$

The value varies both as the ^{7}Li concentration builds up and as the rods are withdrawn during the fuel cycle. Also the B_4C shim rods burn out and must be replaced periodically.

The source from $^7Li(n,nt)\alpha$ reactions in the shim and safety rods in the axial blanket was estimated to be 1000 Ci/yr after one year of operation. This value would increase as ^{7}Li is built up in the safety rods, which would not require replacement as often as the shim rods. The rate of increase in the safety rods would be ~ 500 Ci/yr per year, assuming the neutron balance for the GE 1000 MWe design,[18] which assumes a particular amount of B_4C safety control in the axial blanket.

Adding the 1500 and 1000 Ci/yr values gives a total of 2500 Ci/yr for the tritium production rate from the $^7Li(n,nt)\alpha$ reaction as listed in Table 5.1.

For comparison tritium production rates in boron in a light water reactor can be estimated from Reference 1. For a 1000 MWe PWR (2940 MW(th)), the estimated annual tritium production in the chemical shim for the equilibrium fuel cycle is ~ 700 Ci from the $^{10}B(n,t)2\alpha$ reaction and ~ 1250 Ci from the $^7Li(n,nt)\alpha$ reaction. Tritium production rates in BWR control rods are much higher, but the tritium does not escape from the control rods.

5.1.2.3 Lithium Contamination

Lithium is present as an impurity both in reactor fuel and in the sodium coolant. Neutron capture by lithium-6 leads to tritium production through the reaction $^6Li(n,t)\alpha$.

Although fresh fuel is expected to have less than 1 ppm lithium, reprocessed fuel may contain as high as 20 ppm lithium.[21] Kabele included this source (20 ppm) in his estimates for FFTF.[4] Extrapolating Kabele's calculation to a 1000 MWe LMFBR results in an estimated 4000 Ci/yr tritium production rate from 20 ppm of lithium in the fuel.

Lithium content in the FFTF sodium is specified to be less than 5 ppm. The tritium production rate from this lithium is <100 Ci/yr. This value can be estimated from the above 4000 Ci/yr source from lithium in the fuel since the sodium and fuel volumes in the core are comparable, the lithium mass concentration is 5 ppm in sodium instead of 20 ppm in fuel, and the sodium density is a factor of 10 lower than the fuel density.

5.1.3 Transport of Tritium in an LMFBR System

5.1.3.1 Escape into Sodium System

Escape from Fuel Pins

Tritium produced in the fuel from ternary fission and from lithium in the fuel diffuses through the steel cladding into the sodium. Roy, Rubin, and Wozadlo[9] report experimental results of irradiated mixed-oxide fuel pins with austenitic stainless steel cladding which show that less than 1% of the tritium produced is retained in the fuel pin. Hence nearly all tritium gets into the sodium and little is available for release during fuel reprocessing.

Additional data on tritium leakage from fuel is available for EBR-II driver fuel.[7,8] The data is of less interest since the driver fuel is metallic uranium. Assuming 2 x 10^{-4} tritons produced/fission, EBR-II staff report that nearly 100% of the tritium diffuses out of the driver pins at average fuel temperatures greater than 1000°F and that 80% escapes when the average fuel temperature is 800°F.[8]

This situation is different from the case of light water reactors. Little of the tritium diffuses through the zirconium cladding, so most of the tritium is retained in the fuel pin in light water reactors. The difference may be caused by the difference in cladding temperature more than by the difference in cladding material. The cladding in an LMFBR operates at ∿ 400°F higher than that in a light water reactor.

Control Rods

No published data were found on diffusion of tritium from control rods in an LMFBR. It has generally been assumed by LMFBR designers that tritium produced in B_4C rods would diffuse through the cladding since the cladding is steel at high temperature, as is the fuel cladding.

Some data have been received directly from the EBR-II staff, however, that differs from the above assumption. The EBR-II experience is that all of the tritium produced in B_4C clad in steel stays within the rod. It was assumed at EBR-II that this resulted from irradiation at lower B_4C temperature (1100°F) and higher B_4C densities (2.5 gm/cm^3) than planned for power reactors. Later, these B_4C rods were heated to 1500°F for 120 hours and still no loss of tritium occurred. However, EBR-II staff learned that HEDL experimentors who irradiated B_4C control assemblies in EBR-II at 1600°F centerline temperatures and 2.1 gm/cm^3 density--similar to power reactor conditions--found that 70 to 75% of the tritium produced was retained in the cladding. Unfortunately, so much of the experimental work done by HEDL for FFTF is unavailable to the public that details on this question are unavailable; it is still not clear what fracton of the tritium produced in B_4C rods will escape to the sodium.

This question may be rendered academic if a different design approach is taken. Boron carbide control rods may be designed to vent the helium produced from $^{10}B(n,\alpha)^{7}Li$ reactions to the coolant in order to avoid the large pressures resulting from helium production. In that case, the tritium produced would also escape to the sodium.

5.1.3.2 Transport in the Sodium and Steam Systems

Tritium is removed in cold traps. The reaction that removes tritium is unclear. Two possible mechanisms are deposition of sodium hydride and exchange of ^{1}H and tritium in the steel mesh in the trap.

Some tritium, however, can escape elsewhere--to the cover gas from which it could leak to the reactor building and the environment, through the primary system boundaries (piping and vessels) to the reactor building and the environment, and to the secondary sodium across the tube walls of the intermediate heat exchanger.

Most of the tritium which finds its way to the secondary sodium is trapped in the secondary-sodium cold trap. Some, however, escapes through the secondary-system boundaries to the environment, and some enters the steam system through the steam generators and superheaters.

Proof that tritium is removed in the cold traps comes from operation represented by Figure 5.1 which is reproduced from Reference 7. The measured tritium concentrations in the primary sodium with and without cold trap operation clearly indicate the effectiveness of the cold trap in removing tritium. Also at EBR-II, during one month when the secondary-system cold trap was not being operated, tritium concentrations in water samples taken from the steam system were 5 to 8 times higher than for normal operation with the secondary cold traps in service.[8]

Most of the tritium which reaches the steam system would be expected to get into the environment eventually; the modes and rates of leakage will depend on how the steam system is designed and operated.

EBR-II has reported both tritium production rates and distribution of the tritium in the EBR-II complex.[7,8,3] The results of References 7, 8, and 3 are summarized in Table 5.2. All losses to the reactor building should appear in the air to the stack since the reactor building atmosphere is continually exhausted to the stack. The known tritium losses to the environment during operation are $\sim$ 1 Ci/yr. This is about 0.2% of the tritium that enters the primary sodium. About 10% of the tritium at EBR-II remains in the fuel.[8]

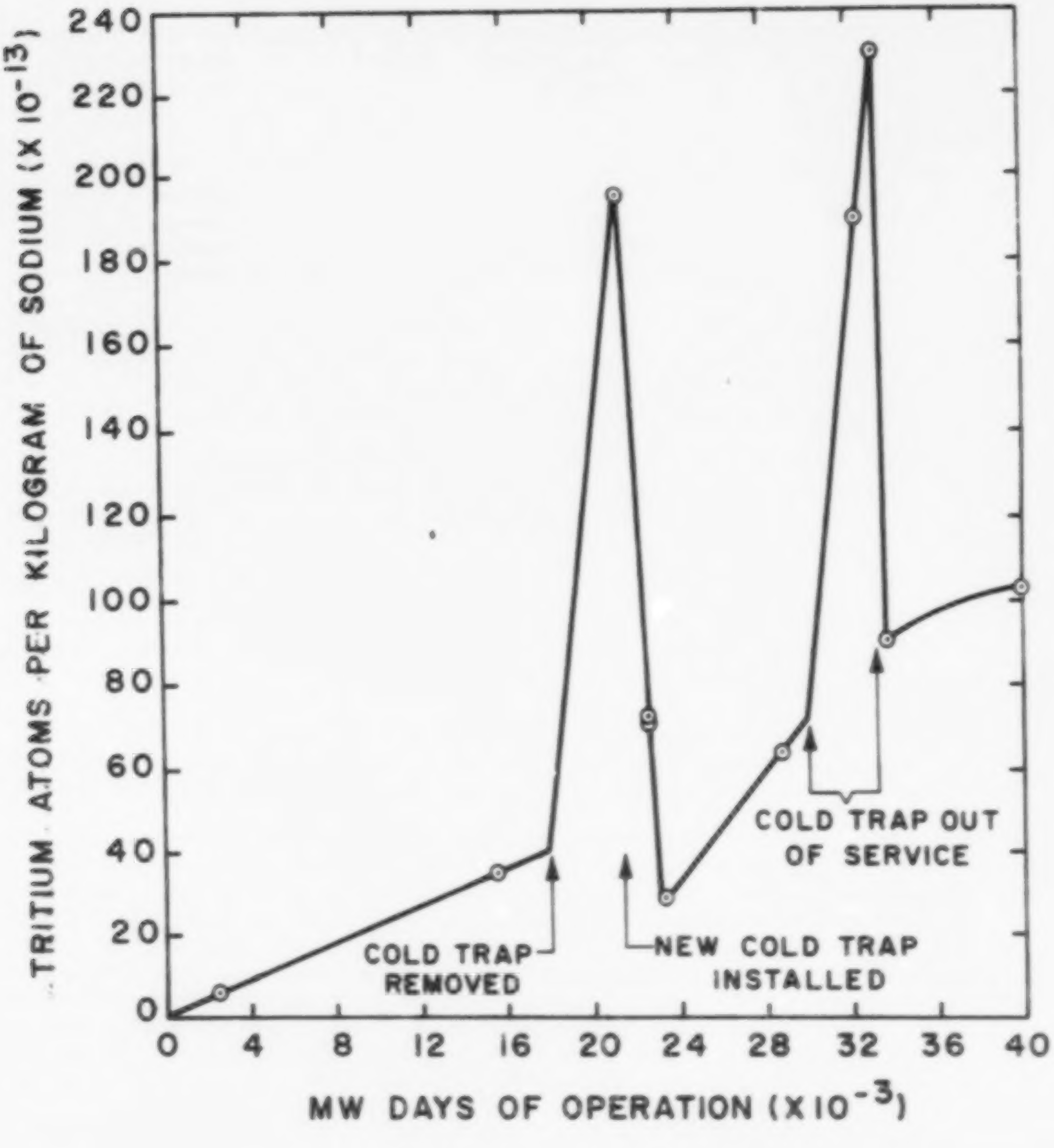

Figure 5.1 Tritium in Primary Sodium (EBR-II)

Table 5.2

Summary of EBR-II Tritium Data

	Reference 7[a]	Reference 8[b]	Reference 3[b]
Production Rate			
Ternary Fission	100%	420 Ci/yr[c]	190 Ci/yr[d]
Boron	Neglected	----	510
Total			700
Known Loss Rates			
In air to stack		0.9 Ci/yr	
In condenser water		0.05 Ci/yr	
Tritium Distribution			
Percent distribution from Ref. 7 (boron control not included)			
Fuel	20-25%	∼ 10%	
Primary sodium	4%		
Primary cold trap	68-70%		
Outside fuel and primary system	3-7%		
Loss from power plant	<1.5%		
Absolute activities of typical sampling data (Ref. 8)			
Primary sodium		15.5 Ci	
Primary argon		0.0015 Ci	
Secondary sodium		0.083 Ci	
Secondary argon		0.00018 Ci	
Steam system		0.00058 Ci	

a. Based on 50 MW(th) operation
b. Based on 62.5 MW(th) at 0.7 load factor
c. Based on 2.0×10^{-4} tritons/fission in ^{235}U
d. Based on 0.8×10^{-4} tritons/fission in ^{235}U

The latest public documentation of EBR-II tritium concentration was found in Reference 22 in which the following results were reported:

Table 5.3

Tritium Concentrations in EBR-II

Region	Concentration	Date of Sample	Secondary Cold Trap Operating?
Primary Sodium	4.2×10^{-2} μCi/gm	April, 1971	No
	6.3×10^{-2} μCi/gm	May, 1971	No
Secondary Sodium	6.7×10^{-3} μCi/gm	April, 1971	No
	9.2×10^{-3} μCi/gm	May, 1971	No
	2.9×10^{-3} μCi/gm	June, 1971	Yes
Turbine Condensates	72 pCi/ml	May, 1971	No
	13 pCi/ml	June, 1971	Yes

These values are consistent with the results from Reference 8 quoted in Table 5.2.

Additional data is now being reported in the non-public ANL reactor progress reports. For example starting in September, 1972 (Reference 23) tritium in the steam system is being reported regularly. The value in Reference 23 is ∿ 10 pci/gm with the secondary cold trap operating, which is similar to the result in Table 5.3. The tritium activity reported in Reference 23 in the primary argon cover gas is 16 pci/cm^3. This result is about a factor of 10 lower than the concentration that would be calculated from the primary cover gas result from Reference 8 data in Table 5.2 above.

The source terms in the EBR-II analysis of Reference 7 include only ternary fission, and assume 0.8×10^{-4} tritons per fission,[3,7] since boron control was not used at that time. Sehgal and Rempert calculate more than 2 1/2 times as much tritium from boron control rods as from ternary fission[3]. However, the tritium in the boron control rods may not contribute to the source in proportion to its production rate since, according to Reference 10, the tritium produced in the B_4C rods does not escape from the rods in EBR-II.

An extrapolation of tritium leakage from a 1000 MWe LMFBR can be made by assuming that the same fraction of tritium that enters the primary sodium escapes to the environment as in EBR-II (i.e. ∿ 0.2% to the atmosphere and 0.01% to the condenser water). Based on ∿ 30,000 Ci/yr entering the sodium in a 1000 MWe LMFBR (see Table 5.1), the amount leaving the reactor through the stack would be ~ 60 Ci/yr. The amount leaving in the condenser water would be ~ 3 Ci/yr. Such an extrapolation may be misleading for several reasons. Leakage of argon to the reactor building is excessive in EBR-II (See Section 8.2) and much higher than could be tolerated in an oxide-fuel power plant; hence the stack leakage extrapolation may be too high. Also the steam generators, a principal component in the pathway to the condenser, contain double wall piping which may not be used in a power reactor; hence the fraction of leakage to the condenser could be higher in a power reactor not using the double wall design. Also, since EBR-I is a pot design extrapolation to a loop-type design may not be valid because of different bulk sodium and wall temperatures, etc.

For comparison, the AEC has calculated tritium leak rates in the liquid effluent for a BWR and PWR.[24] For a 1100 MWe BWR, the annual tritium release rate in the liquid effluent was predicted to be 110 Ci/yr (or 100 Ci/yr for a 1000 MWe plant). For a 870 MWe PWR the corresponding release rate was 500 Ci/yr (or 600 Ci/yr for a 1000 MWe plant). The AEC report did not consider tritium in gaseous effluents.

The EBR-II experience, therefore, indicates that although the tritium production rate in an LMFBR is higher than in a LWR, the amount that finds its way to the liquid effluent is smaller in an LMFBR.

REFERENCES (Section 5.1)

1. H. T. Peterson, J. E. Martin, C. L. Weaver, and E. D. Harward, "Tritium Contamination from Increasing Utilization of Nuclear Energy Sources," Proceedings of the International Conference on Environmental Contamination of Radioactive Materials, SM-117/78, IAEA, Vienna, 1969.

2. C. L. Weaver, E. D. Harward, and H. T. Peterson, "Tritium in the Environment from Nuclear Power Plants," Public Health Reports, 84, 363, 1969.

3. B. R. Sehgal and R. H. Rempert, "Tritium Production in Fast Reactors Containing B_4C," Trans. Am. Nucl. Soc., 14, 779, 1971.

4. T. J. Kabele, "Tritium Distribution in FFTF," Trans. Am. Nucl. Soc., 15, 79, 1972.

5. Reply to Aug. 18, 1972 request to H. Bullinger for HEDL-TM-7219, Report on Tritium Distribution in FFTF", by T. J. Kabele.

6. Westinghouse staff, personal communication, August, 1972.

7. E. R. Ebersole, W. R. Vroman, and J. R. Krsul, "Tritium in the EBR-II Reactor Complex," Trans. Am. Nucl. Soc. 14, 321, 1971.

8. EBR-II Staff, Revision of Data in Reference 7, supplied to participants in an LMFBR workshop sponsored by ANL, AUA, and AEC, December 11-15, 1972

9. C. P. Wozadlo, B. F. Rubin, P. Roy, "Tritium Analysis of Fast Flux Irradiated Mixed-Oxide Fuel Pins," Trans. Am. Nucl. Soc., 15, 200, 1972.

10. EBR-II Staff, personal communication, December, 1972.

11. Reactor Development Progress Report, NAL-RDP-2, p. 7.35, February 1972.

12. N. D. Dudey, M. J. Fluss, and R. L. Malewicki, "Tritium and Alpha Particle Yields in Fast and Thermal Neutron Fission of Uranium-235," Phys. Rev., C6(6), 2252 (1972).

13. D. L. Horrocks and E. B. White, "Tritium Yield in the Thermal Fission of U-233", Nucl. Phys., A151, 65 (1970).

14. P. Cavallini, et al., "Application of New Fast Chemical Separation, to the Determination of Charge Distribution in Low-Energy Fission", Proceedings of the Second Symposium on the Physics and Chemistry of Fission, IAEA, Vienna, 1969.

15. T. Krogulski, et al., "Emission of Light Nuclei in Thermal Neutron Fission of Pu-239", Nuclear Physics, A1[illegible]8 219 (1969).

16. N. D. Dudey, personal communication, July 24, 1972.

17. Five papers on 1000 MWe Follow-on Designs of GE, W, AI, CE, and B & W Proceedings of the International Conference on Sodium Technology and Large Fast Reactor Design, ANL-7520, Part I, November, 1968.

18. "Task II Report, Conceptual Plant Design, Systems Descriptions, and Costs for a 1000 MWe Sodium-Cooled Fast Reactor," GEAP-5678, pages 91-101, December, 1968.

19. D. C. Irving, "Evaluation of Neutron Cross Sections for Boron-10", ORNL-TM-1972, October, 1967.

20. BNL-325, Second Edition, Supplement No. 2, "Neutron Cross Sections, Vol. I, Z = 1 to 20," J. R. Stehn, M. D. Goldberg, B. A. Magurno, and R. Wiener-Chasman--Editors, May, 1964.

21. G. R. Taylor, WARD, personal communication, August, 1972.

22. Reactor Development Progress Report, ANL-7845, July, 1971.

23. Reactor Development Progress Report, ANL-RDP-9, September, 1972.

24. Staff, Directorate of Regulatory Standards, USAEC, "Draft Environmental Statement Concerning Proposed Rule Making Action: Numerical Guides for Design Objectives and Limiting Conditions for Operation to Meet the Criterion 'As Low as Practicable' for Radioactive Material in Light-Water-Cooled Nuclear Power Reactor Effluents," (Proposed Appendix I to 10 CFR50), January, 1973.

5.2 Activated Corrosion Products

Sodium slowly corrodes metallic surfaces in and near the core. These metallic surfaces are radioactive as a result of neutron activation. Radioactive corrosion products may remain in solution in the sodium or may be deposited on other surfaces in the primary system, such as the reactor vessel, piping, intermediate heat exchangers, pumps, and cold traps.

Both corrosion rates and deposition rates are influenced by surface and sodium temperature, flow velocity, and oxide concentration in the sodium. Corrosion and deposition rates and the dependence of these rates on the above parameters vary for different metals. Although experimental information on corrosion and deformation rates has been obtained by General Electric, [1,2] by Hanford Engineering Development Laboratory[3] (HEDL), and in the United Kingdom[4] (as discussed in References 5 and 6), analysis of the distribution of corrosion product activity throughout the primary sodium system is still quite uncertain. In the analysis of activated corrosion product distribution, the primary sources of uncertainty are associated with corrosion rates and deposition patterns; uncertainties involving reaction rates and amounts of target nuclides present are less important.

The best analyses available are two analyses* for FFTF. The most recent and complete analysis was performed by HEDL,[5] and a slightly earlier analysis was made by General Electric.[6] The corrosion data of GE and other data and methods used by HEDL were applied here to extrapolate corrosion product activity and distribution to a 1000 MWe LMFBR. Additional data on corrosion product reactions appear in AI's STP-1 code[7] and in an ORNL reference[8] which quotes data from their reference library.

The principal corrosion products, the reactions that produce them, and their half lives, are given in Table 5.4.

---

* The principal purpose of the two reports was to estimate dose at primary system components for maintenance purposes. However, production and distribution of the activation products were intermediate steps in both reports.

Table 5.4

Activation Reactions in Stainless Steel

Nuclide	Reaction	$T_{1/2}$
^{60}Co	$^{59}Co(n,\gamma)^{60}Co$	5.24 yr
	$^{60}Ni(n,p)^{60}Co$	
^{58}Co	$^{58}Ni(n,p)^{58}Co$	71 d
^{54}Mn	$^{54}Fe(n,p)^{54}Mn$	313 d
^{59}Fe	$^{58}Fe(n,\gamma)^{59}Fe$	45 d
^{55}Fe*	$^{54}Fe(n,\gamma)^{55}Fe$	2.4 yr
^{51}Cr	$^{50}Cr(n,\gamma)^{51}Cr$	28 d
	$^{54}Fe(n,\alpha)^{51}Cr$	
^{182}Ta	$^{181}Ta(n,\gamma)^{182}Ta$	115 d

The following additional reactions are possible, but they contribute little to corrosion product activity:

$^{58}Ni(n,\gamma)^{59}Ni$

$^{62}Ni(n,\gamma)^{63}Ni$

$^{52}Cr(n,2n)^{51}Cr$

$^{55}Mn(n,2n)^{54}Mn$

$^{59}Co(n,2n)^{58}Co$

The above reactions have cross sections that are too low to make them of interest except possibly the reactions that produce ^{59}Ni and ^{63}Ni since their half lives are so long, (8×10^4 yr and 92 yr respectively); these two products are included in the section on Cladding Activation (Section 5.3.2).

---

*This corrosion product was not included in the HEDL calculation[5] because ^{55}Fe decays only by electron capture, giving up a maximum of 0.22 MeV energy as internal bremsstrahlung, and this energy is of little consequence to primary system maintenance.

5.2.1 Estimated Corrosion Product Activity in 1000 MWe LMFBR

Estimates of the corrosion rate and activity of each activated corrosion product in the primary system of a 1000 MWe LMFBR are presented here. It is important to emphasize that great uncertainty exists in the estimates. The methods used here show how to estimate corrosion product activity, and provide an order-of-magnitude result. The large differences between the GE and the HEDL calculations for FFTF are then discussed in order to indicate the degree of uncertainty in the calculations.

Corrosion product inventories in the primary system are given for 30 years of reactor operation. ^{58}Co, ^{51}Cr, ^{59}Fe and ^{182}Ta achieve equilibrium during the first year. ^{54}Mn takes somewhat longer, and ^{60}Co and ^{55}Fe still longer. The data used to estimate these inventories are listed in Table 5.5. Estimated inventories are given in Table 5.6.

Table 5.5

Data for Corrosion Product Calculation

Region	Corrosion Rate (mils/yr)	Surface Area (ft^2)	Average Neutron Flux (n/cm^2 sec)
Core	0.13*	17,000	7×10^{15}
Upper axial blanket	0.3	8,000	3×10^{15}
Gas Plenum (above core)	0.3	17,000	0.5×10^{15}
Radial blanket (upper half)	0.1	10,000	$.2 \times 10^{15}$

---

*Based on corrosion vs. temperature curve in Reference 6 and an inlet temperature of 800°F and outlet temperature of 1100°F.

Table 5.6

Estimates of Activated Corrosion Products in the Primary System of the 1000 MWe LMFBR After 30 Years Operation[a]

Isotope	Formation Reaction	Contribution to the Primary System Activity				Total Primary System Activity
		Core	Axial Blanket	Gas Plenum	Radial Blanket	
		(Ci)	(Ci)	(Ci)	(Ci)	(Ci)
^{60}Co	(n,γ)	1400[b]	9300[b]	6600[b]	2200[b]	20,000
	(n,p)	1000	---	---	---	
^{58}Co	(n,p)	20,000[c]	2800	300	400	23,000
^{54}Mn	(n,p)	16,000[d]	2400	---	300	19,000
^{55}Fe	(n,γ)	26,000	f	f	f	>26,000
^{59}Fe	(n,γ)	300	500	300	---	1,000
^{51}Cr	(n,γ)	2500	2800	1800	---	7,000
	(n,α)	200				
^{182}Ta	(n,γ)	800	3200	2400	---	6,000[e]

---

a. All values based on stoichiometric corrosion, assuming 316 stainless steel (see Table 5.9 for composition).

b. Based on only 0.02% by weight cobalt in stainless steel. (HEDL[5] assumed 0.02%, GE[6] assumed 0.1%).

c. This value was calculated using $\phi(E)$ and $\sigma(E)$ (see page 66). For comparison the value calculated from ϕ of Table 5.5 and σ of Table 5.7 was 21,000 Ci.

d. This value was calculated using $\phi(E)$ and $\sigma(E)$ (see page 66). For comparison the value calculated from ϕ of Table 5.5 and σ of Table 5.7 was 15,000 Ci.

e. The assumption of stoichiometric corrosion is believed by HEDL[5] to be particularly poor here. (HEDL assumed only 1% of stoichiometric corrosion).

f. Cross sections were unavailable for the soft spectra in these regions. It is expected that the ^{55}Fe generation from the n,γ reaction would be higher outside than inside the core. It was decided not to pursue this calculation further, however, because of the low importance of the ^{55}Fe isotope since it is neither a β or γ emitter (see footnote, Table 5.4)

The corrosion rates are based on a curve presented in the GE report[6] for a sodium flow rate of 15 to 28 ft/sec and an oxygen concentration of 2.6 ± 1.5 ppm. The 0.13 mils/yr corresponds to an average corrosion rate over the core for an inlet of 800°F and an outlet of 1100°F. The 0.3 mils/yr corresponds to 1100°F sodium. The lower value for the radial blanket accounts for both a lower sodium temperature and a lower flow rate.

The HEDL calculation[5] assumed much lower corrosion rates even though the same inlet and outlet temperatures were assumed. Two cases were reported by HEDL--one for an oxygen content of 5 ppm and one for an oxygen content less than 2 ppm. Even for the high oxygen case, the corrosion rates were a factor of 2 to 3 lower than the GE values. Values used by HEDL were: core-0.055 mils/yr; axial reflector-0.13 mils/yr; gas plenum-0.095 mils/yr; and radial reflector-0.025 mils/yr. For the case of <2 ppm oxygen, HEDL assumed a further reduction in corrosion rate of a factor of four, i.e. 0.014 mils/yr was used for the core. The source of such a large discrepancy in corrosion rate was not discussed. GE claims that its curve is based on mass transfer data from GE and UK. GE refers to the experimental results of Brehm of HEDL, indicating agreement in some areas and disagreement in others. HEDL's analysis references only a later paper by Brehm.[3] The GE analysis[6] also used lower corrosion rates than in Table 5.5 but their calculation assumed a 700°F inlet and a 1050°F outlet.

Stoichiometric corrosion rates were assumed by GE[6]. Significant deviation from stoichiometric corrosion was assumed by HEDL,[5] however, based on specific information about corrosion of particular elements. For example, cobalt in stainless steel is assumed by HEDL to corrode at about 20% of the rate of the stainless steel in high oxygen sodium, and manganese is assumed to corrode at twice the rate of stainless steel. Tantalum is assumed to corrode at only 1% of the rate of stainless steel, an assumption which HEDL says is backed up by the fact that no ^{182}Ta is observed in EBR-II and tantalum corrosion rates are low in other stainless-sodium systems. However, ^{182}Ta was observed on the primary pump walls at EBR-II, even though EBR-II staff suggested that the source of the ^{182}Ta was the cladding of an antimony neutron source instead of the stainless steel structure. Only iron and chromium are assumed to be released at stoichiometric rates by HEDL. The GE analysis did not include a calculation of tantalum activation.

The surface area of the core is that calculated for the 1000 MWe

GE follow-on design.[9] The upper axial blanket has half the area in the GE design, and it was assumed that the plenum area is equal to the core area. The sodium in the lower axial blanket has too low a temperature to contribute to corrosion.

The fluxes were based on both the GE 1000 MWe follow-on design report[9] and on the HEDL FFTF report.[5] The average flux of 7.1×10^{15} sec in the core is given in Reference 9. For FFTF the core average flux is 4.2×10^{15}; the value is smaller primarily because of the relatively smaller size of the core. Average fluxes in the rest of the FFTF are: axial reflector--1.5×10^{15}; gas plenum-0.3×10^{15}; and radial reflector-0.9×10^{15}. It was assumed that the average fluxes in the corresponding zones in a 1000 MWe reactor would be in the same ratio to the core flux in both the 1000 MWe LMFBR and FFTF. Since cross sections for n,γ reactions are high in the gas plenum region, the activation rates are sensitive to the correct flux in this region. Also the flux extrapolation from FFTF to a 1000 MWe LMFBR in the gas plenum region may introduce a large error.

As discussed in Section 5.2.3, the actual energy dependent neutron flux was used in the calculations of the ^{58}Ni(n,p) ^{58}Co and the ^{54}Fe(n,p) ^{54}Mn reactions in the core. The flux spectrum was combined with the energy dependent n,p cross sections obtained from BNL-325.[10] This procedure offered an independent check of the HEDL method (and of the HEDL flux averaged cross section), which was useful due to the important contributions from these two reactions in the core. As indicated in Table 5.6 (footnotes c and d), nearly identical results were obtained using the actual $\phi(E)$ and $\sigma(E)$ as were obtained using ϕ(total) and $\bar{\sigma}$.

Flux averaged activation cross sections were taken directly from the HEDL report,[5] as follows:

Table 5.7

Corrosion Product
Neutron Cross Sections (Barns)

	Zone			
Reaction	Core	Axial Reflection in Blanket	Gas Plenum	Radial Reflector or Blanket
$^{59}Co(n,\gamma)^{60}Co$	.122	1.73	3.47	1.95
$^{60}Ni(n,p)^{60}Co$	.0006	.001	.001	Not Determined
$^{58}Ni(n,p)^{58}Co$	.014[a]	.003	.001	.003
$^{54}Fe(n,p)^{54}Mn$	.009[a]	.003	.001	.002
$^{58}Fe(n,\gamma)^{59}Fe$	.012	.042	.070	Not Determined
$^{54}Fe(n,\gamma)^{55}Fe$	.012[b]	---	---	---
$^{50}Cr(n,\gamma)^{51}Cr$	.035	.086	.150	Not Determined
$^{54}Fe(n,\alpha)^{51}Cr$	.0007	---	---	---
$^{181}Ta(n,\gamma)^{182}Ta$	1.12	9.18	19.7	Not Determined

Energy averaged cross sections for a typical LMFBR core spectrum were also given in References 7 and 8. These cross sections, together with values for the less important reactions, are given in Table 5.8 for comparison with the HEDL values[5] used for the present study.

a. As described above, the actual cross sections as a function of energy were used for the $^{58}Ni(n,p)^{58}Co$ and the $^{54}Fe(n,p)^{54}Mn$ reactions in the core and the results are compared to results based on these flux averaged cross sections in Table 5.6.

b. This cross section for $^{54}Fe(n,\gamma)^{55}Fe$ comes from Reference 8.

Table 5.8

Comparison of HEDL,[5] AI,[7] and ORNL[8] Cross Sections Averaged Over an LMFBR Core Energy Spectrum

Reaction	Cross Section (barns) HEDL	AI	ORNL
$^{59}Co(n,\gamma)^{60}Co$	0.122	0.136	0.012*
$^{60}Ni(n,p)^{60}Co$	0.0006	0.0004	0.0003
$^{58}Ni(n,p)^{58}Co$	0.014	0.016	0.017
$^{54}Fe(n,p)^{54}Mn$	0.009	0.010	0.011
$^{58}Fe(n,\gamma)^{59}Fe$	0.012	0.017	0.008
$^{54}Fe(n,\gamma)^{55}Fe$	—	—	0.012
$^{50}Cr(n,\gamma)^{51}Cr$	0.035	0.027	0.012
$^{181}Ta(n,\gamma)^{182}Ta$	1.12	—	—
$^{58}Ni(n,\gamma)^{59}Ni$	—	—	0.007
$^{62}Ni(n,\gamma)^{63}Ni$	—	—	0.005
$^{52}Cr(n,2n)^{51}Cr$	—	2×10^{-5}	1×10^{-5}
$^{55}Mn(n,2n)^{54}Mn$	—	3×10^{-5}	6×10^{-5}
$^{59}Co(n,2n)^{58}Co$	—	3×10^{-5}	4×10^{-5}
$^{54}Fe(n,\alpha)^{51}Cr$	—	0.0007	0.0006

---

*This value, as quoted in the ORNL reference, appears to be a factor of 10 too low.

The composition and isotopic abundances assumed for the stainless steel are given in the following table:

Table 5.9

316 Stainless Steel Composition and Isotopic Abundance

Element	Weight Percent	Isotope	Isotopic Abundance
Fe	65%	^{54}Fe	0.0582
Ni	12	^{58}Fe	0.0033
Cr	18	^{58}Ni	0.6788
Mn	2	^{60}Ni	0.2623
Co	0.02	^{50}Cr	0.0431
Ta	0.01	^{59}Co	1.000
Mo	2	^{181}Ta	1.000

The 0.02% cobalt content was the value assumed by HEDL in Reference 5. This value might vary significantly from one reactor to another, and the ^{60}Co activity is dependent on (nearly directly proportional to) this number. For example, the GE analysis[6] used 0.1% cobalt. RRD standards specify <.05% cobalt in fuel cladding materials.

5.2.2 Distribution of Corrosion Products in the Primary System

The corrosion products are deposited on surfaces throughout the primary system. Graphical data on deposition rates are given in the GE analysis.[6] From this data GE estimated where the activation products were deposited. HEDL quotes some general qualitative experimental results:[5] for example, manganese preferentially deposits in cold parts of the system whereas cobalt is deposited in the hot parts of the system. The uncertainty concerning deposition location is illustrated by comparing, in Table 5.10, the final results of GE and HEDL for deposition in FFTF components. No GE results were presented for ^{51}Cr, ^{59}Fe, and ^{182}Ta.

As discussed in the GE reports, it is unclear whether deposition can continue at the rate indicated by current experiments after a thick deposit has built up on the surfaces. Perhaps the cold traps which will be removed periodically will trap more of the metal corrosion products than indicated in Table 5.10 since the surfaces there will be periodically renewed. Some metallic products will remain dissolved in the sodium and will be part of the coolant activity when the plant is decomissioned. It is likely, however, that most of the corrosion products will plate out onto system components or be removed by the cold traps.

Table 5.10

Fraction of Nuclides Deposited in Primary System Components

HEDL[5] and GE[6] Results

Component	^{60}Co		^{58}Co		^{54}Mn		^{51}Cr, ^{59}Fe, ^{182}Ta
	HEDL	GE	HEDL	GE	HEDL	GE	HEDL
Vessel	.31	---	.51	---	.06	---	1.08
Hot leg piping, Vessel-to-pump	.249	---	.20	---	.12	---	.109
Pump	.12	---	.08	---	.08	---	.030
Hot leg piping Pump-to-IHX	.04	---	.03	---	.01	---	.017
IHX Top Half	.258	.114	.168	.114	.42	.105	.684
IHX Bottom Half		.280		.280		.333	
Cold leg piping	.02	.145	.01	.145	.25	.250	.046
Cold Trap	.003	.300	.003	.300	.03	.035	.005
Primary tank, inlet	---	.034		.034	---	.059	---
Bottom shield	---	.127		.127	---	.218	---

5.2.3 Calculational Method

The method used by HEDL for calculation of activated corrosion product inventories in the primary system was adopted, and the method is outlined here.

The activity (in curies/cm^3 of steel) for a given isotope, j, is:

$$X_j = \frac{f_e f_i \rho N_o}{3.7 \times 10^{10} M_e} \sigma_i \phi (1 - e^{-\lambda_j t}) = K(1 - e^{-\lambda_j t}) \tag{1}$$

where f_e = weight percent of the element, e.

f_i = abundance of reactant nuclide, i.

ρ = Steel density.

N_0 = Avogadro's number.

M_e = atomic weight of element, e

σ_i = activation cross section (average over energy spectrum) for nuclide i which results in production of nuclide j.

ϕ = neutron flux (average over space, integrated over energy).

λ_j = decay constant of radionuclide, j.

t = duration of reactor operation.

The fuel is replaced after it has been in the core for some residence time, T_R, a time which is short compared to the 30 year life of the plant. Hence, an average value of corrosion product activity over the residence time is needed. Assuming X = 0 for fresh fuel, the average value of X is:

$$\bar{X}_j = \int_0^{T_R} K(1 - e^{-\lambda_j t})dt \Big/ \int_0^{T_R} dt = K\left(1 + \frac{e^{-\lambda_j T_R}}{\lambda_j T_R} - \frac{1}{\lambda_j T_R}\right) \qquad (2)$$

where K is defined by Equation 1.

In a 1000 MWe LMFBR, it was assumed that the fuel residence time, T_R, was two years in the core (and axial blanket and gas plenum) and three years in the radial blanket. (Some of the core fuel and the outer part of the radial blanket would probably have longer fuel cycle intervals.) In the core, therefore, half of the fuel would be replaced each year.

An alternate way to derive Equation 2 is to obtain an average activity over a one year period. For example, assuming two-batch loading and a refueling interval of one year ($T_R/2$ = 1 year), the average activity during a typical year is:

$$\bar{X}_j = K \frac{\frac{1}{2}\int_0^{T_R/2} (1 - e^{-\lambda_j t})dt + \frac{1}{2}\int_{T_R/2}^{T_R} (1 - e^{-\lambda_j t})dt}{\int_0^{T_R/2} dt}$$

which is equivalent to Equation 2.

The activity transported to the primary system, Q(curies), is obtained from the corrosion rate C and the corrosion product activity $\overline{X}$, as follows:

$$\frac{dQ_j}{dt} = \overline{X}_j CA - \lambda_j Q_j$$

For $Q_j = 0$ at $t = 0$

$$Q_j = \frac{\overline{X}_j CA}{\lambda_j} (1 - e^{-\lambda_j t})$$

$$= \frac{f_e f_i \rho N_o}{3.7 \times 10^{10} M_e} \frac{\sigma_i \phi CA}{\lambda_j} \left(1 + \frac{e^{-\lambda_j T_R}}{\lambda_j T_R} - \frac{1}{\lambda_j T_R}\right) (1 - e^{-\lambda_j t})$$

where t = total reactor operating time (assumed 30 years for results in this report)

C = corrosion rate of stainless steel (cm/sec)

A = corrosion surface area (cm^2)

For the work reported by HEDL, a further parameter would be needed to account for the deviation from the stoichiometric rate of the corrosion rate of the specific element in stainless steel being condiered.

For the ^{58}Ni(n,p)^{58}Co and the ^{54}Fe(n,p)^{54}Mn reactions in the core, Equation 1 was modified so that $\sigma_i \phi$ was replaced by the integral $\int \sigma(E) \phi(E) dE$. The cross sections were obtained from BNL-325.[10] The flux was obtained by the method described in Section 5.1.2.2 for the tritium production rate calculations, i.e. ϕ(E) below 2.2 MeV was obtained from the multigroup flux in Reference 9 and ϕ(E) above 2.2 MeV was assumed to be the properly normalized fission spectrum, with the energy dependence:

$$\sqrt{E}\, e^{-E/1.41\ \text{MeV}}.$$

5.2.4 Corrosion of ^{182}Ta from Tantalum Control Rods

Tantalum is being considered as a material for shim control. One of the disadvantages of the use of Ta is its high activation rate to

^{182}Ta.

Because of the high activation rate of tantalum, shim rods made of this material will probably be clad in stainless steel. The GE 1000 MWe follow-on design, which includes twelve tantalum shim rods, specifies that the tantalum would be in large (2 to 3 inch diameter) solid rods clad with 5 mil stainless steel. Hence direct corrosion by sodium would not occur unless preceded by cladding failure.

Little information was found on corrosion rates of tantalum by sodium. The HEDL report says that ^{182}Ta was found only in small quantities in LAMPRE, a Los Alamos plutonium fueled, sodium cooled reactor, which had Ta in the core, and HEDL claims that the corrosion rate of Ta in low oxygen sodium is known to be quite low.

The total activation rate of tantalum shim rods can be estimated from the GE 1000 MWe follow-on report.[9] Based on their neutron balance, the tantalum midcycle capture rate is 2.5×10^{18} captures/sec, which corresponds to an equilibrium activity of 7×10^{7} Ci. Since the half-life is 115 days, this activity would remain in the environment long after the rods were removed from the reactor.

5.2.5 Activated Corrosion Product Experience at Operating Sodium-Cooled Reactors

5.2.5.1 Summary

A review article by Zwetzig[11] contains information about corrosion products in sodium or NaK cooled reactors. Table 5.11 summarizes the corrosion products observed, in the manner which he used, with additions as referenced.

Table 5.11
Corrosion Products in Sodium-Cooled Reactors
(Other than Tritium)

	EBR-II[12,13]	Rapsodie[14]	SRE[11,15,16]	HPNF[11]	S8ER[11]
Neutron spectrum	fast	fast	thermal	thermal	thermal
Typical outlet temperature	900^{o}F		1000^{o}F	950^{o}F	1300^{o}F
Corrosion and Activation products in primary coolant	^{54}Mn, ^{124}Sb, ^{110m}Ag, ^{113}Sn, ^{113m}In, ^{117m}Sn		^{51}Cr, ^{54}Mn, ^{59}Fe, ^{60}Co		^{56}Mn, ^{60}Co
Corrosion products on primary system surfaces	^{54}Mn, ^{60}Co, ^{182}Ta	^{54}Mn, ^{58}Co, ^{60}Co	^{54}Mn, ^{59}Fe, ^{60}Co, ^{51}Cr	^{54}Mn, ^{60}Co	^{54}Mn, ^{59}Fe ^{58}Co, ^{60}Co
Corrosion and Activation products in cold traps	^{54}Mn, ^{60}Co ^{65}Zn, ^{124}Sb	^{65}Zn			

5.2.5.2 EBR-II

At EBR-II, the following products in the primary sodium are frequently monitored: ^{54}Mn, ^{110m}Ag, ^{117m}Sn, and ^{112}Sn - ^{113m}In. Of these only ^{54}Mn comes from corrosion of stainless steel; the rest are peculiar to EBR-II.

In December, 1970, the primary pump of EBR-II was replaced and qualitative information on activation products was obtained. Detailed results were reported in July, 1971.[12] Activation products on the pump prior to steam cleaning included ^{22}Na, ^{54}Mn, ^{60}Co, and ^{182}Ta. Also present was the fission product ^{137}Cs. In steam cleaning the pump, the following were removed: all of the ^{22}Na, 44-67% of the ^{54}Mn, 42-92% of the ^{60}Co, and ~ 65% of the ^{137} Cs. None of the ^{182}Ta was removed. On the uncleaned surface the ^{182}Ta activity was less than 0.1 of the ^{54}Mn activity. On the cleaned surface the activation products remaining were ^{54}Mn, ^{60}Co, and ^{182}Ta, listed in decreasing order of activity. Reference 12 speculated that the source of tantalum was the cladding of the antimony neutron source used in EBR-II.

It is noted that the presence of ^{58}Co, ^{59}Fe, and ^{51}Cr was not indicated in either Reference 10 or in any other of the ANL reactor development program progress reports.

Activation products and ^{137}Cs were also reported to be present on the inside surface of the reactor tank at the cover-gas-tank interface.[12] Both ^{54}Mn and ^{60}Co were present. It was postulated that ^{137}Cs vaporized from the sodium and redeposited on the tank wall, but it was not known how the ^{54}Mn and ^{60}Co got there.

Activated corrosion products were identified in the EBR-II cold trap from gamma scans.[13] These included ^{54}Mn, and ^{60}Co. Also activation products ^{22}Na, ^{134}Cs, ^{65}Zn, and ^{124}Sb were observed in the cold trap.

5.2.5.3 Rapsodie

In Rapsodie, the corrosion products ^{58}Co, ^{60}Co, and ^{54}Mn were observed on the primary pump after three years of operation at 24 MW(th) (500 equivalent full power days).[12] The ^{54}Mn activity distribution along the axis of the primary pump is shown in the report. Both ^{54}Mn and ^{58}Co were observed on the pipes of the primary system. The ^{54}Mn was distributed fairly uniformly along the pipes. The ^{54}Mn surface activity on the cold leg piping (400°C) is 2 to 5 times higher than on the hot leg piping (500°C). Values of ^{54}Mn surface activity varied between 0.1 and 1 μ Ci/cm^2.

5.2.5.4 SRE

Corrosion product contamination was observed on the piping walls of SRE.[13] The radionuclides ^{54}Mn, ^{60}Co, and ^{59}Fe were identified. The activity levels of these nuclides were roughly equal to the ^{137}Cs activity level on the piping, ∿ 0.01 μCi/cm^2, at shutdown on July 26, 1959.

As described in Section 7.2.4.4, Table 7.9, corrosion-product elements were concentrated in the primary cold trap at the SRE.[16] However, concentration ratios were not large, ranging from ∿ 10 to ∿ 100 for Fe, Ni, Cr, and Mn.

5.2.5.5 SEFOR

No data on radioactive transport of corrosion products was reported for SEFOR. However, a report on cold trap experience at SEFOR[17] did show some corrosion-product elements in the ∿ 200 lbs of sodium oxide removed from the primary cold traps. The following concentrations of impurities were listed for the SEFOR cold traps (Table 5.12).

Table 5.12

Weight Percent of Impurities in SEFOR Cold Traps

Element	ppm
Cu	200
Fe	50
Cr	20
Ni	6
C-(carbonate)	240
C	130

The copper was an unexplained surprise. The cold traps were not radioactive because the traps reported in Reference 17 were removed and analyzed prior to power operation.

REFERENCES (Section 5.2)

1. G. P. Wozadlo and C. N. Spalaris, "Corrosion of Stainless Steel and Deposition of Particulates in Flowing Sodium Systems," GEAP-13544, September, 1965.

2. P. Roy and M. F. Gebhardt, "Corrosion and Mass Transport of Stainless Steels in Sodium Systems," GEAP-13548, September, 1969.

3. W. F. Brehm, et al., 'Radioactive Material Transport in Flowing Sodium Systems", in Corrosion by Liquid Metals, Draley and Weeks, editor, pp 97-113, Plenum Press, New York, 1970.

4. A. W. Thorley and C. Tyzack, "The Corrosion Behavior of Steels and Nickel Alloys in High Temperature Sodium." Proceedings of Symposium on Alkali Metal Coolants, IAEA, Vienna, Austria, November, 1966.

5. T. J. Kabele, W. F. Brehm, D. R. Marr, "Activated Corrosion Product Radiation Levels Near FFTF Reactor and Closed Loop Primary System Components," HDL-TME 72-71, May, 1972. (Also identical results presented in Trans. Am. Nucl. Soc., 15, No. 1, June, 1973.

6. G. P. Wozadlo, C. E. Boardman, and M. L. Weiss, "Calculated Radioactivity of the FFTF Primary Sodium System Due to Mass Transfer," GEAP-13671, August, 1971.

7. G. B. Zwetzig and R. F. Rose, "Interim Description of a Computer Code (STP-1) for Estimating the Distribution of Fission and Corrosion Product Radioactivity," AI-AEC-12847, June, 1969.

8. Staff, Chemical Technology Division, ORNL, "Aqueous Processing of LMFBR Fuels" Technical Assessment and Experimental Program Definition," ORNL-4436, June 1970.

9. "Task-II Report, Conceptual Plant Design, System Descriptions, and Costs for a 1000 MWe Sodium-Cooled Fast Reactor," GEAP-5678, December, 1968.

10. BNL-325, Second Edition, Supplement No.2, "Neutron Cross Sections, Vol. 1, Z = 21 to 40," J. R. Stehn, M. D. Goldberg, B. A. Magurno, and R. Wiener-Chasman--Editors, May, 1964.

11. G. B. Zwetzig, "Survey of Fission and Corrosion-Product Activity in Sodium-or NaK-Cooled Reactors," AI-AEC-MEMO-12790, February, 1969.

12. Reactor Development Program Progress Report, ANL-7845,.p. 1.15, July, 1971.

13 Reactor Development Program Progress Report, ANL-RDP-7, p. 1.10, July, 1972.

14. R. de Fremont, "Observations on the Behavior of Radioactive Products in Rapsodie," DRNR/STRD, 71.1146, 1971.

15. R. S. Hart, "Distribution of Fission Product Contamination in the SRE," NAA-SR-6890, March, 1962.

16. A. I. Hansen, "The Effects of Long-Term Operation on SRE Sodium Systems Components," NAA-SR-11396, August, 1965.

17. A. D. Gadeken and M. C. Plummer, "SEFOR Cold-Trap Experience," GEAP-10548, April, 1972.

5.3 Activation Products

5.3.1 Sodium Activation

Sodium has the disadvantage that it is activated by neutrons. The principal activation product is ^{24}Na, formed by the absorption of a neutron by ^{23}Na. A second activation product is ^{22}Na also formed from ^{23}Na in an n,2n reaction. Although the ^{24}Na activity is far greater than the ^{22}Na activity during reactor operation, ^{24}Na decays with a 14.7 hour half life while ^{22}Na has a 2.6 year half life. Therefore in considering the long term environmental effects of storage of sodium after its use in an LMFBR, or the effects from dispersion of sodium by a sodium fire, the long half-life isotope ^{22}Na is more important than ^{24}Na. The ^{22}Na activity becomes greater than the ^{24}Na activity about ten days after reactor operation ceases.

5.3.1.1 Sodium-24

Sodium-24 in the Primary System

Calculation of the activity of ^{24}Na is straightforward since it does not result from a threshold reaction. A typical calculation is provided for the General Electric 1000 MWe conceptual design described in Reference 1. The equilibrium activity produced in the primary coolant is 2×10^7 Ci. It would have been of interest to compare this result with a result extrapolated from EBR-II, but Na activity in the primary system is not reported in the ANL Reactor Development Program Reports.

Sodium-24 Activity in the Secondary System

Sodium-24 can enter the secondary system in two ways--by leakage of ^{24}Na from the primary to the secondary system through small leaks in the intermediate heat exchanger and, in a pot-type LMFBR design, by direct activation of the secondary sodium. It should be noted here that leakage of sodium from the primary to the secondary system would normally be minimized by controlling the primary system pressure lower than the secondary so that leakage would be in the other direction.

Activation of secondary sodium in pot-type designs will be made small by shielding the secondary sodium loop from neutrons. No estimate of secondary sodium activation was available from conceptual design reports, and both FFTF and the Demonstration Plant will be loop designs instead of pot designs.

EBR-II is a pot-type design and some secondary ^{24}Na activity is reported. Early values reported in the ANL Reactor Development Progress Reports were corrected for an earlier calibration error in Reference 7. During 1972, the ^{24}Na activity in the EBR-II secondary system varied from 8.6 to 38 nCi/gm, with an average value of $\sim$ 20 nCi/gm. The secondary sodium inventory is 6×10^7 gm Hence the total secondary ^{24}Na activity is of the order of 1 Ci.

5.3.1.2. Sodium-22

Sodium-22 results from the threshold reaction, $^{23}Na(n,2n)^{22}Na$, the threshold for the reaction being 12.5 MeV. On decay a 1.28 MeV gamma and two 0.5 MeV gammas are released from positron annihilation.

Two estimates of ^{22}Na activity produced in a 1000 MWe LMFBR were compared. The first estimate is an extrapolation from measured data in EBR-II. The second is a result quoted by General Electric in their 1000 MWe follow-on report. These two estimates disagreed so greatly a third value was calculated for this report in order to try to understand the possible source of the disagreement. (A third comparison was possible, based on extrapolation from a calculation for SEFOR. However, the methods used for the SEFOR calculation were likely the same as for the GE 1000 MWe calculation so that the extrapolated result is not necessarily an independent calculation.)

EBR-II Extrapolation

Sodium-22 activity in the primary system of EBR-II has been measured. Knowing the ^{22}Na activity in EBR-II, the power level, the operating time, and the load factor, one can extrapolate approximately to the activity produced in a 1000 MWe LMFBR.

The ^{22}Na activity in November, 1972, in EBR-II was 60 nCi per gram of sodium in the primary system.[2] The primary system contains 90,000 gallons of sodium. The accumulated exposure at this time was 60,309 MWd.[2] During the year prior to November, 1972, the exposure was 10,446 MWd,[3] and the exposure had been fairly constant for the last four years. The power level has been 62.5 MW(th)* since 1970, before which it was 50 MW(th). Assuming that reactor operation has always been the same as the year prior to November, 1972, the load factor for EBR-II would be 0.46 and the chronological time for operation would be 5.75 years at 62.5 MWth.

The total activity, A, in November, 1972, was 60 nCi/gm in 90,000 gallons of sodium, or 17 Ci. This activity and the equilibrium activity, A_∞, are related by

$$A = fA_\infty \left(1 - e^{-\lambda_{22} t}\right)$$

where f = load factor

λ_{22} = ^{22}Na decay constant t = chronological operation time

---

*Since completing this investigation, it was learned that since about 1972 the actual power level has been about 9% below 62.5 MW(th), or approximately 57MW(th), even though 62.5 MW is still quoted as the "nominal" power. No modifications were made to the EBR-II calculated results given in this report to account for this lower power level.

Hence A_∞ = 47 Ci.

Next assume that the ^{22}Na equilibrium activity is proportional to the power level. The geometry and sodium volume fractions in EBR-II and a power reactor are different, but still the extrapolation is expected to be a reasonable approximation. Also the fission spectrum for the ^{235}U fuel of EBR-II is sufficiently similar to the fission spectrum for the Pu fuel in a power reactor, even above the 12.5 MeV threshold of the ^{23}Na(n,2n)^{22}Na reaction, that the different fuel does not introduce a large uncertainty in the extrapolation. One can extrapolate the activity after long operation in a 1000 MWe LMFBR (2500 MWth, 0.8 load factor) to:

$$A = (47\ \text{Ci})\ (.8)\ \frac{2500\ \text{MWth}}{62.5\ \text{MWth}} = 1500\ \text{Ci}$$

It is of interest to note that the ^{22}Na activity in EBR-II is increasing in a manner consistent with the equations utilized here. For example in November, 1971, the ^{22}Na activity was 54 $\frac{\text{nCi}}{\text{gm}}$, and the ratio of 60 nCi/gm to 54 is about equal to the ratio of $(1 - e^{-5.75\lambda_{22}})/(1 - e^{-4.75\lambda_{22}})$, where 5.75 yr and 4.75 yr are the chronological operating times for November, 1971 and November, 1972 respectively. (λ_{22} = .266 yr^{-1})

GE 1000 MWe Follow-on Value

The result for the 1000 MWe follow-on design reported by General Electric is:[1]

A = 9600 Ci

SEFOR Extrapolation

The calculated ^{22}Na equilibrium activity for a load factor of unity is 65 Ci[4]. The SEFOR power level was 20 MWth. Extrapolation to a 1000 MWe LMFBR at .8 load factor gives

A = 6500 Ci

This value is closer to the 1000 MWe follow-on result than the EBR-II extrapolation, but both are based on General Electric calculations which may have used the same ^{23}Na(n,2n) cross sections.

Present Calculation

Since the above results varied so widely, the ^{22}Na activity was calculated from the fission spectrum and the ^{23}Na(n,2n) cross section.

The activity was estimated from the equation:

$$A = \left[\sum_k N_{23,k} \int_{12.5\ \mathrm{MeV}}^{\infty} \sigma_{n,2n}(E)dE \right] f(1 - e^{-\lambda_{22}t})$$

where the subscript k refers to the region--core and blanket. The flux was obtained from the fission spectrum, normalized to the first group of a multigroup flux distribution. Details of the first-group flux calculation are given near the end of this section. The fission spectrum was represented by

$$\psi(E) = \sqrt{E}\, e^{-E/T}$$

where T = 1.41 MeV for ^{239}Pu. The cross section for the ^{23}Na(n,2n)^{22}Na reaction was obtained from BNL-325[5] (which used the 1963 data of Picard and Williamson), although a large margin of error was possible in reading the cross section as a function of energy.

The calculated equilibrium ^{22}Na activities generated in the core and blanket were

$$A(\mathrm{core}) = 2.4 \times 10^3\ \mathrm{Ci}$$

$$A(\mathrm{blanket}) = 0.3 \times 10^3\ \mathrm{Ci}$$

The activity of ^{22}Na produced outside the blanket was not calculated. It is probably small since the neutron leakage is small from the blankets, and in calculating the blanket flux (see next section for details) no leakage was allowed. There may be leakage of uncollided high energy neutrons into the sodium pool, however, which might provide a ^{22}Na source that is not negligible. In SEFOR, which was a small reactor with thin reflectors, the calculated ^{22}Na production outside the reflectors was ~25% of the total.

Based on the above results, the total ^{22}Na activity from a 1000 MWe LMFBR is estimated to be:

$$A \approx 3000\ (1 - e^{-\lambda_{22}t})\ \mathrm{curies}$$

One further estimate is possible, based on the recalculation of the integral

$$\int_{12.5\ \mathrm{MeV}}^{\infty} \sigma(E)\ \psi\ (E)dE$$

A value of 8.9×10^{-6} barns MeV$^{3/2}$ was obtained for this integral (see next section). For SEFOR the calculated value for this integral was reported[4] as 2.3×10^{-5}. Since the SEFOR ^{22}Na production rate, together with the extrapolation of 6500 Ci for the 1000 MWe LMFBR from the SEFOR numbers, was based on the SEFOR value for this integral, one would be justified in renormalizing the SEFOR extrapolation to our calculated integral. This renormalization gives:

$$A = 6500 \times \frac{8.9 \times 10^{-6}}{2.3 \times 10^{-5}} = 2500 \text{ Ci}$$

which is close to both the above estimated result of 3000 Ci and the result of 1500 Ci extrapolated from EBR-II.

Further Details of the ^{22}Na Activity Calculation

The sodium-22 activity is given by

$$A = \left[N_{23,c} \int_{\substack{12.5 \\ \text{MeV}}}^{\infty} \sigma_{n,2n}(E)\phi_c(E)dE + N_{23,b} \int_{\substack{12.5 \\ \text{MeV}}}^{\infty} \sigma_{n,2n}(E)\phi_b(E)dE \right] f(1-e^{-\lambda_{22}t}) \tag{1}$$

where $N_{23,c}$ = total # of atoms of Na-23 in the core

$N_{23,b}$ = total # of atoms on Na-23 in the blanket

$\phi_c(E)$ = space averaged, energy dependent flux in the core

$\phi_b(E)$ = space averaged, energy dependent flux in the blanket

$\sigma_{n,2n}$ = n,2n reaction cross section

λ_{22} = decay constant for ^{22}Na = .266 yr^{-1}

t = chronological time since initiation of reactor operation

f = load factor

$\phi(E)$ was obtained as follows: The high energy neutron flux is proportional to the fission spectrum, $\psi(E)$, where

$$\psi(E) = \sqrt{E}\, e^{-E/T}$$

where T = 1.41 MeV for Pu-239 fission

Hence $\phi(E) = \alpha\psi(E) = \alpha\sqrt{E}\, e^{-E/1.41}$ at high energy.

The integrals in Eq'n (1) were rewritten, following the method of reference 4, to obtain:

$$\int_{\substack{12.5\\ \mathrm{MeV}}}^{\infty} \sigma_{n,2n}(E)\ \phi\ (E)dE = \alpha \int_{\substack{12.5\\ \mathrm{MeV}}}^{\infty} \sigma_{n,2n}(E)\sqrt{E}\ e^{-E/1.41}dE = 8.9 \times 10^{-6}\alpha\left(\frac{\text{barn-neutrons}}{\text{Cm}^2 - \text{sec}}\right) \qquad (2)$$

The constant α was determined as follows. In terms of group 1 of a multigroup flux structure,

$$\phi_1 = \alpha \int_{E_{\ell,1}}^{\infty} \psi(E)dE$$

where $E_{\ell,1}$ is the lower energy of the group and $E_{\ell,1}$ is large enough that the energy spectrum throughout group 1 can be approximated by the fission spectrum. Hence, if ϕ_1 can be evaluated, then the proportionality constant α can be determined.

The flux ϕ_1 was estimated for a group structure for which $E_{\ell,1} = 3.7$ MeV. The flux in the core $\phi_{1,c}$ was evaluated from the neutron balance equation (i.e. the multigroup equation for group 1):

$$(DB^2 + \Sigma_a + \Sigma_{er} + \Sigma_{in})_{1,c}\bar{\phi}_{1,c} = \chi_1\ (\bar{\nu}\sum_i \Sigma_{fi}\phi_i)_{core}$$

where

$$(\sum_i \Sigma_{fi}\phi_i)_{core} = \text{total fission/sec in the core}$$

and the subscript 1,c refers to group 1 of the core.

For the blanket the equation for $\bar{\phi}_{1,b}$ was:

$$(\Sigma_a + \Sigma_{er} + \Sigma_{in})_{1,b}\bar{\phi}_{1b} = \chi_1(\nu\sum_i \Sigma_{fi}\phi_i)_{blanket} + D_1B^2\bar{\phi}_{1,c}\frac{V_{core}}{V_{blanket}} \qquad (5)$$

where the sources were both fission in the blanket and group 1 leakage from the core, and no leakage is assumed from the blanket.

The calculated fluxes were:

$$\bar{\phi}_{1,c} = 0.9 \times 10^{14}$$

$$\bar{\phi}_{1,b} = 0.8 \times 10^{13}$$

The integral in Eq'n (3) is $\int_{3.7\ \mathrm{MeV}}^{\infty} \psi(E)dE = 0.23$

Hence the proportionality constants, α, are:

$$\alpha(\text{core}) = 4 \times 10^{14}$$

$$\alpha(\text{blanket}) = 3 \times 10^{13}$$

The sodium-22 activities generated in the GE 1000 MWe Follow-on[1] core and blanket are:

$$A(\text{core}) = \frac{(N_{23,c})\ (9 \times 10^{-6}\alpha_c) f (1 - e^{-\lambda_{22}t})}{3.7 \times 10^{10}\ \text{dis/sec Ci}}$$

$$= 2.4 \times 10^3\ (1 - 3^{-\lambda_{22}t})\ \text{Ci}$$

based on the following numerical values:

$$N_{23,c} = 3.1 \times 10^4\ \frac{\text{atom-cm}^2}{\text{barn}}$$

$$\left(\begin{array}{ll} \text{from:} & \text{core volume} = 3.7 \times 10^6\ \text{cm}^3 \\ & \text{sodium volume fraction} = 0.37 \\ & \text{sodium density} = 0.85 \end{array}\right)$$

$$9 \times 10^{-6}\ \alpha_c = 3.6 \times 10^9\ \frac{\text{barn-neutrons}}{\text{cm}^2 - \text{sec}}$$

$$f = 0.8$$

$$A(\text{blanket}) = .26 \times 10^3\ (1 - e^{-\lambda_{22}t})\ \text{Ci}$$

$$A(\text{total}) = 2.7 \times 10^3\ (1 - e^{-\lambda_{22}t})\ \text{Ci}$$

REFERENCES (Section 5.3.1)

1. "Task 1 Report of 1000 MWe LMFBR Follow-on Work," GEAP-5618, p. 252, June, 1968.
2. Reactor Development Program Progress Report, ANL-RDP-11, November, 1972 (Limited-distribution report).
3. Reactor Development Program Progress Report, ANL-7887 November, 1971.
4. A. B. Reynolds and D. F. Sudborough, "SEFOR Shielding Nuclear Design Calculations," GECR-5199, p. 7-4 to 7-6, March, 1967.
5. J. R. Stehn, M. D. Goldberg, B. A. Magurno, and R. Wiener-Chasman, "Neutron Cross Sections," BNL-325, Second Edition, Supplement No. 2, May, 1964.
6. "Task II Report, Conceptual Plant Design, Systems Descriptions, and Cost for a 1000 MWe Sodium-Cooled Fast Reactor," GEAP-5678, December, 1968.
7. Reactor Development Program Progress Report, ANL-RDP-9, September, 1972 (limited distribution report).

5.3.2 Cladding Activation

The stainless steel structure in and near the core of an LMFBR becomes activated. The only part of this activation considered in this report is the fuel cladding activation, which is to be shipped from the site with the fuel.

For a fuel assembly design that has steel hexagonal cans enclosing the entire assembly (as in present FFTF and demonstration plant design), the steel can would contain from 50 to 100% as much steel as the cladding. The specific activity of this steel would be equal to that of the cladding. Hence the total steel activity shipped from the site would be nearly a factor of two higher than the cladding activity alone.

The cladding activity for the AI 1000 MWe Reference Oxide Design was calculated by ORNL,[1] and these values are reproduced in Table 5.13. These values were checked for order of magnitude by using cross sections and fluxes from Section 5.2 (Activated Corrosion Products) and approximate cladding volumes. The results agreed within factors of 2 to 3, which was considered acceptable for the purpose of this review.

The fuel mass discharged annually from the AI design was 8.517 MT (U + Pu) (see Table 4.1). The cladding activity discharged annually with the fuel is therefore 8.517 times the totals in Table 5.13. These results are given in Table 5.14.

Table 5.13

Cladding Activity of Spent LMFBR Core Fuel as a Function of Cooling Time[1]

Activity [Ci/MT(U + Pu)]

	Cooling Time						
Isotope	0	30d	90d	150d	300d	30yr	Half-life ($T_{1/2}$)
^{51}Cr	6.17×10^4	2.92×10^4	6.55×10^3	1.47×10^3	35		28 d
^{54}Mn	1.50×10^5	1.40×10^5	1.22×10^5	1.07×10^5	7.50×10^4		313 d
^{55}Fe	7.60×10^4	7.43×10^4	7.12×10^4	6.81×10^4	6.00×10^4	25.5	2.4 yr
^{59}Fe	1.03×10^4	6.52×10^3	2.59×10^3	1.03×10^3	1.00×10^2		45 d
^{58}Co	4.10×10^5	3.07×10^5	1.71×10^5	9.55×10^4	2.26×10^4		71 d
^{60}Co	1.35×10^3	1.33×10^3	1.31×10^3	1.28×10^3	1.20×10^3	25.9	5.2 yr
^{59}Ni	2.1	2.1	2.1	2.1	2.1	2.1	8×10^4 yr
^{63}Ni	67.8	67.7	67.6	67.6	67.5	54.1	92 yr
Total	7.09×10^5	5.58×10^5	3.75×10^5	2.74×10^5	1.59×10^5	108	

Table 5.14

Cladding Activity Discharged Annually From 1000 MWe LMFBR

Activity (Ci)

Cooling Time					
0	30d	90d	150d	300d	30 yr
6.0×10^6	4.8×10^6	3.2×10^6	2.3×10^6	1.3×10^6	900

REFERENCES (Section 5.3.2)

1. Staff, Chemical Technology Division, ORNL, "Aqueous Processing of LMFBR Fuels: Technical Assessment and Experimental Program Definition," ORNL-4436 (June, 1970).

5.3.3 Activation Products ^{39}Ar, ^{41}Ar, and ^{23}Ne

5.3.3.1 Argon-39

Argon-39 has a 269 year half life and undergoes β^- decay (0.59 MeV maximum β, no γ). It is produced from ^{39}K in the sodium coolant from the reaction: $^{39}K(n,p)\,^{39}Ar$. Although no reported observations of ^{39}Ar were found from operating fast reactors, Reference 1 estimates that 0.13 Ci/day of ^{39}Ar would be produced in the 975 MWe Clinch River Breeder Reactor (CRBR) if the potassium impurity concentration in the coolant were 1000 ppm. For reference, some potassium concentrations have been ~ 160 ppm in EBR-II (e.g. Ref. 2, and Table A.28 of this report) and ~ 300 ppm in SEFOR[3]. Our independent check on ^{39}Ar activity agrees with the Reference 1 value to within 50%, which is within the accuracy of the (n,p) reaction cross section available[4]. Extrapolating from the CRBR value, and assuming 300 ppm potassium impurity in the coolant, gives a ^{39}Ar activity production rate of ~ 30 Ci/yr for a 1000 MWe LMFBR.

5.3.3.2 Argon-41

This radionuclide has a 1.83-hr half-life and undergoes negatron decay to ^{41}K. ^{41}Ar can be produced in the LMFBR by two mechanisms: $^{41}K(n,p)^{41}Ar$ and $^{40}Ar(n,\gamma)^{41}Ar$. The EBR-II staff suspects that the first reaction is the principal production source in EBR-II.[5] EBR-II cover gas typically contains about 1.5 µCi of ^{41}Ar per liter of cover gas. Rapsodie was reported[6] to have a cover gas ^{41}Ar content of 200 µCi/ℓ and BR-5 a cover gas ^{41}Ar content[3] of 100 µCi/ℓ .

5.3.3.3 Neon-23

This radionuclide has a 37.6 sec half-life and undergoes negatron decay to ^{23}Na. ^{23}Ne is produced by the following reaction

$$^{23}Na(n,p)^{23}Ne$$

SEFOR was reported[8] to have a specific ^{23}Ne cover gas activity of 29,000 µCi/ℓ when operating at 10MW. With a cover gas volume of 0.56×10^6 cc, the total cover gas activity was 16.4 Ci from ^{23}Ne. The ^{23}Ne activity in the SEFOR core sodium was estimated to be 5700 Ci at 10 MW. From these numbers, the average time for disengagement of the ^{23}Ne atoms from the sodium was determined to be 5.5 min.

Rapsodie was reported[6] to have a cover gas ^{23}Ne content of 10,000 µCi/ℓ . Both the primary coolant and the cover gas of the #2 primary pump were analyzed for ^{23}Ne at BR-5.[7] The sodium contained 500,000 µCi/ℓ and the pump cover gas contained 700,000 µCi/ℓ .

REFERENCES (Section 5.3.3)

1. T. A. Nemzek, transmittal of Feb. 21, 1974, to universities, of WARD document, "Assessment of the Demonstration Plant Design Decisions", January, 1974.

2. Reactor Development Progress Report, ANL-7845, July, 1971.

3. G. Billuris, General Electric Breeder Reactor Department, personal communication of a 1967 analysis.

4. J. R. Stehn, M. D. Goldberg, B. A. Magurno, and R. Wiener - Chasman, "Neutron Cross Sections", BNL-325, Second Edition, Supplement No. 2, May, 1964

5. EBR-II Staff, personal communication, Dec. 1972.

6. CEA-R-3626 October, 1968.

7. V. V. Orlov, M. S. Pinkliasik, N. N. Aristarkhov, I. A. Efinov, A. V. Karpov, M. P. Nikulin, "Some Problems of Safe Operation of the BR-5 Plant," Paper Va-7, Proceedings of the Int. Conf. on the Safety of Fast Reactors, Aix-en-Provence, Sept. 19-22, 1967.

8. J. J. Regimbal, W. P. Kunkel, and R. S. Gilbert, "Measurement of Noble Gas Transport Dynamics in SEFOR Sodium," Trans. Am. Nucl. Soc. 14, No. 2, 773-774.

5.3.4 Miscellaneous Activation

5.3.4.1 From Fission Products

A number of radioactive nuclides are produced from activation (n,γ reactions) of fission products. In this report, these radionuclides are included under "fission products." They are listed in Tables 4.3-4.6, and indicated by the footnote "a." The "activation fission products" of importance are: ^{86}Rb, ^{110m}Ag, ^{110}Ag, ^{113m}Cd, ^{134}Cs, ^{148m}Pm, ^{154}Eu, and ^{160}Tb.

5.3.4.2 From Impurities in Sodium Systems

A number of miscellaneous activation products are reported from sodium-cooled-reactor operating experience. These are frequently peculiar to the particular reactor system and are generally low in activity level.

Such activation products observed in EBR-II include ^{65}Zn, ^{124}Sb, ^{125}Sb, ^{113}Sn, ^{113m}Sn, ^{117m}Sn, ^{110m}Ag, and ^{210}Po (see Appendix A Table A25). The ^{210}Po comes from the bismuth (^{210}Bi) in the tin-bismuth seal in the EBR-II cover. It is presumed that the ^{125}Sb, ^{113}Sn, ^{113m}In, and ^{117m}Sn come from activation of the tin. It is unclear whether the ^{110m}Ag results from activation of a fission product or activation of a silver impurity in the sodium. Also the source of ^{124}Sb is unclear--perhaps from activation of ^{123}Sb in the sodium. The ^{65}Zn presumably comes from activation of the ^{64}Zn present in the EBR-II sodium, although, like Sb, zinc is not listed as a trace metal in the sodium in EBR-II reports.

In Rapsodie, ^{210}Po was also observed.[1] Like EBR-II, Rapsodie has a tin-bismuth cover seal. Also ^{65}Zn was observed in Rapsodie.

In SRE, ^{125}Sb was observed.[2] The ^{125}Sb was reported to come from activation of ^{124}Sn. ^{110}Ag was observed in the cold trap of SRE, but the source is unclear.

In SEFOR, ^{110}Ag and ^{124}Sb were both observed in the sodium (see Appendix A, Table A22). Since the only other fission product observed in SEFOR was ^{86}Rb, and since Ag and Sb are listed (Table A21) as impurities in SEFOR sodium one can presume the ^{110}Ag and ^{124}Sb come from activation of these impurities.

REFERENCES (Section 5 3.4)

1. R. deFremont, "Observations on the Behavior of Radioactive Products on Rapsodie," DRNR/STR 71.1146, 1971.

2. R. S. Hart, "Distribution of Fission Product Contamination in the SRE," NAA-SR-6890. (March, 1962).

5.4 Tramp Fuel

Tramp fuel is the term used to describe fuel material present on the outer surface of fuel pins as a contaminant from the process of fuel fabrication. When this tramp fuel is exposed to neutrons in the core it becomes a source for direct introduction of fission products into the primary coolant.

The exact amount of tramp fuel present in any core will be a function of many things but primarily a function of the fuel element fabrication process.

Estimates of the amounts of tramp fuel in SEFOR[1] and in EBR-II[2,3] have been made. Neither of these reactors utilize fuels typical of those which will be found in large LMFBR's. The EBR-II fuel is metal rather than oxide and is therefore fabricated in a significantly different way from oxide fuels. The SEFOR fuel is indeed oxide fuel, but is of significantly different diameter than will be used in future LMFBR's.

Despite the nonprototypic fuel in EBR-II and SEFOR, the tramp fuel information from these reactors will be used to estimate tramp fuel inventories in a 1000 MWe LMFBR. The basic assumption for extrapolation from EBR-II and SEFOR data is that the mass of tramp fuel per unit length of fuel pin in the core will be similar for the large LMFBR.

5.4.1 SEFOR

The total tramp fuel inventory in SEFOR has been estimated[1] as 0.2 mg of fissile material, or about 1 mg of heavy metal fuel atoms. Based on a total pin length estimate[4] of 1740 ft., the inventory per foot of fuel pin in the core is 6×10^{-4} mg/ft.

5.4.2 EBR-II

E. R. Ebersole has estimated[2] the ^{235}U in tramp fuel in EBR-II to be 2 mg based on the normal tramp background of ^{133}Xe and ^{135}Xe observed in the cover gas. G. S. Brunson[3] claims an inventory of roughly 7 mg of unclad ^{235}U in the core. Since the EBR-II fuel is enriched to about 50% ^{235}U, a range of 4 to 14 mg of fuel is indicated for the amount of tramp fuel in EBR-II. On the basis of 6910 ft. of fuel pins in the core[5], a corresponding range of 5.79×10^{-4} to 2.03×10^{-3} mg/ft can be determined.

5.4.3 Rapsodie

No direct data are available for tramp fuel in Rapsodie; however, a tramp fuel inventory for Rapsodie which is in general agreement with that of EBR-II can be inferred from other published information as follows: Differences in fast fluxes, cover gas volumes, fissile fractions of core fuel, and total length of fuel pins in the EBR-II and Rapsodie cores tend to cancel. Therefore, ignoring cold trapping of precursors, the cover gas specific activities due to tramp fuel should be similar. Indeed this is found to be true. The ^{135}Xe activity in the EBR-II cover gas at saturation from tramp fuel[2,3] is about 3 x 10^{-3} μCi/cc. The measured saturation activity of ^{135}Xe in the RAPSODIE cover gas right after initial startup[6] was 1 x 10^{-2} μCi/cc.

5.4.4 Extrapolation to 1000 MWe LMFBR

The information on tramp fuel inventories presented above suggests the use of a value of 10^{-3} mg of heavy metal fuel atoms per foot of fuel pin in the core. Large LMFBR's will contain tens of thousands of fuel pins having total lengths of tens of miles. For an average linear power density of 9 kW/ft, the total core fuel length is ~ 250,000 ft. Hence, a total inventory of 0.25 gm of tramp fuel is estimated.

The coolant fission product inventory due to this load of tramp fuel can be estimated using the data of Reference 7. If no deposition or other removal mechanism is assumed for fission products which enter the primary sodium, about 300 curies of fission product activity could be present in the sodium for the equilibrium fuel cycle. Most of this activity would be from short-lived isotopes. The long-lived isotopes would eventually contribute an activity of a few tens of curies if the same primary sodium were utilized throughout a normal plant life.

The corresponding upper limit activities for the higher actinides would be 20 to 30 curies for the equilibrium fuel cycle with a buildup to a few curies of long-lived actinides over the plant life. It is important to emphasize that these estimates take no credit for cold-trapping, plating out, or other removal mechanisms for the radioactive nuclides.

The activities discussed above are quite small in magnitude compared to that from activation of primary sodium, impurities in the sodium, and corrosion products in the sodium.

REFERENCES (Section 5.4)

1. J. J. Regimbal, R. S. Gilbert, W. P. Kunkel, R. A. Meyer, and C. E. Russell, "Fuel Failure Detection Capability at SEFOR," Trans. Amer. Nucl. Soc., 14, 69 (1971)

2. R. R. Smith, et al., "Effects of Driver-Fuel Cladding Defects on the Operation of EBR-II," ANL-7787, Feb. 1972.

3. G. S. Brunson, "On-Line. Noble Gas Fission Product Monitoring in EBR-II," Nucl. Tech., 10, 33 (Jan. 1971).

4. Massoud T. Simnad, Fuel Element Experience in Nuclear Power Reactors, Gordon and Breach, New York, 1971, p. 596.

5. G. S. Brunson, R. M. Fryer, and R. V. Strain, "Post-Shutdown Surges in Cover Gas Activity in Experimental Breeder Reactor II (EBR-II)" Nucl. Tech. 13, 6 (Jan. 1972).

6. M. Chapelet, et al., "Experimental Study of the RAPSODIE Protections," CEA-R-3626, Oct. 1968. (In French).

7. "Aqueous Processing of LMFBR Fuels: Technical Assessment and Experimental Program Definition," ORNL-4436, June, 1970.

6. TRANSPORT OF FISSION PRODUCTS FROM FAILED FUEL

6.1 Introduction

The task of predicting activity releases to the primary coolant and cover gas from the fuel of an operating LMFBR is extremely complicated. At this time there is no consensus of opinion on almost every major question that arises in answering questions like the following: What fraction of the noble fission gases are released from a mixed oxide pellet operating under specific conditions? What are the release times for the gases from the pellet? What pin failure rate will be observed? How can the failures be characterized, e.g. size, location, time of occurrence, etc. For large cladding failures, how much of each of the various radionuclides will be leached from the exposed fuel by the flowing sodium?

These and other similar questions need to be answered before realistic release predictions can be made. This section contains partial answers to all of the questions listed above, and more. The fuel testing which will accompany operation of the FFTF should provide better answers. There is a considerable amount of art (engineering judgement) involved in the prediction of fuel performance today, due to limited experience.

Radioactivity releases from intact non-vented fuel in normally operating LMFBR's will be limited to tritium. Any non-vented fuel which is not intact will be categorized here as failed fuel; this includes either "leaky" fuel or fuel exhibiting gross cladding failure. These two types of failures will, of course, have significantly different consequences. The distinction between small holes in cladding and relatively large failures has been made with varying degrees of consistency in available literature on fuel failures, thus making it difficult to interpret reported failure rates.

Release from vented-to-coolant fuel will be treated separately, although much information from venting tests (e.g. holdup times, etc.) can be important in defining release rates from non-vented fuel.

The problem of activity release from fuel pins will be handled in two main parts: release of activity from the fuel proper, i.e. from the pellet, powder, etc.; and release of activity from the pin itself to the primary coolant. Each of these main parts of the problem will involve several subproblems and phenomena.

6.2 Brief Background Description of Irradiation Experience Relating to Fission Product Release

The FFTF, the LMFBR Demonstration plant, and probably the first generation of large (~1000 Mwe)LMFBR's will use mixed oxide fuels which are about 20% PuO_2 by weight and 80% UO_2. These fuel pins will probably consist of mixed oxide pellets and helium bond gas in an austenitic stainless steel cladding. Later reactors may employ so-called advanced fuels (carbides and nitrides instead of oxides), but the choice of oxide fuel for early plants is governed by the much more extensive experience and testing that has been achieved with oxide fuels, as opposed to carbide or nitride. However, even though there is considerable information available on oxide fuels, much uncertainty still exists about oxide performance under the extreme operating conditions forecast for LMFBR fuels.

Extremely high burnups (~100,000 MWd/MT)* and fast fluences (~3 x $10^{23}n/cm^2$) are the goals for LMFBR fuels. The fuel pins would undergo these irradiations while operating at peak linear powers of the order of 18 kw/ft with corresponding fuel surface and centerline temperatures of 1800°F and 4900°F, respectively, in flowing sodium with velocities of the order of 25 ft/sec and maximum outlet temperatures of 1300°F.[1,2]

The conditions described above have not been simultaneously achieved for fuel tests to date. Moreover, even while falling short of prototypic test conditions, problems have been encountered in oxide fuel testing which have not been completely solved and which may prevent achieving original performance goals.[3]

The main reason that oxide fuel problems have not been solved is the lack of appropriate test facilities. The fast fluxes of sufficient magnitude needed to achieve ~3 x $10^{23}n/cm^2$ have not been available. EBR-II and DFR require over three years to accumulate desired fast fluences. The FFTF will provide higher fast fluxes (achieving the desired fluence in about 1.5 years) for testing fuels, but its own driver fuel will be operating at slightly lower specific power and lower coolant, cladding, and fuel temperatures than proposed LMFBR's. Still, many of the limitations indicated today in fuel performance should be better quantified by FFTF programs. (Design burnup -- i.e. $\geq$ 100,000 Mwd/MT -- has been readily achieved in low power fast test reactors like EBR-II and DFR and in thermal test reactors by enriching the uranium portion of the UO_2 - PuO_2 fuel. However, the combination of design fast neutron fluence at the cladding and fuel burnup cannot be readily achieved.)

---

* Experimental fuel exposures appear in the literature both as atom percent burnup and as megawatt days per metric ton. The conversion factor is almost exactly: 1 atom % = 10,000 MWd/MT.

Fuel swelling and release of fission gases with resulting cladding stress due both to fuel-cladding mechanical interaction and to high fission gas pressures were early recognized as problems.[4] Satisfactory mitigation of the effects of these two phenomena can probably be achieved by (1) incorporating sufficient voidage within the fuel proper to accommodate solid fission products and any unreleased fission gases,[5] and (2) by providing sufficient plenum volume (or venting) to handle gases released from the fuel. However, knowledge of the amounts of gas released from the fuel but remaining within the pin is important in terms of potential releases.

Two unanticipated problems with the stainless steel cladding were discovered: the significant swelling of stainless steel on irradiation to high fast fluences,[6] and irradiation induced creep.[7,8] Austenitic stainless steels irradiated to fast fluences of the order of $7 \times 10^{22} n/cm^2$ have been observed to exhibit volume increases of as much as 7%.[6] Techniques such as heat treating prior to irradiation may reduce such swelling significantly;[9] however, even with the data on control thimble swelling of EBR-II, extrapolation by factors of two on fluence must be made.[3]

Creep rates of 304 stainless steel in a fast flux of only $5 \times 10^{12} n/(cm^2 sec)$ and a simultaneous thermal flux of $6 \times 10^{13} n/(cm^2 sec)$ have been found to be a factor of 2 to 5 higher than those of an unirradiated specimen.[6] Experiments on 316 stainless irradiated in EBR-II to fast fluences approaching $7 \times 10^{22} n/cm^2$ have shown creep rates increasing about tenfold while linear creep strain decreases fourfold.[10] Again extrapolations to fluences of $3 \times 10^{23} n/cm^2$ are needed.

More recently, Foster, et al.[66] have reported measurements on solution annealed and cold-worked types 304 and 316 stainless steel. The irradiation creep rates are linear with stress and essentially independent of temperature at low fluence levels. At high fluence levels there are limited data which indicate that irradiation creep increases as swelling becomes significant. The relationship between swelling and irradiation creep is of great technological significance to the design of fuel rods and assemblies. In particular, the beneficial role of irradiation creep in relieving the stresses created by differential swelling is becoming more clearly understood, and is being applied to core design.[67]

Because of the sensitivity of predicted total plastic strain to various levels of saturation of cladding swelling (10-15%) and fuel swelling (20-35%),[11] additional prototypic test data at high fluence and burnup is necessary to determine the combined effects of fuel swelling, fission gas pressures, cladding swelling, irradiation-induced cladding creep, and perhaps other, as yet undiscovered phenomena. Indeed, the ultimate limiting phenomena for fuel performance may be the deterioration of the cladding due to fuel-cladding interactions.[12]

The uncertainties indicated above make it difficult to predict failure rates and activity releases for LMFBR fuel pins operating at or near design conditions. Indeed, the ability of the reactor radwaste system to handle released activities from failed fuel will ultimately determine the quantity and quality of failed pins that can be accommodated in the core at one time.

The statistics of LMFBR oxide fuel pin irradiations have recently taken a sizable leap. As shown in Table 6.1, the number of pins irradiated or undergoing irradiation in the world's fast reactors was ∿ 110,000 as of January 1974. This total is up from ∿ 23,000 as a result of the startup of the Russian BN-350 and the French Phenix and replacement of fuel in existing fast reactors. Because the first three prototype LMFBR power stations plan to replace fuel at rather frequent intervals*, continued rapid growth in oxide pin operational statistics is expected.

These three early power stations will provide the first fast neutron irradiation experience on large multipin fuel assemblies at LMFBR prototypic temperatures and flow rates, and much more realistic fluence-to-burnup ratios, than have heretofore been possible.

6.3 Tritium Release from Fuel Pins

Tritium produced in the fuel from ternary fission or from lithium impurities in the fuel can diffuse through the stainless steel cladding of intact pins. Results of fast flux irradiation of stainless-steel-clad mixed-oxide fuel[13] indicate that more than 99% of the tritium produced in the fuel of large operating LMFBR's will be released to the primary coolant. Tritium produced in the fuel could introduce about 24,000 Ci/yr into the primary coolant system, as discussed in Section 5.1 of this report.

6.4 Release Fractions for Noble Gases from Oxide Fuels

Release fractions of 7 to 25% were observed in the initial fast-flux irradiation of PuO_2 - UO_2 fuel in EBR-II even though it was a very short irradiation.[14]

At about the same time information on the Russian BR-5 plutonium oxide fuel became available,[15] indicating release fractions of 40-54% for burnups of less than 3% and about 60% for burnups greater than 3.5%.

---

*BN-350 reportedly will have one-fifth of its fuel replaced every 54 days; Phenix will have one-sixth replaced at 60-day intervals, and the PFR (Prototype Fast Reactor) in Great Britain will have one-sixth replaced at 49-day intervals.

Table 6.1
Oxide Fuel Pins Irradiated in LMFBR's [67]

	Completed	On-Going	Total
USSR			
BR-5	~ 2,490		
BR-10		~1,520	
BOR-60	~ 8,000	3,400	
BN-350	~ 8,000	38,200	61,600
France			
DFR	41		
Rapsodie-Core I	4,305		
Rapsodie-Fortissimo	~13,600	~3,700	
Phenix		23,002	44,650
USA			
SEFOR	648		
EBR-II	~800	~1,000	~2,450
UK			
DRF	~800	~200	~1,000
DEBENELUX			
Rapsodie	73		
DRF	48	60	181
Other			~150
TOTAL	~38,800	~71,100	~110,000

The first data from Rapsodie,[16] which uses mixed-oxide sintered fuel pellets in 316 SS cladding, showed gas releases of up to 60% for pins operated at peak powers of 12.2 kW/ft to burnups of 20,000 MWd/MT.

One of the largest sets of experimental data is that from the General Electric F2 Series. The series consisted of 21 encapsulated fuel pins in an experimental program designed to "investigate such parameters as fuel density, compaction process, stoichiometry, diametral and axial gap, cladding material, and cladding wall thickness."[17] Results of the irradiations have been published as data became available.[5,17-20] The results are summarized in Table 6.2. The fission gas releases are seen to approach 100% at high burnups and are not strongly a function of initial fuel density in this range of burnup.

Table 6.3 shows irradiation results of twelve other mixed-oxide fuel elements irradiated in EBR-II under Argonne National Laboratory's fuel element performance program. The first group of four ANL elements were some of the first unencapsulated elements to achieve large burnups in EBR-II. The NUMEC[21] elements were designed to give a comparison of fabrication processes. The last group of four ANL elements were designed to assess various void deployment techniques in accommodating fuel swelling. The information in Table 6.3 is mostly from Reference 22. The data indicate that fission gas release approaches 90% at 10 at% burnup (~ 100,000 MWd/MT.)

Other irradiations such as the PNL tests[23] could be added to these examples, but the trend is clear. On the basis of data presented here plus other irradiations in EBR-II or DFR, Lambert, et al., have concluded that, for fuel operating in the linear power range expected for LMFBR's (9 to 18 kW/ft), fission gas release increases with burnup in the manner shown in Table 6.4, regardless of initial smear density or form of fuel.[22]

The experimental information presented thus far in this section provides a good basis for estimating fission gas release from fuel in LMFBR pins. Moreover, the proliferation[24] of theoretical models to explain the data will hopefully aid in extrapolation of data to other conditions through an understanding of the phenomena involved.

In order to estimate activity release from failed pins to the coolant from the above information, the burnup of the failed pins must be known. It is a reasonable assumption that failure rates will also increase with burnup. This has certainly been borne out by experience.[25,26] If most of the pins do achieve the goal burnups, then the highest rate of failures would occur at burnups approaching 100,000 MWd/MT. This argument leads to the assumption that the "average" failed pin contains fuel which has released at least 75% of its total inventory of noble fission gases and will continue to release noble gases at about the same rate as they are produced.

Table 6.2

General Electric F2 Series of Fuel Pin Irradiations

Pin	Fuel Density Smeared (% Theoretical)	Fuel Density (% Theoretical)	Max Linear Power (kW/ft)	Peak Burnup (at. %)	% Fission Gas Release
F2A	94.0	95.6	15.6	5.19	49
F2B	94.6	95.2	16.0	5.26	48
F2E	94.4	95.3	16.3	5.35	NA
F2F	94.8	96.1	16.3	5.33	50
F2N	92.6	96.2	17.7	5.42	50
F2P	94.5	95.6	9.7	3.26	32
F2Q	94.9	96.2	16.3	5.25	47
F2S	96.1	97.1	17.4	5.49	55
F2U	87.0	89.5	15.8	5.61	63
F2W	83.8	NA	13.6	5.08	58
F2Y	83.9	NA	13.3	4.91	56
F2Z	87.2	89.2	15.7	5.50	58
F2C	93.1	94.6	16.1	7.20	64
F2H	94.9	95.3	16.7	7.30	67.5
F2R	95.2	95.3	16.1	7.17	60.8
F2T	94.6	96.1	16.9	7.07	59.2
F2O	94.0	95.8	16.1	7.39	NA
F2D	94.3	96.4	16.5	12.8	NA
F2G	93.0	95.6	16.1	12.7	~100
F2V	86.7	89.7	15.7	13.1	NA
F2X	83.9	NA	15.3	11.9	~100

Table 6.3

ANL Irradiations in EBR-II

Pin	Fuel Density Smeared (% Theoretical)	Fuel Density (% Theoretical)	Max Linear Power (kW/ft)	Peak Burnup (at. %)	% Fission Gas Release
ANL-012	78.5	81.1	16.0	2.91	69.1
ANL-007	78.6	79.0	15.7	4.73	82.1
ANL-021	80.2	82.8	16.4	4.7	85.6
ANL-026	82.5	85.2	17.0	4.7	NA
NUMEC B-2	88.8	90.6	15.0	9.8	89.8
NUMEC C-1	88.4	91.1	14.7	10.9	95.7
NUMEC C-11	88.3	89.8	14.0	10.9	90.8
NUMEC C-15	82.7	84.4	12.9	10.6	68.0
ANL SOPC-1	80.0	82.2	14.5	3.6	69.0
ANL SOPC-3	82.7	85.3	14.8	3.5	62.6
ANL SOPC-5	77.1	86.0	12.1	3.2	56.4
ANL SOVG-17	80.0	NA	13.7	3.5	59.5

Table 6.4

Percent of Fission Gas Released vs Fuel Burnup

Fuel Burnup (MWd/MT)	Fission Gas Released (%)
<2000	~30
30,000	~50
50,000	~70
100,000	>85

6.5 Fuel Failure Rates

As discussed previously, failures can be of two types: small leaks and gross cladding failures. No data is available which gives failure rates of either type for fuel pins tested under prototypic 1,000 MWe LMFBR conditions. For this reason, failure rates and failure types will be assumed for example calculations in this report, using available experience as a guideline, but with emphasis on the fact that realistic rates must await future experience. Certainly, the failure rates which will be tolerated will depend on the coolant and cover gas cleanup systems.

Some overall feel for fuel reliability can be obtained from numbers presented by Bernath and Wolfe[27] in April, 1971. In summarizing world-wide fast reactor experience at that time, they pointed out that less than 2% of all rods tested had failed. Ignoring the BR-5 failures,[25] which resulted when pins with very small fission gas plena were pushed well past their design limit, less than 0.5% have failed. This picture gets even better if DRF failures[28] caused by cover-gas entrainment in the coolant are ignored. However, it is important to note that different fuel tests have different goals (conditions at specific burnup, power, etc.) and are not all aimed at achieving high burnups. For example, the first twelve pins of the General Electric F Series tests were removed after burnups between about 35,000 and 60,000 MWd/MT.[19]

The only extensive oxide driver fuel experiences have been obtained from BR-5 and Rapsodie, together with limited experience at SEFOR. The BR-5 experience,[25] as indicated above, was intentionally oriented toward run-to-failure with the goal of learning the effects of operating with leaking fuel elements. Also BR-5 used straight PuO_2 in its first core, not a mixed oxide.

Experience with the 24 MW core at Rapsodie has been encouraging. Through February 22, 1970, when the reactor was shut down for modification, no operation-limiting failures had been observed in Rapsodie test pins in nearly three years of operation.[29] However, the reactor core was known before shutdown to contain at least one failed fuel pin with direct contact between the sodium coolant and the fuel.[30,31] Twenty of the driver fuel subassemblies had obtained a burnup of 50,000 MWd/MT compared to a design value of 30,000 MWd/MT.[32] However, the gross cladding failure did not occur in any of these assemblies. It was found in a pin which had achieved a burnup of 40,000 MWd/MT and a fast fluence of 4 x 10^{22}n/cm^2 at a linear power of only 6.3 kW/ft.[33] It was concluded from instrument records that the rupture had occured in January, 1969, when the pin had experienced a burnup of only 24,000 MWd/MT. Also there were indications that the pin had started leaking at 16,000 MWd/MT.

It is important to note that this is only one pin out of 2300, and no gross cladding failures were observed in the higher burnup pins which had operated at twice the power (~12 kW/ft). However, several leakers have been observed during Rapsodie operation, including at least three during the first year of operation.[34] Conservative overall failure rates of 0.5% with 10% of these gross cladding failures could be inferred from the very limited data.

Reports of fuel failure experience with the Rapsodie "Fortissimo" (40 MW) core are not available. This experience should be followed closely since the failure rate may be significantly higher for the new core.[35]

Experience at SEFOR was even better than at Rapsodie, but this experience is not as significant with regard to fuel operation. No failures of any type were detected in the first two years of operation.[36] Perhaps this was to be expected because of the much thicker cladding in SEFOR, combined with much smaller power densities and fast fluxes as compared to Rapsodie.[37] Indeed SEFOR was designed to check physics characteristics, especially the Doppler effect, rather than to serve as a fuel irradiation facility.

In conclusion, the available experience with fuel failure rates can only give very general guidelines. For purposes of creating a source term for the primary coolant in this report, a failure rate of 1% will be assumed, 10% of which are gross cladding failures (i.e. overall 0.1% gross cladding failure).

6.6 Leakage of Fission Products from Failed Fuels - Gaseous and Solid

An important factor in determining noble gas activity in the primary coolant due to failed fuel is the rate at which gases can escape through the pin defect. The degree of enhancement of concentrations of long-lived vs. short-lived isotopes (or the corresponding daughters of such isotopes) in cover gas samples is an indication of release rates to the coolant and transport times in the coolant to the cover gas.

6.6.1 Escape Rates from Plenum to Sodium

Mixed-oxide pins irradiated to burnups of ~40,000 MWd/MT in EBR-II were punctured at different axial locations to measure escape rates.[38] The results indicate that the fuel and insulator columns provide significant resistance to gas releases. The times required to release 50% of the noble gases varied from less than a minute to about 20 minutes, depending on the puncture location. Punctures at the top of the fuel, at the top insulator, and in the plenum all released over 80% of the gas within about two minutes. One bottom insulator puncture released 80% of the gas in four minutes. From this data, an average release time of about four minutes seems reasonable. Two limiting factors about the experiment were that the test was run out of pile and that the sizes of the punctures were not given.

Carelli and Coffield[39] calculated internal pin pressures as a function of time after failure for punctures of areas 10^{-6} in^2 and 10^{-4}

in^2. The larger hole gave almost complete gas release for various puncture locations in a matter of seconds. The smaller hole held up the gas release to about three minutes, consistent with the measurements of Reference 38.

Other experimental measurements of release times have given quite different results. Studies by Gregoire, Novak, and Murata[40] on two mixed oxide pins in naturally convecting NaK indicate much larger delay times. The pins failed while under irradiations in the General Electric Test Reactor (GETR) at a burnup of about 18,000 MWd/MT. The one pin on which plenum depressurization results were given required about four hours for total gas escape, with the peak escape rates within the first 45 minutes after failure. The pin was continually moved to lower power regions during the time immediately after failure, so the results are not exactly applicable to full power operation either. Moreover, although many cracks were observed in the failed region (14 inches below the plenum), no areas were given.

A more recent GE test[41] showed even longer release times, but is not really applicable to sitations of interest here because the pins had only undergone 3900 MWd/MT irradiation at the time of defection. This test is more applicable to determination of in-fuel diffusion rates.

At this point one is left with a wide range of five minutes to one hour for possible delay times for release of plenum gas from the fuel pin.

6.6.2 Transit Time from Failure to Cover Gas

Delay times for transit to the cover gas from the defected pin may show less uncertainty. These times will, of course, depend on reactor and vessel dimensions, coolant flow rates, etc.

A number of measurements of the transit time between fuel and cover gas have been made. Measurements in SEFOR[36] on disengagement times for ^{23}Ne gas of 5.5 min. from core to cover gas were assumed to be the same as for fission gas bubbles.[36] Studies in Rapsodie[42] (the Tempête tests) were made on disengagement times for noble gases released from the lower region of Rapsodie pins. The results indicated that "once the clad barrier is passed, the transfer of xenon and krypton from clad failures from the pin to the reactor cover gas will be fast and practically complete". The Tempête test results indicated disengagement times of the order of a few minutes, thus agreeing with SEFOR results. This also agrees with previous out-of-pile results from Atena[43] and with observed cladding failures at Rapsodie. An averave assumed disengagement time of 5 to 10 minutes could be inferred from the SEFOR and Rapsodie data.

6.6.3 Time for Diffusion out of the Fuel

From the previous discussion, a delay time of five minutes to one hour seems reasonable for gas which has already been released from the fuel proper but is still inside a leaking pin. Another delay of the order of five to ten minutes might be seen in transporting noble fission gases to the cover gas. However, these total delay times of 10 to 70 minutes may well be insignificant compared to the time required for fission products, whether noble gas, semi-volatile, or solid, to diffuse out of the main body of the fuel proper.

A recent GE test cited previously[41] indicates diffusion times for noble gases of the order of many hours. Perhaps the best data for operating pins is that obtained from Gulf General Atomic experiments at ORNL.[44] From this data a diffusion time of the order of twelve hours is indicated for noble gases. Often the assumption is made that other elements diffuse much more slowly in reactor fuel; however, the results of Davies, Long and Stanaway[45] indicate migration times for iodine, tellurium, and cesium comparable to the noble gases.

6.6.4 Diffusion Direction

The question of diffusion times leads logically to the question of diffusion direction. Elements which tend to diffuse toward the center of the pin, i.e. up the temperature gradient, may contribute significantly less to coolant contamination from gross cladding failures than those elements which diffuse down the temperature gradient. Note, however, that some elements may have high concentrations at both the central void and at the outer surface, with minimal in between. A fair amount of migration behavior has been determined.

In mixed oxide fuels operating at sufficient linear powers (> 11 kW/ft), plutonium will preferentially migrate to the central void,[46] apparently by preferential vapor transport mechanisms. This phenomenon is desirable in the sense that it reduces the amount of plutonium that can be leaked into the coolant. The plutonium migration is undesirable because of its effect on the Doppler Coefficient (small effect) and on the maximum allowable power rating (bigger effect).[47]

Duncan, et al.,[48] have observed fission product migration in the F Series of fuel pin tests. Volatile elements such as I and Cs migrate to the cladding. Some elements, such as the noble metals Mo, Ru, Rh, Tc and Pd, form metallic ingots in the center void of high burnup fuels. Other elements, such as Ba, Zr, and Sr, in the form of oxides, produce nonmetallic deposits on the walls of the central void. These nonmetallic deposits all contain some Pu and U oxides.

Lambert, et. al.,[49] also observed outward radial migration of Cs along with axial migration. They also found the noble metals mentioned above in the form of metallic ingots in the central void. In addition they detected Zr, Nb, and Ce by gamma spectroscopy which indicated the presence of ^{103}Ru, ^{106}Rh, ^{95}Zr, ^{95}Nb, and ^{141}Ce.

Johnson, Steidl, and Crouthamel[50] observed similar behavior for ^{137}Cs as was given in References 48 and 49. Reference 50 also indicated a ^{137}Cs as was given in References 48 and 49. Reference 50 also indicated a ^{137}Cs increase near the central void, with a minimum ^{137}Cs concentration at an intermediate radius. Essentially uniform concentration of Ce and the other rare earths was observed, while Mo increased markedly in concentration in the outward radial direction.

The outward radial migration of cesium is unfortunate in two respects. First of all, cesium oxide is apparently important in cladding corrosion[51] (along with MoO_2). Moreover, when the cladding fails the Cs then has access to the sodium coolant. The same undesirable access to sodium is achieved by I in its migration outward.

6.6.5 Experimental Data on Transport of Specific Fission Products to the Sodium or NaK Coolant

The migration behavior described above is generally borne out by experience. General Electric has run a series of tests on irradiated defected fuel to determine leakage of fission products from the fuel.[40,41,52,53,54] The tests varied greatly in important aspects such as burnup of fuels tested (3900 to 41,000 MWd/MT at failure), environment (in-and-out-of-pile), coolant, coolant velocity, and size of defects (0.0007 in^2 to 0.050 in^2).

Fuel pin B9A[52] was irradiated to only 8700 MWd/MT before being intentionally defected by three 31 mil holes (each of area 0.00075^2 lined up within a one inch notch but in the cladding. The only really non-prototypic condition was the low sodium velocity. Almost no ^{103}Ru or ^{95}Zr was released to the coolant (as opposed to previous tests). However, almost all of the ^{137}Cs left the fuel. Less than 1% of the fuel was lost from the pin. In general leakage of both fuel and non-gaseous fission products from pinhole defects is extremely slow relative to leakage from the large defects in experiments reviewed below.

Rods B9D-1 and B9D-2[41,54] were intentionally defected under irradiation at a burnup of 3900 MWd/MT. The defects were 30 mil holes (area of about 0.0007 in^2). Information on the sodium contamination should be available soon for comparison with B9A.

NaK cooled pins B3B and B3c[40] had ruptures much larger than pinhole defects. The NaK analysis from these tests showed the presence of many radionuclides. Table 6.5 shows the analysis of the B3C coolant. Both pins failed at about 18,000 MWd/MT in GETR, and B3C was left in up to 53,000 MWd/MT. B3B lost 1% of its fuel; B3C lost 5 to 10%. Most of the Cs which got into the NaK of B3C remained there, and only a small amount plated out. The ruptures in B3B were several separate small cracks. There was one large continuous rupture in the B3C cladding.

Table 6.8

Leaching Results from Grossly Befected Oxide Pin (B3C) in NaK[40]

Isotope	Concentrations in NaK (atoms/gm NaK)	Plateout Concentrations (atoms/in^2)
^{134}Cs	2.4×10^{15}	1.23×10^{13}
^{137}Cs	2.1×10^{17}	1.42×10^{15}
^{144}Ce	7.7×10^{10}	$.96\times10^{15}$
^{106}Ru	4.2×10^{11}	2.9×10^{14}
^{103}Ru	9.0×10^{13}	6.1×10^{15}
^{125}Sb	1.3×10^{11}	1.5×10^{14}
^{95}Zr	3.2×10^{12}	3.6×10^{14}
^{91}Y	$<8.9\times10^{14}$	$<9.7\times10^{13}$
^{239}Pu	* $.54\times10^{-3}$	** 12
U	*1.3	—

* μgm/gm NaK

** μgm/in^2

An intentionally defected section of fuel pin F2U which had been irradiated to 41,000 MWd/MT was exposed to 1150^{0}F flowing sodium for 18 hours.[53] The defect had an area of about .050 in^2, versus $\sim$.002 in^2 for B9A. There was substantial loss of selected measured fission products (shown in Table 6.6) but less than 1% loss of fuel, with uranium preferentially escaping compared to plutonium (presumably because of Pu migration toward the center of the pin). Leached fuel deposits showed U/Pu ratios of from 1643/1 to 42/1, compared to an original ratio of 4/1.

The BR-5 experience[25] is generally consistent with the above test results. The first indication of gross cladding failure was detection of ^{137}Cs in coolant samples. The most important results for determining defective fuel source terms is that the escape fractions of ^{137}Cs, ^{136}Cs, and ^{133}Xe, were an order of magnitude higher than the escape fractions of ^{131}I, ^{95}Zr, ^{95}Nb, ^{140}Ba, ^{140}La, and ^{135}Xe. Also, the ^{131}I and ^{136}Cs activities were appreciable only with very large leaks. In addition to the major radionuclides discussed above, small amounts of ^{144}Ce, ^{144}Pr, and ^{106}Ru were found in the BR-5 primary coolant.

6.6.6 Theoretical Models for Fission Product Transport

Theoretical models to describe the migration of the various chemical species and thus their availability for transfer through failed cladding to the coolant, have been available since the late 1950's. A simple diffusion model concerned strictly with fission product concentrations within isothermal particles or grains was developed by Booth.[55] Neglect of the temperature gradient present in operating fuel renders the Booth model inadequate, however. Others[56,57] have used Booth's release equations and have included the effect of fuel surface temperature gradients. These[56,57] models have been widely used. Yuill, et. al.,[58] have derived the relationship between release fraction and temperature gradient directly from equations for diffusion in the fuel controlled by the Gibbs free-energy gradient. Models which incorporate both concentration and temperature effects have been moderately successful, but release estimates used for the example calculation in the present report will be based on experimental work.

6.7 Vented Fuel

Vented fuel is of interest for two reasons. First it may be desirable to use vented fuel, either for safety reasons or simply to maintain cladding integrity to the high burnup goals of LMFBR's. In addition, the experimental work from vented fuels gives added information on release rates from the fuel and from the pin which can be used in analysis of defective non-vented fuel.

A good discussion of vented fuel elements is given by Keilholtz and Battle.[59] Little new work on vented fuel has been reported since their paper. One possible venting design not discussed in

Table 6.6

Loss of Fission Products from Grossly Defected Oxide Fuel in Flowing Sodium[53]

Nuclide	% Loss From Fuel
^{137}Cs	66
^{144}Ce	32
^{106}Ru	85
^{90}Sr	29
^{147}Pm	32
$^{95}Nb\text{-}Zr$	<1
^{125}Sb	<1
U,Pu	<1

Reference 59 was a modified "diving bell" concept[60] with separate inlet and outlet capillaries that is mucy shorter than the original GE "diving bell" design.

The main arguments[62] for vented fuel elements have been ones of long term performance and safety: fewer cladding failures because of reduced fission gas pressure buildup, better transient behavior with respect to coolant voiding because of reduced amounts of gases available, and reduction of failure propagation that might be caused by blanketing of neighboring pins by gas expelled from failed non-vented pins.

If the dominant mechanism for fuel failure turns out to be a combination of fuel and cladding swelling, mechanical property change of the cladding under irradiation, and/or fuel-cladding interactions, the first argument for vented fuel given in the previous paragraph may not carry much weight. Thus, the main arguments may be ones of safety, e.g. no sudden gas bursts to add reactivity, or propagate failures, or possibly transport fuel.

One disadvantage of using vented fuel (other than the obvious complications of increased shielding plus larger cover gas and sodium cleanup system) is the possible transport of non-gaseous fission products from the fuel to the coolant. This could happen by diffusion of volatile elements (such as Cs) or by release of gaseous precursors which subsequently decay to solids. (See the notes on DFR experience at the end of this section).

One additional disadvantage may be a long term buildup of certain radionuclides in the primary sodium, notably ^{134}Cs, produced by neutron activation of ^{133}Cs, a daughter of ^{133}Xe.

Whatever the final judgement is on use of vented fuel, the testing of vented fuel has produced valuable data on release fractions of various radionuclides.

The work of O'Neill, et. al.[61] on mixed oxide fuel exposed to 16,500 MWd/MT in a thermal flux gave the following major results:

1. About 44% of noble fission gases were released from the the fuel proper, i.e. were available for venting.

2. Effective gas delay time was 5 days.

3. Dominant sodium activity after decay of ^{24}Na was ^{134}Cs, although this would be less of a problem for fast fluxes.

4. Release fractions of all isotopes (including fissile) except for the noble gases were extremely small - in the range of 10^{-10} to 10^{-6}.

Table 6.7 gives measured release fractions. It is a reproduction of Table 5.1 from Reference 61. Note that all of the long-lived ^{85}Kr which was released from the fuel proper escapes while smaller amounts of the other, shorter-lived radionuclides escape.

The delay time is due to diffusion through the fuel proper, then flow upward past the fuel pellet and blanket pellets, and finally movement through the venting device.

Other experience with vented fuel has been quite limited with the exception of the Dounreay Fast Reactor (DFR). The Dounreay experience is not entirely applicable, because DFR uses NaK-bonded, niobium-clad, uranium alloy metal fuel rather than gas-bonded mixed-oxide fuel. Concentrations of delayed-neutron emitters in the primary coolant (NaK) were so high that it appears that much of the uranium was, in effect, directly exposed to the primary coolant.[64]

Much experience has been gained from DFR operation, however, which is valuable both in terms of evaluating vented fuel and in terms of fast reactor operation in general.

Many problems have been encountered in the years of DFR operation,[63,64,65] few of which, however, were a direct result of using vented fuel.

Modification of many joints in the blanket gas system was found to be necessary in 1962 after airborne levels of radioactivity in the containment sphere rose to 100 times background.[64] The major activity at that time was found to be ^{88}Rb (17.8 min. half-life) and ^{138}Cs (33 min. half-life), nuclides that are not generally a problem in non-vented fuel operation. For the vented DFR fuel, the noble gas precursors of these nuclides were transported to the containment sphere atmosphere, where they decayed.

Blanket gas samples[64] in normal operation show activities due to ^{133}Xe, ^{135}Xe, and ^{41}A which vary by as much as a factor of 100 depending on the sampling location. Typical values for the Xe isotopes are on the order of 10^7 dpm/cc. A table of possible radionuclides accounting for measured activities in the NaK is given in Reference 64. Amounts of U and Pu in the primary circuit are small (less than 0.5 gm and 20 mg. respectively.) Coolant activity during normal operation is about 100 times that due to ^{24}Na, with ^{138}Cs the major nuclide of interest.

The data presented above for DFR are so different from expected vented oxide fuel behavior (due mainly to the effectively direct exposure of so much of the DFR fuel surface to the primary coolant) that it can contribute little to estimating activities from either vented or failed mixed-oxide fuels.

6.8 Example Calculations of Releases of a Few Selected Radionuclides to the Primary Coolant and the Cover Gas System

Table 6.7

Isotopic Release Fractions from GE Vented Fuel Test

Radionuclide	Half-Life	Release Fraction
Noble Gases:		
^{85}Kr	10.76 yr	0.44
^{131m}Xe	11.96 d	0.30
^{133}Xe	5.27 d	0.27
^{133m}Xe	2.26 d	0.05
^{135}Xe	9.16 h	0.0003
Solids:		
^{103}Ru		$4\text{x}10^{-10}$
^{131}I		$1\text{x}10^{-8}$
^{137}Cs		$1\text{x}10^{-6}$
Other (Sr, Y, Zr, Ba, Ce)		10^{-8} to 10^{-6}

From discussions and data already presented in this section, it is clear that predictions of releases from the fuel are dependent on a large number of complicated factors, the biggest one of which is: how much activity can the cleanup systems and containment handle and still satisfy federal guidelines and regulations. This factor will obviously be the governing one. However, example calculations will be made here using several assumptions (some based on available information and some arbitrary) of possible releases from failed fuel in an operating 1000 MWe LMFBR.

Assumptions will include the following:

1% failed fuel

90% of the failed pins are leakers

10% of the failed pins have gross cladding failures

75% of the fission gas is released from the fuel proper, i.e. pellets, of the failed pins.

For the gross failures, the following percentages of long-lived elements are assumed to escape:

Fuel	1%
Br, I, Cs	15%
Te, Ru, Tc, Mo	5%
All Others	1%

The choice of escape fractions was based on relative volatility of the elements (or their oxides) and release data from References 40 and 53. Escape fractions based on only the volatilities and Reference 40 data would have suggested lower values for the group of Te, Ru, Tc, and Mo and for the group of "all others." On the other hand, Reference 53 suggests much higher release percentages. Neither test was prototypic so a compromise was made. Limited BR-5 data available generally support the choices for long-lived Cs and "all others." Plutonium fractions in the released fuel will be assumed equal to 0.1 of the original fraction based on observed preferential leaching of the uranium, due partially to plutonium migration.

At Westinghouse's Advanced Reactors Division, the following escape rates are assumed:[67]

Noble Gases $$f = \frac{1 - e^{-1.5 \times 10^5 \lambda}}{1.5 \times 10^5 \lambda}$$

Halogens $f = 0.2 \frac{1 - e^{-1.5 \times 10^6 \lambda}}{1.5 \times 10^6 \lambda}$

Alkali Metals (Cs) $f = 1$

All Others $f = 0.01$

where f is the fraction of fission products produced in a defected fuel pin which escapes to the coolant.

Table 6.8 gives calculated equilibrium cover gas activities for several noble gases assuming various total delay times between production and entry into the cover gas. The table is simply a modification of Table 6.2 from Reference 61 to account for 1% failures and 75% gas releases plus slightly different nuclear data available today. The table reflects the same cover gas purge rates as in Reference 51 with the corresponding limitation on long-lived radionuclide activity. Note that the difference in total cover gas activity between no delay and a 15 hour delay is only about a factor of 4. Thus, the results are not too critically dependent on a good knowledge of migration or diffusion rates within the fuel pellets.

Table 6.9 gives calculated annual contamination of the primary system from important long-lived nuclides. The numbers are based on assumptions stated above plus calculated activities from the GE 1000 MWe LMFBR as given in Table 4.6. The activities shown in Table 6.9 are important because much of these will collect in the cold traps and be shipped from the reactor or else will deposit on the colder surfaces of the primary system.

Note also that the ^{85}Kr which is removed by the cover gas cleanup system may also be shipped away eventually, just as all the activity which remains inside the fuel pin will be. The amount of ^{85}Kr removed by the gaseous radwaste system under the conditions described here would be about 1900 Ci/yr.

The last activity source to be discussed here is fuel leached from elements experiencing gross cladding failures. An assumed fuel loss of less than 1% from such pins is consistent with almost all of the references cited above.[40,41,52,53,54] Combined with the assumption of 0.1% gross cladding failures and the assumption that the Pu fraction in leached fuel is only 0.1 of the original fraction, burdens of fuel contamination of the primary circuit can be estimated. The annual leaching rate thus calculated is 130 gm per year of metal fuel atoms, of which about 2.5 gm would be plutonium. This would represent about 20 Ci of plutonium activity, most of which would be beta activity of ^{241}Pu.

It should be emphasized here that the failure rates and release fractions assumed in calculating all types of release from LMFBR fuel were, to a certain extent, arbitrary and may be proven high by

Table 6.8

Example Equilibrium LMFBR Cover-Gas Activity from Failed Fuel for Various Delay Times After Birth for Gaseous Radionuclides (1% fuel failure, 75% release)

		Curies				
Nuclide	"Half-Life"	0	10m	1h	5h	15h
^{89}Kr	3.18m	2.69×10^{5}	3.08×10^{4}	.269		
^{137}Xe	3.82m	8.54×10^{5}	1.36×10^{5}	12.8		
^{138}Xe	14.2m	5.87×10^{5}	3.60×10^{5}	3.14×10^{4}	.256	
^{135m}Kr	15.7m	2.59×10^{5}	1.66×10^{5}	1.84×10^{4}	.471	
^{87}Kr	76m	1.69×10^{5}	1.55×10^{5}	9.90×10^{4}	8.44×10^{3}	59.2
^{83m}Kr	1.86h	5.26×10^{4}	4.91×10^{4}	3.64×10^{4}	789	206
^{88}Kr	2.79h	2.07×10^{5}	1.99×10^{5}	1.62×10^{5}	6.19×10^{4}	5.17×10^{3}
^{85m}Kr	4.4h	9.76×10^{4}	9.50×10^{4}	8.32×10^{4}	4.41×10^{4}	8.99×10^{3}
^{135}Xe	9.16h	1.06×10^{6}	1.03×10^{6}	9.80×10^{5}	7.24×10^{5}	3.14×10^{5}
^{133m}Xe	2.26d	2.79×10^{4}	2.79×10^{4}	2.74×10^{4}	2.61×10^{4}	2.31×10^{4}
^{133}Xe	5.27d	1.14×10^{6}	[illegible]4×10^{6}	1.14×10^{6}	1.10×10^{6}	1.05×10^{6}
^{131m}Xe	11.96d	3.30×10^{3}	3.30×10^{3}	3.30×10^{3}	3.30×10^{3}	3.17×10^{3}
^{85}Kr	10.76y	20.2	20.2	20.2	20.2	20.2
Total		4.73×10^{6}	3.39×10^{6}	2.58×10^{6}	1.97×10^{6}	1.40×10^{6}

Table 6.9

Calculated Annual Activities of Long-Lived Radionuclides Entering Primary Sodium from Failed Fuel

Nuclide	Annual Release (Ci)	Activity Present One Year After 30 Year Operation Period (Ci)
^{85}Kr	1900	25,000
^{90}Sr-Y	30	600
^{106}Ru-Rh	4600	6000
^{125}Sb	--	40
^{125m}Te	--	10
*^{134}Cs	150	350
^{137}Cs-Ba	1100	30,000
^{144}Ce-Pr	900	800
^{147}Pm	100	500
^{151}Sm	--	50
^{154}Eu	--	4
^{155}Eu	--	60
^{241}Pu (β)	20	400
Pu (α)	0.6	20
Pu	2.5 grams	75 grams

*Activation product of ^{133}Cs (daughter of ^{133}Xe); therefore, activities depend on irradiation history of failed pins, i.e., time of failure.

a significant factor in future years. However, the numbers used were reasonably consistent with experience and do serve as a convenient basis for calculating releases. If, for example, overall fuel failure rates are 0.1% instead of 1%, the gas release estimates may be scaled down by a factor of ten, etc.

Returning to the question of fuel leaching from pins having gross cladding failures, this leaching may indeed be the ultimate limiting factor on fuel performance. Little information is available on the magnitude of fuel contamination which can be tolerated in the primary circuit. Certainly BR-5 operated with plutonium contamination from failed elements,[25] and DFR has found no problem with having about 0.5 gm of fuel in the primary coolant;[64] however, only 20 mg of this was plutonium. Perhaps the best estimate of how much fuel leaching will be tolerated can be found by looking at the question of tramp fuel (Section 5.4 of this report). Tramp fuel inventories per unit fuel pin length consistent with those seen in SEFOR, EBR-II, and Rapsodie would indicate total tramp fuel inventories of 0.5 gm in a large LMFBR, of which about 0.1 gm would be Pu. To restrict fuel leaching to this order of magnitude per year would require a reduction by more than a factor of 200 of the leached fuel mass calculated above; however, the observed preferential leaching of U over Pu can result in annual Pu leach rates calculated above that need only be reduced by a factor of 20 to approach the magnitude of Pu inventories in tramp fuel.

REFERENCES (Section 6)

1. "Conceptual Plant Design, System Descriptions, and Costs for a 1000 MWe Sodium-Cooled Fast Reactor-Task II Report," GEAP-5678, p. 18 (December 1968).
2. "1000 MWe LMFBR Follow-on Study," BAW-1328, vol. 5, p. 1-10 (January 1969).
3. E. E. Kintner, "LMFBR Fuel Design - Why Can't We Do Better," Proceedings of the Conference on Fast Reactor Fuel Element Technology New Orleans, La., April 13-15, 1971, p.1, Am. Nucl. Soc. (1971).
4. H. Lawton, et. al., "The Irradiation Behavior of Pu-Bearing Ceramic Fuel," London Symposium on Fast Breeder Reactors, British Nucl. Energy Soc., London (1966).
5. R. N. Duncan, D. A. Cantley, K. J. Perry, and R. C. Nelson, "Fuel Swelling - Fast Reactor Mixed Oxide Fuels," Proceedings of the Conference on Fast Reactor Fuel Element Technology, New Orleans, La., April 13-15, 1971, p. 291, Am. Nucl. Soc. (1971).
6. C. Cawthorne and E. J. Fulton, "Voids in Irradiated Stainless Steels," Nature, 216, 576 (1967).
7. E. E. Bloom and J. R. Weir, "In-Reactor and Postirradiation Creep-Rupture Properties of Type-304 Stainless Steel," Trans.Am. Nucl. Soc., 10, 131 (1967).
8. R. M. Willard, "Design Criteria for 304 and 316 Austenitic Stainless-Steel Cladding for FBR Fuel Element," Trans. Am. Nucl. Soc., 10, 486 (1967).
9. S . Oldberg, D. Sandusky, P. E. Bohaboy, F. A. Comprelli, "Analysis of Swelling of Austenitic Stainless Steels in Fast Reactors," Trans. Am. Nucl. Soc., 12, 588 (1969).
10. A. J. Lovell, J. J. Holmes, "Creep Rupture Properties of Type 316 Stainless Steel after High-Temperature Irradiation," Trans. Am. Nucl. Soc., 14, 153 (1971).
11. A. Boltax, T. P. Soffa, A. Biancheria, "Sensitivity of Fuel Pin Behavior to Void Swelling and Irradiation Creep of Stainless Steels," Trans. Am. Nucl. Soc., 14, 631 (1971).
12. Proceedings of the Conference on Fast Reactor Fuel Element Technology, New Orleans, La., April 13-15, 1971, Session III, pp. 393-458, Am. Nucl. Soc. (1971).
13. G. P. Wozadlo, B. F. Rubin, P. Roy, "Tritium Analysis of Fast Flux Irradiated Mixed-Oxide Fuel Pins," Trans. Am. Nucl. Soc., 15, 200 (1972).

14. S. A. Rabin, R. W. Darmitzel, W. W. Kendall, "Short-Term Fast-Flux (EBR-II) Irradiation of $PuO_2 \cdot UO_2$ Fuel Pins," Trans. Am. Nucl. Soc., 9, 41 (1966).

15. M. T. Simnad, Fuel Element Experience in Nuclear Power Reactors, p. 530, Gordon and Breach, New York (1971).

16. F. Anselin, R. G. Mas, J. P. Mustelier, "Irradiation Behavior of Plutonium Mixed-Oxide Driver Fuel of Rapsodie," Trans. Am. Nucl. Soc. 11, 514 (1968).

17. R. C. Nelson, B. F. Rubin, W. W. Kendall, and W. E. Bailey, "Performance of Mixed-Oxide Fuel Pins Irradiated in a Fast Reactor to 50,000 MWd/T," Trans. Am. Nucl. Soc., 10, 460, (1967).

18. W. E. Bailey, C. N. Spalaris, D. W. Sandusky, and E. L. Zebroski, "Effects of Temperature and Burnup on Fission Gas Release in Mixed Oxide Fuel," Ceramic Nuclear Fuels - International Symposium, May 3-8, 1969, Nuclear Div. of American Ceramic Society (1969).

19. C. N. Craig, R. R. Asamoto, R. N. Duncan, "Fast Reactor $(PuU)O_2$ Fuel Pin Irradiations in EBR-II to 75,000 MWd/Te," Trans. Am. Nucl. Soc., 12, 566 (1969).

20. C. N. Craig, W. K. Appleby, K. J. Perry, R. N. Duncan, W. E. Bailey, and C. N. Spalaris, "Steady-State Performance of PuO_2-UO_2 Fast Reactor Fuel," Proceedings of the Conference on Fast Reactor Fuel Element Technology, New Orleans, La., April 13-15, 1971, p. 555, Am. Nucl. Soc. (1971).

21. "Fabrication of 20 wt% PuO_2-UO_2 Fast Breeder Fuels for Irradiation Testing in EBR-II," NUMEC-3524-74 (June 1970).

22. J. D. B. Lambert, L. A. Niemark, W. F. Murphy, and C. E. Dickerman, "Performance of Mixed-Oxide Fuel Elements - ANL Experience," Proceedings of the Conference on Fast Reactor Fuel Element Technology, New Orleans, La., April 13-15, 1971, p. 517, Amer. Nucl. Soc. (1971).

23. J. E. Hanson, "Experimental Description and Hazards Evaluation for the Pacific Northwest Laboratory Mixed Oxide (UO_2-PuO_2) Irradiations in EBR-II, Task A. Subtask I. Irradiations," BNWL-650 (July 1968).

24. Reference 12, Sessions II and III, pp. 137-493.

25. V. V. Orlov, et. al., "Some Problems of Safe Operation of the BR-5 Plant," Int. Conf. on the Safety of Fast Reactors, Aix en Provence, September, 1967, paper no. Va-7, Commissiat a l'Energie Atomique (1967).

26. N. J. Olson, G. C. McClellan, J. E. Flinn, D. G. Franklin, S. C. Miller, "Analysis of Mark-IA Run-to-Failure Experiments in EBR-II," Trans. Am. Nucl. Soc., 15, 748 (1972).

27. L. Bernath and W. B. Wolfe, "Fuel Design for the AI LMFBR Demonstration Plant," Proc. of the Conf. on Fast Reactor Fuel Element Technology, New Orleans, La., April 13-15, 1971, p. 47, Am. Nucl. Soc. (1971).

28. J. Graham, Fast Reactor Safety, p. 228, Academic Press, New York (1971).

29. G. Vendryes, "A General Survey of the French Fast Reactor Program," Trans. Am. Nucl. Soc., 13, 104 (1970).

30. R. DeFremont, "Observations on the Behavior of Radioactive Products in Rapsodie," DRNR/STRS.71.1146, 1971.

31. D. P. Roux and J. Max, "Detection and Location of a Fuel Pin Failure in Rapsodie Using Noise Analysis," Trans. Am. Nucl. Soc., 14, 304 (1971).

32. C. Moranville, "Fuel Development for French Fast Reactors," Trans. Am. Nucl. Soc., 13, 104 (1970).

33. P. Bussy, "Observations on a Rupture of a Rapsodie Fuel Pin," International Meeting on Fast Fuel and Fuel Elements, Karlsruhe (1970).

34. G. Gajac, J. L. Ratier, L. Reynes, M. A. Valantin, "Rapsodie's First Year of Operation," CEA-CONF-1247 (1969).

35. Personal Communication, EBR-II Staff, December, 1972.

36. J. J. Regimbal, W. P. Kunkel, and R. S. Gilbert, "Measurement of Noble Gas Transport Dynamics in SEFOR Sodium," Trans. Am. Nucl. Soc., 14, 773 (1971).

37. Reference 15, pp. 587, 596.

38. Reference 21, p. 566.

39. M. D. Carelli and R. D. Coffield, Jr., "Fission Gas Ejection Characteristics and their Effect on Adjacent Fuel Pins in an LMFBR," Proc. of the Conf. on Fast Reactor Fuel Element Technology, New Orleans, La., April 13-15, 1971, p. 617, Am. Nucl. Soc. (1971).

40. K. E. Gregoire, P. E. Novak, and R. E. Murata, "Failed Fuel Performance in Naturally Convecting Liquid Metal Coolant," GEAP-13620 (June 1970).

41. J. J. Regimbal, R. S. Gilbert, and P. E. Bohaboy, "Radionuclide Release from Intentionally Defected Fuel in the B9D In-Pile Sodium Loop," Trans. Am. Nucl. Soc., 15, 197 (1972).

42. R. DeFremont, "Tempête Test: In-Pile Experiment on the Transfer of Fission Gases," DRNR/STRS.71.1147, (1971).

43. "Diffusion des produits de fission," Proc. of the Conf. of the French Society for Radiation Protection, Saday, November 4-6, 1969, paper no. 27.

44. A. W. Longest, N. Baldwin, J. A. Conlin, R. B. Fitts, and J. R. Lindgren, "Fission Gas Release Measurement from Fast Breeder $(U,Pu)O_2$ Fuel," Trans. Am. Nucl. Soc., 13, 604 (1970).

45. D. Davies, G. Long, and W. P. Stanaway, "The Emission of Volatile Fission Products from Uranium Dioxide," UK Report AERE-R4342 (1963).

46. R. O. Meyer, E. M. Butler, and D. R. O'Boyle, "Actinide Redistribution in Mixed-Oxide Fuels Irradiated in a Fast Flux," Trans. Am. Nucl. Soc., 15, 216 (1972)

47. W. T. Sha, P. R. Huebotter, and R. K. Lo, "The Effect of Plutonium Migration on Allowable Power Rating and Doppler Broadening," Trans. Am. Nucl. Soc., 14, 183 (1971).

48. Reference 5, pp. 294-296.

49. Reference 22, pp. 542-545.

50. C. E. Johnson, D. V. Steidl, and C. E. Crouthamel, "Distribution of Gaseous Fission Products in Irradiated Mixed Oxide Fuels," Proc. of Conf. on Fast Reactor Fuel Element Technology, New Orleans, La., April 13-15, 1971, p. 603, Am. Nucl. Soc. (1971).

51. C. E. Johnson, I. Johnson, and C. E. Crouthamel, "Fuel-Cladding Chemical Interactions in UO_2-20 wt% PuO_2 Fast Reactor Fuel Clad with Stainless Steel," Proceedings of the Conf. on Fast Reactor Fuel Element Technology, New Orleans, La., April 13-15, 1971, p. 393, Am. Nucl. Soc. (1971).

52. R. E. Murata, C. N. Craig, H. C. Pfefferlen, and P. E. Novak, "Effect of Stoichiometry on the Behavior of Mixed-Oxide Fuel during Extended Operation in Failed Pins," GEAP-13730 (July 1971).

53. D. E. Plumlee and P. W. Novak, "Measured Loss of Fission Products from High-Burnup Mixed-Oxide Fuel in a Miniature Pumped Sodium Loop," GEAP-13731 (August 1971).

54. P. E. Bohaboy, C. N. Craig, and G. L. Stimmell, "Performance of Failed Plutonium-Uranium Oxide Fuel Elements in Flowing Sodium," Trans. Am. Nucl. Soc., 15, 196 (1972).

55. A. H. Booth and G. T. Rymer, "Determination of the Diffusion Constant of Fission Xenon in UO_2 Crystals and Sintered Compacts," AECL-692 (August 1958).

56. G. W. Parker, et. al., "Prompt Release of Fission Products from Zircaloy Clad UO_2 Fuels," ORNL-4228 (April, 1968).

57. D. L. Morrison, et. al., "An Evaluation of the Applicability of Existing Data to the Analytical Description of a Nuclear Reactor Accident," BMI-1810 (July 1, 1967).

58. F. W. A. Yuill, V. F. Baston, and J. H. McFadden, "An Analytical Model Describing the Behavior of Fission Products in Operating Fuel Pins," IN-1467 (June 1971).

59. G. W. Keilholtz and G. C. Battle, Jr., "Fission Product Release and Transport in Liquid Metal Fast Breeder Reactors," ORNL-NSIC-37, section 2.4 (March 1969).

60. A. Gerosa and M. Martini, "Venting Device for Sodium-Cooled Fast Ceramic Reactor Fuel Elements," Trans. Am. Nucl. Soc., 11, 508 (1968).

61. G. L. O'Neill, J. Duffy, D. B. Sherer, J. C. Gilbertson, and F. W. Knight, "A Technical and Economic Evaluation of Vented Fuel for Sodium-Cooled Fast Ceramic Reactors," GEAP-4770 (May 1965).

62. G. L. O'Neill, J. H. Davies and J. L. Johnson, "Demonstration of Fission-Gas Venting from Fast Oxide Reactor Fuel Elements," Trans. Am. Nucl. Soc., 7, 92 (1964).

63. Reference 16, p. 538 ff.

64. J. L. Phillips, "Full Power Operation of the Dounreay Fast Reactor," Proc. of National Topical Meeting on Fast Reactor Technology, Detroit, April 26-28, 1965, ANL-100, p. 7 (1965).

65. J. Kirk, "Radioactive Maintenance on DFR," Trans. Am. Nucl. Soc., 13, 789 (1970).

66. J. P. Foster, et. al., Analysis of Irradiation-Induced Creep of Stainless Steel in Fast Spectrum Reactors, Proceedings of the BNES, London, 1973.

67. Letter from G. W. Hardigg, General Manager, Westinghouse Advanced Reactors Division, to E. D. Harward, Director, Technology Assessment Division, EPA, Comments on Draft Report, February 28, 1974.

7. FISSION PRODUCTS IN SODIUM SYSTEMS

Fission products may enter the primary sodium from the fuel, either through failures in the cladding, or from the purposeful venting of fission product gases to the sodium. The extent of fission product release from fuel is discussed in Section 6.

In that section it was noted that fission product gases (e.g. Xe and Kr) escape from both fuel failures and vented fuel. Iodine is volatile at fuel temperatures and some escapes; some cesium and rubidium enter the sodium by the decay of xenon and krypton precursors before these gases escape from the sodium. The major source of fission products such as ^{137}Cs, ^{90}Sr, ^{140}Ba, ^{95}Zr, and ^{141}Ce is the leaching of fission products from the fuel in large cladding ruptures. The release of fission product tritium was discussed in Section 5.1.3; it can be assumed that all tritium from ternary fission enters the sodium.

Much of the interest in cleanup of solid fission products is generated by analyses of reactor accidents in which relatively large amounts of fuel might melt and come directly into contact with sodium. Although this report is concerned with normal operation, some solid fission products enter the sodium even in normal operation; therefore, results are presented for the behavior of solid fission products in this report.

In the first part of this section, a review of fission product behavior in sodium is presented, including operating experience for sodium-cooled reactors. In the second part, the role of the cold traps in sodium purification is discussed. This second part will include discussions of (a) cold trap operation, (b) cold trap experimental results, and (c) cold trap operating experience for sodium-cooled reactors.

7.1 Fission Product Behavior in Sodium

Fission products entering the sodium generally experience one of the following fates: (a) escape to the cover gas, (b) deposit on system surfaces, (c) removal by a cold trap, or (d) they remain in solution in the sodium. The thermodynamics of vaporization (hence, of process a above) is reviewed by Castleman and Tang.[1]

A review of fission product behavior in sodium is given by Castleman.[2] His article forms the basis of much of the review here, although it has been augmented with additional material. Of particular interest is a loop experiment reported by Plumlee and Novak[3] in which fission products and fuel were leached from a purposely defected fuel pin by flowing sodium, and the fate of the fission products in the loop was determined. (This experiment was also reviewed in Section 6.) In particular the relative retention in the sodium versus deposition on the cold steel surfaces of the system was measured for ^{137}Cs (alkali metal), ^{90}Sr (alkaline-earth metal), ^{144}Ce and ^{147}Pm (rare earths), the results of which are discussed in the sections below. Experiments by Saroul[4,5] also provide information on fission product behavior in sodium. Following the review of each type of fission product, operating from sodium-cooled reactors is reported.

7.1.1 Behavior of Each Fission-Product Type

7.1.1.1 Noble Gases

The noble gases of principal interest are xenon and krypton. Noble gases escape into sodium from leaking fuel (see Section 6). Effectively all of the noble gases then escape from the coolant to the cover gas within a few minutes after entering the sodium (See Reference 6,7 for example).

The time delay before escape, however, allows some decay of xenon to cesium and krypton to rubidium in the sodium. For example, ^{138}Cs results from decay of ^{138}Xe. With the vented fuel of Dounreay the on-line activity of the NaK coolant is 100 times the ^{24}Na activity, with ^{138}Cs reported as being the major contributor.[8] Some ^{138}Xe (half-life 17 min.) may escape from failed fuel, but the half-life of ^{138}Cs is only 32 min.; hence, it would not be an important long-term environmental source in the sodium. Also some ^{137}Cs is produced from decay of ^{137}Xe in the sodium; however the short half-life of ^{137}Xe (4.7 min.) prevents much of it from escaping from failed fuel. Although significant ^{135}Xe (9.2 hr. half-life) escapes from the fuel, its daughter ^{135}Cs is relatively stable (2×10^6 y). Perhaps some ^{88}Rb is produced in the sodium from decay of ^{88}Kr (2.77 hr. half-life) which leaks from failed fuel, but the half-life is short (18 min.) so that it is not a long-term environmental problem. The daughters of ^{87}Kr and ^{85}Kr are stable; the resulting ^{87}Rb and ^{85}Rb could activate to ^{88}Rb and ^{86}Rb, with half-lives of 18 min. and 18.7 days respectively.

Vented fuel elements can be designed to delay fission gas transfer to the sodium and thereby substantially reduce the entrance of the short-lived noble gases into the sodium, as described in Section 6.7. This was not the case for the vented fuel in Dounreay, however, since the NaK was, in effect, able to contact much of the fuel directly in Dounreay. As noted above, in Dounreay ^{138}Cs, which is the daughter of ^{138}Xe, is the main source of activity in the coolant during on-line operation,[8] although the half-life of ^{138}Xe is only 17 min.

Saroul reports experiments in the Pirana and Aetna facilities[4,5] in which fission gases from molten irradiated uranium were allowed to enter first sodium and then an argon cover gas. He reported significant retention of noble gases by the sodium. However, uncertainties concerning whether equilibrium was reached and the meaning of material balances led Castleman[2] to emphasize other noble gas solubility experiments to argue that noble gas retention in the sodium should be negligible.

7.1.1.2 Iodine

Iodine which enters the sodium reacts with sodium to form NaI. Sodium iodide remains in solution in the liquid, with only small amounts being vaporized into the cover gas, still as NaI. Extensive data on NaI volatility have been reported by Castleman and Tang (e.g. Reference 1) and by Pollock, Silberberg, and Koontz (e.g. Reference 9). In Reference 9, relative volatility data for NaI are reported in terms of a distribution coefficient, K_d, defined as the ratio of the mole fraction of solute in the vapor to the mole fraction of solute in the liquid.

Sodium iodide does not generally react chemically with other fission products. Some reaction with cesium to form CsI is possible; but Castleman, Tang, and Mackay[10] showed experimentally that, for the low concentrations and for the sodium temperatures involved in reactors, CsI readily decomposes to NaI and Cs. This lack of reaction between Cs and NaI was also confirmed by Cooper, Grundy, and Taylor.[11]

It has been observed (for example in the Pirana experiments[4]) that in stagnant sodium a large fraction of the iodine is concentrated near the gas-liquid phase boundary. In other Pirana experiments,[4] when argon was bubbled through the sodium the iodine was distributed homogeneously in the sodium.

Fission product isotopes of another halogen, bromine, are of sufficiently short half-life not to be of environmental concern.

7.1.1.3 Alkali Metals

Cesium and rubidium are alkali metals, with cesium being the more important for environmental considerations.

Plumlee and Novak[3] found that cesium is retained in sodium far more than any other fission product, which might be expected since sodium itself is an alkali metal. They report that in their loop experiment, 50% of the ^{137}Cs which was leached from the fuel remained in the sodium and 50% plated out on the colder loop surfaces. This finding is somewhat consistent with EBR-II experience (Section 7.1.2.2) and BR-5 experience (Section 7.1.2.3). It is also consistent with the results of Clifford,[34] which is described in Section 7.2.3.1 on cold trapping of cesium.

Cesium is present in both sodium liquid and sodium vapor as elemental metallic cesium. Cesium reacts little with other fission products. Cesium will react with carbon if present.[12]

Cesium is highly volatile in sodium. Experimental results by Pollock, Silberberg and Koontz[9] and theoretical and experimental results by Castleman and Tang[1] indicated high volatility of cesium relative to sodium (far higher, for example, than NaI). Clough and Wade[12] confirmed these high volatilities. They found, further, that the volatility was decreased significantly either by adding graphite or charcoal to the sodium or the gaseous phase. Cesium apparently both reacts with graphite and is adsorbed on graphite surfaces.

The concentration of cesium does exhibit some inhomogeneity at a sodium liquid-gas interface, with higher concentrations being found near the surface than below the liquid level. On draining steel vessels which contained cesium dissolved in sodium, Saroul found that appreciable cesium remained at the vessel surface and a significant amount had penetrated the vessel wall to a 3 to 4 μ depth[4],[5]

Although less work has been reported on rubidium, its properties are similar to those of cesium. For example Castleman reports thermodynamic properties for rubidium which indicate that it is also highly volatile relative to sodium.[2]

7.1.1.4 Alkaline-Earth Metals

Alkaline-earth fission products include strontium and barium. Little of these materials enter the primary sodium from fuel failures. However some ^{89}Sr, ^{90}Sr, and ^{140}Ba has been observed in the sodium from failed fuel in operating sodium-cooled reactors.

Plumlee and Novak[3] reported that, of the ^{90}Sr that entered the sodium in their loop experiment, only 0.024% remained in the sodium. Hence nearly all of the ^{90}Sr presumably plated out on the system walls.

The alkaline earth metals have low volatility in sodium. Castleman reports that their chemical state in sodium is not well established; they probably interact with dissolved oxygen in sodium, but the nature of the oxygen compounds in sodium is not well known.[2] Clough reports experimental values for strontium volatility in sodium that are lower than expected for elemental Sr, indicating that some relatively nonvolatile oxygen species has been formed.[13] Later Clough and Wade again suggest that barium and strontium are present in sodium as BaO and SrO.[12]

Saroul reported in the Pirana experiments[4] that ^{140}Ba - ^{140}La tended to concentrate near the liquid sodium-argon gas boundary in stagnant sodium.

Saroul also reported[4] that most (83%) of the ^{140}Ba - ^{140}La released from the uranium into the sodium deposited on the stainless steel walls of the sodium vessel upon removal of the sodium at 250°C.

7.1.1.5 Rare Earths

Rare earth fission products include cerium, lanthanum and promethium. Little cerium and promethium enter the sodium from fuel failures although Plumlee and Novak[3] found significant amounts of ^{144}Ce and ^{147}Pm leached in their experiment. Lanthanum-140 is produced by decay of the alkaline earth ^{140}Ba and is found with ^{140}Ba.

Plumlee and Novak[3] report <0.0024% retention of ^{147}Pm in sodium; hence nearly all of these two fission products plated out on the system walls. Saroul also showed that most of the cerium and lanthanum is transported to the walls of sodium systems.[4,5] The rare earths are relatively nonvolatile.

7.1.1.6 Transition Metals

Transition metals include ^{95}Zr - ^{95}Nb among fission products. Information on their behavior in sodium was not found. Such small amounts of these two isotopes were leached in the Plumlee-Novak experiment[3] that relative retention in sodium and deposition on system surfaces could not be measured.

7.1.1.7 Noble Metals

Noble metal fission products include palladium, rhodium, and ruthenium. Little information on their behavior in sodium was found. Plumlee and Novak report that a large amount of ^{106}Ru was leached from the fuel in their experiment and less than 0.023% was retained in the sodium.[3] Presumably, this means that most plated out on the system walls.

7.1.1.8 Tritium

The fission product tritium, and its behavior in sodium, are discussed in Section 5.1.

7.1.2 Operating Experience with Fission Products in Sodium (or NaK) Cooled Reactors (Excluding Experience with Cold Traps)

7.1.2.1 Summary

Zwetzig[14] has reported a summary of fission-product operating experience in the coolant systems of sodium or NaK cooled reactors. Table 7.1 is patterned after Zwetzig's summary; it includes his results plus additional results as referenced in Table 7.1.

7.1.2.2 EBR-II

Activities of various radionuclides in the primary system of EBR-II during 1971 (the last year they were publicly reported) are listed in Table A25 of Appendix A. The principal fission products observed are ^{137}Cs and ^{131}I. Also observed was the activation product ^{134}Cs which results from activation of the fission product ^{133}Cs.

In July, 1971, the fission and activation products on the pump walls of the primary pump were reported.[15] ^{137}Cs was found on the pump walls; 65% of the ^{137}Cs was removed by cleaning the surface.

Also ^{137}Cs was reported[15] in the walls of the primary tank at the argon cover gas level. This was believed to have resulted from vaporization and subsequent recondensation of ^{137}Cs.

Table 7.1
Fission Products Observed in the Primary System of Sodium and NaK Cooled Reactors (other than tritium)

	Fermi[14]	BR-5[17]	EBR-II[15]	Dounreay[8]
Neutron Spectrum	fast	fast	fast	fast
Coolant	Na	Na	Na	NaK
In Primary Coolant	^{140}Ba-La, ^{137}Cs, ^{89}Sr, ^{131}I	^{144}Ce, ^{141}Ce, ^{144}Pr, ^{140}Ba-La, ^{137}Cs ^{136}Cs ^{106}Ru, ^{95}Zr-Nb, ^{90}Sr, ^{131}I	^{137}Cs, ^{131}I	^{141}Ce, ^{144}Ce, ^{132}Te ^{131}I, ^{103}Ru, ^{106}Ru, ^{132}I, ^{137}Cs, ^{95}Zr-Nb, ^{140}Ba-La, ^{138}Cs
On Primary Piping or Pump	^{141}Ce, ^{144}Ce, ^{133}I, ^{103}Ru, ^{95}Zr-Nb		^{137}Cs	^{140}Ba-La
In Cold Trap		^{137}Cs, ^{136}Cs, ^{131}I, ^{133}I ^{135}I, ^{95}Zr-Nb, ^{140}Ba-La	^{137}Cs, ^{134}Cs	^{137}Cs

Table 7.1 (Continued)

	Rapsodie[18]	SEFOR (See Appendix A, Table A21)	SRE[14,20]	S8ER[14]
Neutron Spectrum	fast	fast	thermal	thermal
Coolant	Na	Na	NaK	NaK
In Primary Coolant	^{137}Cs	^{86}Rb	^{141}Ce, ^{131}I, ^{103}Ru ^{137}Cs, ^{83}Sr, ^{90}Sr, ^{95}Zr-Nb, ^{140}Ba-La, ^{144}Ce, ^{106}Ru	^{137}Cs, ^{131}I, ^{132}Te-I
On Primary Piping or Pump	^{141}Ce, ^{137}Cs, ^{131}I, ^{132}I, ^{140}Ba-La, ^{95}Zr-Nb, ^{90}Sr-Y, ^{91}Y		^{89}Sr, ^{90}Sr, ^{95}Zr-Nb, ^{144}Ce, ^{137}Cs, ^{106}Ru	^{89}Sr, ^{90}Sr, ^{95}Zr-Nb, ^{103}Ru ^{144}Ce, ^{106}Ru-Rh, ^{140}Ba-La, ^{141}Ce
In Cold Trap			^{137}Cs, ^{106}Ru, ^{144}Ce-Pr	

An interesting results concerns ^{137}Cs segregation in the primary sodium system of EBR-II at low temperature.[16] After a reactor shutdown on November 15, 1970, the primary pumps were turned off and the sodium was cooled to 350°F on November 17. Sampling of ^{137}Cs and ^{22}Na continued during and after this time. The ^{22}Na activity in the sodium remained constant. The ^{137}Cs activity, however, steadily decreased from 11 nCi/gm Na to 4 nCi/gm in one month. This decrease can be seen in Table A25 of Appendix A, as reported in Reference 16. It was supposed that the ^{137}Cs segregated from the bulk of the quiescent sodium and concentrated at the sodium-metal and sodium-gas interfaces in the primary tank. After the sodium was reheated and operation again started, the ^{137}Cs activity returned to its original value, as can be seen from later results in Table A25, Appendix A.

7.1.2.3 BR-5

The following results for BR-5 operation were obtained from Reference 17.

The USSR sodium-cooled PuO_2-fueled 5MW(th) BR-5 fast reactor was operated for 8 years from 1959 to 1967. At the end of the first stage of operation (1962-1964) there were 63 assemblies with PuO_2 fuel with 5.0 - 6.5% fuel burnup in the core. Between 1964 and 1967, the reactor was operated with PuC fuel, to 2.4% burnup. Integrated power for the 8 years was 4100 MW days.

During the eight years of operation there was no situation endangering the integrity of the reactor because of sodium leakage from the heat-transfer system. No sodium leakage occurred at pipe welds. Isolated leakages did occur in liquid metal fittings, through the level metering devices, in the heat exchanger equipment, and through a fault in the drainage piping of the primary circuit. Four of 65 valves were replaced due to sodium leaks.

A unique feature of BR-5 operation was long-term operation with an excessive number of fuel failures. Before completion of operation with the PuO_2 core, 17 of the 63 fuel assemblies contained failed fuel. The concentrations of fission product activities in the sodium and in the primary system walls at the end of the first stage of operation is given in Table 7.2.

Before 2% burnup, the residual activity in the sodium was due only to ^{22}Na. At 3% burnup, ^{137}Cs was detected (~ 20% of the ^{22}Na activity). At 5% burnup, ^{137}Cs was 200 times its activity at 3% burnup, and other fission products were found in the primary sodium (see Table 7.1).

7.1.2.4 Dounreay

Dounreay fuel is U-Mo alloy and is vented to the NaK coolant. During operation the fission product activity is ~ 100 times the ^{24}Na activity, the dominant isotope being ^{138}Cs (^{138}Cs activity = 0.6 Ci/gm NaK).[8]

Table 7.2

Fission Product Activity in BR-5 During First Stage of Operation (1962-64)

	Isotope	Activity
Primary Sodium	^{131}I	0.8 mCi/liter
	^{137}Cs	7 mCi/liter
	^{95}Zr-Nb	0.3 mCi/liter
	^{140}Ba-La	2 mCi/liter
Walls of Primary System	^{131}I	70 mCi/cm^2
	^{137}Cs	74 mCi/cm^2
	^{95}Zr-Nb	55 mCi/cm^2
	^{140}Ba-La	19 mCi/cm^2

Table 7.3

Gamma Activity of Fission Products in DFR Coolant, 6 Days After Sampling

Energy(MeV)	Possible Isotopes	Activity (μCi/gm NaK)
0.14	^{143}Ce, ^{144}Ce	0.7
0.22	^{132}Te	1.2
0.364	^{131}I	6.8
0.5	^{103}Ru, ^{106}Ru	0.7
0.67	^{132}I, ^{137}Cs	7.3
0.76	^{95}Zr-Nb	2.3
1.6	^{140}Ba-La	8.8

The fission product gamma activities 6 days after sampling in the DFR coolant are given in Table 7.3.[8]

7.1.2.5 Rapsodie

After three years of operation, including 500 equivalent days at 24 MW, Rapsodie was shut down for conversion to 40 MW operation. At that time a study of fission products in the sodium was made and the results are summarized here.[18] Operation had proceeded with one failed fuel pin, with direct contact of sodium coolant and the UO_2-PuO_2 fuel.

^{137}Cs and ^{140}Ba were the main fission products deposited on primary system pipes.

Fission products deposited on the primary pump included: ^{141}Ce, ^{137}Cs, ^{131}I, ^{132}I, ^{140}Ba-La, ^{95}Zr-Nb,and ^{90}Sr-Y. The axial distribution of ^{137}Cs was plotted in Reference 18 for the primary pump.

The ^{137}Cs level in the primary sodium rose steadily to 0.05 μCi/gm Na at the end of the 500 effective days of operation at 24 MW.

The primary pump was decontaminated by alternate washing in water and dilute nitric and phosphoric acids.[19] A 90% decontamination factor was obtained for ^{137}Cs, which was not considered adequate for future work. A sample steel bolt from the pump was washed with alcohol with a resulting 99% decontamination factor, but it was considered too dangerous to use alcohol for the entire pump.

7.1.2.6 SRE

During Run 14 of SRE, from July 12-26, 1959, fuel element cladding failures occured in 14 of the 43 elements. The total accumulated irradiation through Run 14 was 2426 MWd. The fuel in SRE was metallic uranium, bonded with NaK, and clad in stainless steel. The fate of fission products from these failures is well documented[20] and is reviewed here in some detail. Unfortunately some uncertainty exists on its direct applicability to an LMFBR system since 7 to 70 lbs. of carbon were also in the system.

Prior to Run 14, small amounts of fission products were found in the primary sodium. The fission product levels detected prior to Run 14 are given in Table 7.4, which is reproduced from Reference 20.

After Run 14 the fission product levels rose to the values listed in Table 7.5, again reproduced from Reference 20. It is interesting to note in this table that the variation in fraction of isotope released to the primary sodium was only a factor of 10 between the lowest (^{103}Ru) and the highest (^{137}Cs) isotope.

In Table 7.6 are listed primary sodium levels for three sampling dates -- at the end of Run 14, 3 months later, and one year later.

Table 7.4

Typical Radioactivity Levels of SRE Primary Sodium Prior to Run 14 [20]

Sample No.	R-24	R-27	R-32
Sampling Location	Material Evaluation Facility	Reactor Pool	Material Evaluation Facility
Date of Sample Removal	10/2/58	2/6/59	4/14/59
Date of Last Reactor Scram	9/25/58	1/29/59	4/6/59
		Specific Activity (μCi/gm Na)	
^{95}Nb-Zr	—	5.2×10^{-2}	2.9×10^{-3}
^{103}Ru	5.9×10^{-4}	8.0×10^{-4}	—
^{106}Ru	2.2×10^{-3}	—	—
^{131}I	5.1×10^{-3}	1.6×10^{-2}	4.0×10^{-2}
^{137}Cs	5.1×10^{-4}	6.5×10^{-4}	1.5×10^{-2}
^{140}Ba-La	—	2.8×10^{-4}	—
^{141}Ce	—	5.4×10^{-4}	4.3×10^{-2}

Table 7.5

Initial Fission Product Analysis of SRE
Primary Sodium After Run 14[20]

Isotope	Primary Coolant Activity (μCi/gm Na)[a]	Total Coolant Inventory (curies)[a]	Total Reactor Inventory (curies)[a]	Fraction of Inventory Released[b]
^{137}Cs	1.26	2.77×10^{1}	8.70×10^{3}	-3.18×10^{-3}
^{134}Cs	0.02	-4×10^{-1}	2×10^{2}[c]	2×10^{-3}[c]
^{89}Sr	20.0	4.44×10^{2}	1.60×10^{5}	2.78×10^{-3}
^{90}Sr	0.97	2.14×10^{1}	8.15×10^{3}	2.63×10^{-3}
^{131}I	0.74	1.63×10^{1}	1.68×10^{4}	0.97×10^{-3}
^{141}Ce	4.38	9.65×10^{1}	1.27×10^{5}	0.76×10^{-3}
^{144}Ce	5.18	1.41×10^{2}	1.69×10^{5}	0.67×10^{-3}
^{140}Ba-La	1.65	3.63×10^{1}	5.61×10^{4}	0.65×10^{-3}
^{95}Zr-Nb	13.9	3.06×10^{2}	5.53×10^{5}	0.55×10^{-3}
^{103}Ru	0.95	2.09×10^{1}	7.52×10^{4}	0.28×10^{-3}

(a) As of July 26, 1959

(b) Multiply values in this column by -3 to adjust fraction released to average values for those fuel elements which suffered cladding failures (14 of 43 elements failed).

(c) From neutron capture in ^{133}Cs; estimated.

Table 7.6

Fission Product Analyses of SRE Primary Sodium As a Function of Time After Run 14 [20]

	Primary Coolant Activity (µCi/g Na)			
Sample Date	7/26/59	10/31/59	7/26/60	Ratio
Time After Run 14	0	97 days	1 year	$\left[\frac{\text{Oct. 31 (actual)}}{\text{Oct. 31 (decay only)}}\right]$
^{137}Cs	1.26	0.45	0.028	0.36
^{134}Cs	0.02	0.006	Undetectable	0.3
^{89}Sr	20.0	0.25	Not analyzed	0.043
^{90}Sr	0.97	0.060	Not analyzed	0.062
^{131}I	0.74	0.00012	Undetectable	0.63
^{141}Ce	4.38	0.000088	Undetectable	0.00016
^{144}Ce	5.18	0.00031	Undetectable	0.00008
^{140}Ba-La	1.65	—	Undetectable	
^{95}Zr-Nb	13.9	0.0067	Undetectable	0.0013
^{103}Ru	0.95	0.0045	Undetectable	0.024

Also listed are the ratio of the Oct. 31 results to the values which would result if radioactive decay were the only loss mechanism for the isotope. The fact that the ratios are below unity indicates that other mechanism such as deposition on primary system walls or deposition in the cold trap are effectively removing fission products from the sodium. Discussion of cold trap purification of the SRE system is given later in this section (see Section 7.2.4.4). By July 26, 1960 (one year later), the ^{131}I, ^{140}Ba-La, and ^{141}Ce had decayed to the extent that they were undetectable. However the decreases in ^{144}Ce, ^{103}Ru, and ^{137}Cs were attributed to other removal mechanisms, such as cold trap cleanup. A strontium analysis was not made in the final sample.

Analysis of fission product activity on primary pipe samples was also made. Residual sodium on samples of pipe walls was removed by methanol and water. Next the pipe was subjected to a series of etches by hydrochloric acid. Sodium, methanol wash, and HCl etch solutions were analyzed. An example analysis of the etch solution at the surface is given in Table 7.7. In addition, Reference 20 shows a graph of the activities of ^{95}Zr-Nb, ^{144}Ce, and ^{137}Cs as a function of depth into the pipe wall, to a depth of 0.2 mils.

7.1.2.7 SEFOR

The only fission product reported in the SEFOR sodium was ^{86}Rb (see Appendix A, Table A22), which is actually an activation product of ^{85}Rb which results from decay of ^{85}Kr.

7.2 Cold Traps

7.2.1 Brief Description of Cold Trap Technology

Cold traps are used for the purification of sodium in liquid metal cooled reactors. Impurities are removed in cold traps by precipitation, making use of the fact that solubilities are reduced by lowering the sodium temperature, and by adsorption on surfaces in the cold trap.

The principal impurity to be removed by a cold trap is sodium oxide (Na_2O). Operation of the cold trap, including temperature and duration of operation, is governed by the need to reduce the oxygen content of sodium. The principal mechanism for oxide removal is precipitation. Traps operating in the 250°F to 300°F range can hold the oxygen content down to the 1 ppm to 3 ppm (parts by weight) level.*

---

*A recommended equation for oxygen solubility is given by Eichelberger[21] as follows: $\log S = 6.239 - 2447/T(^{\circ}K)$, where S = ppm by weight of oxygen in sodium. This expression was based on 107 solubility determinations from five laboratories. Published work at that time (1969) represented a serious lack of agreement, however, so that better data may be available by now.

Table 7.7

Example of SRE Primary Pipe Wall Fission-Product Contamination from HCℓ Etch at Pipe Surface[20]

Isotope	Contamination Level* ($\mu Ci/cm^2$)
^{89}Sr	15.2
^{90}Sr	0.78
^{95}Zr-Nb	2.7
^{144}Ce	2.1
^{137}Cs	0.022

*Corrected for radioactive decay since 7/26/59 for comparative purposes.

Other nonradioactive impurities removed by cold traps include carbon and hydrogen.

Cold traps are also effective in removing some fission products from the sodium. Removal occurs even when the fission product concentration is lower than the saturated value for the material at the cold trap temperature. For some materials, such as cesium and sodium iodide, the concentration in sodium at a metal surface is higher than the concentration in the bulk liquid, and adsorption or some other transfer mechanism occurs at the surface to remove the material from solution.

A brief review of cold trap operation and experience is given by Hinze.[22]

In a cold trap a bleed stream from the main sodium system (i.e. the primary or secondary system) is cooled, and precipitation of the impurity (e.g. Na_2O) occurs. A large surface on which the impurities are collected is present in the trap, frequently in the form of stainless steel mesh. The collection process includes one or more of the following processes and operations: crystal formation and retention on metal surfaces, filtration, and settling. After leaving the cold trap (or the steel mesh part), the sodium is reheated and returned to the main system. Initial reheating is generally done in an economizer (usually, but not necessarily, external to the cold trap) in which the exiting stream is heated by cooling the incoming bleed stream.

Hinze[22] describes early designs and experience for the cold traps for the Submarine Intermediate Reactor (SIR), Fermi, EBR-II, Sodium Reactor Experiment (SRE), Hallam (HNPF), and Dounreay, and also reports some USSR experience. Both the Fermi and the EBR-II primary cold traps were 500-gallon traps containing stainless steel mesh. Only one trap was in each primary system. The traps were run until they "plugged" with oxide, i.e. until the pressure drop across the trap due to oxide deposition increased such that insufficient flow could be maintained. In some cases (e.g., the primary trap in Fermi and the secondary trap in EBR-II) the trap plugged early during the purification of the sodium. Then a new trap was installed which has not yet required replacing. The primary cold trap in EBR-II lasted until June, 1968, when it was replaced.

SEFOR had two primary cold traps, only one of which was operated at any one time. Each trap had to be replaced after one year ($\sim$1500 hours of operation each) due to plugging.[23] Total Na_2O collected was $\sim$200 lb. Excessive oxide buildup had resulted from zero power operation with the vessel cover removed, when the argon in the refueling cell and over the sodium was contaminated from excessive leakage of nitrogen (and oxygen impurity) from adjacent cells.

The first Fermi primary trap was also removed prior to power operation. The trap was examined by Westinghouse; however, the report[24]* is not available to the public and no final public report was issued. The report was available to Hinze, however, because he reports in Reference 22 that the trap was found to contain 50 lb. of oxygen, 1 lb. of carbon, and lesser amounts of hydrogen, nitrogen, and metallic impurities.

The above experience indicates that it is difficult to predict how long a cold trap will last in an LMFBR power plant. Hence, it is difficult at this stage to estimate how often cold traps, with their accompanying charge of fission and activation products, will be shipped away from the reactor for decontamination or storage in the environment.

Brief descriptions of cold traps appear in the 1000 MWe follow-on reports. For example Reference 25 (the GE design) shows four primary system cold traps operating in parallel and six secondary system cold traps. Each trap (in both systems) has a 20 cu ft volume (150 gallons) and a maximum oxide capacity of 560 lbs. The traps are constructed of 304 stainless-steel, each with a 35 inch high and 35-inch diameter bed of stainless-steel packing. The traps are cooled by forced convection of the cell atmosphere nitrogen. The economizers are not "built-in", but are separate from the cold trap.

7.2.2 Cold Trap Decontamination Terminology

It is useful to review some of the theory and definitions concerning cold traps in order to appreciate the data on fission product removal reported in the literature. Different reports quote a variety of measured or design quantities but no summary of the relations between these quantities was found. Hence, this background is provided in this section.

A number of reports on removal of fission products by cold traps report values for a surface deposition constant K. This constant, with units of length, is defined as:

$$K = \frac{\text{grams deposited/cm}^2\text{ of deposition surface area}}{\text{grams/cm}^3\text{ concentration in sodium}}$$

This constant is generally found to be inversely proportional to the absolute temperature of the sodium. Experimental information for cesium and iodine is reviewed below in Section 7.2.3.

Another parameter that is used in cold trap technology is a "decontamination factor," D. For a particular nuclear species, this factor is defined as:

$$D = \text{Decontamination factor} = \frac{\begin{array}{l}\text{Concentration in coolant}\\ \text{without cold traps operating}\end{array}}{\begin{array}{l}\text{Concentration in coolant}\\ \text{with traps operating}\end{array}}$$

---

* Personal communication, P. Cohen, Westinghouse, December 21, 1972.

Another related term in use is a "Concentration ratio", C, defined for a particular nuclear species as:

$$C = \text{Concentration ratio} = \frac{\text{Grams in trap/cm}^3\text{ sodium in trap}}{\text{Concentration in remainder of the system}}$$

The factors D and C are related as follows:

Let X = concentration in the system without a trap

Y = concentration in the system outside the cold traps, with cold traps operating.

V_s = system volume

V_T = cold trap volume

If traps are operating, the concentration in a trap is CY. From conservation of total production of the particular nuclide with or without trap operation,

$$XV_s = YV_s + CYV_T$$

The decontamination factor, D, is related to X and Y by: D = X/Y. Therefore

$$D = 1 + C\,\frac{V_T}{V_s}$$

Values of concentration ratio found at SRE are given in Section 7.2.4.4.

Cold trap efficiency, ε is frequently reported, where ε is the efficiency for precipitation, defined as:

$$\varepsilon \equiv \frac{\text{entering concentration - exit concentration}}{\text{entering concentration - saturation concentration at the minimum cold trap temperature}}$$

None of the parameters listed above are related to rate of deposition in a cold trap. The experimental work found on cold trap deposition did not provide information on deposition rate. Atomics International does, however , provide for a rate calculation of cold trap deposition in their STP-1 fission product transport code.[26,27]

Shown below is an equation similar to one proposed by Atomics International[26] to describe the removal rate of material i from the sodium in a cold trap:

$$\frac{dN_c^i}{dt} = -F\left[\varepsilon^i\left(\frac{N_c^i}{V_c} - \sigma^i\right) + \frac{N_c^i}{PZ}\left(1 - e^{-\kappa^i PZ/F}\right)\right] \quad (1)$$

where N_c^i = atoms of nuclide i in coolant (atoms)

V_c = volume of coolant in total primary (or secondary) system (cm^3)

ε^i = cold trap efficiency for removal of nuclide i

F = flow rate in the trap (cm^3/sec)

σ^i = solubility of nuclide i in the trap at the minimum cold trap temperature (atoms/cm^3)

P = surface area per unit length of traps (cm^2)

κ^i = deposition rate parameter of the trap $\left(\frac{\text{atoms deposited/sec/cm}^2}{\text{atoms/cm}^3}\right)$

Z = length of trap (cm)

Only depletion is considered in the above equation (no source term is included).

The factor $\left(\frac{N_c^i}{V_c} - \sigma^i\right)$ is a measure of the excess of the concentration above saturation, and therefore the first term of Equation (1) represents removal by precipitation. This term is assumed to be positive or zero in the AI codes.

The second term of Equation (1) represents deposition by adsorption. The following derivation of the second term is useful to provide an understanding of it:

Let $N_c(t)/V_c$ = Concentration of an impurity entering the trap (equal to the average concentration in the total system, (atoms/cm^3)

$N_c(z,t)/V_c$ = concentration at height z in the trap

The change in N_c as a function of height is:

$$\frac{\partial}{\partial z}\left[\frac{N_c(z,t)}{V_c}\right] = - \frac{N_c(z,t)}{V_c} \quad \frac{\kappa P}{F}$$

Integrating from $z = 0$ to Z, and letting $N_c(Z,t) = N_c(t)$ at $z = 0$, gives

$$N_c(Z,t) = N_c(t)\, e^{-\kappa PZ/F}$$

Next we consider the time dependence of $N_c(t)$. The transit time of the sodium in the cold trap is PZ/F. Hence,

$$\frac{dN_c(t)}{dt} = - \frac{N_c(Z,t) - N_c(t)}{PZ/F}$$

$$= - \frac{N_c(t)\ (1-e^{-\kappa PZ/F})}{PZ/F}$$

which is the second term of Equation (1).

Information on the deposition rate parameter κ was not found. Perhaps it is dependent on conditions in the cold trap which vary with time, thus making κ time dependent.

It is noted further that the parameter κ in Equation (1) is a deposition rate (i. e. per sec) whereas the deposition constant K is an equilibrium-type value and not related to a rate. Although many of the experiments which report K are made in flowing sodium, it remains unclear how the two constants κ and K are related -- a relation that is necessary before using Equation (1).

7.2.3 Experiments on Cold Trapping of Particular Radionuclides

7.2.3.1 Cesium

Cooper and Taylor[28] of Westinghouse studied cesium sorption from sodium by the following surfaces: polished 304 stainless-steel, as-received 304 stainless-steel, polished nickel, single-crystal aluminum oxide, and oxidized zirconium. Cesium concentrations from <0.1 apm (atom parts per million) to 46 apm were studied.

It was concluded that cesium was sorbed by Van der Waal forces as opposed to chemisorption. Numerical results showed the sorbed cesium surface concentration (atoms/cm^2) to be inversely proportional to temperature and directly proportional to cesium concentration in the sodium (atoms/cm^3).

Later the same experimenters ran experiments on cesium trapping by 304 stainless steel to study the effect of Na_2O on deposition rate.[29] Cesium was cold trapped from almost oxygen-free sodium and from sodium containing oxygen. Initial cesium concentrations were 0.13 and 0.059 apm. Their results are reported as fraction of the initial cesium removed by cold trapping, and this fraction varied from 0.18 to 0.52.

Among their conclusions were:

1. Cesium is removed from flowing sodium by reversible physical adsorption on metal surfaces in the absence of precipitated Na_2O, or by adsorption on both metal and Na_2O surfaces in the case of Na_2O precipitation.

2. Precipitation of Na_2O increased the Cs fraction removed from the sodium. Values are given for atoms of cesium deposited per cm^2 of surface and per gram of sodium for various conditions (particularly oxygen concentrations) and for various flow rates (flow rate had little effect).

3. Adequate LMFBR Cs traps can be designed based on adsorption on clean metal surfaces. Precipitation of Na_2O in this trap would increase the capacity.

Zwetzig, Guon, and Silberberg[26] of Atomics International showed relative trapping levels by stainless steel for cesium concentrations of 65 ppm and three different oxygen concentrations (5, 55, and 105 ppm), as a function of temperature. The deposition levels increased with increasing Na_2O concentration, and the log of the deposition level was inversely proportional to temperature. Deposition occurred at temperatures above which Na_2O had not precipitated, indicating that adsorption occurs directly on metal instead of on Na_2O. Later studies of deposition of cesium on 304 stainless steel in the range of cesium concentrations of 0.7 to 6 ppm and oxygen concentrations from 10 to 25 ppm were reported by Guon of AI.[30] Among the conclusions were:

1. Cesium deposition requires the presence of a third constituent.

2. Cesium deposition and dissolution kinetics are rapid with no apparent hysteresis.

3. A deposition constant, K, (defined in Section 7.2.2) can be used to express the partition of cesium between the sodium solution and stainless-steel wall, in agreement with earlier results from Westinghouse[28] for different cesium concentrations.

4. Surface treatments of stainless steel prior to sodium loading can result in increased cesium deposition by a factory of 10 and possibly 100. The surface treatment referred to concerned the temperature history of the surface prior to deposition; the report shows a relation between K and surface temperature.

Further studies by Guon[31] showed further distribution coefficients (called a "partition parameter" in Reference 31) for cesium, barium, and manganese on stainless-steel surfaces.

Recently Colburn of Westinghouse has presented two papers summarizing work there on cold trapping of cesium and iodine.[32,33] In the first[32] he reports distribution coefficients for both ^{137}Cs and ^{131}I. Further conclusions presented in the paper were:

1. Large Cs deposits observed were not due to physically adsorbed metallic Cs but, rather, are part of a nonmetallic precipitate.

2. The distribution coefficient for Cs and I at cold-trap temperature is strongly influenced by non-metallic contaminants in sodium.

In the second work[33] Colburn studied mechanisms for cesium and iodine deposition in sodium on stainless steel which had been previously exposed to hydrogen or oxygen. Examination showed that the deposition behavior was dominated by interactions with the nonmetallic contaminants, i.e. hydrogen or oxygen. Tests showed that hydrogen was more effective than oxygen. Colburn suggests that the importance of the surface impurities and possible differences in impurity concentrations between experiments could have led to earlier discrepancies in cesium surface distribution coefficients, K, reported in the literature. He reports experimental values for "phase distribution coefficients," D, at 250°F of 8.5×10^5 for Cs and 2.27×10^6 for I, where

$$D \equiv \frac{\text{atoms of Cs (orI)/gram hydrogen in the deposit}}{\text{atoms of Cs (orI)/gram sodium in bulk solution}}$$

He suggests that the intentional addition of hydrogen to the sodium may enhance the ability to cold trap cesium and iodine (while simultaneously enhancing tritium removal by isotopic substitution in the hydride precipitate).

Clifford[34] showed that some cesium could be removed by cold trapping, although most of the cesium remained in the sodium in his experiments. In two loops which operated for 2300 to 2500 hours, equilibrium was believed to have been achieved with the following cesium distribution: one third of the ^{137}Cs deposited in the cold trap, one half remained in the sodium, and the remainder was distributed around the system on stainless steel surfaces. Adding 100 ppm oxygen to the sodium had little effect on the amount of trapped ^{137}Cs, although the cause could have been that the oxygen was absorbed elsewhere in the system than the cold trap. The hot leg of the loops were operated at 500°C, the cold leg at 300°C, and the cold trap in the range from 110°C to 175°C. A total of 3 to 4 mCi of ^{137}Cs was in each trap but no data was provided concerning loop or trap sodium inventories.

7.2.3.2 Iodine

Cold trapping of iodine fission products appears to be effective. Two reports on iodine deposition by Colburn[32,33] also gave results for cesium; hence they were discussed in the previous section on cesium.

Cooper, Grundy, and Taylor[35] reported experimental values of the distribution coefficient, K, for NaI in sodium. They found that log K is inversely proportional to the sodium absolute temperature, as was the case with cesium. This relationship held both for low iodine concentrations ($\sim 10^{-6}$ to 10^{-9} apm) and for high concentrations (0.05 apm), although the distribution coefficients for the high concentration were about a factor of five larger than those at low concentrations. In all cases, more than 90% of the iodine was removed by cold trapping at 250°F. They also conclude that 99% of iodine may be cold trapped in high oxygen/hydrogen systems or by the addition of sufficient natural iodine to increase the concentration beyond the NaI solubility limit at the cold trap temperature.

7.2.3.3 Strontium, Barium, and Zirconium

Clifford[36] reported some experience with strontium in cold traps. He reported that strontium deposited on the stainless-steel and zirconium surfaces of a cold trap at 300° to 500°C, with the strontium collection at 300°C being an order of magnitude higher than at 500°C. Slightly more deposition occurred on stainless steel than on zirconium.

At BR-5, barium and zirconium were collected in the cold trap, but much less effectively than iodine and cesium.[17]

7.2.3.4 Tritium

Cold trapping of tritium (a fission product as well as an activation product) was discussed in Section 5.1.3.2.

7.2.4 Operating Experience on Cold Trapping of Fission Products at Sodium-Cooled Reactors

7.2.4.1 Summary

Experience at each reactor for which data are available is reported in Section 7.2.4.

Fission products which have been observed in cold traps are listed in Tables 7.1 and 7.8.

Table 7.8

Fission Products Observed in Primary Cold Traps of Sodium or NaK Cooled Reactors

EBR-II[38]	^{137}Cs, ^{134}Cs, I
BR-5[17]	^{137}Cs, ^{136}Cs, ^{131}I, ^{133}I, ^{135}I, ^{95}Zr-Nb, ^{140}Ba-La
Dounreay[8]	^{137}Cs
SRE[39]	^{137}Cs, ^{106}Ru, ^{144}Ce-Pr

7.2.4.2 EBR-II

Despite experimental work reviewed in this report and results from other reactors that show the success of ^{137}Cs removal by cold traps, EBR-II personnel maintain that the primary system cold trap does not reduce ^{137}Cs satisfactorily at EBR-II.[37] This result is shown by observing the reported ^{137}Cs activity levels in the primary sodium, as shown in Table A25 of Appendix A. In 1971 the level built up to 20 nCi/gm Na from failed fuel, and stayed there.

Experience with iodine (and tritium--see Section 5.1.3.2) at EBR-II was different. The cold trap does remove ^{131}I so that the levels are generally below 0.1 nCi/gm in the primary sodium (see Table A25, Appendix A). Also EBR-II personnel can observe increases in the ^{131}I levels in the cover gas when the primary cold trap is cut off.[37]

A primary system cold trap was removed from operation from EBR-II in 1965. Unfortunately the contents of this cold trap were never analyzed; the trap still sits in a field near EBR-II.

Recently limited data have been reported concerning the EBR-II primary cold trap.[38] A gamma spectral scan of the trap during a shutdown period in 1972 identified radiation from ^{22}Na, ^{54}Mn, ^{60}Co, ^{65}Zn, ^{124}Sb, ^{125}Sb, ^{134}Cs, and ^{137}Cs. The ratio of the ^{137}Cs to ^{22}Na activities was ~18. The same ratio in the primary sodium was ~0.36. Hence, the ^{137}Cs concentration ratio in the cold trap for this measurement was ~50. This is far below the value reported by SRE (see Table 7.9 below).

The dose rate from the cold trap during the 1972 shutdown was 90% higher than the value during a shutdown one year before, in 1970-71. The measurements in the previous shutdown are reported in Reference 15. The dose rate 2 in. from the surface was 290 mR/hr at 132 days after the 1972 shutdown, compared to 153 mR/hr at 132 days after the 1970-71 shutdown.

7.2.4.3 BR-5

The BR-5 cold trap was reported to trap ^{131}I, ^{137}Cs, and ^{136}Cs.[17] More than 90% of the I and Cs activity was trapped. The cold trap also collected zirconium and barium, but much less efficiently than I and Cs.

The ^{135}Xe and the ^{133}Xe activities in the cover gas were reduced by factors of two and three, respectively, when the cold trap was operating, due to trapping of the precursors ^{135}I and ^{133}I.

7.2.4.4 SRE

Extensive data are available from SRE cold trapping experience because the cold traps were used to clean up the sodium system after

Table 7.9

Comparison of Impurity Levels in SRE Cold Trap to those in Sodium Coolant [22,39]

Impurity	In Cold Trap	In Coolant	Concentration Ratio
Carbon	144-1550 p.p.m.	18-60 p.p.m.	2-80
^{137}Cs	4.0x10^{2} μCi/g	1.5x10^{-2} μCi/g.	2.7x10^{4}
^{125}Sb	4.3 μCi/g	0.6x10^{-2} μCi/g.	7.2x10^{2}
Fe	200- >500 p.p.m.	50 p.p.m.	4- >10
Si	200- >500 p.p.m.	50 p.p.m.	4- >10
Mn	50- 500 p.p.m.	<5 p.p.m.	10- >100
Pb	5 >500 p.p.m.	10 p.p.m.	0.5- >50
Cr	5- >500 p.p.m.	5 p.p.m.	1- >100
Ni	10- 300 p.p.m.	5 p.p.m.	2- 60

extensive fuel cladding failure.[22,39] There was a large amount of carbon in the system, however, which leads to uncertainty in applying the results directly to a cold trap system without carbon. Hansen[39] provides arguments that oxide impurity in the sodium was responsible for the greater retention of ^{137}Cs instead of the carbon impurity.

The most interesting results are the concentration ratios, which are reported in Table 7.9. The large concentration ratio for ^{137}Cs is particularly noted. The total ^{137}Cs trapped was ~10 Ci. In addition to those shown in Table 7.9 (only one of which is a fission product), the fission products ^{106}Ru, ^{144}Ce-Pr, and ^{110}Ag were also observed in the cold trap.

7.2.4.5 SEFOR and Fermi

Although reports on oxide removal by cold traps in SEFOR[23] and Fermi[22] are available (as discussed in Section 7.2.1), no results were found on fission product removal by cold traps at these facilities.

REFERENCES (Section 7)

1. A. W. Castleman, Jr., and I. N. Tang, "Fission Product Vaporization from Sodium Systems." Proceedings of the International Conference on Sodium Technology and Large Fast Reactor Design, ANL-7520, I, 540, November 7 - 9, 1968.

2. A. W. Castleman, Jr., "LMFBR Safety, I. Fission-Product Behavior in Sodium," Nuclear Safety, II, 379 (September - October 1970).

3. D. E. Plumlee and P. E. Novak, "Measured Loss of Selected Fission Products from High-Burnup Mixed-Oxide Fuel in a Miniature Pumped Sodium Loop," GEAP-13731, August 1971.

4. J. Saroul, "Investigation on the Behavior of Fission Products in Sodium and Argon--Pirana Experiments," Proceedings of the International Conference on the Safety of Fast Reactors," Aix-en-Provence, France, Session Vb-1, September 19-22, 1967.

5. J. Saroul, "Out of Pile Studies and Diffusion of the Contamination in Liquid Sodium and Fast Reactor Containment, New Experimental Program," Proceedings of the International Congress on the Diffusion of Fission Products, Saclay, France, November 4-6, 1969.

6. R. deFremont, "TEMPÊTE Test: In Pile Experiment on the Transfer of Fission Gases. Comparison to Out of Pile Tests," DRNR/STRS, 71.1147 (France), 1971.

7. J. J. Regimbal, W. P. Kunkel, and R. S. Gilbert, "Measurement of Noble Gas Transport Dynamics in SEFOR Sodium," Trans. Am. Nucl. Soc., 14, 773, (1971).

8. J. L. Phillips, "Full Power Operation of the Dounreay Fast Reactor," Proceedings of the National Topical Meeting on Fast Reactor Technology, ANS-100, p. 23, April 26-28, 1965.

9. B. D. Pollock, M. Silberberg, and R. L. Koontz, "Vaporization of Fission Products from Sodium," Proceedings of the International Conference on Sodium Technology and Large Fast Reactor Design," ANL-7520, I, 549, November 7-9, 1968.

10. A. W. Castleman, Jr., I. N. Tang, and MacKay, "Fission Product Behavior in Sodium Systems," Proceedings of the Symposium on Alkali Metal Coolants, IAEA, Vienna, 1966, p. 729.

11. M. H. Cooper, B. R. Grundy, and G. R. Taylor, "Behavior of Iodine in Sodium Systems," Trans. Am. Nucl. Soc., 15, 232 (1972).

12. W. S. Clough and S. W. Wade, "Caesium Behavior in Liquid Sodium -- The Effect of Carbon," Proceedings of the Eleventh AEC Air Cleaning Conference, 1, 393, September, 1970.

13. W. S. Clough, "The Behavior of Barium and Strontium Fission Products in Liquid Sodium," Proceedings of the International Congress on the Diffusion of Fission Products, Saclay, France, November 4 - 6, 1969.

14. G. B. Zwetzig, "Survey of Fission - and Corrosion - Product Activity in Sodium - or NaK-Cooled Reactors," AI-AEC-MEMO-12790 (February 1969).

15. Reactor Development Program Progress Report, ANL-7845, Section 1 (July 1971).

16. Reactor Development Program Progress Report, ANL-7776, 1 - 24 (January 1971).

17. V. V. Orlov, M. S. Pinkhasik, N. N. Aristarkhov, I. A. Efimov, A. V. Karpov, M. P. Nikulin, "Some Problems of Safe Operation of the BR-5 Plant," Proceedings of the International Conference on the Safety of Fast Reactors, Aix-en-Provence, France, Session Va-7, September 19 - 22, 1967.

18. R. deFremont, "Observations on the Behavior of Radioactive Products on Rapsodie," DRNR/STRS, 71.1146, 1971.

19. R. deFremont, "Decontamination Experience on Rapsodie," DRNR/STRS, 71.1145, 1971.

20. R. S. Hart, "Distribution of Fission Product Contamination in the SRE," NAA-SR-6890 (March 1962).

21. R. L. Eichelberger, "A Recommended Expression for the Solubility of Oxygen in Liquid Sodium," Trans. Am. Nucl. Soc., 12, 613 (1969).

22. R. B. Hinze, "Cold Trap Performance Limitations (A State-of-the-Art Review)," Chem. Eng. Prog., Symposium Series, 66, No. 104, 94 (1970).

23. A. D. Gadeken and M. C. Plummer, "SEFOR Cold-Trap Experience," GEAP-10548 (April 1972).

24. J. Herb, "Examination of the Enrico Fermi Sodium Cold Trap," WCAP-4321 (November 1965) (Limited distribution report).

25. "Task II Report, Conceptual Plant Design, System Descriptions, and Costs for a 1000 MWe Sodium-Cooled Fast Reactor," GEAP-5678, p. 206 (December 1968).

26. G. B. Zwetzig, J. Guon, and M. Silberberg, "The Distribution of Fission Products in LMFBR Sodium Systems," Proceedings of the International Conference on Sodium Technology and Large Fast Reactor Designs, ANL-7520, I, 527, November 7 - 9, 1968.

27. G. B. Zwetzig and R. F. Rose, "Interim Description of a Computer Code (STP-1) for Estimating the Distribution of Fission and Corrosion Product Radioactivity," AI-AEC-12847 (June 1969).

28. M. H. Cooper and G. R. Taylor, "Cesium Sorption from Liquid Sodium, Trans. Am. Nucl. Soc., 11, 525 (1968).

29. M. H. Cooper and G. R. Taylor, "Cesium Cold Trapping in a Forced-Convection Na System," Trans. Am. Nucl. Soc., 12, 611 (1969).

30. J. Guon, "Studies of Cesium Deposition in a Sodium/Stainless-Steel System," Trans. Am. Nucl. Soc., 12, 612 (1969).

31. J. Guon, "Effect of Surface/Liquid Partition on the Analysis of Impurities in a Sodium System," Trans. Am. Nucl. Soc., 14, 625 (1971).

32. R. P. Colburn, "Nature of Cs and I Deposits in Sodium Systems," Trans. Am. Nucl. Soc., 14, 626 (1971).

33. R. P. Colburn, "Fission Product Removal from Sodium by Hydride Slagging," Trans. Am. Nucl. Soc., 15, 235 (1972).

34. J. C. Clifford, Advanced Plutonium Fuels Program, Second Annual Report, LA-3993, September, 1968.

35. M. H. Cooper, B. R. Grundy, and G. R. Taylor, "Behavior of Iodine in Sodium Systems," Trans. Am. Nucl. Soc., 15, 232 (1972).

36. J. C. Clifford, "Behavior of Fission Products in Sodium," Proceedings of Symposium on Alkali Metal Coolants, I.A.E.A., Vienna, 759 (1967).

37. EBR-II personnel, personal communication, December, 1972.

38. Reactor Development Program Progress Report, ANL-RDP-7, p. 110 (July 1971).

39. A. I. Hansen, "The Effects of Long-Term Operation on SRE Sodium System Components," NAA-SR-11396 (August 1965).

8. GASEOUS RADWASTE MANAGEMENT

The proposed gaseous radwaste systems of FFTF and EBR-II together with some review of present systems for EBR-II, Fermi, SEFOR, Rapsodie, and Dounreay are discussed in this section. Also a comparison is made with LWR gaseous radwaste systems.

The quantities of gaseous activity that will be released from FFTF are expected to be trivial. This results from two factors: (a) a sophisticated gaseous radwaste system will be used on FFTF, and (b) there is virtually no liquid coolant leakage from an LMFBR from which noble gases can escape to the environment. Although sophisticated gaseous radwaste systems have not been used heretofore on fast reactors, such systems will probably be used on future LMFBR power plants. Nevertheless, results are presented here for ^{85}Kr releases both with and without such systems since their future use is not assured.

The current situation in LWR power plants differs from expected future LMFBR plants for two reasons: (a) generally, gaseous radwaste systems on present LWR's are not as effective as the FFTF system and (b) significant coolant leakage occurs in LWR components, providing a pathway for fission-product gas transport to the environment not present in the LMFBR. In Section 8.4 current "typical" LWR gaseous effluents are described together with projected reductions in these effluents if such reductions are warranted.

The ^{85}Kr releases from an LWR can be reduced to about the same levels as an LMFBR, assuming that sophisticated gaseous radwaste systems are used on both. However, it is more difficult in the LWR due to coolant leakage. Without an elaborate gaseous radwaste system on either the LMFBR or the LWR, the ^{85}Kr release rate would be comparable for the two reactors, with a slightly lower rate for the LMFBR.

The large contributors to total gas releases from an LWR are the short-lived isotopes. These can be reduced to low values, but this requires reduction or containment of coolant leakage, which is difficult. Since there is no routine coolant leakage from an LMFBR, these short-lived isotopes are not released even from an "unsophisticated" gaseous radwaste system that depends only on holdup time.

8.1 FFTF Gaseous Radwaste Systems[1,2,3]

The Fast Flux Test Facility (FFTF) is a 400 MWt sodium-cooled reactor, being designed and constructed at Hanford under the management of the Westinghouse Hanford Company for the USAEC Division of Reactor Development and Technology. The purpose of FFTF is to provide experimental data in support of the LMFBR program in a number of areas, including: fast neutron effects on fuels and materials; fast reactor fuel performance; and system and component performances. In keeping with this purpose, the design will allow reactor operation with continuous noble gas release to the primary system from up to 1% of the fuel pins. Also, four special sodium-cooled closed loops will permit testing of vented or defective fuel. FFTF is designed to release practically zero quantities of radionuclides to the environment. This "near zero release" operation will be achieved primarily by means of high-integrity sealing of the primary sodium systems and through the use of two gas processing systems, namely, the Radioactive Argon Processing System (RAPS) and the Cell Atmosphere Processing Systems (CAPS). Salient details of these features are discussed below.

8.1.1. Primary Sodium System Seals

The FFTF reactor will operate with a maximum outlet temperature of the coolant of approximately 1050°F. At this temperature, the vapor pressure of sodium is only 0.018 atmospheres absolute. In order to prevent inleakage of air into the reactor, it is necessary to pressurize the reactor with an inert gas. At FFTF argon has been chosen for this service; the reactor cover gas pressure is nominally 10 inches WG or approximately 1.025 atmospheres absolute. The closed loops require an argon cover gas pressure of about 55 psig in order to prevent sodium pump cavitation. Since the argon cover gas lies on top of the sodium in the reactor and closed loops, certain gaseous fission products, primarily the Kr and Xe isotopes, which escape from defective or vented fuel pins can disengage from the sodium and collect in the argon cover gas. Consequently, it is important to reduce the leakage of this potentially contaminated cover gas into the reactor building.

To accomplish this, gas buffered seals are used in the reactor head and in the closed loops. Each buffered seal consists of two seals in series, with positive argon buffer gas pressure (e.g., 2 psig in the reactor head seal) maintained in the annular space between the two seals. Since all seals leak to some extent, there is some argon buffer gas continuously leaking into the reactor and into the reactor building from the inter-seal spaces. Therefore, it is necessary to vent argon cover gas from the primary system, at a rate which depends on the amount of leakage, in order to maintain the cover gas pressure in the proper range. The flow rate of argon from the reactor cover gas region is expected to be about 4 standard cubic feet per minute (scfm). The closed-loop cover gas will contribute an additional 0.02 scfm. This flow of contaminated argon cover gas goes to the Radioactive Argon Processing System (RAPS), where its activity is substantially reduced. The relatively "clean" argon leaving the RAPS is recycled for use as cover gas or for pressurization of the buffered seals.

The buffer gas which leaks into the reactor building from the interseal spaces should present no significant radiation hazard, as it has practically the same specific activity as the effluent from RAPS. Although the references[1,2,3] report no values for the volumetric leak-rates into the reactor building, it is reasonable to assume a value equal to the total leak-rate from the inter-seal spaces into the reactor and the closed loops, i.e., about 4 scfm. The specific activity of the buffer gas is estimated in Reference 1 to be 10^{-5} Ci/ml, most of which is ^{85}Kr. Assuming this activity and the leak rate of 4 scfm, the rate at which activity leaks into the reactor building and thence to the environment via the reactor building ventilation system is:

$$\frac{4\ \mathrm{ft}^3}{\mathrm{min}} \times \frac{28317\ \mathrm{ml}}{\mathrm{ft}^3} \times \frac{10^{-5}\ \mu\mathrm{Ci}}{\mathrm{ml}} \times \frac{1440\ \mathrm{min}}{\mathrm{day}} = 1.63 \times 10^{-3}\ \frac{\mathrm{Ci}}{\mathrm{day}}$$

Thus, the annual discharge of activity to the environment stemming from leakage of buffer gas into the reactor building is only about 0.5 Ci.

8.1.2 Radioactive Argon Processing System (RAPS)

This system (RAPS) is designed to receive the contaminated argon cover gas from the reactor and the four closed loops and to process it on a continuous basis. The system is designed to process an inflow of about 700,000 Ci of noble gases per day,[2] yielding a purified argon effluent having a specific noble gas activity of 10^{-5} μCi/ml or less, which corresponds to a maximum allowable specific activity of 1 MPC* for Kr-85.

The basic flow-sheet of RAPS is shown in Figure 8.1 Contaminated argon, vented by pressure controllers from the various cover gas regions, is piped to a surge tank, from which it is metered into a processing loop consisting of four cryogenic charcoal delay beds, four heat exchangers for removal of decay heat, a fractionation column, a gas circulator, a surge gas storage tank, and various control elements.

The delay beds are quite effective in holding up xenon (and iodine, if any exists in the cover gas), less so for krypton. Table 8.1 summarizes the delay times under design conditions.[2] For these delay times, virtually all radioactive xenon and most of the short-lived krypton is eliminated in the decay beds.

Argon leaving the last decay bed is recooled to -280°F before being injected into the fractionation column. The stable xenon isotopes and the krypton isotopes are concentrated in a pool of liquid argon in the bottom of the fractionation column by the refluxing action

---

* From 10CFR20, Appendix B, Table 1 (maximum permissible average concentration in restricted areas to persons of age 18 or more).

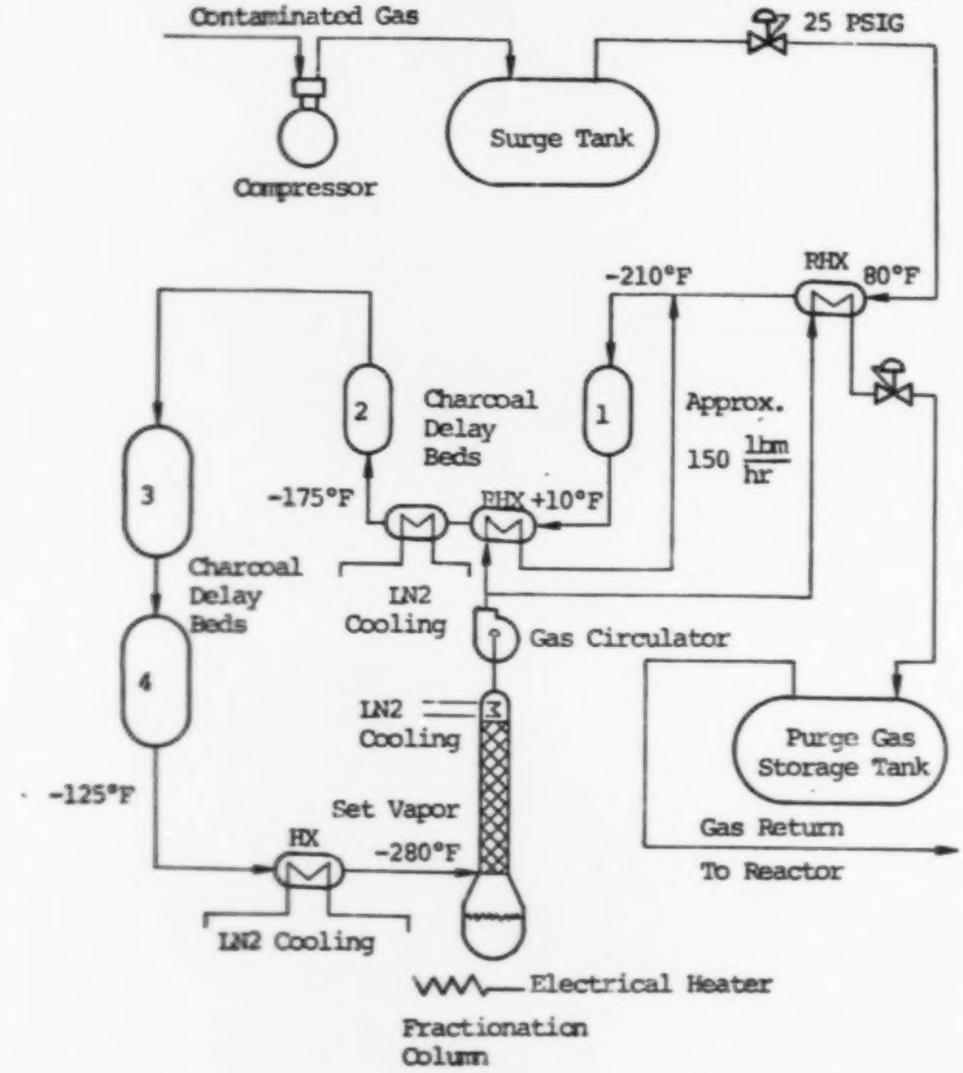
Contaminated Gas
25 PSIG
Surge Tank
Compressor
-210°F
RHX
80°F
Charcoal
Delay
Beds
2
1
Approx.
150 lbm/hr
3
-175°F
RHX
+10°F
Charcoal
Delay
Beds
LN2
Cooling
Gas Circulator
4
LN2
Cooling
Purge Gas
Storage Tank
-125°F
Set Vapor
HX
-280°F
Gas Return
To Reactor
LN2 Cooling
Electrical Heater
Fractionation
Column

Figure 8.1 Radioactive Argon Processing System

Table 8.1

Radioactive Argon Processing System Delay Times

	Delay Bed No. 1	Delay Bed No. 2	Delay Bed No. 3	Delay Bed No. 4
Xenon Delay, Days	9	45	42	40
Krypton Delay, Days	0.27	0.78	0.76	0.73

of the column. The fractionation column is expected to remove 99.9% of the xenon and krypton isotopes from the gas stream. The purified argon gaseous effluent from the column is expected to have a specific noble gas activity of 10^{-5} μCi/ml or less. The purified argon is recycled back to the buffered seals.

When it becomes desirable to remove the accumulation of noble gas nuclides in the bottom of the column, the column is isolated and its contents are gasified and transferred to an ambient-temperature tank for long term storage. Under design operating conditions (1% defective fuel), the annual accumulation of Kr-85 in the fractionation column will be about 300 Ci. Other noble gas nuclides will be present in only trace quantities.

If it is assumed that leakage from RAPS is negligible, there is virtually no release of radioactivity from this system to the environment.

8.1.3 Cell Atmosphere Processing System (CAPS)

The primary sodium equipment cells are provided with virtually inert atmospheres of nitrogen with approximately one percent oxygen. The cells are sealed and the atmospheres are maintained by feed-and-bleed pressure controls. Effluents from these cells are processed by the Cell Atmosphere Processing System (CAPS) before release to the environment.

The basic flow-sheet for CAPS is shown in Figure 8.2. Gas vented from the inert atmosphere cells is pumped into a surge tank, from which it is metered into the processing equipment, consisting of a disiccant unit, two cryogenic charcoal delay beds, two liquid nitrogen cooled heat exchangers for removal of decay heat, a gas circulator, and various control elements. The effluent from CAPS is mixed with air passing through the FFTF heating and ventilation system and exhausted to the environment.

Although the final design of CAPS has not yet been made, an estimate of the delay times associated with the charcoal delay beds is 53 days for xenon and 2 days for krypton at a flow rate of 25 scfm and a temperature of -100°F.[3] CAPS should be able to process between 0 and 50 scfm of contaminated inert gas, depending on the demand.

The normal release of activity from CAPS is virtually zero, since there should be no release of activity from the primary system under normal conditions.

8.2 EBR-II Gaseous Radwaste Systems

8.2.1 Present Operation

EBR-II is used to test fuel for the LMFBR development program. The driver fuel is metallic U-235. Test pins are made of potential

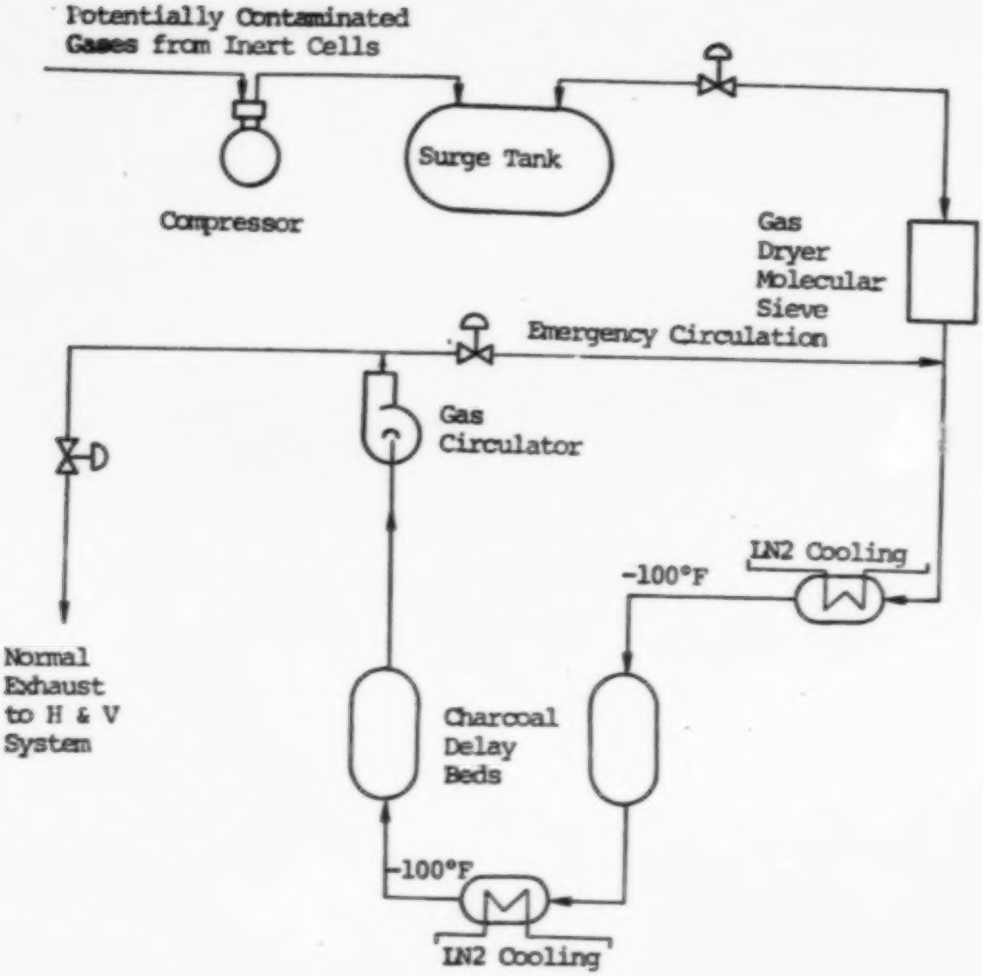
Potentially Contaminated
Gases from Inert Cells
Compressor
Surge Tank
Gas
Dryer
Molecular
Sieve
Emergency Circulation
Gas
Circulator
LN2 Cooling
-100°F
Normal
Exhaust
to H & V
System
Charcoal
Delay
Beds
-100°F
LN2 Cooling

Figure 8.2 Cell Atmosphere Processing System

LMFBR fuels such as oxides, carbides, and nitrides, with oxide test pins predominating.

At present EBR-II cannot operate with failed test pins. When oxide pins fail, fission product gas is rapidly released. Leakage from the cover gas to the reactor building is sufficiently high that EBR-II must be shut down when a test pin fails and remain shut down until the failed pin is located and removed.

EBR-II can operate with failed driver fuel, however. Failed metallic fuel releases fission product gas at such a slow rate that the present cover gas cleanup system can reduce the activity from failed driver fuel adequately.

The present gas radwaste system is designed: (a) to operate during normal reactor operation and (b) to purge the cover gas when a failure occurs in a test pin.

8.2.1.1 Normal Operation

During normal operation the escape rate of the cover gas from the reactor tank is ∿1000 ml/min. Of this ∿130 ml/min passes through the various monitoring systems and then is discharged to the atmosphere through the stack. The remainder (i.e. ∿900 ml/min) leaks to the reactor building. The air in the reactor building is continually being purged, with the exhaust being discharged to the atmosphere through the stack. Hence all 1000 ml/min of cover gas eventually is discharged directly to the atmosphere via the stack.

8.2.1.2 Fast Gas Purge System

In the event of a test fuel pin failure the reactor is shut down, and the Fast Gas Purge System is put into operation. This system removes the cover gas and eventually sends it to the atmosphere through the stack.

The flow rate to the system can be varied up to 3 standard cubic feet per minute (scfm). The purged argon is replaced with fresh argon while monitoring the cover gas at slightly above atmospheric pressure. The activity in the cover gas can be returned to a tolerable level in 3 to 4 hours.

In the Fast Gas Purge System, the first step is to remove sodium vapor in a vapor trap. An aerosol trap filters out particles of size greater than 5μ . This is followed by a gas sampling and monitoring station. Finally there is a variable speed pump and a flowmeter. The gas is then sent out of the containment to the suspect exhaust stack and to the atmosphere.

8.2.2 Proposed Gas Radwaste System

A system has been proposed[4] for use at EBR-II which would allow operation with failed test fuel. The proposed system is described here because of its educational value. It is an example of a system that has been extensively analyzed and one for which the analysis is available. If it is implemented, it will serve as a useful demonstration that operation with failed oxide fuel is feasible, or at least it will identify problems involved with such operation.

8.2.2.1 Criteria

The first step toward designing a system for operation with failed test fuel was to determine the required design criteria.[5] Ultimately this meant specifying the flow rate to the proposed cover gas cleanup system and the activity of the gas to be processed by the system.

The design criteria were:

- Operation with 12 defective oxide fuel pins at a linear power density of 16 kW/ft.
- Detection of a new test pin failure by a step release of ^{133}Xe.
- Activity in the reactor building below the maximum permissible concentration as defined by 10 CFR 20.
- Gas release to the environment from the stack to be below the maximum permissible concentration at ground level as defined by 10 CFR 20.

The number of defective fuel pins and linear power density were based on proposed fuel failure test requirements by the General Electric Co. Calculations were made of fission gas release rates from defective oxide pins to determine the rate at which activity of each isotope would be added to the cover gas.[5] The Booth diffusion model was used for these calculations.

Detection of failed oxide pins by xenon tagging has been successfully demonstrated in EBR-II, and test fuel pins are now being tagged. In order for the xenon tagging method to work, the level of xenon isotopes in the cover gas must be kept low. The fact that a new failure has occurred is indicated by a rise in ^{133}Xe activity. It was determined that a 25% rise in ^{133}Xe activity due to a new fuel pin failure was sufficient for detection. A pin failure is expected to increase the cover gas activity by 0.25 μCi/ml. Therefore, the second design criteria meant that the cover gas ^{133}Xe activity from 12 failed fuel pins must be held to $<$1.0 μCi/ml.

In order to meet the 1 μCi/ml ^{133}Xe activity from 12 failed pins, the required cover gas purge rate was determined to be 10 scfm.

For the resulting activity levels in the cover gas, the present leakage rate of ~1000 ml/min from the cover gas to the reactor building is too great. In order to reach 10 CFR 20 MPC levels, the leakage rate must be reduced by a factor of 100, to 10 ml/min. It is anticipated that this can be done by replacement of seals known to be principal sources of the current high leakage.

8.2.2.2 Cover Gas Cleanup System

The 10 scfm of cover gas purged must be treated in order to remove radioactive krypton and xenon isotopes from it. The method selected for the proposed EBR-II system is the use of charcoal adsorption beds. This method was selected over other possibilities (e.g. cryogenic distillation, permselective membranes, and selective absorption in liquid fluorocarbons) on the basis of relative costs, relative effectiveness, complexity, possible material problems, and space requirements.

Before passing through the charcoal delay beds, the gas passes through an aerosol removal system. This system will remove sodium liquid entrainment and fine particles. Aerosol traps will be followed by high efficiency filters, but the specific design for neither has yet been selected. A gas flowmeter will also be in the aerosol removal system. There will be two redundant modules, each containing a trap, filter, and flowmeter, and each module will have sufficient capacity to perform the entire aerosol removal function independently.

Two conceptual charcoal delay-bed systems have been designed from which a final selection will be made. The simpler design is a 7-day-delay system.

8.2.2.3 Seven-Day-Delay System

The 7-day-delay system is shown in Figure 8.3. Flow capacity through the system is 10 scfm, although lower flow rates (and longer delay times) would be used if fewer than 12 fuel pins had failed. For seven days flow is directed through one delay bed, e.g. T1. The argon cover gas is cooled in cooler HX1 to -136°F. At this low temperature, the xenon and krypton in the cover gas are adsorbed on the charcoal. Decay heat from Xe and Kr in the delay bed causes the temperature to rise to -64°F as the argon passes through the bed. The argon is then filtered (F3), reheated to 80°F, and returned to the reactor. The delay bed provides a seven-day holdup of xenon and a seven-hour holdup of krypton.

After seven days of service, the cover gas flow is switched to the second delay bed, T2, and the first bed, T1, is regenerated, i.e. the xenon and krypton isotopes are removed. Regeneration is accomplished by heating the bed to 400°F (at which temperature the adsorbed xenon and krypton are released from the charcoal) and backflushing the bed with a small flow of cover gas diverted from the outlet of the operating delay bed, T2. This hot gas from T1, which now contains the

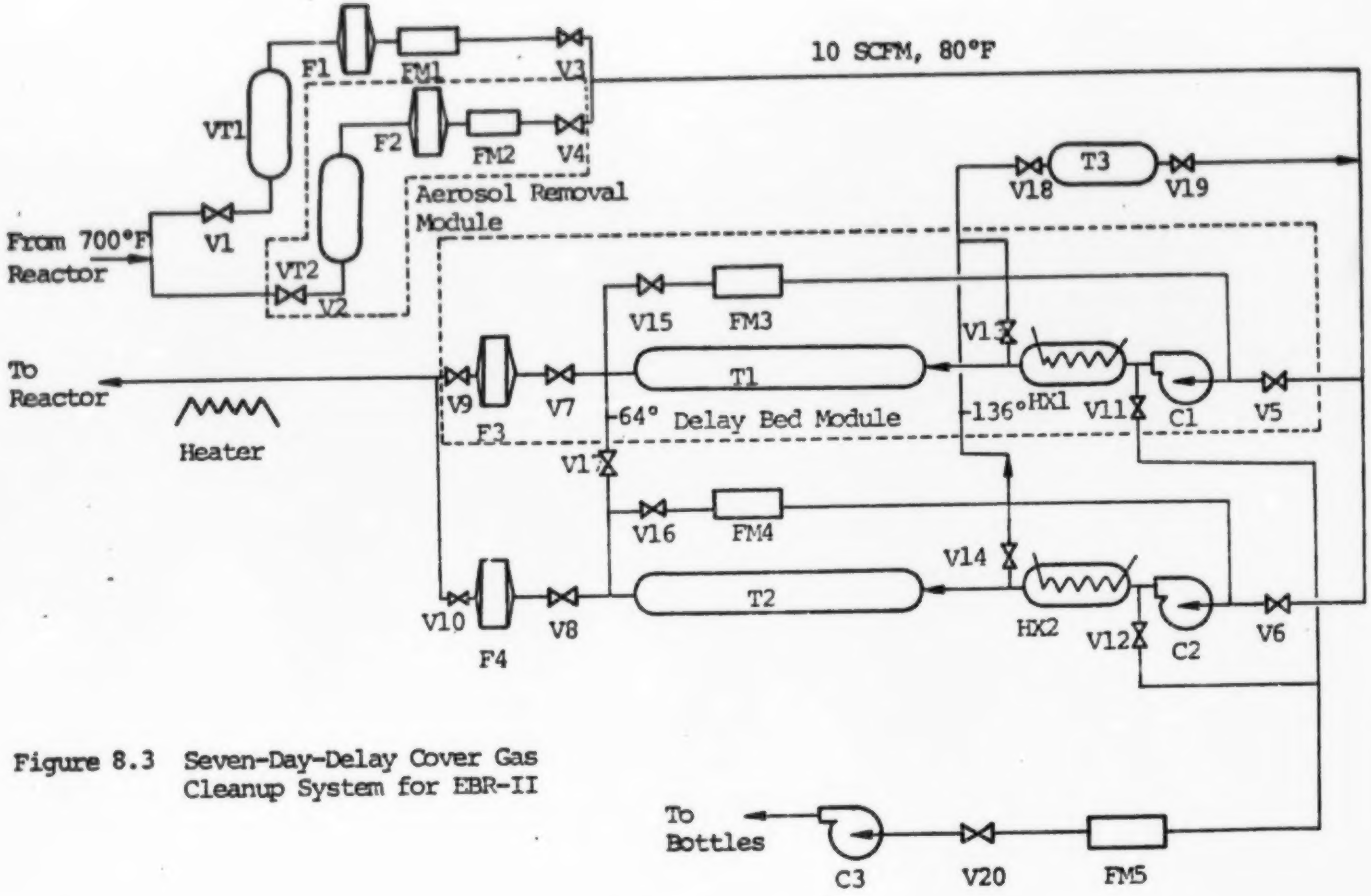
10 SCFM, 80°F
F1
FM1
V3
VT1
F2
FM2
V4
Aerosol Removal Module
From 700°F Reactor
V1
VT2
V2
T3
V18
V19
V15
FM3
V13
To Reactor
Heater
V9
F3
V7
T1
-64° Delay Bed Module
-136° HX1
V11
C1
V5
V17
V16
FM4
V14
V10
F4
V8
T2
HX2
V12
C2
V6
To Bottles
C3
V20
FM5

Figure 8.3 Seven-Day-Delay Cover Gas Cleanup System for EBR-II

xenon and krypton from T1, is cooled in HX1 and is compressed into bottles. The volume of gas bottled each week is 162 standard cubic feet. The bottles are shipped off site for further processing or storage. After regeneration, the gas in the bed is recirculated through the blower and cooled until the bed returns to operating temperature (-100°F).

Another small bleed stream is sent to a Xe-tag cold trap, T3. The xenon is held up in this trap for about one hour. In the event of a fuel element failure, the trap will collect and retain the xenon tag sample for later analysis.

This delay bed system removes nearly all of the xenon activity from the cover gas stream before it is returned to the reactor. Since the krypton is held a shorter time on the beds, some of it returns to the reactor. The fraction returned for each krypton isotope is listed in Table 8.2. Also shown in Table 8.2 are the calculated activities and decay heat rates in the delay bed in service for both xenon and krypton for operation with 12 failed fuel rods.

8.2.2.4 24-Hour Delay System

The 24-hour-delay-system is shown in Figure 8.4. Three delay beds are used on a 24 hour cycle each.

The most fundamental change in this system compared to the 7-day system is the addition of the secondary delay beds T4 and T6. After regeneration of one of the 24-hour-delay beds, the argon is cooled and sent to the secondary delay beds T6 and T4. The delay bed T4 operates at room temperature and provides a 50-day holdup of xenon isotopes. The outlet gas from T4 is cooled to -60°F and flows through the krypton retention bed, T6. The regeneration flow rate is approximately 9 scfh and approximately 6 hours is required, so that approximately 54 standard cubic feet of gas is used for regeneration. The outlet from T6 is either sent to the stack or recirculated back through the primary delay beds and to the reactor. The krypton holdup time in T6 is 7 days. Hence all of the krypton isotopes will decay in T6 except ^{85}Kr.

Once each week the krypton retention bed, T6, is regenerated, and the effluent is compressed into bottles, for storage or shipment off-site. During regeneration, T6 is heated to 300°F. Regeneration of this bed is accomplished during regeneration of a primary delay bed; hence the same flow rate (9 scfh) is used. Regeneration requires only 2.1 hr., hence only 18.9 standard cubic feet each week must be bottled.

8.3 Gaseous Radwaste Experience in Other Operating Fast Reactors

8.3.1 Fermi

Tables of cover gas data for Fermi are given in Appendix A of this

TABLE 8.2

Xenon and Krypton Conditions in Delay Beds

Isotope	Half Life	Fraction Returned To Reactor	Activity On Bed	Decay Heat (Including Daughters)
			(Ci)	(Btu/hr)
^{83m}Kr	1.86 hr	0.209	19.8	0.02
^{85m}Kr	4.4 hr	0.517	32.9	0.36
^{85}Kr	10.76 hr	1.00	0.0032	2.8 x 10^{-5}
^{87}Kr	76 min	0.102	83.5	4.02
^{88}Kr	2.8 hr	0.355	55.5	3.52
^{89}Kr	3.2 min	$<10^{-6}$	10.2	0.49
^{90}Kr	33 sec	$<10^{-6}$	0.76	0.07
				8.48 total
^{131m}Xe	11.9 d	$\sim$0	0.87	0.00
^{133m}Xe	2.3 d	$\sim$0	15.1	0.07
^{133}Xe	5.27d	$\sim$0	384	1.53
^{135m}Xe	15.6 min	$\sim$0	17.3	0.18
^{135}Xe	9.2 hr	$\sim$0	92.4	1.07
^{137}Xe	3.8 min	$\sim$0	92.0	2.75
^{138}Xe	14 min	$\sim$0	41.1	1.60
^{139}Xe	41 sec	$\sim$0	0.45	0.02
^{140}Xe	13.7 sec	$\sim$0	0.05	0.00
				7.22 total

Total decay heat = 15.70 Btu/hr

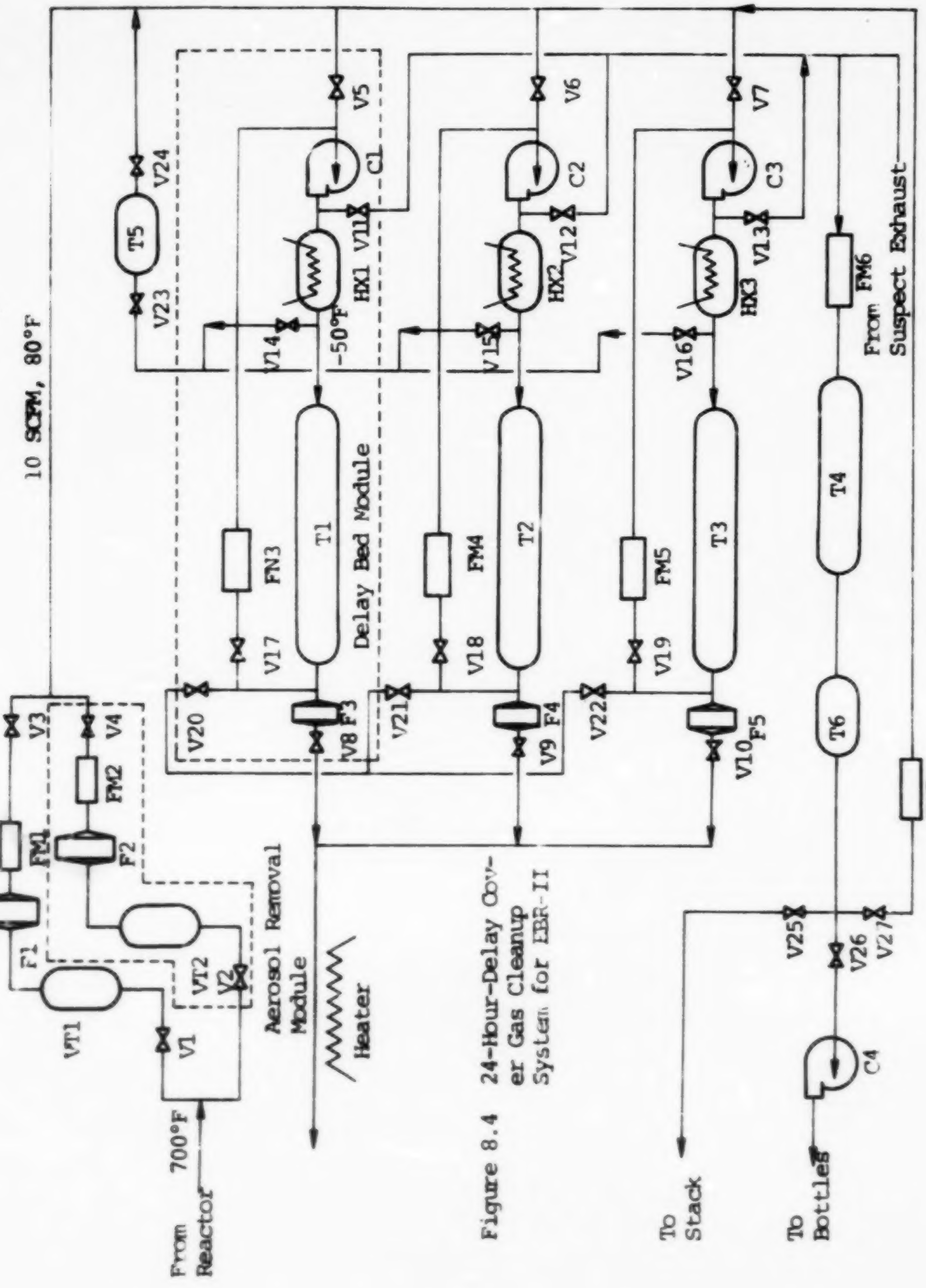

Figure 8.4 24-Hour-Delay Cover Gas Cleanup System for EBR-II

From Reactor
700°F
V1
VT1
F1
FM1
V3
VT2
V2
F2
FM2
V4
Aerosol Removal Module
Heater
10 SCFM, 80°F
V20
V8 F3
V17
FN3
T1
Delay Bed Module
V14
-50°F
HX1
V11
C1
V5
V23
T5
V24
V21
V9 F4
V18
FM4
T2
V15
HX2
V12
C2
V6
V22
V10 F5
V19
FM5
T3
V16
HX3
V13
C3
V7
To Stack
To Bottles
C4
V25
V26
V27
FM7
T6
T4
FM6
From Suspect Exhaust

report. Initially there was a problem of achieving tight sealing of the cover gas system,[6] but there was no real problem in keeping the cover gas clean as long as the primary sodium temperature was kept below 600°F. The waste-gas system was quite oversized for the associated systems. In fact, Bruzzi et al.[7] calculated that the Fermi waste-gas system could adequately handle the large activities which would result if the original fuel were replaced by vented-to-coolant fuel, i.e. it could handle perhaps 100 times more activity than expected in normal operation.

8.3.2 SEFOR

Performance of the gaseous radwaste system is only partially indicated in the tables of cover gas activity in SEFOR in Appendix A of this report. The main reasons that the cover gas showed so little activity were that the pins were not pushed to excessive performance limits, i.e. little leakage, and that tramp fuel background was so low.[8]

8.3.3 Rapsodie

During its first year of operation, Rapsodie had a few releases of fission gas,[9] but the cover gas cleanup system, combined with the relatively small releases, prevented any operational problems. These first releases did permit location and sealing of small leaks in the primary argon circuit. The only problem with the system was an anticipated gradual plugging of the argon cover gas lines of the primary system, caused by deposits of a mixture of sodium and sodium oxide. Also the gate valves in the system lost their air-tightness due to these deposits.[10]

8.3.4 Dounreay

The use of vented fuel places stringent requirements on the gaseous radwaste containment and cleanup systems. The first problem encountered was excessive leakage from the cover gas to the main sphere.[11] Modification of several joints corrected this problem. The radwaste treatment system is basically just a holdup system, and the turnover rate of cover gas volume is so small that extremely high activities are found in the cover gas. Activities of 10^{10} and 4×10^9 dpm/liter for ^{133}Xe and ^{135}Xe and argon activity of 2×10^7 dpm/liter are typical, but variations by two orders of magnitude are possible at various points around the system. Indeed, the gas control panel at one time was inaccessible for 48 hours after shutdown due to radiation fields surrounding the panel.

8.4 Comparison of LWR and LMFBR Radgas Effluents

A comparison was made between the radioactive gaseous releases from light-water reactors (LWR's) and an LMFBR having a radgas system similar to the FFTF system.

8.4.1 LWR Gaseous Releases

Two recent studies provide excellent summaries of radioactive gas emission from LWR's, the first an ORNL study[12] and the second a comprehensive USAEC Regulatory study.[13] The ORNL and the Regulatory studies both assumed 0.25% failed fuel for the calculated fission-gas releases. Although this assumption leads to generally higher estimates for activity releases to the environment than is warranted by actual LWR operating experience, these results are used here for the purpose of comparison with LMFBR results (for which 1% failed fuel has been assumed).

8.4.1.1 ORNL Study

A comprehensive survey of LWR gaseous waste systems was presented by ORNL staff members at the 12th AEC Air Cleaning Conference.[12] This survey involved a detailed study of roughly 100 LWR plants based upon information contained in docketed documents such as the Preliminary Safety Analysis, the Final Safety Analysis, the Applicant's Environmental Report, and the Amendments thereto, as well as information obtained by direct questioning of the applicants, reactor vendors, and architect engineers.

As a result of this study, it was determined that those radionuclides which are normally available for escape in gaseous form include the noble fission product gases (Kr and Xe), the fission product halogens (Br and I), certain activation products such as ^{16}N, ^{13}N, ^{19}O, and ^{41}Ar, and tritium, which may originate either from ternary fission or activation. Experience has shown that the noble gases and the iodines contribute virtually all of the radiologically significant gaseous activity released from LWR's of current design.

The sources of emission can be divided into two major categories: (1) inadvertent leaks from tanks, piping, valves, etc. which allow gaseous activity to escape without being processed by the radgas system, and (2) operational releases in which fluid is deliberately withdrawn from the cooling system of the reactor. The latter category would include steam generator blowdown, exhaust from the condenser air ejectors and releases from various system degassing operations.

The ORNL study presents tables of "typical" gaseous releases from PWR's and BWR's, identifying sources as well as isotopes. Table 8.3 is a summary of releases from a typical 1000 MWe PWR, based on numbers taken from the ORNL study. It is seen that a 1000 MWe PWR with 0.25% defective fuel will "typically" release roughly 2,500 Ci annually of noble gas radionuclides, most of which consists of ^{133}Xe with a 5.77-day half-life. More important, because of its 10.7-year half-life, is ^{85}Kr, which has an estimated annual release of about 800 Ci.

Table B.3

Typical Annual Gaseous Release from a 1000 MWe PWR Operating
With 0.25% Defective Fuel (based on Reference 12)

Release Rate, Ci/yr

	Coolant Concentration μ Ci/ml	Auxiliary Building	Containment Purge	Primary Degasification	Shim Bleed Degasification	Steam Generator	Total
Kr-83m	3.865E-02	1.068E 00	2.643E-03	0.0	0.0	1.079E 00	2,150E 00
85m	2.076E-01	5.737E 00	3.359E-02	0.0	0.0	5.796E 00	1.157E 01
-85	1.219E-01	3.368E 00	6.751E 00	9.252E 01	7.194E 02	3.403E 00	8.254E 02
-87	1.125E-01	3.110E 00	5.240E-03	0.0	0.0	3.142E 00	6.257E 00
-88	3.604E-01	9.960E 00	3.708E-02	0.0	0.0	1.006E 01	2.006E 01
-89	8.546E-03	2.362E-01	1.665E-05	0.0	0.0	2.386E-01	4.748E-01
Xe-131m	1.518E-01	4.196E 00	1.573E 00	7.729E 00	2.239E 01	4.239E 00	4.013E 01
-133m	3.724E-01	1.029E 01	7.428E-01	2.625E-04	1.623E-04	1.040E 01	2.143E 01
-133	2.775E 01	7.669E 02	1.292E 02	5.277E 01	7.481E 01	7.747E 02	1.798E 03
-135m	2.393E-02	6.614E-01	2.302E-04	0.0	0.0	6.682E-01	1.330E 00
-135	6.003E-01	1.659E 01	2.033E-01	0.0	0.0	1.676E 01	3.355E 01
-137	1.756E-02	4.852E-01	4.109E-05	0.0	0.0	4.902E-01	9.754E-01
-138	8.317E-02	2.298E 00	8.657E-04	0.0	0.0	2.322E 00	4.621E 00
I -131	6.166E-01	8.519E-02	4.375E-01	0.0	0.0	9.907E-01	1.513E 00
-133	6.845E-01	9.458E-02	5.283E-02	0.0	0.0	7.078E-01	8.552E-01

It should be stressed that most of the activity releases in the above "typical" PWR stem from leaks of reactor coolant in the Reactor Building, Auxiliary Building, and steam generators. Gaseous activity from these sources are, for the most part, vented directly to the environment. Over 90% of the ^{133}Xe, and virtually all of the other short half-life isotopes, escape to the environment in this fashion. Consequently, the effect of adding a cryogenic "cleanup" system to the tail-end of the radgas system would be to reduce the ^{85}Kr emission rate substantially (by about 80-90%), but to diminish the emission of the short half-life isotopes only marginally (since these isotopes come principally from points outside the radgas system). The net effect of such a cryogenic system would be to reduce off-site radiation exposure rates by marginal amounts. In view of these considerations, it does not seem practical for PWR's to incorporate cryogenic units into existing radgas systems until sources stemming from coolant leaks can be reduced to insignificant levels.

8.4.1.2 USAEC Regulatory Study

Another recent and very comprehensive study of the radioactive liquid and gaseous releases from LWR's was performed by the USAEC Directorate of Regulatory Standards.[13] In this report, a number of alternative gaseous radwaste systems were considered and evaluated for both PWR's and BWR's. Results for six PWR radgas systems are presented in Table 8.4 based on 0.25% (defective fuel). Annual releases were estimated for each system. The total annual releases for the six systems are summarized in Table 8.5. (A more detailed presentation of the releases from each system, indicating sources for for each radionuclide, is found in Reference 13.)

For all radgas systems represented in these two tables, the annual emission of noble gas radionuclides ranged from 1300 Ci to 170,000 Ci, with ^{133}Xe (5.77 day) accounting for the larger part of the released activity. The more important (radiologically) ^{85}Kr annual releases ranged from 5 Ci to 800 Ci. The upper limit represents releases from PWR radgas systems of current design. (Note the excellent agreement between this value and the corresponding value reported in the ORNL study).

Results for gaseous releases from a BWR were similar to those for a PWR (except for the total noble gas release with little radwaste equipment), and therefore are not presented here in detail. For example, based on the Regulatory Report,[13] the annual emission of noble gases from a 1000 MWe BWR for 0.25% defective fuel would range from 2300 Ci to 2 x 10^6 Ci, and the ^{85}Kr annual releases would range from 1 Ci to 600 Ci.

8.4.2 Comparison of LWR and LMFBR Radioactive Gas Releases

In Section 8.1.1 it was estimated that the FFTF would discharge about 0.5 Ci/yr of ^{85}Kr to the environment. Normalizing this value to a 1000 MWe (2500 MWt) unit, the annual release of ^{85}Kr from a

TABLE 8.4

Summary of Variables for PWR Gaseous Radwaste Treatment Systems

	PWR Gas Case No 1	2	3	4	5	6
	Degree of Removal					
Xe	low	high	high	high	high	high
I	low	medium	medium	high	high	high
Kr	low	low	low	low	high	high
	Equipment Units, Functions, and Flow Paths*					
Primary system gases	None	60-day decay storage tanks, HEPA filter	60-day decay on charcoal bed, HEPA filter	60-day decay on charcoal bed, HEPA filter	Recombiner, 60-day decay storage tanks, selective absorption	Cover gas recycle
Secondary system gases	None	None	Charcoal adsorber for iodine, HEPA filter, clean steam for gland seal, blowdown tank vented to condenser	Charcoal adsorber for iodine, HEPA filter, clean steam for gland seal, blowdown tank vented to condenser	Charcoal adsorber for iodine, HEPA filter, clean steam for gland seal, blowdown tank vented to condenser	Charcoal adsorber for iodine, HEPA filter, clean steam for gland seal, blowdown tank vented to condenser
Reactor containment purge	None	Charcoal kidney adsorber for iodine	Charcoal kidney adsorber for iodine	Charcoal kidney adsorber for iodine, charcoal adsorber for iodine, HEPA filter	Charcoal kidney adsorber for iodine, charcoal adsorber for iodine, HEPA filter	Charcoal kidney adsorber for iodine, charcoal adsorber for iodine, HEPA filter
Auxiliary building ventilation	None	None	None	Charcoal adsorber for iodine, HEPA filter	Charcoal adsorber for iodine, HEPA filter	Charcoal adsorber for iodine, HEPA filter
Turbine building ventilation	None	None	None	Charcoal adsorber for iodine, HEPA filter	Charcoal adsorber for iodine, HEPA filter	Charcoal adsorber for iodine, HEPA filter

*All gases to 50-meter roof vent unless stack is indicated.

Table 8.5

Estimated Annual Releases (Ci/yr of Radioactive Gaseous Effluents from 1000 MWe PWR with 0.25% Defective Fuel (Based on Reference 13)

Nuclide	System 1	System 2	System 3	System 4	System 5	System 6
Kr-83m	210	3	3	3	3	3
85m	1,100	19	19	19	19	17
85	800	800	800	800	26	5
87	620	10	10	10	10	10
88	2,000	33	33	33	33	33
89	31	1	1	1	1	1
Xe-131m	920	35	35	35	18	5
133m	2,100	36	36	36	36	20
133	160,000	2,900	2,900	2,900	2,900	1,200
135m	120	2	2	2	2	2
135	3,400	55	55	55	55	48
137	70	2	2	2	2	2
138	420	7	7	7	7	7
Total Noble Gas	170,000	3,900	3,900	3,900	3,000	1,300
I-131	1.8	1.2	0.3	0.04	0.04	0.04
133	0.7	0.6	0.2	0.03	0.03	0.03

LMFBR operating with 1% defective fuel and an FFTF-type radwaste system would be only about 3 Ci. Unlike the LWR, there should be almost no release of short-lived fission gas to the environment from an LMFBR. Confirmation of these low release rates, of course, must await actual operating experience since these are only estimates at this time.

The ^{39}A production rate for a 1000 MWe LMFBR with 30 ppm potassium impurity in the coolant was estimated in Section 5.3.3.1 to be $\sim$30 Ci/year. All of this would eventually leak to the environment regardless of whether argon or helium is used as the cover gas (unless argon is deliberately separated from helium in a purification system for a helium cover gas). This radioactive source is not present in a LWR.

These values compare favorably with gaseous activity releases from light water reactors. As indicated in Section 8.4.1 for an assumed 0.25% defective fuel, even the most sophisticated PWR radgas system[13] would release 1300 Ci of noble gases annually, including about 5 Ci of ^{85}Kr, whereas "typical" PWR annual radioactive gaseous releases amount to roughly 2500 Ci of noble gases, including about 800 Ci of ^{85}Kr. The most sophisticated BWR radwaste system would release only 1 Ci of ^{85}Kr annually.[13]

REFERENCES (Section 8)

1. Fast Flux Test Facility Design Safety Assessment HEDL-TME 72-92, July 1972, HEDL Section 2.3.

2. C. J. Foley, "Fission Gas Control at FFTF," Proceedings of the 12th AEC Air Cleaning Conference, Oak Ridge, August, 1972.

3. FFTF Environmental Statement, WASH-1510, USAEC, May 1972, pp. IV-28 to IV-32.

4. A. Panek, C. McPheeters, P. Nelson, "Cover Gas Cleanup System for EBR-II Conceptual Design," ANL report, October 27, 1972.

5. ANL Memo, J. F. Koenig to R. C. Matlock, "Considerations for Cover Gas Cleanup System," Sept. 13, 1972.

6. E. L. Alexanderson, C. E. Branyon, and W. R. Olson, Proceedings of the ANS National Topic Meeting on Fast Reactor Technology, ANS-100, p. 41 (196).

7. L. Bruzzi, G. Gondoni, P. S. Lindsey, and R. E. Mueller, "Plant Design Problems Associated with the Application of Vented Fuel to a Fast Breeder Reactor," Proceedings of the International Conference on Sodium Technology on Large Fast Reactor Design, ANL-7520 II, p. 154 (1968).

8. J. J. Regimbal, R. S. Gilbert, W. P. Kunkel, R. A. Meyer, and C. E. Russell, "Fuel Failure Detection Capability at SEFOR," Trans. Am. Nucl. Soc., 14, 69 (1971).

9. G. Gajac, J. L. Ratier, N. Reboul, L. Reynes, and M. A. Valantin, "Rapsodie's First Year of Operation," Proceedings of the International Conference on Sodium Technology and Fast Reactor Design," ANL-7520 II, p. 52 (1968).

10. G. Gajac, "Experience de Fonctionnement de Rapsodie en ce qui Concerne la Fiabilite des Composants," Proceedings of the Internation Conference on the Engineering of Fast Reactors for Safe and Reliable Operation, Karlsruhe, October 9 - 13, 1972.

11. J. L. Phillips, "Full Power Operation of the Dounreay Fast Reactor, Proceedings of the ANS National Topical Meeting on Fast Reactor Technology, ANS-100, p. 1 (1965).

12. Binford, F. T.; Hamrick, T. P.; Parker, G. W.; Row, T. H., "Analysis of Power Reactor Gaseous Waste Systems," Proceedings of the 12th AEC Air Cleaning Conference, Oak Ridge, Tenn., August, 1972.

13. Directorate of Regulatory Standards, USAEC, "Draft Environmental Statement Concerning Proposed Rule Making Action: Numerical Guides for Design Objectives and Limiting Conditions for Operation to Meet the Criterion 'As Low as Practicable' for Radioactive Material in Light-Water-Cooled Nuclear Power Reactor Effluents," January, 1973.

9. LIQUID AND SOLID RADWASTE MANAGEMENT AT EBR-II

The only information collected on liquid and solid radwaste from an operating fast reactor was for EBR-II.[1,2] This is a test reactor with elaborate hot cell facilities that would not normally be present at an LMFBR power plant. For example, irradiated fuel test pins are routinely dismantled in the hot cells, and irradiated cladding and other materials must be stored.

In Section 9.2, it is shown that the high level solid waste stored at the EBR-II is of the order of 10^6 Ci/yr, while the intermediate solid waste is ~ 3000 Ci/yr. For comparison, for a 1000 MWe light water reactor the solid waste activity is 5000 to 10,000 Ci/yr.[2]

9.1 Liquid Radwaste System

Suspect liquid waste from EBR-II is liquid waste that contains radioactive material, generally in water solutions. Approximately 100,000 gallons per year of suspect waste is processed. No estimate of the activity in this waste is available. After processing, this waste is added to non-radioactive industrial waste which is sent to a leach pit, where it either evaporates or settles into the lava below. Typical sources of this suspect waste include decontamination of equipment, solutions from chemical laboratories, and emergency showers.

In the early days of EBR-II the suspect waste was pumped directly to the leach pit. Later this method was changed to an evaporation process, carried out several times each week. This process is shown schematically in Figure 9.1(A). The present system provides a decontamination factor of 10^2 to 10^3.

A decontamination factor of 10^4 is now desired at EBR-II. Therefore, the liquid waste system will be modified to add a settling tank for solids before the liquid enters the evaporators and to add additional equipment after evaporation. These additions are shown schematically in Figure 9.1(B).

The solid sludge from the evaporators is stored in 55 gallon drums, which are encased in concrete for shielding. This sludge is eventually processed as solid radwaste.

9.2 Solid Radwaste Management

Solid waste from EBR-II is classified as low, intermediate, or high level waste. The concern here is with solid waste other than the irradiated fuel itself, which is shipped offsite for reprocessing. About 90% of the solid waste volume is low level; nearly all of the activity is high level. In Table 9.1 are listed the activity concentration ranges for the different levels, together with typical annual volumes and the 1971 activity totals for each level. The activity levels are values after 15 days of storage.

The intermediate wastes are placed into 1 cu ft shielded containers and sent, together with the low level waste, to the National Reactor Testing Station (NRTS) Burial Ground. Typical sources of low level wastes are dry decontamination and filters. Intermediate wastes come mostly from analytical cells and chemical facilities.

High level wastes are stored in a 7 acre storage facility at EBR-II. About half of this capacity had been used through 1972. The wastes are placed in 1 ft. or 2 ft. high containers, these are then placed in a 6 ft. high can, and the can is inserted in a 12 ft. deep, 16 inch diameter hole in the ground, or on grids at 6 ft. intervals. Finally the 6 ft. above the can is filled with gravel shielding.

Any solid waste that contains plutonium or other transuranium elements is wrapped several times in plastic bags, placed in 55 gallon drums and stored outdoors on an asphalt pad at an interim storage facility at NRTS. On the order of 3 mg of plutonium was stored in 1971.

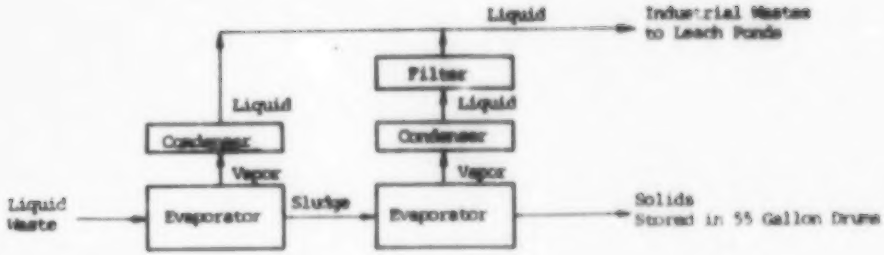
Liquid
Industrial Wastes to Leach Ponds
Filter
Liquid
Liquid
Condenser
Condenser
Vapor
Vapor
Liquid Waste
Evaporator
Sludge
Evaporator
Solids Stored in 55 Gallon Drums

(A) Present System

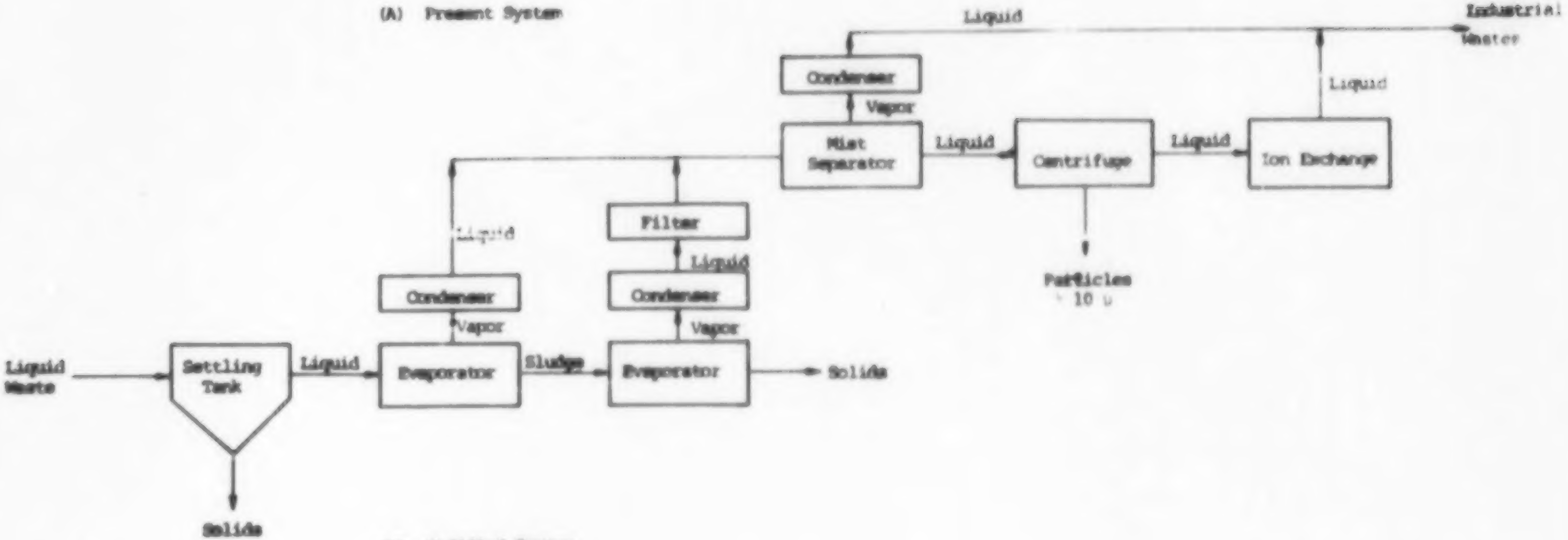
Liquid
Industrial Waster
Condenser
Liquid
Vapor
Mist Separator
Liquid
Centrifuge
Liquid
Ion Exchange
Filter
Liquid
Liquid
Condenser
Condenser
Particles
> 10 μ
Vapor
Vapor
Liquid Waste
Settling Tank
Liquid
Evaporator
Sludge
Evaporator
Solids
Solids

(B) Modified System

Figure 9.1 EBR-II Liquid Radwaste System

Table 9.1

EBR-II Solid Waste Management

Annual Production ∿ 5×10^7 Ci

Shipped from site with fuel ∿ 90% of production

Processed at site ∿ 5×10^6 Ci

Level	Range (Ci/ft^3)	Volume (ft^3)	1971 Activity (Ci)	Disposal Site
Low	1×10^{-5} to .1	13,000	3×10^2	NTRS Burial Ground
Intermediate	.1 to 5	1,000	3×10^3	NTRS Burial Ground
High	> 5	150	1.5×10^6	EBR-II Site High Level Storage Facility
Pu & Other Transuranium Materials				Stored in 55 gallon drums, wrapped in plastic, on asphalt pad above ground at NTRS (interim storage)

REFERENCES (Section 9)

1. M. Jackson and W. Grady, EBR-II Liquid Radwaste System, Personal Communication, Fast Reactor Workshop, EBR-II Site, Idaho Falls, December 1972.

2. P. Stoddart, EBR-II Solid Radwaste Management, Personal Communication, Fast Reactor Workshop, EBR-II Site, Idaho Falls, December 1972.

3. Directorate of Regulatory Standards, U.S.A.E.C., "Draft Environmental Statement Concerning Proposed Rule Making Action: Numerical Guides for Design Objectives and Limiting Conditions for Operation to Meet the Criterion 'As Low as Practicable' for Radioactive Material in Light-Water-Cooled Nuclear Power Reactor Effluents," January 1973.

APPENDIX A:

Environmental Operating Data for Fermi, SEFOR, and EBR-II

Environmental radiation data for Fermi was reported monthly to the AEC, and data for SEFOR was reported quarterly. These reports are available in the AEC's public documents room in Washington, D. C.

Similar data for EBR-II are reported in the ANL monthly Reactor Development Program Progress Reports. Data for the EBR-II are tabulated only through 1971 because the AEC did not make the 1972 and 1973 progress reports (the ANL-RDP series) available to the general public while this review was in progress. Since completion of this review, these progress reports have been made available to the public.

The data are summarized in the following tables. Much of the data is quoted as total γ, β, or α activity. These data are of limited usefulness since specific isotopes are not identified. It is useful, however, to observe the type of environmental data that must be reported to the AEC by the reactor operations. It is also of limited use to observe that apparently no significant differences in radiation in the environment surrounding Fermi and SEFOR were observed over the background present before plant operation. The integrated power for SEFOR is very low since it was an experimental reactor which operated at low load factor and at a power level of 20MW(th). Total exposure data (MWd) were not reported for SEFOR.

LIST OF TABLES

Fermi:

		Page
A 1	Integrated Power and List of Reports	179
A 2	Liquid Waste Discharge	180
A 3	Gaseous Waste Discharge	181
A 4	Environmental Surveys -- Airborne Dust	182
A 5	Environmental Surveys -- Precipitation	183
A 6	Environmental Surveys -- Surface Water	184
A 7	Environmental Surveys -- Drinking Water	185
A 8	Environmental Surveys -- Milk	186
A 9	Environmental Surveys -- Fish	187
A10	Environmental Surveys -- Gamma Radiation	188

Page

A11 Activity of Liquid and Gaseous Samples 189

A12 Primary Sodium Composition 193

A13 Primary Sodium Activity 194

A14 Uranium in the Sodium in the Transfer Tank System 195

SEFOR:

A15 Off-Site Radioactivity Release in Gaseous Waste -- Noble Gases and Activation Products 196

A16 Off-Site Radioactivity Release in Gaseous Waste -- Halogens and Particulates 197

A17 Off-Site Radioactivity Release in Liquid Waste -- Fission Products and Activation Products 198

A18 Off-Site Radioactivity Release in Liquid Waste -- Tritium and Carbon-14 199

A19 Environmental Sampling of Vegetation, Soil, and Water 200

A20 Environmental Film Monitoring 202

A21 Primary Sodium Composition 203

A22 Primary Sodium Radioactivity 204

A23 Cover Gas Activity 205

EBR-II:

A24 Integrated Power and List of Reports (1971) 206

A25 Radionuclide Activity in Primary Sodium 207

A26 Radionuclide Activity in Secondary Sodium 215

A27 Gamma Activity in Cover Gas Due to Tramp Source 217

A28 Primary Sodium Composition -- Trace Metals 218

A29 Primary Sodium Composition -- Non-metals 220

A30 Secondary Sodium Composition -- Trace Metals 221

A31 Secondary Sodium Composition -- Non-metals 223

Table A1

Integrated Power and List of Reports (FERMI)

Report # & Date	Operation Period	Integrated Power MWd
EF-101, January 1972	January 1972	0
	July 16, 1970-January 31, 1972	5941
EF-100, December 1971	December 1971	0
	July 16, 1970-December 31, 1971	5941
EF-99, November 1971	November 1971	1491
	July 16, 1970-November 1971	5856
EF-98, October 1971	October 1971	0
	July 16, 1970-October 1971	4365
EF-97, September 1971	September 1971	0
	July 16, 1970-September 1971	4365
EF-96, August 1971	August 1971	0
	July 16, 1970-August 1971	4365
EF-95, July 1971	July 1971	0
	July 16, 1970-July 1971	4365
EF-94, June 1971	June 1971	1029
	July 16, 1970-June 1971	4365
EF-93, May 1971	May 1971	19
	July 16, 1970-May 31, 1971	3336
EF-92, April 1971	April 1971	155
	July 16, 1970-April 1971	3317
EF-91, March 1971	March 1971	0
	July 16, 1970-March 1971	3162
EF-90, February 1971	February 1971	142
	July 16, 1970-February 1971	3162
EF-89, January 1971	January 1971	427
	July 16, 1970-January 1971	3020
EF-88, December 1970	December 1970	145
	July 16, 1970-December 1970	2593
EF-87, November 1970	November 1970	1381
	July 16, 1970-November 1970	2448

Table A2

Liquid Waste Discharge (FERMI)

	Total amount of discharge (gallons)	Total activity mCi
EF-101, January 1972	0	0
EF-100, December 1971	6467	4.02 (a)
EF-99, November 1971	0	0
EF-98, October 1971	6937	0.72 (a)
EF-97, September 1971	0	0
EF-96, August 1971	7068	1.1 (a)
EF-95, July 1971	0	0
EF-94, June 1971	0	0
EF-93, May, 1971	6967	1.376 (a) (b)
EF-92, April 1971	0	0
EF-91, March 1971	0	0
EF-90, February 1971	6967	4.62 (a)
EF-89, January 1971	0	0
EF-88, December 1970	6967	9.14 (a)
EF-87, November 1970	1810	4.23 (a)

(a) All effluents released to the environment after dilution with the circulating pump discharge were below MPC.

(b) This value was reported in EF-93 as 1376 mCi. By letter of Oct. 18, 1972, from W. C. Morison, Fermi Assistant Plant Superintendent, to A. B. Reynolds, it was learned that the correct number was 1.376, not 1376 as reported.

Table A3

Gaseous Waste Discharge (FERMI)

The following paragraph appeared in every monthly report:

"Approximately 1×10^9 cubic feet of gaseous effluent were released through the plant stack. The concentration of particulates and halogens with half-lives greater than 8 days was less than 0.143 MPC at the waste gas stack outlet. The concentration of all other isotopes was less than 100 MPC at the gas stack outlet. These levels meet the requirements of the Technical Specifications."

Table A4

Environmental Surveys - Airborn Dust (FERMI)

Report # and Date	Period	No. of Samples	Reactor Area* Gross α μCi/ccx10^{-15}	Reactor Area* Gross β μCi/ccx10^{-14}	Background Group Gross α μCi/ccx10^{-15}	Background Group Gross β μCi/ccx10^{-14}
EF-101	A (Aug. 5 - Sept. 2, 1971)	39	2.18	33.7	1.84	33.6
Jan., 1972	B (Sept. 2 - Sept. 30, 1971)	40	1.70	14.2	1.75	13.5
	1967		2.67	7.5	3.31	7.7
EF-100	No reports on environmental surveys were received during this period.					
Dec., 1971						
EF-99						
Nov., 1971						
EF-98	A (June 10 - July 8, 1971)	40	1.97	62.7	1.85	60.3
Oct., 1971	B (July 8 - Aug. 5, 1971)	40	1.87	58.8	1.55	57.9
	1967		2.67	7.5	3.31	7.7
EF-97	A (April 15 - May 13, 1971)	40	2.32	53.1	2.25	56.8
Sept., 1971	B (May 13 - June 10, 1971)	40	1.77	60.3	1.93	65.5
	1967		2.67	7.5	3.31	7.7
EF-96	March 18 - April 15, 1971	40	1.77	29.5	1.77	30.5
Aug., [illegible]	1967		2.67	7.5	3.31	7.7
EF-9[illegible]	No reports on environmental surveys were received during this period.					
Ju[illegible] 1971						
[illegible]4	A (Jan. 21 - Feb. 18, 1971)	40	1.87	10.5	1.76	10.6
June, 1971	B (Feb. 18 - March 18, 1971)	40	1.48	14.1	1.63	15.5
	1967		2.67	7.5	3.31	7.7
EF-93	No reports on environmental surveys were received during this period.					
May, 1971						
EF-92	No reports on environmental surveys were received during this period.					
April, 1971						
EF-91	No reports on environmental surveys were received during this period.					
March, 1971						
EF-90						
Feb., 1971						
EF-89						
Jan., 1971						
EF-88	A (Sept. 3 - Oct. 1, 1970)	40	1.50	12.8	1.59	12.4
Dec., 1970	B (Oct. 1 - Oct. 29, 1970)	40	1.39	12.9	1.70	13.0
	1967		2.67	7.5	3.31	7.7
EF-87	A (June 11 - July 9, 1970)	40	1.70	63.4	1.85	61.4
Nov., 1970	B (July 9 - Aug. 6, 1970)	40	1.55	42.4	1.86	44.9
	C (Aug. 6 - Sept. 3, 1970)	40	2.07	40.8	1.97	40.2
	1967		2.67	7.5	3.31	7.7

*There are five sampling stations around the reactor area and five stations away from the reactor area where samples are continuously collected and removed weekly. Collected samples during the periods were analyzed and averaged, and compared to the 1967 yearly average results (background group).

Table A5

Environmental Surveys - Precipitation (FERMI)

			Reactor Area*		Background	
Report # and Date	Period	No. of Samples	Gross α mCi/sq. mile	Gross β mCi/sq. mile	Gross α mCi/sq. mile	Gross β mCi/sq. mile
EF-101	A (Aug. 5 - Sept. 2, 1971)	9	0.151	12.2	0.173	10.4
Jan., 1972	B (Sept. 2 - Sept. 30, 1971)	10	0.113	5.03	0.156	4.85
	1967		0.205	5.1	0.337	6.04
EF-100	No reports on environmental surveys were received during this period.					
Dec., 1971						
EF-99						
Nov., 1971						
EF-98	A (June 10 - July 8, 1971)	10	0.151	20.7	0.219	25.1
Oct., 1971	B (July 8 - Aug. 5, 1971)	10	0.083	10.7	0.138	11.8
	1967		0.205	5.1	0.337	6.04
EF-97	A (April 15 - May 13, 1971)	10	0.117	17.96	0.130	18.08
Sept. 1971	B (May 13 - June 10, 1971)	10	0.202	33.3	0.177	28.3
	1967		0.205	5.1	0.337	6.04
EF-96	March 18 - April 15, 1971	10	0.090	15.5	0.140	12.7
Aug., 1971	1967		0.205	5.1	0.337	6.04
EF-95	No reports on environmental surveys were received during this period.					
July, 1971						
EF-94	A (Jan. 21 - Feb. 18, 1971)	10	0.164	7.82	0.174	6.86
June, 1971	B (Feb. 18 - March 18, 1971)	10	0.106	11.2	0.197	10.3
	1967		0.205	5.1	0.337	6.04
EF-93	No reports on environmental surveys were received during this period.					
May, 1971						
EF-92	No reports on environmental surveys were received during this period.					
April, 1971						
EF-91	No reports on environmental surveys were received during this period.					
March, 1971						
EF-90						
Feb., 1971						
EF-89						
Jan., 1971						
EF-88	A (Sept. 3 - Oct. 1, 1970)	10	0.090	7.80	0.108	7.57
Dec., 1970	B (Oct. 1 - Oct. 29, 1970)	9	0.057	6.99	0.067	8.76
	1967		0.205	5.1	0.337	6.04
EF-87	A (June 11 - July 9, 1970)					
Nov., 1970	B (July 9 - Aug. 6, 1970)					
	C (Aug. 6 - Sept. 3, 1970)					

---

*Two groups of samples were collected from five locations around the reactor site and five locations away from the reactor area to indicate background. The samples were analyzed for gross α, β and γ-activity, and compared to the 1967 yearly average results.

Table A6

Environmental Surveys - Surface Water (FERMI)

Report # and Date	Period	No. of Samples*	Swan Creek x10^{-9} µCi/ml	Lake Erie (Intake) x10^{-9} µCi/ml	Reactor Channel x10^{-9} µCi/ml	Reactor (Outlet) x10^{-9} µCi/ml
EF-101	A (Aug. 5 - Sept. 2, 1971)	16	6.73	5.68	5.17	4.91
Jan., 1972	B (Sept. 2 - Sept. 30, 1971)	16	5.92	6.29	5.58	5.45
	1967		8.68	5.60	5.79	Not Collected
EF-100	No reports on environmental surveys were received during this period.					
Dec., 1971						
EF-99						
Nov., 1971						
EF-98	A (June 10 - July 8, 1971)	12	8.22	6.97	6.77	—
Oct., 1971	B (July 8 - Aug. 5, 1971)	12	7.13	5.78	6.13	—
	1967		8.68	5.60	5.79	—
EF-97	A (April 15 - May 13, 1971)	12	10.2	6.47	6.53	—
Sept., 1971	B (May 13 - June 10, 1971)	12	9.74	8.50	10.8	—
	1967		8.68	5.60	5.79	—
EF-96	March 18 - April 15, 1971	12	6.35	8.87	7.00	—
Aug., 1971	1967		8.68	5.60	5.79	—
EF-95	No reports on environmental surveys were received during this period.					
July, 1971						
EF-94	A (Jan. 21 - Feb. 18, 1971)	12	14.5	15.2	6.70	—
June, 1971	B (Feb. 18 - March 18, 1971)	12	8.49	7.12	7.08	—
	1967		8.68	5.60	5.79	—
EF-93	No reports on environmental surveys were received during this period.					
May, 1971						
EF-92	No reports on environmental surveys were received during this period.					
April, 1971						
EF-91	No reports on environmental surveys were received during this period.					
March, 1971						
EF-90						
Feb., 1971						
EF-89						
Jan., 1971						
EF-88	A (Sept. 3 - Oct. 1, 1970)	12	9.14	1.58	6.80	—
Dec., 1970	B (Oct. 1 - Oct. 29, 1970)	12	8.59	5.21	5.42	—
EF-87						
Nov., 1970						

*Two groups of samples were collected from four or three locations (one sample a week from each) and analyzed for gross activity. The results were compared to 1967 yearly averaged results.

Table A7

Environmental Surveys - Drinking Water (FERMI)

Report #	Period	No of Samples*	Monroe $x10^{-9}$ µCi/ml	Flat Rock $x10^{-9}$ µCi/ml	Dundee $x10^{-9}$ µCi/ml	Toledo $x10^{-9}$ µCi/ml	Detroit $x10^{-9}$ µCi/ml	Allen Park $x10^{-9}$ µCi/ml	Ann Arbor $x10^{-9}$ µCi/ml	Colchester $x10^{-9}$ µCi/ml
EF-101	A	32	4.18	6.83	6.17	4.20	3.86	3.76	3.99	6.47
	B	32	4.64	6.41	7.14	3.65	3.87	4.27	3.76	3.54
	1967		3.26	3.73	3.17	2.51	2.64	Not Collected	2.23	Not Collected
EF-100	No reports on environmental surveys were received during this period.									
EF-99	No reports on environmental surveys were received during this period.									
EF-98	A	32	5.58	7.49	7.37	5.60	4.24	5.25	5.47	8.24
	B	32	4.60	7.68	6.99	4.88	4.16	4.07	4.76	5.24
	1967		3.26	3.73	3.17	2.51	2.64	Not Collected	2.23	Not Collected
EF-97	A	32	5.14	6.04	6.69	4.34	4.98	4.30	6.38	5.57
	B	32	5.06	7.27	5.37	3.89	4.64	4.96	4.89	4.94
	1967		3.26	3.73	3.17	2.51	2.64	Not Collected	2.23	Not Collected
EF-96	3/18/71 4/15/71	32	4.16	6.26	5.83	6.05	3.16	4.32	5.18	4.66
	1967		3.26	3.73	3.17	2.51	2.64	Not Collected	2.23	Not Collected
EF-95	No reports on environmental surveys were received during this period.									
EF-94	A	32	11.8	12.6	13.9	9.36	8.25	9.89	9.67	19.8
	B	32	7.15	10.6	11.4	7.69	4.22	6.15	38.7	7.93
	1967		3.26	3.73	3.17	2.51	2.64	Not Collected	2.23	Not Collected
EF-93	No reports on environmental surveys were received during this period.									
EF-92	No reports on environmental surveys were received during this period.									
EF-91	No reports on environmental surveys were received during this period.									
EF-90	No reports on environmental surveys were received during this period.									
EF-89	No reports on environmental surveys were received during this period.									
EF-88	A	32	4.32	6.54	7.20	4.14	4.01	3.82	4.49	3.29
	B	32	4.02	5.83	6.24	3.53	3.66	3.77	4.22	9.18
	1967		3.26	3.73	3.17	2.51	2.64	Not Collected	2.23	Not Collected
EF-87	No reports on environmental surveys were received during this period.									

*Two groups each containing thirty-two samples (daily composite samples collected weekly) from neighboring cities were analyzed for gross β activity, and compared to the 1967 results.

Table A8

Environmental Surveys - Milk (FERMI)

			Reactor Area		Background Group	
Report #	Period	No. of Samples*	Monroe $\beta (\times 10^{-7}\ \mu Ci/ml)$	Newport $\beta (\times 10^{-7}\ \mu Ci/ml)$	Ypsilanti $\beta (\times 10^{-7}\ \mu Ci/ml)$	Ann Arbor $\beta (\times 10^{-7}\ \mu Ci/ml)$
EF-101	A	4	12.6	13.1	13.1	14.0
	B	4	11.0	11.9	13.4	11.2
EF-100	No reports on environmental surveys were received during this period.					
EF-99						
EF-98	A	4	13.3	10.8	11.4	15.1
	B	4	11.4	11.9	12.9	10.5
EF-97	A	4	14.5	14.7	14.1	13.0
	B	4	14.1	13.3	14.5	15.1
EF-96	3/18/71 4/15/71	4	12.8	13.7	11.1	13.0
EF-95	No reports on environmental surveys were received during this period.					
EF-94	A	4	12.6	10.2	14.0	15.6
	B	4	13.0	13.6	14.3	13.1
EF-93	No reports on environmental surveys were received during this period.					
EF-92	No reports on environmental surveys were received during this period.					
EF-91	No reports on environmental surveys were received during this period.					
EF-90						
EF-89						
EF-88	A	4	11.3	13.2	12.8	11.9
	B	4	12.7	11.6	12.2	11.0
EF-87						

*Two groups each containing four milk samples were collected two from the reactor area and two away from the reactor area for background. These samples were analyzed for gross beta and gamma activity.

Table A9

Environmental Surveys -- Fish (FERMI)

EF-101: Twelve samples of Lake Erie fish (six from the reactor area and six from the Buffalo area) were taken and analyzed for gross β and γ activity during period A. No significant change in the results was noted when compared to previously analyzed samples.

EF-94: Twelve samples of Lake Erie fish (six from the reactor area and six from the Buffalo area) were taken and analyzed for gross β and γ activity during period B. No significant change in the results were noted when compared to previously analyzed samples.

Table A10

Environmental Surveys --- Gamma Radiation (Fermi)

Two groups (A,B) each containing ten gamma radiation exposure analyses were conducted (ten locations of one, four week exposure) by the usage of environmental film packets. No gamma exposures above normal were reported.

The same analyses were done for each period and the same results were reported.

Table All

Activity of Liquid and Gaseous Samples (FERMI)

Liquid				Gaseous		
Report # and date reported	Date Taken	Location	Gross β activity (highest concentration) μCi/cm^3	No. of Samples	Location	Gross β activity (highest concentration) μCi/cm^3
EF-101 Jan. 1972	Jan. 19	Demineralized water	$1.22x10^{-8}$	4	Primary Shield Tank	$3.5x10^{-8}$
				4	Auxiliary Fuel Storage Facility	$1.6x10^{-6}$
	Jan. 19	Potable Water	$1.22x10^{-8}$	3	Reactor Cover Gas	$3.5x10^{-5}$
				1	Waste Gas Storage Tank No: 2	$3.1x10^{-5}$
EF-100 Dec. 1971	Dec. 7	MK-15 Liquid Waste Tank	$3.1x10^{-5}$	4	Primary Shield Tank	$3.5x10^{-8}$
	Dec. 10	MK-15 Liquid Waste Tank	$1.7x10^{-4}$	5	Auxiliary Fuel Storage Facility	$1.4x10^{-6}$
	Dec. 14	Cut-up Pool before Ion Exchange	$6.8x10^{-8}$	4	Reactor Cover Gas	$4.2x10^{-3}$
	Dec. 14	Cut-up Pool after Ion Exchange	$1.8x10^{-8}$	1	Waste Gas Storage Tank No: 2	$2.2x10^{-4}$
	Dec. 14	Decay Pool before Ion Exchange	$2.0x10^{-7}$	1	Waste Gas Storage Tank No: 1	$4.1x10^{-4}$
	Dec. 14	Decay Pool after Ion Exchange	$3.9x10^{-9}$			
	Dec. 20	Demineralized Water	$1.2x10^{-8}$			
	Dec. 20	Potable Water	$4.5x10^{-8}$			
EF-99 Nov. 1971	Nov. 18	Demineralized Water	$4.76x10^{-8}$	5	Primary Shield Tank	$2.75x10^{-3}$
				4	Auxiliary Fuel Storage Facility	$4.55x10^{-6}$
	Nov. 18	Potable Water	$1.22x10^{-8}$	5	Reactor Cover Gas	$1.82x10^{-1}$
				1	Waste Gas Storage Tank	$1.32x10^{-4}$
				1	Waste Gas Discharge Line No: 1	$3.19x10^{-5}$
EF-98 Oct. 1971	Oct. 15	Demineralized Water	$1.95x10^{-8}$	4	Auxiliary Fuel Storage Facility	$1.24x10^{-6}$
	Oct. 15	Potable Water	$5.86x10^{-8}$	4	Primary Shield Tank	$3.16x10^{-8}$
	Oct. 18	Waste Liquid Tank MK-15	$2.73x10^{-5}$	4	Reactor Cover Gas	$5.39x10^{-5}$
				1	FARB Transfer Tank	$5.94x10^{-7}$

Table All

Activity of Liquid and Gaseous Samples (FERMI)
(continued)
page 2

Liquid				Gaseous		
Report # and date reported	Date Taken	Location	Gross β activity (highest concentration) μCi/cm³	No. of Samples	Location	Gross β activity (highest concentration) μCi/cm³
EF-97 Sept. 1971	Sept. 13	Cut-up Pool before Ion Exchange	9.62×10^{-8}	5	Auxiliary Fuel Storage Facility	1.37×10^{-6}
	Sept. 13	Cut-up after Ion Exchange	3.54×10^{-8}	5	Primary Shield Tank	7.49×10^{-7}
	Sept. 13	Decay Pool before Ion Exchange	1.66×10^{-7}	5	Reactor Cover Gas	9.8×10^{-4}
	Sept. 13	Decay Pool after Ion Exchange	1.22×10^{-8}			
	Sept. 20	Demineralized Water	1.22×10^{-8}			
	Sept. 21	Potable Water	1.34×10^{-8}			
EF-96 Aug. 1971	Aug. 18	Waste Liquid Tank MK-15	4.08×10^{-5}	4	Auxiliary Fuel Storage Facility	1.55×10^{-6}
	Aug. 24	Demineralized Water	2.1×10^{-8}	4	Primary Shield Tank	2.83×10^{-8}
	Aug. 24	Potable Water	1.22×10^{-8}	3	Reactor Cover Gas	5.84×10^{-5}
EF-95 July 1971	July 19	Demineralized Water	Below detectable limits	5	Auxiliary Fuel Storage Facility	1.6×10^{-6}
	July 19	Potable Water	Below detectable limits	5	Primary Shield Tank	4.9×10^{-7}
				5	Reactor Cover Gas	1.2×10^{-3}
EF-94 June 1971	June 7	Decay Pool before Ion Exchange	2.24×10^{-7}	4	Auxiliary Fuel Storage Facility	1.32×10^{-6}
	June 7	Decay Pool after Ion Exchange	1.68×10^{-7}	5	Primary Shield Tank	2.15×10^{-4}
	June 7	Cut-up Pool before Ion Exchange	5.5×10^{-7}	6	Reactor Cover Gas	1.8×10^{-1}
	June 7	Cut-up Pool after Ion Exchange	1.22×10^{-8}	3	Waste Gas Tank No: 1	1.28×10^{-4}
	June 18	Demineralized Water	1.34×10^{-8}	3	Waste Gas Tank No: 2	9.94×10^{-5}
	June 18	Potable Water	5.81×10^{-8}			
EF-93 May 1971	May 6	Liquid Waste Tank MK-15	5.18×10^{-5}	5	Reactor Cover Gas	9.94×10^{-5}
	May 19	Demineralized Water	2.6×10^{-8}	4	Primary Shield Tank	1.97×10^{-7}
	May 19	Potable Water	7.32×10^{-8}	4	Auxiliary Fuel Storage Facility	1.16×10^{-6}

Table All

Activity of Liquid and Gaseous Samples (FERMI)

(continued)
page 3

		Liquid		Gaseous		
Report # and date reported	Date Taken	Location	Gross β activity (highest concentration) μCi/cm^3	No. of Samples	Location	Gross β activity (highest concentration) μCi/cm^3
EF-92 April	April 16	Demineralized Water	1.2×10^{-8}	5	Reactor Cover Gas	9.1×10^{-4}
	April 16	Potable Water	1.2×10^{-8}	5	Primary Shield Tank	2.3×10^{-7}
				5	Auxiliary Fule Storage Facility	1.5×10^{-6}
EF-91 March 1971	March 1	Demineralized Water	1.2×10^{-8}			
	March 1	Potable Water	3.5×10^{-8}	4	Reactor Cover Gas	5.6×10^{-5}
	March 2	Cut-up Pool before Ion Exchange	9.9×10^{-8}			
	March 2	Cut-up Pool after Ion Exchange	3.3×10^{-8}	3	Primary Shield Tank	3.7×10^{-8}
	March 2	Decay Pool before Ion Exchange	1.7×10^{-7}	2	Auxiliary Fuel Storage Facility	1.3×10^{-6}
	March 2	Decay Pool after Ion Exchange	8.6×10^{-8}			
	March 22	Potable Water	1.2×10^{-8}			
	March 22	Demineralized Water	1.2×10^{-8}			
EF-90 Feb. 1971				1	Containment Building	8.7×10^{-7}
				4	Primary Shield Tank	1.2×10^{-3}
				4	Reactor Cover Gas	1.2×10^{-1}
				3	Auxiliary Fuel Storage Facility	1.6×10^{-6}
				1	Waste Gas Storage Tank No: 1	2.0×10^{-5}
				1	Transfer Tank	1.1×10^{-6}
EF-89 Jan. 1971	Jan. 13	Potable Water	2.44×10^{-8}	2	Containment Building	1.26×10^{-5}
				3	Reactor Cover Gas	1.57×10^{-1}
	Jan. 13	Demineralized Water	1.22×10^{-8}	4	Primary Shield Tank	9.19×10^{-5}
				4	Auxiliary Fuel Storage Facility	5.05×10^{-6}
	Jan. 20	Condenser out-Fall	1.68×10^{-7}	1	Machinery Dome	1.37×10^{-5}
				1	Waste Gas Tank No: 1	8.69×10^{-5}

Table All

Activity of Liquid and Gaseous Samples (FERMI)
(continued)
page 4

Liquid				Gaseous		
Report # and date reported	Date Taken	Location	Gross β activity (highest concentration) $\mu Ci/cm^3$	No. of Samples	Location	Gross β activity (highest concentration) $\mu Ci/cm^3$
EF-88 Dec. 1970	Dec. 7	Decay Pool before Ion Exchange	$1.7x10^{-6}$	5	Primary Shield Tank	$1.6x10^{-6}$
	Dec. 7	Decay Pool after Ion Exchange	$1.4x10^{-7}$	5		
	Dec. 7	Cut-up Pool before Ion Exchange	$7.4x10^{-7}$	4	Auxiliary Fuel Storage Tank	$1.6x10^{-6}$
	Dec. 7	Cut-up Pool after Ion Exchange	$7.4x10^{-7}$	4	Reactor Cover Gas	$2.9x10^{-3}$
	Dec. 9	Waste Liquid Tank MK-15	$3.4x10^{-4}$	1	Waste Gas Tank No: 1	$3.8x10^{-5}$
	Dec. 15	Demineralized Water	$2.6x10^{-8}$			
	Dec. 15	Potable Water	$2.8x10^{-8}$			
EF-87 Nov. 1970				5	Containment Building	$1.7x10^{-6}$
				4	Primary Shield Tank	$2.6x10^{-4}$
				4	Reactor Cover Gas	$8.1x10^{-2}$
				4	Auxiliary Fuel Storage Facility	$2.8x10^{-6}$
				1	Waste Gas System FARB	$3.2x10^{-7}$
				1	Waste Gas Tank No: 2	$6.4x10^{-5}$
				1	Waste Gas Tank No: 1	$4.6x10^{-5}$
				1	Waste Gas Tank No: 2	$2.5x10^{-3}$
				1	Waste Gas Tank No: 1	$2.7x10^{-4}$

Table A12

Primary Sodium Composition (FERMI)

Chemical Analysis

Report #	Sample #	Date taken	C (ppm)	Cl (ppm)	Cr (ppm)	F (ppm)	Fe (ppm)	H Non-hydroxide (ppm)	Ni (ppm)	O (ppm)
EF-93	Purity variation of Primary sodium test was concerned with the effect that temperature and radiation would have on the shield plug graphite for releasing impurities into the primary sodium. Comparison of analyses of a sodium sample taken prior to the power demonstration program and one taken immediately following the 200 MW(t) operation showed negligible changes in impurity levels. Oxygen level remained below 10 ppm; carbon level was less than 35 ppm; and the indicated hydrogen level was less than 3 ppm. There was no apparent correlation between power operation and impurity level. Operation of the cold trap during power operation apparently maintained the low level impurities in the sodium.									
EF-92	Coil #58	April 5, 1971	0.7	0.3		0.8				
	Coil #59	April 12, 1971	- - - - - - - - - - - - - - - - - Results are not published - - - - - - - - - - - - - - - -							
EF-88	Coil #54	Oct. 22, 1970	33		0.078		0.268	0.66	0.138	8.0
					Hydroxide H = 2.30 ppm					

Table A13

Primary Sodium Activity (FERMI)

Report #	Fission Products activity (μCi/cc of Na)	Na^{24} activity (mCi/cc of Na)	Date Reported
EF-101	$2.5x10^{-2}$	***	January 1972
EF-100		13	December 1971
EF-99		13	November 1971
EF-98		$2.3x10^{-5}$	October 1971
EF-97		$2.3x10^{-5}$	September 1971
EF-96		$2.5x10^{-5}$	August 1971
EF-95		$2.5x10^{-2}$	July 1971
EF-94		12.23	June 1971
EF-93		0.865	May 1971
EF-92		2.68	April 1971
EF-91	$1.8x10^{-2}$		March 1971
EF-90		0.5	February 1971
EF-89		1.0	January 1971
EF-88		1.6	December 1970
EF-87		13	November 1970

Secondary System: No radiation levels greater than instrument background were detected at the surface of the steam generators which indicates that the radioactivity was well below $2.5x10^{-4}$ μCi of Na^{24} per cc of sodium as required by the Technical Specifications.

***Purpose of the sample taken is an investigation to determine the cause of Na^{24} found in the containment building atmosphere in December, 1971. The sample is being analyzed to establish base data on Na^{22} and other constituents.

Table A14

Uranium in the Sodium in the Transfer Tank System (Fermi)

A sodium sample taken from the electromagnetic pump line of the FARB cold trap room transfer tank system on May 27, 1970 was analyzed in two parts for December, 1970 (EF-88) as follows:

	Sample A	Sample B
^{238}U	11.8±0.7 ppb	2.9±0.4 ppb
^{235}U	1.9±0.5 ppb	$<$ 0.5 ppb

Table A15

Off-Site Radioactivity Release in Gaseous Waste—
Noble Gas and Activation Products (SEFOR)

Report #	Total Activity Released (Noble Gases and activation products) (Ci)	Total Volume of Gas Released (ft^3)	Time Average Release Rate (μCi/sec)	MPC$^{(a)}$ used (μCi/ml)	Licensed Limit for Annual Average (μCi/sec)	Percent of Annual Limit	Maximum Hourly Average Release Rate (μCi/sec)	Licensed Limit for Hourly Average (μCi/sec)	Percent of Hourly Limit
10th Quarterly	8.99×10^{-3}	261,000	1.14×10^{-3}	2×10^{-8}	800	1.4×10^{-4}	544	3400	16
9th Quarterly	6.38×10^{-3}	127,000	$.81\times10^{-3}$	2×10^{-8}	800	1×10^{-4}	5.1×10^{-2}	3400	1.5×10^{-3}
8th Quarterly	1.37	155,700	.174	2×10^{-8}	800	2.2×10^{-2}	18	3400	.53
7th Quarterly	7.1×10^{-2}	124,500	9.0×10^{-3}	2×10^{-8}	800	1.1×10^{-3}	.19	3400	5.6×10^{-3}

			Maximum Radioactivity Measured		
			Long-lived Gross α (μCi/ml)	Long-lived Gross β (μCi/ml)	Noble Gas Concentration (μCi/ml)
6th Quarterly		390,000	$<1\times10^{-12}$	1×10^{-10}	$<1\times10^{-9}$
5th Quarterly		125,280	$<1\times10^{-12}$	1×10^{-10}	$<1\times10^{-9}$
4th Quarterly		153,380	$<1\times10^{-12}$	$<1\times10^{-11}$	$<1\times10^{-9}$
3rd Quarterly		108,650	$<1\times10^{-12}$	$<1\times10^{-11}$	$<1\times10^{-9}$
2nd Quarterly		265,200	$<1\times10^{-12}$	$<1\times10^{-11}$	$<1\times10^{-9}$
1st Quarterly		234,350	$<1\times10^{-13}$	$<1\times10^{-11}$	$<1\times10^{-9}$

(a) Based on ^{87}Kr observed in the cover gas.

Table A16

Off-Site Radioactivity Release in Gaseous Waste—Halogens and Particulates (SEFOR)

Report #	Total Activity Released (Halogens and Particulates)(a) (Ci)	Total Volume of Gas Released (ft^3)	Time Average Release Rate (µCi/sec)	MPC used(b) (µCi/ml)	Licensed Limit for Annual Average (µCi/sec)	Percent of Annual Limit	Maximum Hourly Average Release Rate (µCi/sec)	Licensed Limit for Hourly Average (µCi/sec)	Percent of Hourly Limit
10th Quarterly	$<7.39\text{x}10^{-5}$	261,000	$<9.4\text{x}10^{-6}$	$1\text{x}10^{-10}$	$5.6\text{x}10^{-3}$	.17	<.34	$5.6\text{x}10^{-2}$	6
9th Quarterly	$<3.6\text{x}10^{-8}$	127,000	$<4.6\text{x}10^{-9}$	$1\text{x}10^{-10}$	$5.6\text{x}10^{-3}$	$<1\text{x}10^{-4}$	$<9.4\text{x}10^{-7}$	$5.6\text{x}10^{-2}$	$<1.7\text{x}10^{-3}$
8th Quarterly	$<4.4\text{x}10^{-7}$	155,700	$<5.6\text{x}10^{-8}$	$1\text{x}10^{-10}$	$5.6\text{x}10^{-3}$	$<1.0\text{x}10^{-3}$	$<9.4\text{x}10^{-7}$	$5.6\text{x}10^{-2}$	$<1.7\text{x}10^{-3}$
7th Quarterly	$3.5\text{x}10^{-7}$	124,500	$4.4\text{x}10^{-8}$	$1\text{x}10^{-10}$	$5.6\text{x}10^{-3}$	$.79\text{x}10^{-3}$	$9.4\text{x}10^{-7}$	$5.6\text{x}10^{-2}$	$1.7\text{x}10^{-3}$

6th - 1st Quarterlies: None Observed

(a) Halogens and particulates with half-lives > 8 days.

(b) Based on the possible presence of ^{131}I.

Table A17

Off-Site Radioactivity Release in Liquid Waste—Fission Products and Activation Products (SEFOR)[a]

Report #	Total activity of Fission Products and Activation Products Released (Ci)	Total volume of liquid waste discharged (gallons)	Total volume of dillution water (gallons)	Volume average concentration at discharge point (μCi/ml)	MPC used (μCi/ml)	Percent of limit (%)	Maximum concentration released, averaged over not more than 24 hours (μCi/ml)
10th Quarterly	1.28x10^{-5}	5.29x10^{3}	5.0x10^{4}	6.8x10^{-8}	3.0x10^{-5} (b)	0.22	9.0x10^{-6}
9th Quarterly	<3.3x10^{-6}	1.15x10^{4}	5.0x10^{4}	<1.9x10^{-8}	3.0x10^{-5} (b)	<0.06	3.0x10^{-7}
8th Quarterly	4.6x10^{-7}	12x10^{3}	62x10^{3}	<1.9x10^{-9}	1.0x10^{-7}	<1.9	<5x10^{-8}
7th Quarterly	<7.2x10^{-7}	4.8x10^{3}	50x10^{3}	<3.8x10^{-9}	1.0x10^{-7}	<3.8	<3x10^{-8}

	Maximum radioactivity level measured (Fission products and activation products)		Volume discharged (gallons)
	α (μCi/ml)	β (μCi/ml)	
6th Quarterly	<1x10^{-8}	1.6x10^{-5} (Identified as tritium and C-14. No γ emitters observed above 1x10^{-8} μCi/ml)	1773
5th Quarterly	<1x10^{-8}	8x10^{-8}	7774
4th Quarterly	<1x10^{-8}	3x10^{-8}	7399
3rd Quarterly	<1x10^{-8}	<1x10^{-8}	4154
2nd Quarterly	<1x10^{-8}	<1x10^{-8}	6718
1st Quarterly	<1x10^{-8}	<1x10^{-8}	3750

(a) All liquids are released to a tile field. Measured concentrations refer to values at the point of discharge into the tile field.

(b) Na^{22} identified as gamma emitter.

Table A18

Off-Site Radioactivity Release in Liquid Wastes-
Tritium and Carbon-14 (SEFOR)

Report #	Tritium Total Curie Activity Released (Ci)	Volume Average Concentration at Discharge Point (a) (μCi/ml)	(b) Percent of Limit %	Carbon-14 Total Curie Activity Released (Ci)	Volume Average Concentration at Discharge Point (a) (μCi/ml)	(c) Percent of Limit %
10th Quarterly	$1.35\text{x}10^{-2}$	$7.1\text{x}10^{-5}$	2.4	$1.3\text{x}10^{-6}$	$6.9\text{x}10^{-9}$	$8.6\text{x}10^{-4}$
9th Quarterly	$4.4\text{x}10^{-2}$	$2.3\text{x}10^{-4}$	7.7	$4\text{x}10^{-3}$-estimated		
8th Quarterly	$9.4\text{x}10^{-2}$	$4.0\text{x}10^{-4}$	13.4	$3.5\text{x}10^{-4}$-estimated		
7th Quarterly	$8.0\text{x}10^{-3}$	$4.2\text{x}10^{-5}$	1.4	$3.0\text{x}10^{-4}$-estimated		
6th Quarterly	Total activity of tritium and carbon-14 is 1.6×10^{-5} μci/ml.					
5th Quarterly	Not reported.			Not reported.		
4th Quarterly	Not reported.			Not reported.		
3rd Quarterly	Not reported.			Not reported.		
2nd Quarterly	Not reported			Not reported.		
1st Quarterly	Not reported.			Not reported.		

(a) All liquids are released to a tile field. Measured concentrations refer to values at the point of discharge into the tile field.

$$\text{Volume average concentration at discharge} = \frac{\text{Total activity released}}{\text{Total volume of dilution water}}$$

(b) MPC used 3×10^{-3} μCi/ml for one week breathing (soluble in water)

(c) MPC used 8×10^{-4} μCi/ml for one week breathing (soluble in water)

Table A19

Environmental Sampling of Radioactivity in Vegetation, Soil, and Water (SEFOR)

Report #	Month	Vegetation[(a)]		Soil[(b)]		Water[(b)]	
		α activity	β activity	α activity	β activity	α activity	β activity
		pCi/gm-ash		pCi/gm		µCi/ml	
All Quarterlies	Recheck level	50	1820	32	45	3×10^{-8}	1.5×10^{-7}
	pre-operational average	13	987	25	34	$<2 \times 10^{-9}$	6.1×10^{-8}
10th Quarterly	August, 1971	16	549	<15	27	$<1 \times 10^{-8}$	$<3 \times 10^{-8}$
	September, 1971	18	861	22	19	$<1 \times 10^{-8}$	$<3 \times 10^{-8}$
	October, 1971	<15	862	19	44	$<1 \times 10^{-8}$	$<3 \times 10^{-8}$
9th Quarterly	May, 1971	<15	1108	24.3	25	$<1 \times 10^{-8}$	3×10^{-8}
	June, 1971	<15	1151	22	27	$<1 \times 10^{-8}$	3×10^{-8}
	July, 1971	<15	917	23	22	$<1 \times 10^{-8}$	4.6×10^{-8}
8th Quarterly	February, 1971	32.6	1497	26	29	$<1 \times 10^{-8}$	3.2×10^{-8}
	March, 1971	30	1657	<15	55	1.9×10^{-8}	$<3 \times 10^{-8}$
	April, 1971	20.7	1640	20	23.3	$<1 \times 10^{-8}$	3.2×10^{-8}
7th Quarterly	November, 1970	16	1332	26	21	$<1 \times 10^{-8}$	7.0×10^{-8}
	December, 1970	23	1509	15	23	$<1 \times 10^{-8}$	7.3×10^{-8}
	January, 1971	19	1463	18	15	$<1 \times 10^{-8}$	3.1×10^{-8}
6th Quarterly	August, 1970	<15	964	<15	48	$<1 \times 10^{-8}$	2.3×10^{-8}
	September, 1970	16.6	1471	15.4	43	$<1 \times 10^{-8}$	1.2×10^{-7}
	October, 1970	<15	1395	20	22	$<1 \times 10^{-8}$	3×10^{-8}
5th Quarterly	May, 1970	15	762	16	35	$<1 \times 10^{-8}$	$<3 \times 10^{-8}$
	June, 1970	17	949	15	29	$<1 \times 10^{-8}$	3.3×10^{-8}
	July, 1970	18	1317	22	26	$<1 \times 10^{-8}$	7.3×10^{-8}

Table A19

Environmental Sampling of Radioactivity in Vegetation, Soil, and Water (SEFOR) (continued - page 2)

Report #	Month	Vegetation[a] α activity pCi/gm-ash	Vegetation[a] β activity pCi/gm-ash	Soil[b] α activity pCi/gm	Soil[b] β activity pCi/gm	Water[b] α activity μCi/ml	Water[b] β activity μCi/ml
4th Quarterly	February, 1970	18	1007	16	22	$<1\times10^{-8}$	$<3\times10^{-8}$
	March, 1970	15	2154*	15	27	$<1\times10^{-8}$	$<3\times10^{-8}$
	April, 1970	15	762	16	35	$<1\times10^{-8}$	$<3\times10^{-8}$
3rd Quarterly	November, 1969	<15	951	22	24	$<3\times10^{-8}$	$<5\times10^{-8}$
	December, 1969	<15	966	21	32	$<3\times10^{-8}$	$<5\times10^{-8}$
	January, 1970	18	705	31	38	$<1\times10^{-8}$	$<3\times10^{-8}$
2nd Quarterly	August, 1969	<15	941	22	28	$<5\times10^{-9}$	$<7\times10^{-8}$
	September, 1969	20	1003	<15	25	$<5\times10^{-9}$	$<7\times10^{-8}$
	October, 1969	<15	1055	31	32	$<3\times10^{-8}$	$<5\times10^{-8}$
1st Quarterly	May, 1969	18	1026	22	29	$<5\times10^{-9}$	$<7\times10^{-8}$
	June, 1969	<15	966	22	17	$<5\times10^{-9}$	$<7\times10^{-8}$
	July, 1969	<15	941	21	28	$<2\times10^{-9}$	4.3×10^{-8}

*Only long-lived fission products (fallout) were noted in gamma scan.

(a) No evidence of Co^{60}, I^{131}, or Na^{24} was observed.

(b) No evidence of Co^{60} or Cs^{137} was observed above detection limits.

Table A20

Environmental Film Monitoring (SEFOR)

Number of Stations: 17

Total Films Analyzed during Each Quarter: 51

Report # and Report Period	Maximum Radiation Level Reported	Maximum Radiation Level Reported during Pre-Operational Survey (millirad/month)
10th Quarterly Aug. 1, 1971 thru Oct. 31, 1971	17 millirad/quarter	8
9th Quarterly May 1, 1971 thru July 31, 1971	16 millirad/quarter	8
8th Quarterly Feb. 1, 1971 thru April 30, 1971	12 millirad/quarter	8
7th Quarterly Nov. 1, 1970 thru Jan. 31, 1971	0 millirad/month	8
6th Quarterly Aug. 1, 1970 thru Oct. 31, 1970	0 millirad/month	8
5th Quarterly May 1, 1970 thru July 30, 1970	0 millirad/month	8
4th Quarterly Feb. 1, 1970 thru April 30, 1970	0 millirad/month	8
3rd Quarterly Nov. 1, 1969 thru Jan. 31, 1970	0 millirad/month	8
2nd Quarterly Aug. 1, 1969 thru Oct. 31, 1969	4 millirad/month	8
1st Quarterly May 1, 1969 thru July 31, 1969	4 millirad/month	8

Table A21

Primary Sodium Composition (SEFOR)

Concentration (ppm)

Report #	Date Taken	Al	Ag	B	Ba	Be	Bi	C	Ca	Co	Cr	Cu	Fe	Li	Mg
10th Quarterly (8/1/71-10/31/71)	8/16/71	20	<.2	<20	<6	<.6	<.2	25	6	<.6	<.6	.2	8		.6
9th Quarterly (5/1/71-7/31/71)	6/16/71	100	2	<10	<5	<.1	<.1	22	6	6	4	<3	4	<10	6
8th Quarterly (2/1/71-4/30/71)	3/17/71	<2		2		<12	<12	13	5		6		6	<20	6
7th Quarterly (11/1/70-1/31/71)	12/18/70	< 6	<.6	<.6	<6	<.6		24	6	<6	< 6	<.6	4		<6

Primary Sodium Composition (SEFOR)

Concentration (ppm)

(part 2 - continued)

Report #	Date Taken	Mn	Mo	Nb	Ni	P	Pb	Sb	Si	Sn	Ti	U^{235}	U^{238}	V	Zn	Zr
10th Quarterly (8/1/71-10/31/71)	8/16/71	<.2	<.2	<60			<6	<60	5	<.6	<.2	.2(a)	7(a)	<.2		<6
9th Quarterly (5/1/71-7/31/71)	6/16/71	.6	<.3	<30	<1	<100	<1	<30	2	< 3	< 1	.2(a)	5(a)	<.3	<1	
8th Quarterly (2/1/71-4/30/71)	3/17/71		<12						20	< 2		(4±2)(a)	(200±50)(a)	<12		
7th Quarterly (11/1/70-1/31/71)	12/18/70	<.6	<.6		<6		<.6		12	<.6	<.6			<.6		<6

< Represents lower limit of detection for instrument used.

(a) ppb

Table A22

Primary Sodium Radioactivity (SEFOR)

Report #	Date Taken	Ag^{110}	Co^{60}	I^{131}, I^{133}	Na^{22}	Na^{24}	Rb^{86}	Sb^{124}
				dpm/16g sample				
10th Quarterly (8/1/71-10/31/71)	8/16/71	$3.1x10^4$		(a)	$1.2x10^6$			None
9th Quarterly (5/1/71-7/31/71)	6/16/71	$4.4x10^4$			$1.1x10^6$			$<4x10$[illegible]
8th Quarterly (2/1/71-4/30/71)	3/17/71	$4.9x10^4$		(b)	$1.9x10^6$			$1.1x10$[illegible]
7th Quarterly (11/1/70-1/31/71)	12/18/70	$2.0x10^4$	$4.4x10^2$	(b)	$4.1x10^5$	$\sim 1x10^{11}$	$1.6x10^5$	$4.8x10$[illegible]

(a) No evidence of I^{131} or I^{133} above detection limits was observed.

(b) I^{131} activity was below the limits of detection.

Table A23 .

Cover Gas Activity (SEFOR)

Report #	
10th Quarterly	The cover gas monitor was in service during the quarter and indicated no anomalous gas activity. Cover gas samples were obtained at monthly intervals before and after the Subprompt Test Series and each Superprompt Transient Test. No significant increase in the concentration of the fission products in the cover gas was observed. Examination of this data continues to indicate good correlation with cover gas samples obtained since December, 1970.
9th Quarterly	The cover gas monitor was in service during the quarter and indicated no anomalous fission gas activity. Ten cover gas samples were obtained between May 6, 1971 and May 8, 1971; six in June, and one in July to quantitatively measure the isotopic constituents. These samples consistent of routine monthly cover gas analysis, special experiments to further refine sampling and identification techniques, and pre- and post-FRED transient samples. No significant increase in the concentration of the fission products in the cover gas was observed. Preliminary examination of these data indicate good correlation with other cover gas samples obtained since December, 1970.
8th Quarterly	The cover gas monitor was in service during the quarter, and indicated no anomalous fission gas activity. Cover gas samples were obtained to quantitatively measure the isotopic constituents. These samples consisted of routine monthly cover gas analyses, special experiments to further refine sampling and identification techniques, and pre- and post-FRED transient samples. These results indicate no fission gas levels other than those normally anticipated from tramp uranium and/or pin hole cladding penetrations.
7th Quarterly	The cover gas monitor was in service continuously during the quarter. Cover gas samples were obtained to quantitatively measure the isotopic constituents. Two samples were obtained in November, 1970, five during January, 1971. A special series of measurements were also conducted in December to further refine the techniques for sampling the low level fission gas (Xe and Kr) components. These results indicated no fission gas levels other than those normally anticipated from tramp uranium and/or pin hole cladding penetration.
6th Quarterly	The cover gas monitor operated during the quarter and data were obtained as a function of reactor power level. These results were supplemented with a cover gas sampling technique which used 50 ml charcoal filter and a millipore filter in addition to the 400 ml cylinder gas sample which was used on previous gas samplings. With the edition of these filters the sensitivity of the sampling technique was increased sufficiently to observe a background level of xenon radioactivity. The magnitude of xenon corresponded to that anticipated from the low level "tramp" uranium. On-line spectrometric studies were conducted also which revealed the presence of neon-23, a short lived ($T_{1/2} = 38$ sec) isotope resulting from fast neutron activation of Na^{23}. This isotope has been observed at EBR-II and RHAPSODIE.
5th Quarterly	Reactor cover gas activity was monitored and samples were taken for spectrographic analysis. The A-41 activity was near the levels anticipated. No other isotopic activity was observed.
4th Quarterly	Reactor cover gas activity was monitored and samples were taken for spectrographic analysis. The A-41 activity was near the anticipated level for short term operation at low power levels.

Table A24

Integrated Power*and List of Reports (1971) (EBR-II)

Report No. and Date	Operated Period of Time	Integrated Power MWd
ANL-7776, January 1971		Not Reported
ANL-7783, February 1971		Not Reported
ANL-7798, March 1971	March 2, 1971-March 15, 1971 November 1963-March 15, 1971	505 42321
ANL-7825, April-May 1971	March 15, 1971-May 15, 1971 November 1963-May 15, 1971	1467 43788
ANL-7833, June 1971		Not Reported
ANL-7845, July 1971	May 15, 1971-July 15, 1971 November 1963-July 15, 1971	1752 45540
ANL-7854, August 1971		Not Reported
ANL-7861, September 1971	July 15, 1971-September 15, 1971 November 1963-September 15, 1971	1969 47509
ANL-7872, October 1971		Not Reported
ANL-7887, November 1971	September 15, 1971-November 15, 1971 November 1963-November 15, 1971	2354 49863
ANL-7900, December 1971		Not Reported

* See footnote on page 79 concerning EBR-II power level.

Table A25

Radionuclide Activity in Primary Sodium (EBR-II)

Report No. and Date	Sampling Data	^{22}Na (nCi/g)	^{137}Cs (nCi/g)
ANL-7776 January 1971	9/30/70	48	11
	10/6/70	49	11
	10/13/70	51	11
	10/28/70	51	12
	11/2/70	50	12
	11/9/70	53	13
	11/13/70	53	11
	11/18/70	51	10
	11/23/70	52	7
	11/30/70	54	8
	12/4/70	51	6
	12/9/70	51	6
	12/14/70	50	3
	12/30/70	51	4
	1/4/71	51	4

Table A25

Page 2 (continued)

Report No. and Date	Sampling Date	^{131}I (pCi/g)	^{137}Cs (nCi/g)	^{210}Po (pCi/g)
ANL-7798 March 1971	2/11/71	None detected	5	
	2/16/71	None detected		15.7
	2/18/71	None detected	12	
	2/19/71	None detected	12	
	2/22/71	None detected	10	
	2/24/71	28	13	
	3/2/71	12	12	

Table A25

Page 3 (continued)

Report No. and Date	Sampling Date	^{131}I (pCi/g)	^{137}Cs (nCi/g)	^{54}Mn (pCi/g)	^{110m}Ag (nCi/g)	^{113}Sn-^{113m}In (nCi/g)	^{117m}Sn (nCi/g)	^{125}Sb (nCi/g)
ANL-7825 April-May, 1971	3/5/71	25	11					
	3/10/71	67	12					
	3/12/71	150	13					
	3/15/71	140	13					
	3/26/71	86	13					
	4/5/71	47	14					
	4/12/71	79	14					
	4/16/71	140	18					
	4/21/71	150	18					
	4/27/71	143	19					
	4/27/71	130	18					
	4/16/71			None detected	0.614	5.10	0.08	.148
	4/23/71			50.6	0.651	5.46	4.81	.506

Table A25

Page 4 (continued)

Report No. and Date	Sampling Date	^{131}I (pCi/g)	^{137}Cs (nCi/g)
ANL-7833 June 1971	4/12/71	79	14
	4/16/71	140	18
	4/21/71	150	18
	4/27/71	136	18
	5/5/71	110	17
	5/14/71	58	17
	5/19/71	25	16
	5/24/71	66	17
	5/28/71	72	17
	6/1/71	147	
	6/4/71	97	
	6/7/71	310	17
	6/8/71	463	~21

Table A25

Page 5 (continued)

Report No. and Date	Sampling Date	^{3}H (nCi/g)	^{131}I (pCi/g)	^{137}Cs (nCi/g)	^{54}Mn (pCi/g)	^{110m}Ag (nCi/g)	^{113}Sn-^{113m}In (nCi/g)	^{117}Sn (nCi/g)	^{125}Sb (nCi/g)
ANL-7845 July 1971	5/5/71		110	17					
	5/14/71		58	17					
	5/19/71		25	16					
	5/24/71		66	17					
	5/28/71		72	17					
	6/1/71		147	18					
	6/4/71		97	17					
	6/7/71		31	20					
	6/8/71		463	22					
	6/11/71		294	23					
	6/14/71		196	21					
	6/18/71		113	22					
	6/23/71		82	21					
	6/28/71		68	23					
	4/29/71	42							
	5/24/71	63							
	5/13/71				28.9	.651	5.96	4.34	.542
	6/18/71				72.3	.578	5.78	3.61	.108
	7/2/71				61.4	.687	6.47	5.06	.867

Table A25
Page 6 (continued)

Report No. and Date	Sampling Date	^{3}H (nCi/g)	^{22}Na (nCi/g)	^{131}I (pCi/g)	^{137}Cs (nCi/g)	^{54}Mn (pCi/g)	^{110m}Ag (nCi/g)	^{113}Sn-^{113m}In (nCi/g)	^{117}Sn (nCi/g)	^{125}Sb (nCi/g)
ANL-7861 September 1971	1/6/70					28	.50	4.4	4.1	.59
	2/5/70					59	.41	5.0	4.1	.66
	3/19/70					24	.47	5.6	5.6	.23
	6/16/70					53	.53	3.8	5.3	.10
	7/31/70					84	.59	7.2	4.4	.50
	8/21/70					19	.59	6.6	4.4	.17
	9/21/70					49	.47	4.7	2.2	.17
	11/24/70					None Detected	.69	7.2	3.8	.20
	1/8/71					None Detected	.59	5.7	0.38	None Detected
	2/16/71					None Detected	.53	4.4	0.07	.13
	4/23/71					44	.56	4.7	4.2	.44
	5/13/71					25	.57	5.2	3.8	.48
	6/18/71					63	.50	5.0	3.0	.094
	7/2/71					53	.59	5.6	4.4	.75
	7/9/71		51	42	19					
	7/14/71		52	50	21					
	7/16/71	34								
	7/16/71	30								
	7/19/71		51	49	20					

continued on next page....

Table A25

Page 7 (continued)

Report No. and Date	Sampling Date	^{3}H (nCi/g)	^{22}Na (nCi/g)	^{131}I (pCi/g)	^{137}Cs (nCi/g)	^{54}Mn (pCi/g)	^{110m}Ag (nCi/g)	^{113}Sn-^{113m}In (nCi/g)	^{117}Sn (nCi/g)	^{125}Sb (nCi/g)
ANL-7861 September 1971	7/23/71		53	63	20					
	7/28/71		53	76	20					
	8/3/71		53	59	20					
	8/6/71		51	49	21					
	8/19/71					18	.59	6.0	4.7	.20
	8/20/71	20								
	8/27/71		53	41	20					

Table A25

Page 8 (continued)

Report No. and Date	Sampling Date	^{3}H (nCi/g)	^{22}Na (nCi/g)	^{131}I (pCi/g)	^{137}Cs (nCi/g)	^{54}Mn (pCi/g)	^{110m}Ag (nCi/g)	^{113}Sn-^{113m}In (nCi/g)	^{117}Sn (nCi/g)	^{125}Sb (nCi/g)
ANL-7887 November 1971	9/1/71		51	43	21					
	9/8/71		52	53	21					
	9/13/71			45		28	.59	6.1	4.2	.35
	9/24/71		51		21					
	9/29/71	46								
	10/4/71		51	65	20					
	10/6/71		51	69	20					
	10/18/71						.59	5.8	3.6	.28
	10/20/71		53	35	22					
	10/21/71		53	47	22					
	10/27/71		53	66	21					
	10/29/71		54	65	21					

Table A26

EBR-II Radionuclide Activity in Secondary Sodium (1971)

Concentration (nCi/g)

Report No. and Date	Sampling Date	^{3}H (nCi/g)	^{24}Na (nCi/g)
ANL-7845 July 1971	4/29/71	6.7	
	5/24/71	9.2	
	6/23/71	2.9	
ANL-7861 September 1971	7/16/71	0.83	
	7/16/71	2.4	
	7/16/71	3.6	
	8/2/71	0.98	
	8/2/71	0.73	
	9/10/71		30
ANL-7887 November 1971	9/29/71	1.2	
	10/27/71		41
	11/30/68		6.5
	4/5/68		31
	5/20/68		32
	6/12/68		32
	9/4/68		30
	12/20/68		25
	3/26/69		10
	4/23/69		6.5
	5/19/69		26
	6/10/69		27
	7/10/69		22
	8/19/69		22
	9/26/69		24
	10/17/69		9.3
	1/29/70		11
	3/10/70		30
	6/22/70		28

continued....

Table A26

EBR-II Radionuclide Activity in Secondary Sodium (1971) (continued)

Concentration (nCi/g)

Report No. and Date	Sampling Date	^{3}H (nCi/g)	^{24}Na (nCi/g)
ANL-7887 November 1971 (continued)	7/15/70		24
	9/29/70		33
	10/6/70		34
	4/21/71		16
	6/30/71		30
	7/29/71		36

Table A27

Gamma Activity in EBR-II Cover Gas due to Tramp Source

(data taken Sept. 7-8, 1971)

Report No. and Date	Nuclide	Absolute Activity [(a)] μCi/ml
ANL-7872 October 1971	^{133}Xe	4.34×10^{-4}
	^{135}Xe	2.05×10^{-3}
	^{85m}Kr	3.07×10^{-4}
	^{88}Kr	5.0×10^{-4}
	^{87}Kr	2.48×10^{-4}
	^{138}Xe	4.22×10^{-5}
	^{135m}Xe	2.1×10^{-5}
	^{23}Ne	2.5×10^{-3}

(a) Normalized to grab-sample determination of 2.05×10^{-3} μCi/ml for ^{135}Xe during this period. Principal nuclides identified in the EBR-II cover gas are: ^{85m}Kr, ^{133}Xe, ^{135}Xe, ^{85}Kr, ^{87}Kr, ^{88}Kr, ^{135m}Xe, ^{138}Xe, ^{131m}Xe, ^{133m}Xe, ^{137}Xe, ^{23}Ne, ^{41}A, ^{88}Rb, ^{138}Cs (ANL-7872, October 1971).

Table A28

EBR-II Primary Sodium Composition
(trace metals)
Concentration, ppm

Report No. and Date	Sampling Date	Ag	Al	Bi	Ca	Cd	Co	Cr	Cu	Fe
ANL-7776 January 1971	10/27/1970	0.06	<0.6	1.9	<0.02		<0.02	<0.02	<0.02	0.09
	11/24/1970	0.05	<0.6	1.9	<0.02		<0.02	<0.02	<0.02	0.1
ANL-7798 March 1971	1/8/1971	0.05	<0.6	0.9	<0.02		<0.02	<0.02	<0.02	0.28
	2/16/1971	0.05	<0.6	1.3	<0.02		<0.02	<0.02	<0.02	0.08
ANL-7825 April-May 1971	4/23/1971	0.05	<0.6	3	<0.02		<0.02	<0.02	0.03	0.23
ANL-7845 July 1971	5/13/1971	0.07	<0.6	3.2	<0.02		<0.02	0.02	0.04	0.97
	7/2/1971	0.13	<0.6	1.1	<0.01		<0.02	<0.02	0.03	0.45
	6/18/1971									
	5/19/1971					0.02				
ANL-7861 September	7/7/1971	0.045	0.027	1.4	<0.001		<0.002	0.063	0.02	0.55
	7/14/1971			∼1.0		0.03				
	7/16/1971	0.1		2.0						
	8/19/1971	0.06	<0.6	1.5	<0.01		<0.002	<0.02	<0.02	0.25
ANL-7887 November 1971	1/4/1971			1.1						
	9/13/1971	0.06	<0.6	1.8	<0.01		<0.02	0.07	<0.02	0.18
	10/18/1971	0.05	<0.6	1.6	<0.01		<0.02	<0.02	<0.02	0.48
	10/20/1971					0.08				

continued....

Table A28

Continued

EBR-II Primary Sodium Composition
(trace metals)

Concentration, ppm

Report No. and Date	Sampling Date	In	K	Mg	Mn	Mo	Ni	Pb	Sn	Zn
ANL-7776 January 1971	10/27/1970	<0.06		0.009	<0.005	<0.07	<0.04	11.3	24.2	
	11/24/1970	<0.06		0.01	0.009	<0.07	<0.04	10.6	23.1	
ANL-7798 March 1971	1/8/1971	<0.06		0.005	<0.005	<0.07	<0.04	2.9	24.6	
	2/16/1971	<0.06		<0.005	<0.005	<0.07	<0.04	7.11	28.8	
ANL-7825 April-May 1971	4/23/1971	<0.06		0.009	<0.005	<0.07	<0.04	9.8	23.5	
ANL-7845 July 1971	5/13/1971	<0.06		0.013	0.009	<0.07	<0.04	5	26.9	
	7/2/1971	<0.06		0.018	0.005	<0.07	<0.04	1.8	25.5	
	6/18/1971									
	5/19/1971									<0.06
ANL-7861 September 1971	7/7/1971	0.008		0.007	0.015	<0.01	0.056	8.27	28.0	
	7/14/1971							~9.0		<0.06
	7/16/1971							11.0		
	8/19/1971	<0.06		0.023	<0.005	<0.07	<0.04	9.1	26.7	
ANL-7887 November 1971	1/4/1971							11.0		
	9/13/1971	<0.06		0.007	<0.005	0.07	<0.04	11.0	25.0	
	10/18/1971	<0.06		0.015	<0.005	0.07	<0.04	12	24.0	
	10/20/1971									<0.06

Table A29

EBR-II Primary Sodium Composition
(Non-metals)

Report No. and Date	Sampling Date	B	C	O	Si	Total H	Hydride H	Hydroxide H	N
		Concentration, ppm							
ANL-7776 January 1971	11/24/1970			1.1 ± 0.2					
	11/13/1970					<0.1			
ANL-7798 March 1971	2/16/1971			2.2 ± 1.0					
	11/24/1970		0.8 ± 0.06						
	2/16/1971		1.6 ± 0.4						
	12/23/1971					<0.06			
	2/18/1971					0.22			
ANL-7825 April-May 1971	4/7/1971			1.3 ± 0.4					
	4/23/1971			1.8 ± 0.7					
	2/11/1971				1.6				
	4/29/1971				0.9				
	4/29/1971	<0.05							
ANL-7845 July 1971	5/14/1971		1.0 ± 0.5	1.6 ± 0.6					
	6/11/1971		1.1 ± 0.2	1.2 ± 0.3					
	6/28/1971								<0.1
ANL-7861 September 1971	7/16/1971				1.2				
	8/20/1971	<0.05			3.1				
	5/13/1971						0.09	0.10	
	6/11/1971						0.07	0.08	
	7/19/1971		1.9 ± 0.1	0.8 ± 0.25		<0.0	0.10	0.07	
	8/20/1971								0.16
ANL-7887 November 1971	9/29/1971	<0.05			0.4				
	10/21/1971	<0.05			0.8				
	8/19/1971					0.09 ± 0.02			
	9/13/1971					0.16 ± 0.05			
	9/24/1971		0.07						
	10/20/1971		1.0 ± 0.5						<0.1
	10/21/1971			1.0 ± 0.4					

Table A30

EBR-II Secondary Sodium Composition
(Trace Metals)

Concentration, ppm

Report No. and Date	Sampling Date	Ag	Al	Bi	Ca	Co	Cr	Cu	Fe
ANL-7798 March 1971	2/16/1971	0.01	<0.6	<0.1	0.03	<0.02	0.58	<0.02	3.6
	2/22/1971	0.048	0.05	0.019	0.026	<0.002	0.004	0.007	0.11
ANL-7825 April-May 1971	3/10/1971	0.011	0.02	0.013	<0.001	0.002	0.001	0.045	0.08
	3/16/1971	0.03	<0.6	<0.1	0.013	<0.02	0.009	0.015	0.07
	4/16/1971	0.06	<0.6	<0.1	<0.01	<0.02	0.016	0.02	0.08
ANL-7845 July 1971	5/13/1971	0.16	<0.6	<0.1	0.04	<0.02	0.06	0.05	1.27
	6/16/1971	0.05	<0.6	<0.1	0.11	<0.02	0.05	<0.02	0.23
	7/13/1971	0.08	<0.6	<0.1	0.02	<0.02	0.03	0.02	0.21
ANL-7861 September 1971	8/10/1971	0.23	<0.06	<0.01	0.01	<0.02	0.05	0.04	0.11
ANL-7887 November 1971	9/7/1971	0.39	<0.06	<0.1	<0.01	<0.02	0.06	<0.02	0.17
	10/12/1971								
	10/21/1971	0.02	<0.06	<0.1	<0.03	<0.02	0.02	0.04	0.20

continued....

Table A30

(continued)

EBR-II Secondary Sodium Composition
(Trace Metals)
Concentration, ppm

Report No. and Date	Sampling Date	In	K	Mg	Mn	Mo	Ni	Pb	Sn
ANL-7798 March 1971	2/16/1971	<0.06		0.005	0.031	<0.07	0.37	0.5	<0.5
	2/22/1971	<0.01		0.013	0.001	<0.01	0.005		
ANL-7825 April-May 1971	3/10/1971	0.01		0.007	0.002	<0.015	0.008	0.67	0.06
	3/16/1971	<0.06		0.043	<0.006	<0.07	<0.04	0.30	<0.5
	4/16/1971	<0.06		0.007	<0.006	<0.07	<0.04	0.55	<0.5
ANL-7845 July 1971	5/13/1971	<0.06		0.038	0.021	<0.007	0.06	0.20	<0.5
	6/16/1971	<0.06		0.028	<0.006	<0.07	<0.04	0.18	<0.5
	7/13/1971	<0.06		0.032	0.014	<0.07	<0.04	0.23	<0.5
ANL-7861 September 1971	8/10/1971	<0.06		0.038	<0.06	<0.07	<0.04	0.77	<0.5
ANL-7887 November 1971	9/7/1971	<0.06		0.04	<0.006	<0.07	0.08	0.66	<0.5
	10/12/1971		158						
	10/21/1971	<0.06		0.02	<0.005	0.11	<0.04	0.11	<0.5

Table A11

EBR-II Secondary Sodium Composition
(Non-metals)

Report No. and Date	Sampling Date	Concentration, ppm B	C	O	Si	Total H	Hydride H	Hydroxide H	N
ANL-7776 January 1971	11/18/1970			0.8 ± 0.4					
	10/27/1970					<0.06			
ANL-7798 March 1971	2/17/1971			3.7 ± 0.5					
	2/17/1971		1.0 ± 0.3						
	3/3/1971		1.2 ± 0.2						
	2/17/1971					0.27			
ANL-7825 April-May 1971	3/3/1971			1.0 ± 0.1					
	4/14/1971			0.4 ± 0.1					
	4/14/1971		1.4 ± 0.4						
	2/16/1971				1.6				
	3/15/1971				0.8				
	4/21/1971				0.9				
	4/26/1971	<0.05							
ANL-7845 July 1971	5/11/1971		1.6 ± 0.2	1.3 ± 0.9					
	6/7/1971		1.3 ± 0.4	1.0 ± 0.5					
	6/17/1971								<0.1
	5/19/1971				0.4				
	6/24/1971				4.4				
	5/20/1971	<0.05							
	6/18/1971	<0.05							
ANL-7861 September 1971	7/12/1971	<0.05							
	7/27/1971				1.3				
	8/11/1971	<0.05							
	8/12/1971				0.5				
	3/25/1971						0.08	0.10	
	4/19/1971						0.07	0.04	
	5/18/1971						0.04	<0.04	
	6/29/1971					0.09	0.12	0.03	
	7/28/1971					0.2	0.06	0.11	
ANL-7887 November 1971	9/20/1971				2.3				
	9/21/1971	<0.05							
	10/25/1971	<0.05							
	10/29/1971				0.7				
	3/26/1971					0.00 ± 0.05			
	9/14/1971								0.12
	9/28/1971		0.7			0.04 ± 0.02			
	10/19/1971			1.2 ± 0.3					

APPENDIX B:

Fission Product Data

Half lives, decay constants, and fast fission yields for ^{239}Pu and ^{238}U are given in Table B1. The reference is:

> M. E. Meek and B. F. Rider, "Compilation of Fission Product Yields, Vallecitos Nuclear Center, 1972," NEDO-12154 (January 1972).

The results in this reference are output of a computer tabulation at General Electric which is frequently updated and which weights in importance the different experimental data assembled.

The decay schemes of the fission products for which the activities were calculated during the present study are shown in Figure B1. These decay schemes ignore nuclides of very short half lives that occur before the first nuclide shown in each chain in the figure, i.e. nuclides of such short half life that they do not affect the results in Section 4.

Table B1

Half Lives and Fission Yields of Fission Products Listed in Section 4.

Nuclide	Accumulated Percent Yield (Fast Fission)		Half-Life	Decay Constant
	^{239}Pu	^{238}U	$T^{1/2}$	λ, sec^{-1}
^{85m}Kr	0.642	0.811	4.4h	4.375×10^{-5}
^{85}Kr	0.142	0.173	10.76y	2.042×10^{-9}
^{86}Rb[a]	1.810×10^{-5}	1.510×10^{-7}	18.66d	4.298×10^{-7}
^{89}Sr	1.719	3.016	50.8d	1.579×10^{-7}
^{90}Sr	2.089	3.282	28.9y	7.604×10^{-10}
^{90}Y	2.089	3.282	64.0h	3.008×10^{-6}
^{91}Sr	2.464	4.506	9.67h	1.991×10^{-5}
^{91m}Y	1.503	2.748	50.5m	2.287×10^{-4}
^{91}Y	2.464	4.506	58.8d	1.364×10^{-7}
^{95}Zr	4.586	5.579	65.5d	1.225×10^{-7}
^{95m}Nb	0.060	0.073	87h	2.213×10^{-6}
^{95}Nb	4.586	5.579	35.1d	2.285×10^{-7}
^{99}Mo	5.609	6.424	66.6h	2.890×10^{-6}
^{99m}Tc	4.936	5.653	6.007h	3.208×10^{-5}
^{103}Ru	6.533	6.395	39.8d	2.015×10^{-7}
^{103m}Rh	6.468	6.331	55m	2.100×10^{-4}
^{106}Ru	4.517	2.835	368d	2.180×10^{-8}
^{106}Rh	4.519	2.835	30s	2.310×10^{-2}
^{110m}Ag[a]	7.300×10^{-6}	2.050×10^{-10}	253d	3.170×10^{-8}
^{110}Ag[a]	8.250×10^{-6}	2.310×10^{-10}	24.6s	2.817×10^{-2}
^{111}Ag	0.367	0.103	7.48d	1.072×10^{-6}
^{113m}Cd[a]	4.180×10^{-6}	3.330×10^{-9}	13.6y	1.616×10^{-9}
^{115m}Cd	0.006	0.003	44.1d	1.819×10^{-7}
^{119m}Sn	0.001	0.001	245d	3.274×10^{-8}
^{121m}Sn	0.001	7.860×10^{-6}	76y	2.891×10^{-10}
^{123m}Sn	0.043	0.0210	129d	6.218×10^{-8}
^{125}Sn	0.064	0.068	9.65d	8.312×10^{-7}
^{125}Sb	0.192	0.113	2.73y	8.049×10^{-9}

Table B1

(continued-page 2)

Half Lives and Fission Yields of Fission Products Listed in Section 4.

Nuclide	Accumulated Percent Yield (Fast Fission)		Half-Life	Decay Constant
	^{239}Pu	^{238}U	$T^{1/2}$	λ, sec^{-1}
^{125m}Te	0.040	0.024	58d	1.383×10^{-7}
^{126}Sb	0.301	0.063	12.4d	6.466×10^{-7}
^{127}Sn	0.209	0.049	2.12h	9.080×10^{-5}
^{127}Sb	0.500	0.098	3.8d	2.111×10^{-6}
^{127m}Te	0.086	0.190	109d	7.359×10^{-8}
^{127}Te	0.501	1.067	9.3h	2.070×10^{-5}
^{129}Sb	0.687	0.513	4.34h	4.435×10^{-5}
^{129m}Te	0.335	0.222	34.1d	2.352×10^{-7}
^{129}Te	0.801	0.573	69m	1.674×10^{-4}
^{129}I	0.922	0.653	1.6×10^{7}y	1.373×10^{-15}
^{131m}Te	0.609	0.367	30h	6.417×10^{-6}
^{131}Te	3.548	3.361	25m	4.620×10^{-4}
^{131}I	4.196	3.662	8.065d	9.945×10^{-7}
^{131m}Xe	0.025	0.024	11.96d	6.706×10^{-7}
^{132}Te	5.265	5.298	78h	2.468×10^{-6}
^{132}I	5.366	5.300	2.284h	8.428×10^{-5}
^{133}I	6.817	6.471	20.8h	9.255×10^{-6}
^{133m}Xe	0.195	0.181	2.26d	3.549×10^{-6}
^{133}Xe	6.824	6.471	5.27d	1.522×10^{-6}
^{134}Cs[a]	1.440×10^{-4}	1.020×10^{-7}	2.06h	9.345×10^{-5}
^{136}Cs	0.151	0.011	13.0d	6.170×10^{-7}
^{137}Cs	6.625	5.952	30.2y	7.276×10^{-10}
^{137m}Ba	6.195	5.563	2.551m	4.528×10^{-3}
^{140}Ba	5.142	5.947	12.8d	6.266×10^{-7}
^{140}La	5.150	5.947	40.23h	4.785×10^{-6}
^{141}La	6.094	5.447	3.87h	4.974×10^{-5}
^{141}Ce	6.094	5.447	32.53d	2.466×10^{-7}
^{143}Ce	4.312	4.533	33h	5.833×10^{-6}

Table B1

(continued-page 3)

Half Lives and Fission Yields of Fission Products Listed in Section 4

Nuclide	Accumulated Percent Yield (Fast Fission)		Half-Life	Decay Constant
	^{239}Pu	^{238}U	$T^{1/2}$	λ, sec^{-1}
^{143}Pr	4.313	4.533	13.58d	5.906×10^{-7}
^{144}Ce	3.604	4.543	284.4h	6.769×10^{-7}
^{144}Pr	3.609	4.543	17.3m	6.676×10^{-4}
^{147}Nd	2.022	2.564	11.06d	7.252×10^{-7}
^{147}Pm	2.023	2.565	2.623y	8.378×10^{-9}
^{148m}Pm^{a}	3.110×10^{-4}	5.39×10^{-8}	41.5d	1.933×10^{-7}
^{151}Pm	0.819	0.925	28.4h	6.778×10^{-6}
^{151}Sm	0.820	0.925	93y	2.363×10^{-10}
^{154}Eu^{a}	4.488×10^{-3}	3.300×10^{-6}	7.8y	2.817×10^{-9}
^{155}Eu	0.258	0.139	5.0y	4.395×10^{-9}
^{156}Sm	0.125	0.074	9.4h	2.048×10^{-5}
^{156}Eu	0.154	0.075	15.2d	5.277×10^{-7}
^{160}Tb^{a}	0.005	4.580×10^{-6}	72.4d	1.108×10^{-7}
^{161}Tb	0.014	0.002	7.0d	1.146×10^{-6}
^{162}Gd		4.080×10^{-4}	10.4m	1.111×10^{-3}
^{162m}Tb		2.210×10^{-4}	2.24h	8.594×10^{-5}

[a] These isotopes are produced more by activation of other fission products than by accumulated yield from fission.

Figure B1. Fission Product Decay Schemes Used for Calculations in Section 4.

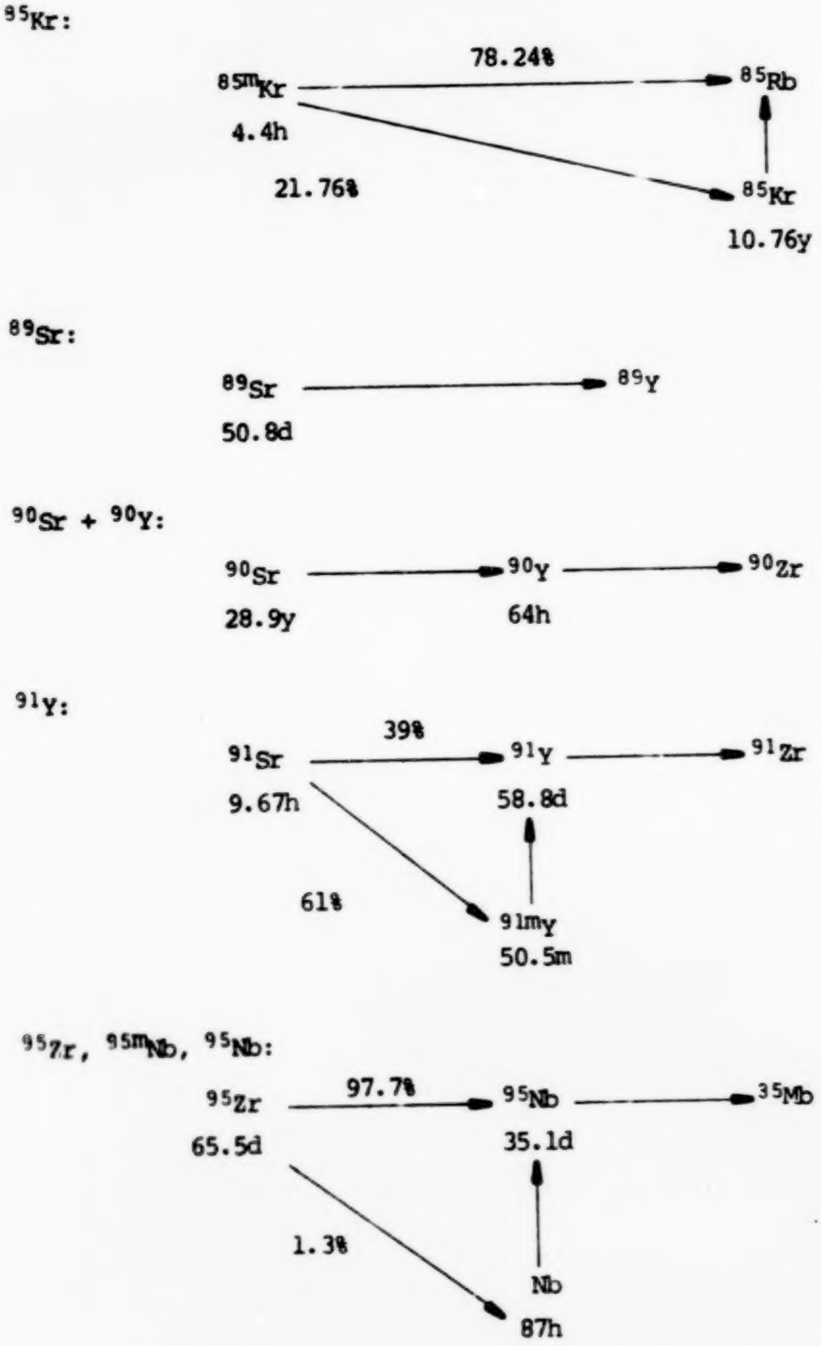
^{85}Kr:
78.24%
^{85m}Kr
4.4h
^{85}Rb
21.76%
^{85}Kr
10.76y
^{89}Sr:
^{89}Sr
50.8d
^{89}Y
^{90}Sr + ^{90}Y:
^{90}Sr
28.9y
^{90}Y
64h
^{90}Zr
^{91}Y:
39%
^{91}Sr
9.67h
^{91}Y
58.8d
^{91}Zr
61%
^{91m}Y
50.5m
^{95}Zr, ^{95m}Nb, ^{95}Nb:
^{95}Zr
65.5d
97.7%
^{95}Nb
35.1d
^{35}Mb
1.3%
Nb
87h

Figure B1. Fission Product Decay Schemes Used for Calculations in Section 4. (continued)

^{103}Ru + ^{103m}Rh:

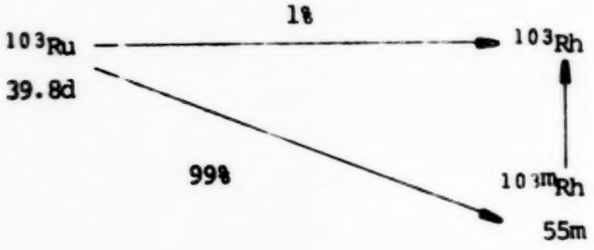
^{103}Ru
39.8d
1%
^{103}Rh
99%
^{103m}Rh
55m

^{106}Ru + ^{106}Rh:

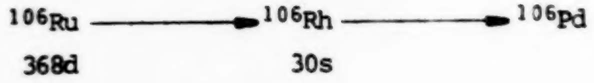
^{106}Ru
368d
^{106}Rh
30s
^{106}Pd

^{125}Sb:

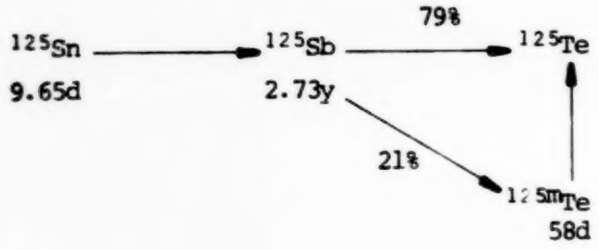
^{125}Sn
9.65d
^{125}Sb
2.73y
79%
^{125}Te
21%
^{125m}Te
58d

^{127}Sb:

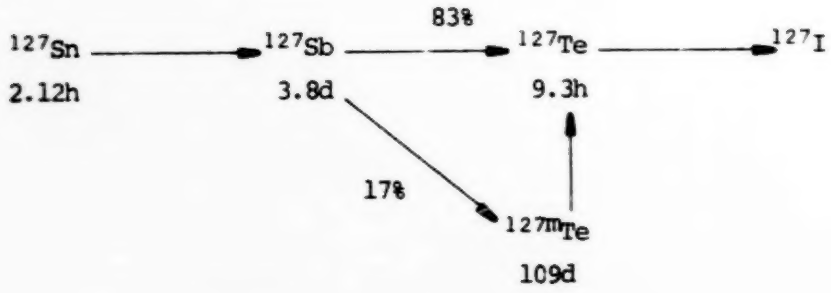
^{127}Sn
2.12h
^{127}Sb
3.8d
83%
^{127}Te
9.3h
^{127}I
17%
^{127m}Te
109d

^{131}I:

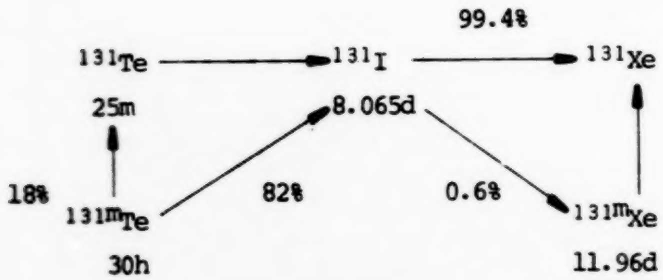
99.4%
^{131}Te
25m
^{131}I
8.065d
^{131}Xe
18%
^{131m}Te
30h
82%
0.6%
^{131m}Xe
11.96d

Figure B1. Fission Product Decay Schemes Used for Calculations in Section 4. (continued)

^{133}Xe:

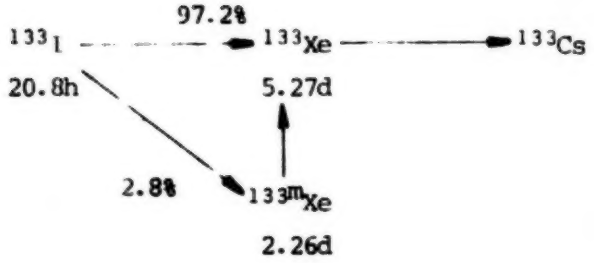

97.2%
^{133}I
20.8h
^{133}Xe
5.27d
^{133}Cs
2.8%
^{133m}Xe
2.26d

^{137}Sc + ^{137m}Ba:

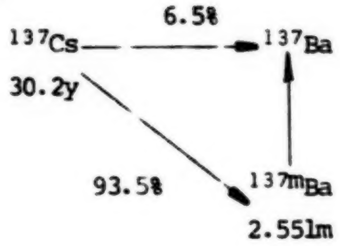

6.5%
^{137}Cs
30.2y
^{137}Ba
93.5%
^{137m}Ba
2.551m

^{141}Ce:

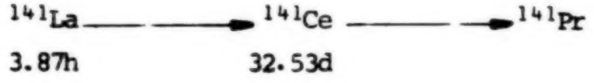

^{141}La
3.87h
^{141}Ce
32.53d
^{141}Pr

^{144}Ce + ^{144}Pr:

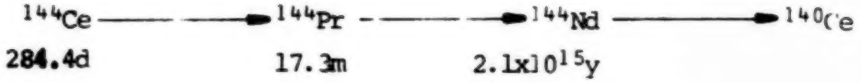

^{144}Ce
284.4d
^{144}Pr
17.3m
^{144}Nd
2.1x10^{15}y
^{140}Ce

^{147}Nd, ^{147}Pm:

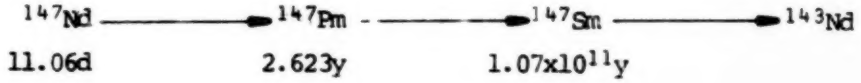

^{147}Nd
11.06d
^{147}Pm
2.623y
^{147}Sm
1.07x10^{11}y
^{143}Nd

^{151}Sm:

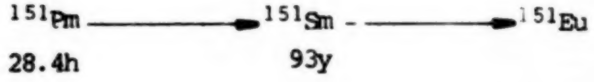

^{151}Pm
28.4h
^{151}Sm
93y
^{151}Eu

^{155}Eu:

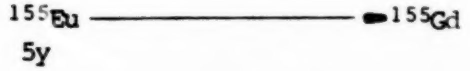

^{155}Eu
5y
^{155}Gd